2007

Distributed parameter sensitivity analysis of laterally loaded piles in non-homogeneous soil (soft clay overlying sand under cyclic loading)

Dahlia Hisham Hafez
University of Windsor

Distributed Parameter Sensitivity Analysis of Laterally Loaded Piles in Non-Homogeneous Soil (Soft Clay Overlying Sand Under Cyclic Loading)

By

Dahlia Hisham Hafez

A Dissertation
Submitted to the Faculty of Graduate Studies
through the Department of Civil and Environmental Engineering
in Partial Fulfillment of the Requirements for
the Degree of Doctor of Philosophy at the
University of Windsor

Windsor, Ontario, Canada

2007

© Dahlia Hisham Hafez

To My Mother

ABSTRACT

Laterally loaded piles are widely used to support many structures such as high-rise buildings, bridge abutments and offshore structures. This dissertation presents the study of the sensitivity of laterally loaded piles embedded in non-homogeneous soil consisting of soft clay overlying sand subjected to cyclic loading. The study is divided into three parts.

In the first part, the theoretical formulation for the sensitivity of the pile's head lateral deflection and rotation to changes in the design parameters was derived for single and group piles. The distributed parameter sensitivity approach was used in the derivation with three different formulation techniques of the adjoint method. The design parameters considered were those defining the pile and the adjacent clay and sand. Five forms of sensitivity results were obtained.

In the second part, various numerical sensitivity investigations were conducted including single piles and pile groups. Different pile lengths, pile head boundary conditions, and pile loadings were studied. In addition, the effect of pile spacing and pile location for a pile group, and the thickness of the overlying clay were investigated. More than 700 different cases for single and pile groups were studied using developed MATLAB programs, COM246P for single piles and FB-Pier for pile groups. The obtained results were verified by conducting an error analysis assessment.

In the third part of this research, a user-friendly sensitivity program for laterally loaded piles was developed which allows the engineer to input his own data. The program is based on the theoretical formulation and is developed using MATLAB. It offers the numerical and graphical presentation of the five forms of sensitivity results.

The results presented in this study enhance the understanding of the behavior of the laterally loaded pile-soil system. In addition, they allow the engineer to detect the critical locations of influence of each parameter along the pile length and quantitatively assess and compare that influence. Further more, an engineering tool for sensitivity is provided. Accordingly, the proposed research has considerable practical application in improving the design of the pile systems, solving infrastructure aging problems, monitoring processes, and helping in rehabilitation and renovation activities.

ACKNOWLEDGEMENTS

I would like to thank almighty Allah first and foremost for giving me the will, energy and guidance without which I couldn't accomplish this prestigious degree.

I express my deep and sincere appreciation and gratitude to my supervisor Dr. Budkowska for her guidance, inspiration and encouragement in shaping this dissertation. My gratitude for Dr. Zamani, Dr. Madugula, and Dr. Das for their suggestions, comments and overall involvement.

A very sincere appreciation and special thanks go to my mother Mona Sadek who extended her help for me beyond childhood to the deep involvement and help in writing the dissertation leaving her work and family back home. To my father Hisham Hafez who guided me and helped me in following his path of studies and would give without limits to see me happy and progressing.

My deep gratitude to my husband Ahmed Deif for his continuous support and guidance. I couldn't have done it without his unlimited patience at all times. To my children Hamza, Mariam and Mahmoud who in their own way understood as to why mummy had a lot of work on the computer. To my mother and father in law who kept praying for me.

To my friends who helped me out during my studies especially with the kids: Heba, Mona, Naglaa, Hanan, Ola, Horeya, Hajar, Hala, Laila, Reem, Fatma, Sumayia and more.

A final appreciation to all those who taught me that knowledge is the way for honor and helped me to create my mission to continue seeking knowledge throughout my life.

TABLE OF CONTENT

LIST OF TABLES

xiv

LIST OF FIGURES

xvii

xix

xx

NOMENCLATURE

$\overline{\lambda}$: a virtual displacement

θ : angle of rotation,

γ'_c : effective unit weight of clay

$\delta y''$: increment of change of angle of flexural rotation of primary structure

$\hat{\delta}(x)$: Dirac measure at zero.

σ_a : stress in the adjoint structure

λ : adjoint variable

$\delta a_{\delta u}$: first variation of the calculus of variation with respect to explicit dependence of the energy bilinear form a_u on design u evaluated in the direction δu.

γ'_s : the submerged unit weight of sand

ϕ : friction angle of sand

Λ : a column vector of design derivatives

λ: (n × 1) adjoint variables vector or an (n x 1) Lagrange multiplier vector

δG : the first-order change in the function G

θ_t : the angle of rotation at the top of the pile (the counter clockwise rotation at the pile head)

δu : change (first variation) of the design variables

δy_t : change (first variation) of lateral top deflection caused by the change of the design variables δu

α, β : values used in $p\text{-}y$ models for sand where $\alpha = \phi/2$, $\beta = 45 + \phi/2$

$$\delta PE = \int_0^l [EIz''\bar{z}'' - f\bar{z}]dx = 0 : \text{first variation of } PE$$

δy : increment of deflection of primary structure

$\delta(..)_N$: normalized variations of design variables corresponding to each design variable $(..)$

ε_{50} : strain corresponding to one-half the compressive strength of clay

ε_a : the strain in the adjoint structure.

$$a_u(z,\bar{z}) = \int_0^l EIz''\bar{z}''dx = \text{energy bilinear form where } u \text{ denotes dependence of energy}$$

bilinear forms on the design vector u.

$A_{(.)}$: the sensitivity factors corresponding to each design variable $(..)$ which is equal to the integration of the sensitivity operators S which gives the magnitude of the influence of each design variable

$\widetilde{A}_c$, B_c : non-dimensional coefficients used for p-y model for piles in sand subjected to cyclic loading given as function of x/b by Reese el. 1974.

$\widetilde{A}_s$, B_s : non-dimensional coefficients used for p-y model for piles in sand subjected to static loading given as function of x/b by Reese el. 1974.

A_s : non-dimensional coefficient used for p-y model for piles in stiff clay below water table subjected to static loading given as function of x/b by Reese et al. (1975).

$A_{tot} = |A_{\gamma c}| + |A_c| + |A_{\varepsilon 50}| + |A_{\gamma s}| + |A_\phi| + |A_k| + |A_{EI}| + |A_b|$: summation of the absolute values of the all the sensitivity factor

b or D : width or diameter of the pile

c : undrained shear strength or undrained cohesion

C: (n × m) matrix defined in Eq. (3.4)

c_a : average undrained soil shear strength over the depth x

xxii

C_m : moment amplification factor

C_y : deflection amplification factor

EI: bending stiffness of beam

F : $(n \times 1)$ vector of external loads

$f(u)$: cost (objective) function to be optimized

$f(x)$: distributed lateral load

f_m: p-multiplier used for pile groups

$g(r)$: performance function (or failure function or limit state function)

G: a general function (or functional) that may represent any of the performance measures (or a constraint function)

G_c : group reduction factor

$g_c(u)$: constraints function

GF : group relative sensitivity factor where each design variable is compared with the design variables in its group

H_1 : depth of upper layer of soft clay

H_2 : depth of embedment of the pile in the lower sand layer

h_2 : equivalent depth of sand that determines local coordinates for the lower sand layer

J : a model constant needed for calculation of ultimate soil resistance of clay

k : modulus of subgrade reaction for the linear part of the p-y sand curve.

K_a: coefficient of active lateral earth pressure used in p-y models for sand where $K_a = \tan^2(45 - \phi / 2)$

$K(u)$: $(n \times n)$ stiffness matrix

l : length of pile

$l_u(\bar{z}) = \int_0^l f\bar{z}dx$: load linear form where u denotes dependence of load linear forms on the design vector u.

L: Lagrangian

L_a : length of pile below which the pile deflections become negligible

M : the bending moment

$M_{g(max)}$: maximum moment in a pile in the group

$M_{s(max)}$: maximum moment in a single pile under the same load

N : number of cycles of loading used for p-y model for stiff clay above water table

p : soil reaction given as a force per unit length

PCR: percent change ratio which determines percent change in the lateral deflection or rotation at the pile head if the parameter changes with a certain percent.

PE: potential energy

Pg : lateral load applied to the pile group

$(Pg_1)_j$: the lateral force applied to the adjoint structure pile cap that will produce unit shear force at the pile number j under consideration

p_m : the soil resistances of sand occurring at deflections y_m for p-y model for sand

p_s ; the ultimate soil resistance per unit length of the pile for sand

p_{sd} : the ultimate soil resistance for sand, p_s, for the lower part of the system $(x \geq x_{rs})$

p_{st} : the ultimate soil resistance for sand, p_s, for the upper part of the system $(x \leq x_{rs})$

p_u : the soil resistances of sand occurring at deflections y_u for p-y model for sand

p_{ult}, : ultimate soil resistance per unit length of the pile for clay

$R(u, z) = K(u)z$- $F(u) = 0$: state or equilibrium equations

$R(z, z', u) \equiv z' - F(z, u) = 0$: equilibrium equations for one-dimensional structural systems that are described by a set of first order differential equations

r: random variables vector

s': center to center pile spacing in a pile group (perpendicular to the direction of load)

s: center to center pile spacing in a pile group (spacing in direction of load)

$\tilde{s}$: nonlinear stress strain relationship

T: relative stiffness factor used to determine length of pile

TF: total relative sensitivity factors that compares each design variable to all the design variables in the study

TF: total relative sensitivity factor which compares the effect of each parameter relative to all studied parameters.

u: (m ×1) design variables vector, $u = \{EI, b, \gamma'_c, c, \varepsilon_{50}, \gamma'_s, \phi, k\}^T$

V: shear force

Vj: shear force produced at the top of pile number j under consideration by the application of the force Pg to the pile cap of the primary structure.

x_{rc}: depth of reduced resistance for clay

x_{rs}: depth of reduced resistance for sand

y: pile lateral deflection

y: pile lateral deflection

y_g: group deflection

y_k: deflection differentiating between the linear elastic stage and the parabolic nonlinear stage for p-y model for sand

y_m: deflection differentiating between the parabolic nonlinear stage and the linear hardening stage for p-y model for sand

y_s: single pile deflection under the same load

y_t: lateral pile-head displacement occurring at the top of the pile and

y_u: deflection differentiating between the linear hardening stage and the plastic flow stage for p-y model for sand

z : $(n \times 1)$ nodal displacement (or state) vector for discrete systems or a displacement field for distributed parameter systems

z' : $z' = \dfrac{\partial z}{\partial x}$: the gradient of z

$\tilde{z}$: state z with dependence on τ suppressed and $\bar{z}$ is independent of τ

$\bar{z}(x)$: arbitrary function or can be viewed as a virtual displacement

$z(\hat{x})$: value of the displacement z (or y) at an isolated point $\hat{x}$

Z : the space of kinematically admissible displacements.

xxvi

CHAPTER 1

INTRODUCTION

1.1 PROBLEM STATEMENT

The sensitivity of a system to variations of its parameters is one of the most important aspects needed to properly understand the system performance. It is considered as an important complementary part of the analysis in the design stage. In addition, it is important for dealing with unavoidable parameter imperfections and in the rehabilitation process.

Sensitivity analysis is concerned with the relationship between parameters defining the system at hand and the system behavior (Kleiber et al., 1997). It found broad application in various branches of science, engineering and economy. However, its application needs to be better established in the geotechnical field. Its application to the geotechnical field is of special importance due to the soil's nature associated with parameter uncertainties.

The study area of laterally loaded piles is an important area in the geotechnical engineering field. This field is receiving more attention since laterally loaded piles are an important part of many infrastructural facilities. They are widely used in engineering practice to support structures such as high-rise buildings, bridge abutments, and offshore structures. The behavior of a laterally loaded pile embedded in soil is typically considered to be a soil-structure interaction system (Poulos and Davis, 1980).

The importance of sensitivity analysis of the soil-structure interaction system is embodied in two facts. The soil is a nature-made material that affects the system's performance and the sensitivity theory constitutes an inherent part of the behavior of the system. Moreover, the access to the supporting system is limited. Therefore, it is essential to have

1

a reliable basis for the assessment of how changes of the parameters of the system affect its performance.

The performance of laterally loaded piles is dependent on the maximum deflections. The maximum generalized deflections are those that mainly occur at the top of the pile. They are the pile-head lateral deflection and the pile-head rotation. These quantities are crucial quantities for the behavior of the superstructure which are used as an indicator or a tool to measure serviceability. Good and safe performance of the pile system and superstructure will be achieved if certain measures of these deflections are satisfied.

Application of sensitivity analysis to laterally loaded pile foundations thus represents a powerful tool and an innovative method of the analysis of piles. The sensitivity analysis of distributed parameter type allows the consideration of material properties of both the pile and the surrounding soil as spatial functions. The sensitivity results can allow the engineer to indicate the critical locations of the changes that the design variables have on the system performance. In addition, the results permit the view of the influence of each variable along the pile length and the quantitative assessment of the impact of each change.

Application of sensitivity analysis to laterally loaded piles started as a continuing research program in the last few years at the University of Windsor, Windsor, Ontario, Canada. However, the previous studies were limited to cases of homogeneous soils (Budkowska, 1998, Priyanto, 2002, Suwarno, 2003, Abedin, 2004, Liu, 2004, Rahman, 2004 and Mora, 2006). In addition, previous research concentrated on analysis of certain dimensions and parameters of the system. A flow chart showing the applications of sensitivity analysis is given in Figure 1.1.

2
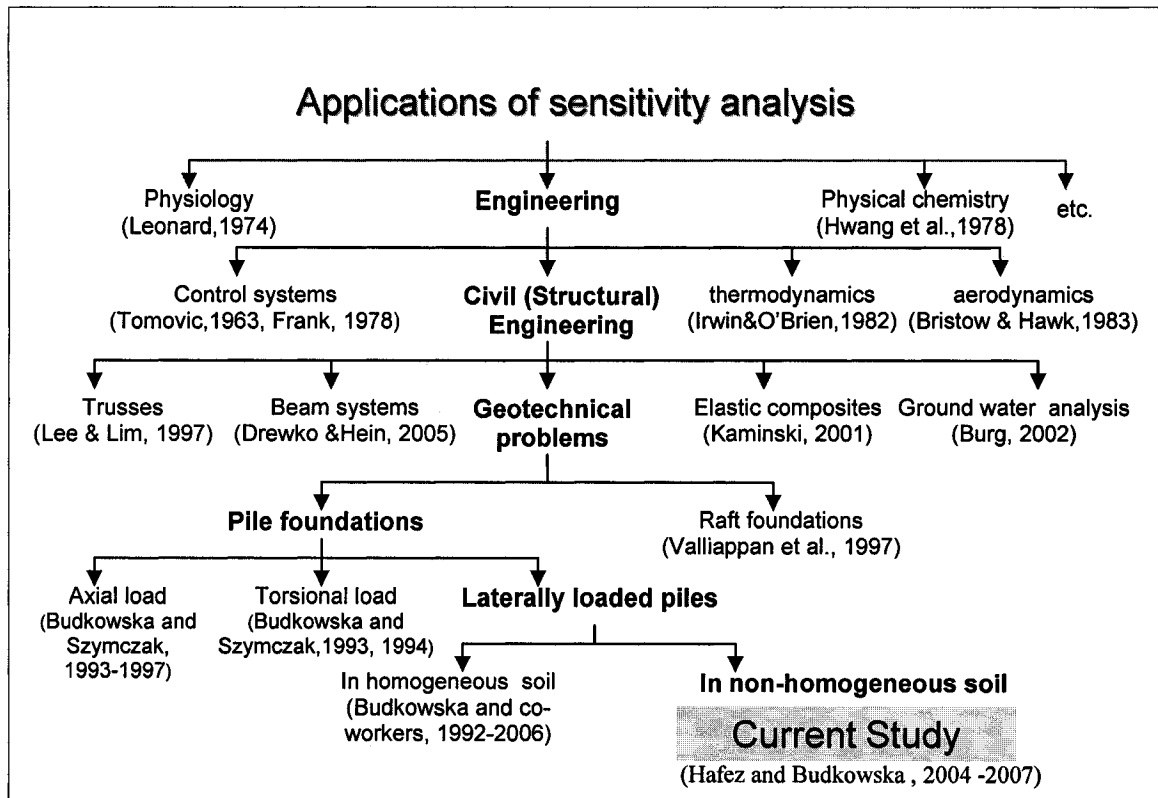
**Figure 1.1 Application of sensitivity analysis in different fields
and engineering areas**

The current study applies the sensitivity analysis to non-homogeneous soil, which is a more common and complex case (Hafez and Budkowska, 2004, 2005a, b, 2006a, b, c, d, 2007a and 2007b). The present research work allows the engineer to broaden our understanding of the pile-soil system. It has considerable practical application in improving the design of the pile systems, solving problems of infrastructure aging, monitoring processes and helping in rehabilitation and renovation activities. In addition, the present research is not limited to certain dimensions and parameters of piles. The current research offers engineers a user-friendly sensitivity analysis program to allow for the applicability of the study to general cases. Engineers can apply specific cases and obtain the sensitivity analysis results.

3

1.2   STUDY OBJECTIVES

The key objective of the present research study is to apply the distributed parameter nonlinear sensitivity analysis to laterally loaded piles embedded in non-homogeneous soil subjected to cyclic loading. The focus is towards determination of how sensitive the structural response of the pile-soil system is to the changes of the design variables. The structural response is described as the lateral top deflection and rotation of the pile head due to their importance as serviceability measures for the superstructure supported by the pile system. In addition, an important objective of the study is to offer a sensitivity analysis tool to the engineer.

Accordingly, three specific objectives of this study are to:

1. Develop a theoretical formulation for sensitivity analysis of laterally loaded piles embedded in non-homogeneous soil consisting of soft clay overlying sand.

2. Perform numerical analysis based on the theoretical formulation for different cases of piles with different cases of non-homogeneity.

3. Develop a user-friendly program as a tool for engineers to obtain sensitivity analysis results relevant to their different studied cases.

1.3   SCOPE OF WORK

The current research is divided into three parts. Each part deals with one of the three objectives listed above. The scope of work of each of the three parts studied in this dissertation (theoretical, numerical and programming) is discussed below. It should be noted that the scope of the current work doesn't include experimental or field studies; however, it is recommended that this be an extension for future research to the current work as mentioned in Chapter 8.

1.3.1   Part I: Theoretical formulation

There are many methods of sensitivity analysis that can be applied to engineering problems (Kleiber et al, 1997 and Haug et al., 1986). Comparisons between different

methods and approaches are summarized in Chapter 3. The distributed parameter type of sensitivity analysis using the adjoint method was found to be the most suitable method to be used. The adjoint method can be theoretically formulated for nonlinear problems using different formulation techniques such as those based on the virtual work equation, energy forms and those based on the Lagrange multiplier method (Budkowska, 1997a, Haug et al., 1986 and Belegundu, 1985). These three different techniques are used to derive formulations for the laterally loaded piles. Comparisons are provided between these formulations and a final form resulting from these three techniques is obtained to be used in the current research.

Non-homogeneity of the soil surrounding the piles is considered in a layered fashion. The investigated piles are assumed to penetrate soft clay that overlies a sand layer. The nonlinear pile-soil behavior is described by the well established "p-y curves", relating the soil reaction p to the pile deflection y. The state-of-the-art of the analysis of laterally loaded piles shows that the p-y method of analysis, based on full scale tests, can be adequately used to model the nonlinear soil behavior (Reese and Van Impe, 2001).

The cyclicity of the loading is introduced to the p-y models in an implicit fashion. The incorporation of two homogeneous p-y models to the non-homogeneous soil profile is achieved by means of an equivalent thickness approach proposed by Georgiadis (1983). This method employs the continuity of ultimate soil reaction resultant. The effect of the non-homogeneity is investigated by considering different thicknesses of each layer.

The sensitivity of the system performance, described by the lateral head deflection and rotation, to changes of the system parameters is theoretically formulated. Eight system parameters for clay, sand, and pile are considered in the present study. The studied clay parameters are: the undrained cohesion c, the submerged unit weight of clay γ_c' and the strain corresponding to one-half of the compressive strength ε_{50}. The sand parameters are the angle of friction ϕ, the submerged unit weight of sand γ_s' and the modulus of subgrade reaction k while the pile diameter b and its bending stiffness EI are the studied pile parameters.

5

In summary, the theoretical formulation includes the following:

1. Using three different formulation techniques of the adjoint method to develop a theoretical formulation of the sensitivity of lateral head deflection and head rotation of single laterally loaded piles to changes in the design variables.

2. Comparing the different techniques to reach a final theoretical form to be used in the study.

3. Implementing non-homogeneity in the formulation. The piles are embedded in non-homogenous soil consisting of soft clay overlying sand below water table subjected to cyclic loading.

4. Extending the proposed theoretical formulation for single piles to pile groups

1.3.2   Part II: Numerical analysis

Based on the developed formulation in Part I, a comprehensive numerical study is conducted. The numerical study includes single piles and pile groups. The numerical sensitivity analysis is obtained by developing computer programs using MATLAB that facilitate in the calculation of the values of the different forms of sensitivity results and present them graphically. The developed MATLAB programs use the finite difference program COM624P for single laterally loaded piles and the finite element computer program for pile groups, FB-Pier, to obtain deflections and internal forces of piles that are required for the sensitivity analysis.

The numerical sensitivity analysis is applied to laterally loaded piles embedded in non-homogeneous soil subjected to cyclic loading. Different cases of non-homogeneous soil (11 different soil stratifications) are analysed. The soil stratifications cover different thicknesses of the upper clay layer, which increases in an incremental fashion. These cases start from the special case of no clay and the pile fully embedded in sand (0% of the pile's length embedded in clay), followed by 10%, 20%, 30%, 40%, 50%, 60%, 70%, 80%, 90% and finally reaches 100% of the pile's length embedded in clay.

The study includes short and long piles, free and fixed head piles, and piles subjected to different ranges of lateral loads and bending moments applied at their top. In addition, the

6

study extends the sensitivity analysis for the above cases to pile groups (3×3 arrangement) to take into account the interactive group effect existing among the piles.

The forms of sensitivity results for each performance measure (lateral head deflection and rotation) are obtained for 297 cases for single piles given in Table 1.1 (in Table 1.1, T denotes the relative sensitivity factor used to determine the length of pile). For the pile groups, the forms of sensitivity results of the lateral deflection are obtained for 396 cases shown in Table 1.2. In addition, the numerical sensitivity results are verified using an error analysis assessment.

The following effects on the sensitivity results are investigated:
1. Effect of nonlinearity
2. Effect of non-homogeneity of the soil (thickness of overlying clay layer)
3. Effect of boundary condition (free and fixed head)
4. Effect of the load type (lateral load and bending moment)
5. Effect of soil response studied (lateral top deflection and lateral top rotation)
6. Group effect (single pile and pile in a group)
7. Effect of pile location in a group of piles
8. Effect of pile spacing for pile groups

Table 1.1 Scope of analysis for single piles

Support type	Pile length	Soil stratification	No. of cases
Free head pile subjected to lateral load	9 cases (2T, 3T, 4T, 5T, 6T, 7T, 8T, 9T &10T) T = 2 m	11 cases (Clay layer thickness = 0, 10, 20, 30, 40, 50, 60, 70, 80, 90 & 100%)	99 cases
Fixed head pile subjected to lateral load	9 cases (2T, 3T, 4T, 5T, 6T, 7T, 8T, 9T &10T) T = 1.8 m	11 cases (Clay layer thickness = 0, 10, 20, 30, 40, 50, 60, 70, 80, 90 & 100%)	99 cases
Free head pile subjected to bending moment	9 cases (2T, 3T, 4T, 5T, 6T, 7T, 8T, 9T &10T) T = 2 m	11 cases (Clay layer thickness = 0, 10, 20, 30, 40, 50, 60, 70, 80, 90 &100%)	99 cases

7

Table 1.2 Scope of analysis for pile groups

Support type	Pile location	Pile spacing	Soil stratification	No. of cases
Piles pinned to pile cap subjected to lateral load (18 m long)	**3 cases** (1 pile from each row)	**4 cases** (2D, 3D, 4D & 5D) D = pile diameter	**11 cases** (Clay layer thickness = 0, 10, 20, 30, 40, 50, 60, 70, 80, 90 & 100%)	**132 cases**
Piles fixed to pile cap subjected to lateral load (18 m long)	**3 cases** (1 pile from each row)	**4 cases** (2D, 3D, 4D & 5D) D = pile diameter	**11 cases** (Clay layer thickness = 0, 10, 20, 30, 40, 50, 60, 70, 80, 90 & 100%)	**132 cases**
Piles pinned to pile cap subjected to bending moment (18 m long)	**3 cases** (1 pile from each row)	**4 cases** (2D, 3D, 4D & 5D) D = pile diameter	**11 cases** (Clay layer thickness = 0, 10, 20, 30, 40, 50, 60, 70, 80, 90 &100)	**132 cases**

1.3.3 Part III: Sensitivity analysis program

This part concentrates on developing a user-friendly program for sensitivity analysis of laterally loaded piles. The program is developed using MATLAB with the aid of COM624P. The program offers the sensitivity of the lateral top head deflection and head rotation to changes in the design parameters of the three following cases of single piles:

1. Pile embedded in a homogeneous layer of soft clay below water table subjected to cyclic loading

2. Pile embedded in a homogeneous layer of sand below water table subjected to cyclic loading

3. Pile embedded in a non-homogeneous layer of soft clay overlying sand, both layers being below water table, subjected to cyclic loading.

By employing the program, the user can obtain the different forms of sensitivity results in both numerical and graphical forms.

8

1.4 STRUCTURE OF DISSERTATION

The work in this dissertation is presented through Chapters 1 to 8, Appendices A to C and the attached CD. An introduction about the studied topic of sensitivity analysis of laterally loaded piles was presented in the current chapter. Chapter 2 presents a review of the literature of laterally loaded piles including single piles and pile groups. Chapter 3 gives a detailed review of sensitivity analysis presenting the different methods and comparing between different approaches of the sensitivity analysis. The different soil models that are needed for developing the theoretical formulation of sensitivity analysis and the incorporation of the non-homogeneity of the soil are presented in Chapter 4.

Part I of the study, which includes the theoretical part, is presented in Chapter 5. The theoretical formulation of the sensitivity analysis problem is derived for both single piles and pile groups using different formulation techniques. Part II of the study, which includes the numerical analysis, is presented in Chapter 6. In Chapter 6, numerical investigations are performed based on the theoretical formulation developed in Part I. A thorough analysis of the numerical results is performed for both single piles and pile groups.

Part III of the study is presented in Chapter 7. Chapter 7 provides details on the user-friendly sensitivity analysis program developed in this study and offers a guide for how to execute the program conveniently and effectively. Summary, conclusions and further recommendations for engineers who use laterally loaded piles in their practice are given in Chapter 8.

The equations for sensitivity operators are given in Appendix A. The programs developed for the numerical sensitivity analysis conducted in Chapter 6 are discussed in Appendix B. The contents of the attached CD and how to obtain data from it are outlined in Appendix C. The attached CD contains the numerical sensitivity results for single and pile groups studied in Chapter 6. In addition, it contains the user-friendly sensitivity analysis program.

9

CHAPTER 2

REVIEW OF LATERALLY LOADED PILES

2.1 INTRODUCTION

Piles are considered as deep foundations and are commonly selected as a cost effective option for the support of many structures in a variety of circumstances. The lateral load besides an axial load is one of the most frequently applied loads the pile foundations have to resist. Sources of lateral loads on pile foundations are manifold. Forces from wind act against overhead signs and high rise buildings. Loads from waves and current are critical to the design of offshore structures and bridges. Waterfront structures must support horizontal loads from the berthing of ships while retaining walls must withstand lateral earth pressure. The soil-structure interaction is the mechanism that governs the pile response behavior and ultimate capacity.

Laterally loaded piles gained a significant amount of study when offshore platforms were being installed in significant numbers in the late 1950s. Full scale tests were extensively conducted sponsored by the petroleum industry. These tests and the advances in the computer technology led to the emergence of the p-y methodology (where p is the soil resistance and y is the deflection) which is still commonly used for laterally loaded pile analysis. With regard to pile analysis, laterally loaded piles can be divided into single isolated piles and pile groups. The analysis of single piles and pile groups are presented in Sections 2.2 and 2.3, respectively.

2.2 ANALYSIS OF SINGLE LATERALLY LOADED PILES

2.2.1 Models used for single pile analysis

Two approaches have been generally employed in modeling single laterally loaded piles.

10

1. The Winkler or subgrade-reaction approach, in which the pile is considered to be supported by an array of uncoupled springs.

2. The elastic approach in which the soil is considered as an ideal elastic homogeneous continuum.

Some of the models used for single piles are presented below:

2.2.1.1 Elastic pile and elastic soil model

In this model, the pile is embedded in an elastic soil. Terzaghi (1955) suggested values of subgrade modulus that can be used to solve for deflection and bending moments. The standard beam equation, such as the one suggested by Hetenyi (1946) can be applied in this model. This model has been widely used, but there were no comparisons between this model and experiments nor recommendations for the computation of bearing capacity (Reese and Van Impe, 2001). Poulos and his colleagues significantly contributed to the development of this model (Poulos and Davis, 1980 and Poulos and Hull, 1989). The elastic solution has gained a substantial attention but cannot be easily used to compute the larger deformation or collapse of the pile foundation in nonlinear soil. In addition, the applicability of this method yet faces the difficulty of the determination of the soil modulus.

2.2.1.2 Elastic pile and finite element for soil

In this model, soil is modeled through finite elements. In view of the computational power that is available, nonlinear geometry can be employed and the elements can be fully three dimensional and nonlinear (Reese and Van Impe, 2001). In spite of this, some problems appear besides the selection of the basic nonlinear element of the soil. Among these problems are the tensile stress in the soil, modeling layered soil, accounting for the separation between pile and soil during cyclic loading, the collapse of sand against the back of the pile, and accounting for the changes of the soil characteristics associated with different types of loading (Reese and Van Impe, 2001).

11

Two dimensional finite element studies were performed by Yegian and Wrigth (1973) and Thompson (1977). Thompson presents a plane stress model and obtained through his study soil response curves that agreed well with results at near the ground surface from full scale field tests. The utilization of three dimensional finite elements approach to develop *p-y* curves was described by Kooijman (1989) and Brown et al. (1989). Bhowmik et al. (1991) investigated the behavior of piles using two and three dimensional linear and nonlinear finite element models. Bransby (1999) used two dimensional finite element analyses to find load-transfer relationship for translation of an infinitely long pile through undrained soil for a variety of soil-constitutive models.

2.2.1.3 *Rigid pile and plastic soil*

The rigid pile and plastic soil model was presented by Broms (1964a, b and 1965) for both cohesive and cohesionless soils. In this method, the pile is assumed as a rigid element, and a solution is found by use of the equations of statics for the distribution of ultimate resistance of the soil that puts the pile in equilibrium. After the ultimate loading is computed for a pile of particular dimensions, Broms suggests that the deflections for the working load may be computed by the equations suggested by the theory.

The method presented by Broms used several simplifying assumptions but still can be useful for the initial selection of piles. The solutions for the equations will yield the size and length of the pile for the expected loading and the pile can then be employed at the starting point for the *p-y* method of analysis. Further benefits from the Broms method are that the mechanics of the problem of lateral loading is clarified and that the method may be used as a check of some of the results from the *p-y* method of analysis (Reese and Van Impe, 2001).

2.2.1.4 *Characteristic load method*

The characteristic load method presented by Duncan et al. (1994) has been widely used. It is based on the earlier work of Evans and Duncan (1982) and states numerous solutions

that were made with nonlinear p-y curves for a range of soils and for a range of pile-head conditions. The method provides simple equations and curves that could be used for rapid prediction of the response of piles under lateral loading. Dimensionless variables were employed in the predicted equations and characteristic shear and moment loads were used. The method can be used to solve for ground-line deflections due to lateral load or bending moment for different pile-head conditions. The soil may be either clay or sand, both limited to uniform strength with depth. In addition, the value of the maximum bending moment and where it occurs along the pile can be determined.

In spite of the limitations in the method with respect to applications that were noted by the authors, an important advantage of this method is that the analysis can be obtained quickly and directly and thus can be used to check results from more sophisticated analyses. In addition it can be used to determine the relative stiffness factor T used to differentiate between short and long piles.

2.2.1.5   Strain wedge model

Ashour et al. (2002) presented the strain wedge model and demonstrated its capability of analyzing laterally loaded isolated piles. The strain wedge model relates one-dimensional beam on an elastic foundation analyses to a three-dimensional response modeled by the strain wedge method by relating the deflection of a pile versus depth, or rotation, to the relative soil strain that exists in the passive wedge which develops in front of a pile under horizontal load. The method allows for the assessment of the nonlinear p-y curve response of a laterally loaded pile based on the envisioned relationship between the three-dimensional response of a flexible pile in the soil to its one-dimensional beam on elastic foundation parameters.

In addition, the strain wedge model employs stress-strain-strength behavior of the soil as established from the triaxial test and the effective stress condition to evaluate the mobilized soil behavior. The strain wedge model assumes that the deflection of a pile under lateral load is due solely to the deformation of the soil within the passive wedge,

13

plane stress change conditions exist within the wedge, and soil strain is constant with depth in the wedge. The strain wedge model was extended to assess the lateral response of an isolated pile in saturated sands as liquefaction develops in response to dynamic loading such as that generated during earthquake shaking (Ashour and Norris, 2003).

2.2.1.6 p-y model

The *p-y* method is a widely used method of design of laterally loaded piles that has been suggested for over 40 years (McClelland and Focht, 1958 and Reese and Matlock, 1956). The development of the method was possible in the 1950s due to two factors. The first factor is the performance of full scale tests sponsored by the offshore industry and the remote-reading strain gauge for use in obtaining soil-response (*p-y*) curves from these full scale tests. The second factor is the existence of the digital computers for solving the problem of the nonlinear fourth order differential equation for the beam column.

The non-linear *p-y* models are based on full scale tests performed for many kinds of soils. Basically the most important attribute of the *p-y* method is the ability to define the lateral load-deflection relationship between the foundation element and the soil. This relationship is expressed as *p-y* curves, where *p* is the lateral soil resistance per unit length of the foundation and *y* is the lateral deflection (Figure 2.1).

(a) After Installation and before lateral load is applied

(b) After lateral load is applied
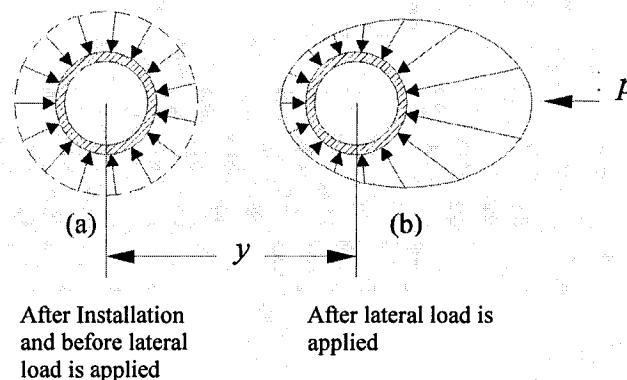
Figure 2.1 A cross-section view showing the deflection *y* and soil resistance *p*

14

The *p-y* method considers the pile structure as an elastic beam supported by a series of nonlinear, discrete uncoupled springs (Winkler approach). Figure 2.2 demonstrates the model proposed for a pile under lateral loading where the soil around the pile is replaced by a set of mechanisms that merely indicate that the soil resistance *p* is a nonlinear function of a pile deflection *y*. As seen in the figure, the *p-y* curves are fully variable with respect to distance *x* along the pile and pile deflection *y*.
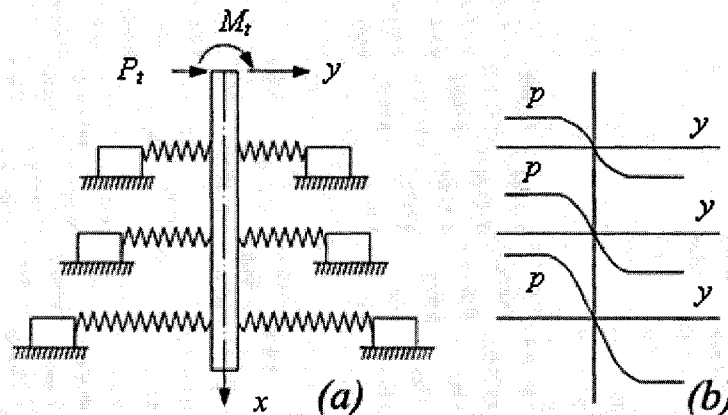
Figure 2.2 The model for a pile under lateral load with *p-y* curves (Reese and Van Impe, 2001)

The most serious criticism directed against the *p-y* method of analysis is that the soil is not treated as a continuum. Reese and Van Impe (2001) pointed out, as a reasonable response to the valid criticism of the method, that *p-y* curves are based for the most part on results of full-scale experiments in which the continuum effect was explicitly satisfied.

Besides the advantage of the *p-y* method of being based on full scale tests;(1) it employs commonly used soil strength parameters to simulate the *p-y* relationship;(2) it is capable to consider many variables as variations of the load-deflection curve with depth, variations in the foundation stiffness, *EI,* with depth, any defined head constraint condition, including free, restrained, pure moment; (3) it allows to take in account the complex relationship developed between the deflection and the soil resistance; (4) it showed good to excellent agreement with experimental results as pointed out by Reese and Van Impe (2001). Therefore, the *p-y* method is used in the current research.

15

2.2.2 Experimental and numerical studies of single laterally loaded piles

New methods of analysis are being applied in the research field of laterally loaded piles in an attempt to apply modifications to the *p-y* curves to cover more cases and to introduce several factors that influence their behavior. Some of the experimental and numerical studies conducted on laterally loaded single piles in the last decade are presented below.

Gabr et al. (1994) developed a model for the construction of static *p-y* curves in clay deposits based on dilatometer test data. They presented strength modification values as a function of the over consolidation ratio (OCR). The influence of close-ended pile installation on the soil properties around the pile was accounted for. A procedure for the construction of *p-y* curves using a hyperbolic model was proposed. Predictions of the pile-soil response using the proposed model were conducted and results indicated reasonable agreement between predicted and measured field behavior.

Long and Vanneste (1994) studied the effects of repetitive lateral loads on deflection of two drilled piers in Tampa Bay. The results showed that deflections were significantly greater than predicted by a *p-y* procedure commonly used in practice. In addition; they developed two methods for predicting the effects of repetitive lateral loads using results of 34 cyclic lateral load tests to quantify model parameters important to the behavior of piles subjected to repetitive lateral loading. The two methods modeled the cyclic lateral load behavior of a pile by degrading soil resistance as a function of number of cycles of load, method of pile installation, soil density, and character and cyclic load. The two methods provide a simple means for estimating effects of cyclic lateral load.

Rajashree and Sundaravadivelu (1996) developed a nonlinear hyperbolic model for static load condition based on the undrained shear strength and modulus of subgrade reaction. They adopted an iterative procedure to perform a nonlinear finite element analysis and the effect of static lateral load and deflection was studied. Based on the lateral deflection at the end of the first circle (static load), the degradation factor is assumed and the *p-y*

16

curve is modified. The cyclic load analysis was carried out using the static analysis program idealizing the soil by modified p-y curve, which considers the effect of the number of cycles and magnitude of cyclic lateral load. The results of the proposed analytical model compared well with published experimental results on piles subjected to one-way cyclic loading for different magnitudes of cyclic loading and number of cycles.

El Naggar and Novak (1996) studied the dynamic lateral pile nonlinear response with the aid of full scale field tests on single piles that were conducted at the University of Houston. Piles were loaded with a static cyclic load and a dynamic load. Their study showed that single pile stiffness and damping parameters, as well as interaction between the piles, were greatly affected by the level of the loading. In addition they pointed out that the effect of nonlinearity is that it reduces single pile stiffness as well as damping.

Prakash and Kumar (1996) presented a method developed to predict the load-displacement relationship for single piles subjected to lateral load, embedded in sands, considering soil nonlinearity using subgrade reaction. Their study presented the first systematic study to develop lateral load-deflection curves using modulus degradation with strain. Based on the analysis of 14 full scale lateral pile load tests, an empirical equation of modulus degradation with strain was proposed. The computed load-deflection relationships based on this method were compared with the observed ones and with those based on p-y analysis. The authors stated that the method demonstrates considerable promise over the p-y solutions and predicts upper and lower bound load deflection curves, which can be valuable guides in making informed engineering decisions.

Hsiung and Chen (1997) presented another simplified method for the analysis and design of long piles under lateral load in uniform clays. The method is based on the concept of the coefficient of subgrade reaction with consideration of the soil properties being extended to include elastoplastic behavior. Under the lateral load the maximum deflection and moments were evaluated using the finite element method. Using this simplified method, the solution of maximum deflections and moments of laterally loaded piles can be estimated quickly and easily either directly from figures, or using a hand calculator.

17

Guo and Lee (2001) developed a load transfer approach to simulate the response of laterally loaded single piles embedded in a homogeneous medium, by introducing a rational stress field. Generalized solutions for a single pile and the surrounding soil under various pile head and base conditions were established and presented in compact forms. With the solutions, a load transfer factor, correlating the displacement of the pile and the soil, was estimated and expressed as a simple equation. Expressions were developed for the modulus of subgrade reaction for Winkler model as a unique function of the load transfer factor. Critical pile length, maximum bending moment, and the depth at which the maximum moment occurs can be estimated by simple expressions. The method gave satisfactory results when compared with available, more rigorous numerical approaches.

Kim et al. (2004) described the results of a model testing of piles embedded in Nak-Dong River sand, located in South Korea under monotonic lateral loadings. The lateral resistance of piles, the effect of the installation method, and the pile head restrained condition were studied. The study led to recommendation of p-y curves for laterally loaded piles. Modification factors were developed to allow both a different pile installation method and different pile head restrained conditions by comparison to existing model load tests. The study revealed that the proposed p-y curves show significant differences in shapes and magnitudes when compared with existing p-y curve models. The accuracy of the proposed p-y curve model, considering the effect of installation method and pile head restrained condition, is reasonable as shown by comparing measured and predicted lateral behavior of the pile.

Shen and The (2004) presented a variational solution and its spreadsheet calculation procedure for the analysis of laterally loaded piles in a soil with stiffness increasing with depth. Solutions can be used simply with resource only to spreadsheet calculation to solve the displacement and bending moment of laterally loaded piles. The proposed method can be easily applied in practice as an alternative approach to analyze the response of laterally loaded piles.

18

2.3 ANALYSIS OF LATERALLY LOADED PILE GROUPS

The previous section was directed primarily at single or isolated piles under lateral loading. However, most piles are installed in groups. The response of pile group to lateral loading is discussed in this section. A pile group is a system made up of two or more piles connected with each other at the end with a pile cap. A pile group may contain battered piles and may be subjected to simultaneous axial load, lateral load, moment, and possibly, torsional load. A variety of methods of analysis exists to analyze the pile group system.

2.3.1 Early theories for response of pile groups

Analysis of pile groups first considered only the axial resistance of the pile group. A simple static method of analysis was first used to analyze pile groups that can resist axial loads. This method assumed that both the structure and the pile are rigid, ignoring the effect of the soil. This method can be employed either in an analytical or a graphical way. A graphical solution was presented by Culman in 1866 (Terzaghi, 1956). A force polygon was used to analyze the equilibrium state of the resultant external load and the axial reaction of each pile in the group. In 1930, Brennecke and Lohmeyer (Terzaghi, 1956) presented a supplemental method to this graphical solution. In 1917, Wetergaaard (Karol, 1960) first took into consideration the elastic displacement of pile tops. However, axial loading only was still considered. Westergaard assumed linearly elastic displacement of pile heads under a compressive load and developed a method to find the center of rotation of a pile cap. With the center of rotation known, the displacements and forces in each pile could be analyzed accordingly.

Later, lateral resistance of pile groups started to be considered. Hrennikoff (1950) presented a comprehensive structural treatment for the two-dimensional case where axial, transverse, and rotational resistance of piles on the cap were considered. The load-displacement relationship of the pile head was assumed to be linearly elastic and all piles were assumed to have the same load-displacement relationship. The laterally loaded pile

19

was regarded as an elastic beam on an elastic foundation with uniform stiffness. The method consisted of obtaining influence coefficients for cap displacements by summing the influence coefficients of individual piles in terms of spring constants which represent the pile-head reactions onto the pile cap. The significance of this method is that it presented the potential for the analytical treatment of the soil-pile interaction systems. Almost all the subsequent work followed the approach taken by Hrennikoff (1950).

Asplund (1956) formulated the matrix method for both two-dimensional and three-dimensional cases. The stiffness matrix of the pile group was calculated and an elastic center method was employed to treat laterally loaded piles. The importance of the pile arrangement for economical reason was noted. In this method, laterally loaded piles were merely regarded as elastic beams on an elastic bed with uniform spring constant.

Francis (1964) computed the two-dimensional case using the influence-coefficient method. The lateral resistance of the soil was taken as uniform or increasing in proportion to depth. Aschenbrenner (1967) later presented the three-dimensional case using the influence-coefficient method. The method was restricted to pin-connected piles. This analysis was an extension to Hrennikoff's method to the three-dimensional case.

Saul (1968) gave the most general formulation of the matrix method for a three dimensional foundation with rigidly connected piles. The cantilever method was employed to describe the behavior of laterally loaded pile. Reese and O'Neill (1967) developed the theory for the general analysis of a three-dimensional group of piles using the matrix formulations. Their theory was an extension of the theory of Hrennikoff, in which springs are used to represent the piles.

Reese and Matlock (1960 and 1966) and Reese et al. (1970) presented a method for coupling the analysis of the grouped-pile foundation with the analysis of laterally loaded piles by the finite difference method. Their method presumed the use of a digital computer. The formulation of equations of the movement of the pile cap was done by the influence method, similar to Hrennikoff's method.

20

2.3.2 Pile-soil-pile interaction

Pile Groups can be classified into two categories (O'Neill, 1983; Ooi and Duncan,1994): (1) groups of widely spaced piles, (2) groups of closely spaced piles. In the first category, the deflection of one pile in the group does not affect the other piles, because there is enough space between the pile members, so that piles interact only through the pile cap. These groups of widely spaced piles can be analyzed by distributing the lateral loads equally among the piles and considering the behavior of any one pile in isolation. In the second category, where the piles are closely spaced, the response of one pile affects the nearby piles by causing deflection of the soil between them.

In closely spaced piles, the deflection of any pile in a group causes movement of the surrounding soil and piles. This leads to larger deflection for the pile group than for single piles subjected to the same load per pile. This behavioral mechanism is called "pile-soil-pile interaction". In addition, the maximum bending moment in the group is larger than that for a single pile, because the soil allows the group to deflect more for the same load per pile, thus the soil behaves as if it was softer.

Reliable methods of analyzing closely spaced pile groups should account for pile-soil-pile interaction. Methods accounting for pile-soil-pile interaction in the behavior of pile groups include the following:

1. Continuum methods
2. Modified unit load transfer method
3. Winkler interaction model, empirical stiffness model, hybrid model
4. Group reduction method and group amplification method
5. Single beam analogy
6. Strain wedge model
7. *p*-multipliers method

2.3.2.1 Continuum methods

One of the continuum methods was presented by Poulos (1971). The method was developed to predict the pile-head response at the surface support. This method uses Mindlin's three dimensional elasticity equations to calculate the stresses and displacements due to horizontal point loads applied in an elastic half space (Reese and Van Impe, 2001). Soil was assumed to be elastic and the effect of the pile to other pile was taken into account by using influence factors based on the linear elastic theory. The variations of deflection and bending moment along the length of the piles were not taken into account. Limitations of the method are that piles have constant cross sections, the pile head restraint is fully-fixed (no rotation) or fully-free (no bending moment) and that there is a difficulty in determining the soil modulus between two piles.

The boundary element method (Banerjee and Davies, 1980) and the finite element method are also considered as continuum methods. Shibata et al. (1988) performed a three dimensional finite element analysis for group piles. This method can incorporate nonlinear soil behavior and account for the stiffness of the soil and piles separately and accurately, even if the piles are battered. Complexity is the main disadvantage of this method (Ooi and Duncan 1994).

2.3.2.2 Modified unit load transfer method

Bogard and Matlock (1983) developed the modified unit load transfer method for the analysis of pile groups. This method involves the development of *p-y* curves for a group of piles considered as a single pile. The modified single pile has a diameter that is equal to the width of the pile group. This width is equal to the width of the piles and the soils in between the piles. This procedure is used for circular pile embedded in soft clay with the assumption that the distribution of the lateral resistance is equal among the piles. This method is less suitable for non-circular groups of piles (Ooi and Duncan, 1994). Excellent agreement was obtained between their computed results and results from field experiments (Matlock et al. 1980 and Reese and VanImpe, 2001)

22

2.3.2.3 Winkler interaction model, empirical stiffness model, hybrid model

In the Winkler interaction model, a network of springs is used to represent the pile-soil-pile reaction (Nogami and Paulson, 1985 and Hariharan and Kumarasamy, 1982). This method only considers the pile-soil-pile interaction in horizontal direction.

The Empirical Stiffness model was developed by Dunnavant and O'Neill (1986). This method considers the effect of "shadowing" for estimating the load distribution among piles in the group. Shadowing is the effect whereby leading piles (row of piles further form the load) are more heavily loaded than trailing or shadowed piles. This method depends on the proper selection of the soil elastic modulus.

Focht and Koch (1973) proposed the hybrid model that combined Poulos' (1971) elastic continuum model and nonlinear p-y analysis. The procedure is based on the concept that the deflection of a group of piles results from two components. The first is due to nonlinear soil behavior occurring close to the individual piles, and the second is due to pile-soil-pile interaction through the less highly stressed soil further from the piles. They recommended that the first component can be estimated using the nonlinear p-y analysis or the characteristic load method (Duncan et al. 1994) and that the second component can be estimated using Poulos' (1971) elastic interaction coefficients.

Their method (Focht and Koch, 1973) developed influence coefficients that are related to the geometry of the piles arrangements. By using this method, different values of stiffnesses can be used to represent the highly stressed soil near the piles and the less highly stresses soil further from the piles. Deflections and bending moments in pile groups can thus be obtained. Modifications of the hybrid model have been developed by O'Neill et al. (1977), O'Neill and Tsai (1984), and Horsnell et al. (1990).

2.3.2.4   Group reduction factor method and group amplification procedure

The group reduction factor method and group amplification method are based on single pile analysis and use a modified modulus or factor to account for group effect. These two methods are highly empirical because they depend on limited test results. But they provide an effective and simple way to calculate the pile group behaviors through the analysis of single piles.

Group reduction factor method

In the group reduction factor method, the lateral load resistance of the pile group is determined based on the single pile analysis but modified according to the pile distance. Based on the model tests of pile groups in sands by Prakash (1962), Davisson (1970) suggested that the piles would work independently, i.e. no pile-soil-pile interaction, if the pile distances are more than eight diameters of piles. Davisson (1970) also proposed that the subgrade reactions are equal to 75% of those of single pile if the distance between piles were three pile diameters. For the piles, with spacing between three and eight diameters, the reduction factor for the subgrade modulus can be obtained by linear interpolation (Davisson, 1970).

The group reduction factor proposed by Davisson (1970) for analysis of pile groups in granular soils has been widely used by practicing engineers. In the proposed method, recommendations for the group reduction factor, G_c, were made. Prakash and Prakash (1989) studies showed that recommendations by Davison(1970) appear to be somewhat conservative. Arsoy and Prakash (2001) performed 14-full scale tests on piles in sand and analyzed them to re-evaluate the group reduction factor, G_c. In this study it was shown that the group reduction factor, G_c, was a function of pile spacing, displacement and relative density. In addition, they concluded that the group action disappears at 6-diameter pile spacing for 2×2 groups and 7-diameter pile spacing for groups having six piles or less in the direction of loading.

24

Group amplification procedure

Ooi and Duncan (1994) presented the group amplification procedure (GAP) which is based on the original Focht and Koch (1973) procedure. The deflections and bending moments of pile groups will be greater than those of single piles, so that this procedure tried to determine amplification factors for deflection, C_y and amplification factor for moments C_m, that formulated as:

$$y_g = C_y y_s \tag{2.1}$$

$$M_{g(max)} = C_m M_{s(max)} \tag{2.2}$$

where C_y = deflection amplification factor

$\quad\quad C_m$ = moment amplification factor

$\quad\quad y_g$ = group deflection

$\quad\quad y_s$ = single pile deflection under the same load

$\quad\quad M_{g(max)}$ = maximum moment in a pile in the group

$\quad\quad M_{s(max)}$ = maximum moment in a single pile under the same load

The values of C_y and C_m are greater than or equal 1.0. They depend on the soil type, diameter of single pile, spacing of piles, passive earth pressure coefficient, angle of internal friction for sand and undrained shear strength for clay. The GAP has the following limitations: (1) it can be used for a rectangular (not a circular) group with uniform or non uniform spacing, (2) it can be applied for vertical piles not battered ones, (3) it cannot determine the distribution of load, (4) the arrangement of piles in a group is not taken into account, (5) it is applied for long pile embedded in a uniform, homogenous soil. It has been found that there is good agreement between the results of this method and field load test results (Ooi and Duncan, 1994).

25

2.3.2.5 Single beam analogy

Konagai et al. (2003) proposed a single beam analogy for describing soil-pile group interaction. In their method, piles closely grouped together beneath a superstructure are viewed as a single equivalent upright beam whose stiffness matrix determines the active pile length, L_a (where L_a is the length below which the pile deflections become negligible). The value of L_a is an important parameter that governs the overall behavior of rigidly capped pile group. Their idea was verified for different cases of pile spacing. It was also extended to nonlinear behavior of soils surrounding grouped piles.

2.3.2.6 Strain wedge model

The strain wedge (SW) model for pile groups was proposed by Ashour et al. (2004). The pile group analysis was based on the concepts and assumptions of the strain wedge model analysis of isolated pile presented by Ashour et al. (1998a, b) and Ashour and Norris (2000). The model presented had the capability of assessing the response of a laterally loaded pile group. The SW model characterized the interaction among the piles in the group based on the envisioned three-dimensional interaction of the associated developing passive wedges. This allowed the calculation of the associated variation in modulus of subgrade reaction for each pile in the group. Thereafter, each pile in the group was analyzed individually by beam on elastic foundation analysis procedure. This approach allowed the calculation of the amount of interaction among the piles in the group according to soil and pile properties and the level of loading. The approach presented showed the capability of analyzing the behavior of a pile group in layered and uniform soil (sand and /or clay).

2.3.2.7 The p-multipliers method

The development of the computer technology made it possible to use different computer techniques to solve several engineering problems such as the finite difference and the finite element techniques. The most commonly used method for analyzing the lateral

response of piles uses these computer techniques to solve beam bending equation, in which the pile is represented as a beam supported laterally by the soil, which is modeled using nonlinear load versus deflection (p-y) curves. The p-y curve method used to analyze single piles has been explained briefly in the previous section.

For pile groups, measurements of displacements and stresses in full-scale and model pile groups indicated that piles in a group carry unequal lateral loads, depending on their location within the group and the spacing between them. This phenomenon occurs due to soil-pile-soil-interaction or shadowing. Shadowing is the term used to describe the overlap of zones of resistance, and the consequential reduction of lateral soil resistance. This fact indicates that the p-y curves of the soil should be modified when it is used for the analysis of the piles in a group. Piles in different rows shares different fraction of load applied to the group. Thus, to incorporate group effect the soil resistance values, p, in a family series of p-y curves for a given pile or a pile in a row is reduced by a constant factor, called p-multiplier.

Brown et al. (1988) were the first to propose the p-multiplier concept. The p-y curves of single pile are modified to account for the influence of the interaction between the different piles in the group. As shown in Figure 2.3, the p-multiplier, f_m, is the reduction factor of soil resistance p for the same deflection of y. The p-y curve is compressed in the direction of p, so that the soil resistance p of the piles-in the group will be smaller than the soil resistance of single piles. Because these p-multipliers are determined from load test results, the multipliers include both the elastic effects and shadowing effects that occur when closely spaced piles are loaded laterally.

The values of p-multiplier proposed by Brown e al. (1988) were based on the results of an isolated pile embedded in dense sand subjected to cyclic loading and full-scale test for pile group. Brown and Shie (1991) also presented the p-multipliers from the results of three dimensional finite element analysis. Cox et al. (1984), Brown and Reese (1985), Morrison and Reese (1986), McVay et al. (1995), Ruesta and Townsend (1997) , McVay

27

et al. (1998) and Rollins et al. (1998) suggested different values for the p-multiplier, f_m, based on the centrifuge or full scale tests in different type of soils.
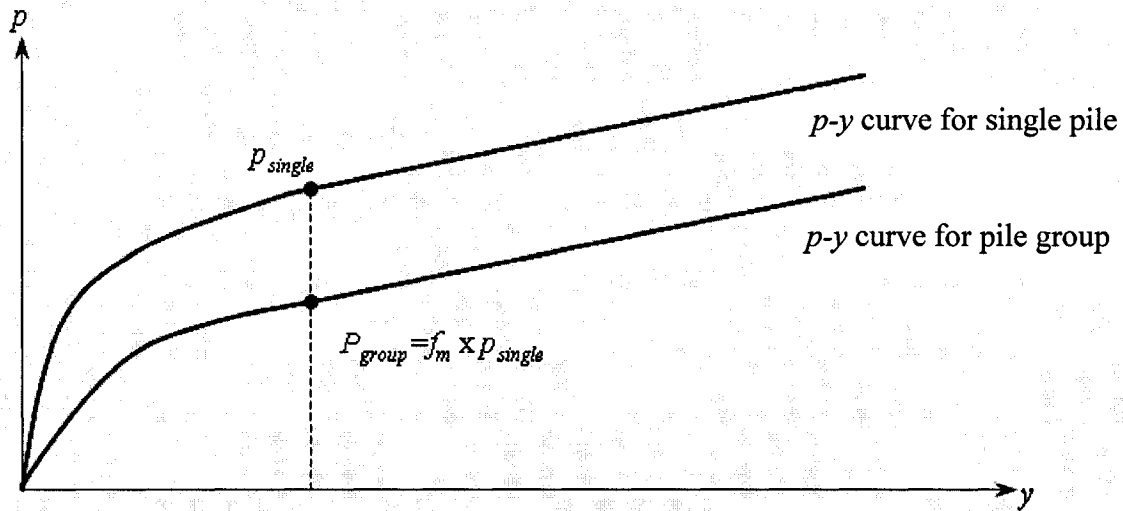
Figure 2.3 The concept of p-multiplier (f_m) (Brown et al., 1988)

Mostafa and El Naggar (2002) considered the concept of the p-multiplier for the dynamic loading case. The dynamic p-multipliers were found to vary with the spacing between piles, soil type, peak amplitude of loading, and the angle between the line connecting any two piles and the direction of loading. The study indicated the effect of pile material and geometry, pile installation method, and pile head conditions on the p-multipliers. Their calculated p-multipliers compared well with p-multipliers back-calculated from full scale field tests.

By combining the research work that has been done before, Mokwa and Duncan (2001b) presented design charts for estimating p-multipliers, f_m, for all kinds of soil as function of pile group arrangement and pile spacing. They collected and reviewed over 350 journal articles and other publications pertaining to lateral resistance, testing, and analysis of pile caps, piles, and pile groups. The results from theses studies were assimilated into tables and charts, from which the trends and similarities can be observed.

28

Since p-multipliers suggested by Mokwa and Duncan (2001b) are based on the research of many geotechnical engineers and are treated as state-of-the-art values, they will be employed in this research. In addition, the proposed p-multipliers can be used for any kind of soil, thus they are suitable since the soil studied in the current research is non-homogeneous consisting of soft clay and sand. Their method is introduced in detail in Chapter 5.

2.3.3 Other factors affecting group behavior

2.3.3.1 Effect of Pile Cap

Additional restraint to the group of piles can be provided through the pile cap that remains in contact with the ground. Settlement or scour of the soil around the piles, however, may reduce or eliminate the cap-soil contact causing a reduction in the lateral restraint provided by the cap. Therefore, the resistance of the pile cap is usually neglected. However, pile caps are usually stiff in bending and provide effective rotational restraint at the tops of the piles. This rotational restraint is an extremely important factor in the behavior of pile groups since a single fixed head pile deflects only about one-fourth as much as a free head pile subjected to the same load (Ooi and Duncan, 1994).

Mokwa and Duncan (2001a) reported that only four publications were found that described tests performed to investigate the lateral-load resistance of pile caps (Beatty 1970; Kim and Singh 1974; Rollins et al. 1997; Zafir and Vanderpool 1998). In most of the tests, the cap resistance was found to be as large as the lateral resistance provided by the piles themselves. However, the test results did not provide sufficient information for developing a method for including cap resistance in design calculations.

Accordingly, Mokwa and Duncan (2001a) conducted thirty-one field load tests to evaluate the lateral-load resistance of pile caps by comparing the response of pile groups with caps fully embedded and with soil removed from around the caps. The results of the tests showed that pile caps provide significant resistance to lateral load; the pile caps

29

embedded in the natural soil at the test site provided approximately 50% of the overall lateral resistance of the pile groups to lateral loads. They concluded that neglecting this resistance can lead to excessively conservative estimates of lateral-load capacities of pile groups. They showed that the lateral resistance increases as the stiffness and strength of soil around the cap increases and by increasing the thickness of the cap or the depth of embedment.

2.3.3.2 Effect of Batter

Awshika and Reese (1971) studied the effect of batter on the behavior of laterally loaded piles. The lateral soil resistance curves of a vertical pile were modified by a constant to account for the effect of pile inclination. The values of that constant were deduced from model tests in sand and also from full-scale tests that are reported in the literature by Kubo, 1965. The modifier constant is given as a function of the batter angle (Reese and Van Impe, 2001).

Other studies on batter piles were performed by Rajashree and Sitharam, (1999 and 2001), Veeresh (1996), Meyerhof and Ranjan (1973) and Poulos and Madhav (1971). However, in the current study only vertical piles will be considered.

2.3.3.3 Effect of pile installation on pile group behavior

O'Neill and Gazioglu (1984) performed experimental studies to investigate the installation effect on performance of group of piles. The test took place on a flat coastal plain of Chaiyi, Taiwan. They have tested group of piles consisting of bored piles and group of driven piles. The classification and properties of soil were experimentally found through drilling bores. They have identified experimentally that p-multipliers differ in value in driven piles from that of bored piles. The difference in p-multipliers reflected the differing effect of pile installation on the density and stress state in the soil within the pile group. No numerical values for correction were suggested by the researchers in the paper.

30

Haung et al. (2001) studied the effect of construction on laterally loaded pile groups. They performed full-scale lateral load tests on groups of bored and a group of driven precast piles. These tests were part of a research project for the proposed high-speed rail system in Taiwan. The effect of construction was obtained by performing standard penetration tests, cone penetration tests and Marchetti dilatometer tests (DMT) before and after pile installation. Numerical analyses of the laterally loaded piles were conducted using p-y curves derived from preconstruction and post construction DMT and by applying the concept of p-multipliers. They showed, through comparison of preconstruction and post construction, that the installation of bored piles softened the surrounding soil, while the driven piles caused a densifying effect. The construction effects were limited to the top 15 m from ground surface, where soil conditions have greatest effect on the behavior of laterally loaded piles.

O'Neill and Haung (2003) compared the behavior of bored and driven piles in cohesionless soil. The comparison was performed on two piles groups. The results of the study showed that the effect of installation was found to reduce the soil stiffness within the bored pile group, making the soil less efficient in resisting lateral pile movements than in the driven pile group. However, structurally, the bored piles were more resistant to flexural loading. The net effect was that the system of bored piles was stiffer than the system of driven displacement piles. Their study showed that the p-multipliers for the bored pile group were, on average, lower than those for the driven pile groups.

2.3.4 Experimental and numerical studies of laterally loaded pile groups

Some of the experimental studies and full-scale tests performed for groups of laterally loaded piles in the previous years are presented below.

Gandhi and Selvam (1997) studied the behavior of a pile group under lateral load through laboratory experiments on aluminum pipe piles. Piles were driven in medium to fine sand in different configurations and were subjected to lateral load under fixed head conditions. The results of analysis of pile groups with various spacings were presented in a non-

31

dimensional form and a method for the prediction of field group behavior was illustrated. The results of their method were compared with field results from the literature which demonstrated favorable agreement with the actual field results. In addition, the behavior of a single driven pile was compared with that of a bored pile to quantify the effect of pile driving.

A static lateral load test on a full-scale pile group was performed by Rollins et al. (1998) to study pile-soil-pile interaction effects. The soil profile consisted of soft to medium-stiff clays and silts underlain by sand. A pile group 3×3 was installed at three-diameter spacing and instrumented with inclinometers and strain gages. A single pile test was conducted for comparison. The load test results showed that the pile group deflected over two times more than the single pile under the same average load. Maximum moments in the group piles were 50-100% higher than in the single pile. Trailing rows carried less than the leading row, and middle row piles carried the lowest loads. Design curves were presented to estimate p-multipliers over a range of pile spacings. Good agreement between the measured and computed pile group responses was obtained using the p-multiplier approach.

Patra and Pise (2001) performed experimental investigations on model pile groups with different configurations and with different embedment length to diameter and pile friction angles. Spacing between piles ranged from three to six pile diameter. Piles were embedded in dry Ennore sand obtain from Chennai, India and were subjected to lateral loads. The load-displacement response and the ultimate resistance, and group efficiency with spacing and number of piles in a group were quantitatively and qualitatively investigated. The authors proposed analytical methods to predict the ultimate lateral capacity of single pile and pile groups that accounted for pile friction angle, embedment length-to-diameter ratio, the spacing of piles in a group, pile group configuration, and soil properties. By comparison with the experimental results of the writers and other researchers, it was shown that these methods were capable of predicting the lateral capacity of groups reasonably well.

32

Ng et al. (2001) presented results of full-scale lateral load tests of one single pile and pile groups in Hong Kong. The test piles were 1.5 m in diameter and approximately 30 m long. They were embedded in superficial deposits and decomposed rocks. The large-diameter bored pile groups tested had different configurations (2×2 and 3×3) and different pile spacings (three-diameter and six-diameter spacing). The nonlinear response of laterally loaded large-diameter bored pile groups was investigated. The design parameters for large-diameter bored piles associated with p-y method were studied using a three dimensional finite element program, FLPIER. Predictions using soil parameters based on published correlations and back analysis of the single-pile load test were compared. It was found that a simple hyperbolic representation of load-deflection curves provided an objective means to determine ultimate lateral load capacity.

McVay et al. (1998) performed centrifuge testing of large laterally loaded pile groups in sand. They developed an apparatus to load large pile groups (3×3 to 7×3) founded in sand in the centrifuge laterally. The instrumentation allowed the determination of both bending moments and shear forces at the head of each pile. The tests were conducted in both loose and medium dense sands. Single pile tests were also completed for comparison purposes. The pile group interaction effects were investigated based on the test results. The results emphasized the validity of the p-y multiplier concept. The tests showed that the p-multipliers are independent of soil density and only a function of the pile group geometry. In addition, they were found to be only a function of row position for that study where the pile spacing was fixed at three diameter spacing.

Zhang et al. (1999) investigated numerically, using the finite-element code FLPIER, the lateral response of the centrifuge pile tests performed by McVay et al. (1998). It was found that the numerical code FLPIER did an excellent job of predicting the response of both the single piles and the pile groups. The predicted lateral load versus lateral deflection of the group, the shears and bending moments developed in the individual piles, and the distributions of the lateral loads in each pile row were all in good agreement with the measured results.

Illyas et al. (2004) proposed a centrifuge model study of laterally loaded pile groups in clay. A series of centrifuge model tests has been conducted in their research to examine the behavior of laterally loaded pile groups in normally consolidated and over consolidated kaolin clay. The pile groups have different symmetric pile configurations with a center-to-center spacing of three or five times the pile width. The piles were connected by a solid aluminum pile cap placed just above the ground level. The test results revealed the presence of the shadowing effect phenomenon and showed that it was most significant for the lead row piles and considerably less significant for subsequent rows of trailing piles. They also pointed out that the approach adopted by many researchers of taking the average performance of piles in the same row was found to be inappropriate for the middle rows of piles for large pile groups as the outer piles in the row carry significantly more load and experience considerably higher bending moment than those of the inner piles. They also compared their p-multiplier results with those of other researchers.

Rollins et al. (2005a) performed a lateral load test on a full-scale pile group with configuration a 3×3 at 3.3 pile diameter spacing. Piles were driven open ended into a profile consisting of loose to medium dense sand underlain by clay. The tests confirmed that trailing rows carried fewer loads than the leading row. In contrast to tests in clay, lateral resistance was also consistently lower for middle piles within each row. The p-multipliers were back calculated from the test results and were found to be consistent with results from previous centrifuge tests and full-scale tests where different installation methods were used. Based on centrifuge and full-scale tests in sands, design curves were presented to estimate p-multipliers over a range of pile spacings. In addition, the authors computed analytically the results for pile groups using the computer programs GROUP and SWM. Good agreement between measured and computed pile group response was obtained. However, the computer program SWM was able to match the measured group response without the use of p-multipliers which are needed in the computer program GROUP.

Rollins et al. (2005b) also performed a lateral load test on a full-scale pile group with a 3×3 configuration at 3.3 pile diameter spacing but installed in liquefied sand. In contrast

34

to pre-liquefaction tests, group interaction effects were insignificant after liquefaction. The lateral resistance of each pile in the group was similar and about the same as that for the single pile test. They developed p–y curves based on the bending moment versus depth data. It was found that while the slope of p–y curves for nonliquefied sand typically decreases with continued deflection, the slope of the back calculated p–y curves for liquefied sand increases with deflection. This phenomenon was connected with load-induced dilation and a decrease in excess pore pressure locally around the pile. The p–y curves stiffened with depth and as the excess pore pressure ratio decreased. Equations accounting for the effect of variations in pile diameter were developed for p–y curves in liquefied sand.

CHAPTER 3

REVIEW OF SENSITIVITY ANALYSIS

3.1 HISTORY AND BASIC IDEA

3.1.1 History

Sensitivity analysis can be broadly defined as the variation that occurs in the system performance due to the variation in its parameters; i.e. evaluation of the gradients of response quantities with respect to design parameters. In its early stages, sensitivity analysis found its use in assessing the effect of varying parameters in mathematical models of control systems in the engineering field (Tomovic, 1963, Frank, 1978, Radanovic, 1966). In addition, interest in optimal control in the early 1960s, and automated structural optimization led to the use of gradient-based mathematical programming methods in which derivatives were used to find search directions toward optimum solutions. Examination of the optimization procedures indicated that the predominant contributor to the cost and time was the calculation of derivatives. As a consequence, emerging interest in sensitivity analysis has emphasized efficient computational procedures.

Later, the sensitivity methodology has been used in many other disciplines to assess the effects of parameter variations in the analytical models and create designs insensitive to parameter variation. Examples of these disciplines are physiology (Leonard, 1974), thermodynamics (Irwin and O'Brien, 1982), physical chemistry (Hwang et al., 1978), and aerodynamics (Dwyer and Peterson, 1980, Dwyer et al. 1976, and Bristow and Hawk, 1983).

In the 1980s, sensitivity analysis also emerged as a fruitful area of engineering research (Adelman and Haftka, 1986). This was due to the recognition of the variety of uses for the sensitivity derivatives. Researchers have developed and applied sensitivity analysis

36

for approximate analysis, analytical model improvement, and assessment of design trends, so that structural sensitivity analysis has become more than a utility for optimization but a versatile design tool in its own right.

3.1.2   Basic idea of structural sensitivity analysis

An abstract structural system in the form of a single block shown in Figure 3.1 is used to present the basic idea of structural design sensitivity analysis (Kleiber et al., 1997).The abstract system is simply a set of equations that defines the relationship between an input signal F (external loads, prescribed displacements, etc.) and an output signal z (displacements, stresses, etc.) The properties of the system are characterized by the set of parameters u, called the design parameters (or variables). This system may represent a continuous static or dynamic model or a discrete static or dynamic model depending on the way it is described.

Input signal F
(F constant)

Structural System with parameters u
(u varies)

Output Signal z
(Variation of z required)
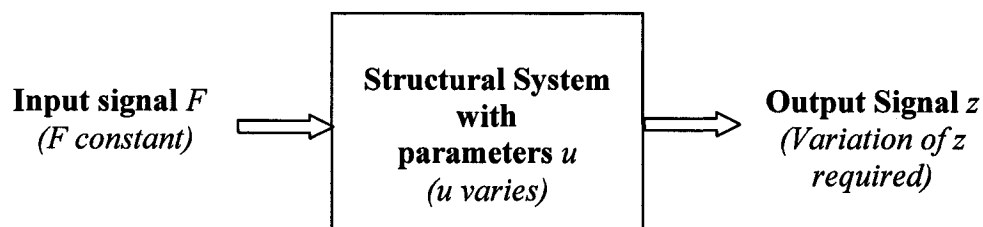
Figure 3.1 Basic idea of sensitivity analysis

The traditional mechanics of structures is concerned with the analysis of system behavior (described by z) subject to the 'load' F, assuming that the system itself (i.e. the values of design parameters u) is kept unchanged. However, structural sensitivity analysis is concerned with studying system behavior as a function of the design parameters, i.e. for a given vector F the parameters u are subject to variations and the resulting variations of z are sought.

Kleiber et al. (1997) summarized the definition of the structural design sensitivity analysis as follows:

37

"Structural design sensitivity is a measure of the change in structural response under the change in the system design parameters; by the structural response we mean here any quantity that may be used to characterize system behavior such as the displacement component, stress component or energy at a selected point in time-space, the time averaged displacement component, stress component or energy at a selected point in space, etc."

Variation in parameters may be due to an imaginary experiment performed by the analyst to determine the direction of changes in the system performance to be able to come up with an improved or optimized design. It can also be due to unavoidable imperfections in the structure geometry and material properties that have to be analyzed.

The natures of these design parameters can differ. One class of design parameters includes the member cross-sectional dimensions and material constants. Another class includes the shape variables. A third class is constituted by parameters entering problem formulation through support and loading conditions. Finally a fourth class involves parameters defining some initial strain fields associated with self-equilibrated stress fields within the structure (Kleiber et al., 1997).

In the present dissertation, the first class which includes the member cross-sectional dimensions and material constants will be the focus of our study. Shape design sensitivity analysis, in which the shape of the physical domain of the structural component must be treated as a design variable, will not be addressed. In the systems studied currently, a function that specifies the shape of a structural component is defined on a fixed physical domain; i.e. integrations are taken over a fixed domain. Shape sensitivity analysis has been investigated by many researchers such as Choi and his co-workers (Choi and Haug, 1983, Yoo et al., 1984, Choi, 1985 and Yang and Choi, 1985). For a thorough study of shape sensitivity analysis reference is made to Haug et al. (1986) for linear systems and Kleiber et al. (1997) for nonlinear systems.

38

3.2   IMPORTANCE OF SENSITIVITY ANALYSIS

The importance of sensitivity analysis can be summarized in the following two points:

1. Sensitivity analysis is concerned with the evaluation of derivatives (gradients). These sensitivity derivatives are important for solving fundamental problems of engineering such as system optimization problems.

2. The gradients are also important in their own right as they represent trend for the structural performance, which is important in understanding the system behavior.

Due to the above reasons, sensitivity analysis is considered as a versatile design tool. These two points are discussed in greater detail below.

3.2.1   Importance of sensitivity derivatives for use in fundamental engineering problems

Derivatives of functions describing system behavior with respect to parameters are necessary in the majority of algorithms used for fundamental problems of engineering. Examples of these problems are the system optimization, reliability assessment, system identification, analysis of the so-called stochastic finite element method and control problems. The computational costs required for such algorithms depend strongly on the efficiency of calculating the gradients. The importance of parameter sensitivity to some of the engineering problems is briefly discussed below (Kleiber et al., 1997).

3.2.1.1   Importance of sensitivity in system optimization

Any formulation for the optimum selection of parameters requires proper identification of:

i)   design variables (parameters) describing the system denoted by vector u

ii)   cost (objective) function to be optimized, denoted by $f(u)$

iii)   constraints assuring safe system performance ; divided into a number of equality constraints denoted by $g_c(u) = 0$, c=1,2,3, ... C_e and a number of inequality constraints denoted by $g_c(u) \leq 0$, c= C_e+1, ..,C.

39

A general optimization problem can be defined as follows:

Find a design variable vector u that minimizes the cost function $f(u)$ with u satisfying the constraints $g_c(u) = 0$, $c=1,2,3, \ldots C_e$ and $g_c(u) \leq 0$, $c= C_e+1, ..,C$.

There exist many computational algorithms that can be used for solving the optimization problem. Most of these algorithms involve the computation of the following vectors: $\partial g_c/\partial u$ and $\partial f/\partial u$.

It can be shown that these gradients of functions that are generally implicitly as well as explicitly dependent on design variables are the core of the numerical methods of optimization. In fact, the gradient computations constitute a major task in the overall optimization problems that efficient algorithms for handling sensitivity evaluation are the decisive factors in assessing any specific optimization strategy.

3.2.1.2 Importance of sensitivity in reliability-based system design

The reliability of structural system is defined in terms of a performance function (or failure function, or limit state function) $g(r)$ such that, by convention, $g \leq 0$ and $g > 0$ represent failure and safe regions for the system, respectively. The system has random parameters collected into the vector r therefore the limit state $g(r)$ is also expected to be random.

It can be shown that the formulation of the reliability problem can be reduced to that of the design optimization problem discussed in the previous section. The design variables u and the constraints function $g_c(u)$ of the latter problem correspond to the random variables r and the failure surface $g(r) = 0$ of the former problem.

Solving the optimization problem yields the best design according to a given cost function, while the reliability problem similarly yields the set of random parameters corresponding to the most likely system failure defined by the minimum distance from the random variable coordinates to the failure surface. Having efficient algorithms for

40

calculating gradients of functions defining the failure surface is crucial for effective reliability evaluation.

3.2.1.3 Importance of sensitivity in system identification and in the stochastic finite element method

A discrete system can be described by a set of equations in terms of a number of generalized coordinates given in the form of vector z and a number of parameters given in the form of vector u. The generalized coordinates z depend implicitly on the parameters u. The question in system identification is how all the parameters u should be fixed to obtain an 'optimal' model of the system. The way the derivatives $(\partial z / \partial u)$ are computed is most essential for the efficiency of any specific identification technique. Since ways to compute parameter derivatives of functions implicitly dependent on these parameters are the very essence of sensitivity theory, the identification procedures are again an area of high potential gains resulting from improved computational sensitivity techniques.

The stochastic finite element method is a computational technique for solving problems involving some random effects. The basic computational procedure of the stochastic finite element method reduces the problem to finding sensitivities of the displacement components with respect to random variables. Accordingly, the importance of sensitivity is again emphasized.

3.2.2 Importance of sensitivity derivatives in their own right

The question of parameter sensitivity particularly arises in the fields of engineering, where mathematical models are used for the purposes of analysis and synthesis. There is always a certain discrepancy between the actual system and its mathematical model. This is due to the following reasons (Frank, 1978):

1. a real system cannot be identified exactly because of the restricted accuracy of the measuring devices

41

2. a theoretical concept cannot be implemented exactly because of manufacturing tolerances.

3. the behavior of any real system changes with time in an often unpredictable way caused by environmental, material property, or operational influences.

4. Mathematical models are often simplified or idealized in order to simplify the mathematical problem or to make it solvable at all.

Thus, the sensitivity of a system to variations of its parameters is one of the basic aspects in the treatment of that system. Accordingly, the design derivatives are important in their own right. Their importance is emphasized in the following three points:

3.2.2.1 Importance in understanding system behavior

Any realistic large-scale engineering simulation has to be complemented by an extensive study on the sensitivity of the system response with respect to system parameters. This is important to broaden our understanding of the system behavior.

3.2.2.2 Importance as a versatile design tool

Design derivatives represent trends for the structural performance that are important to the designer in changing his/her design estimate. The value of this sensitivity information to the designer is perhaps even greater than simply response data with no trend information. In addition, the designer may use this information directly in interactive computer-aided design procedures.

In other words, the derivatives are quite useful from the designer's point of view since they represent what effect a design change will have on a response quantity. Specifically, if the derivative of a response quantity with respect to a certain design variable is positive, an increase in that design variable will increase the response quantity and if it is negative, an increase in the design variable will cause a decrease of the response quantity. Further, the order of magnitude of the various sensitivity coefficients will tell the

42

designer which design variables have significant effect on the response quantity and which have little effect (Haug and Arora,1978).

3.2.2.3 Importance in rehabilitation and detection of sensor location

The derivatives are also important for assessment of structural degradation. Thus they are important for use in the rehabilitation process of structures. This degradation may be due to unavoidable imperfections in the structure geometry and material properties that have to be analyzed.

In addition, locating the critical positions in the structures where certain parameters have the most effect will allow the engineer to place the sensors in the appropriate positions in the structure. Thus performing a parameter sensitivity analysis prior to placing any sensor is of great importance.

3.3 METHODS OF DESIGN SENSITIVITY ANALYSIS

As defined above, in structural sensitivity analysis, it is necessary to determine the rate of change of some response measure-such as stress or displacement at a point- with respect to a set of design parameters. Therefore, the core of sensitivity analysis is to evaluate the gradients (derivatives) of response quantities with respect to design variables. Only first-order design sensitivity (first derivatives) will be considered in the current study. Studies of second-order sensitivity were performed by many researchers (Haftka and Mroz, 1986, Haug, 1981, Haftka, 1982, Haug and Ehle, 1982, Haug et al., 1986, Dems and Mróz, 1985, Van Belle, 1982 and Jawed and Morris, 1984).

In general, there are two approaches to calculate the design derivatives. These approaches are:

1. The finite difference approach, which is the simplest method of sensitivity analysis.

43

2. The analytical approach, which can be divided into two methods to calculate the design derivatives. The first is the direct differentiation method and the second is the adjoint method.

3.3.1 Finite difference method

The traditional method of design sensitivity analysis is simply to change the design, reanalyze the structure, and compare the two calculated measures of structural response. This is simply the finite difference calculation of sensitivities based on successive perturbation of parameter values followed by reanalysis of the system. This approach is the easiest to implement but is often inefficient or may have accuracy problems. In addition, when the design variable is a parameter, this approximation can be obtained. If the deign variable is a function such as beam cross-section or variable plate thickness, however, this approach is not applicable (Haug and Rousselet, 1980).

For a nonlinear response problem, there are also two shortcomings of using this approach. First, there is an uncertainty in the choice of perturbation. An improper choice may cause truncation or condition errors in the computation. Second, when the number of design variables is large, there is an enormous increase in the number of nonlinear finite element analyses. The procedure can, therefore, be prohibitively expensive (Wu and Arora, 1987).

3.3.2 Analytical methods

The analytical methods of structural design sensitivity analysis can be applied using the discretized system approach or distributed parameter (continuum system) approach. These analytical methods can also be applied to linear or nonlinear systems. To present the basic idea of the analytical methods a linear discretized system is considered. Discussion and comparison between the different approaches and systems will be discussed in following sections.

44

In most problems of engineering design, the system being designed is required to behave according to some laws of physics. This behavior can be described analytically by a set of variables called state variables. Further, there is a second set of variables that describe the system, rather than the system behavior. These variables are called design variables since they are to be chosen by the designer and serve to assure the specifications for fabrication. The equations that determine the state of mechanical and structural systems generally depend on the design variables, so the two sets of variables are related.

For a structural design problem, consider the state (equilibrium) equation given in the form:

$$K(u)\, z = F(u) \tag{3.1}$$

where $K(u)$ is an (n×n) structural stiffness matrix, z is an (n×1) displacement (state) vector and $F(u)$ is an (n×1) load vector. The stiffness matrix and load vector are functions of the design variables given in an (m×1) vector denoted by u. It is clear from this equation that the solution z is design dependent in an implicit way; i.e. $z = z(u)$

Consider now a general function G that may represent any of the performance measures for a structure (or a constraint function), written in the form:

$$G = G(u, z(u)) \tag{3.2}$$

The dependence of this function on design arises in two ways. The first is the explicit design dependence of the function on u and the second is the implicit design dependence of G on u through the solution z of the state (equilibrium) equation.

The objective of the design sensitivity analysis is to determine the total dependence of such functions on design (i.e. to find dG/du). Then the following two questions should be asked: (1) given that the function G is differential in its arguments, is the total dependence of G on design differentiable? (2) if the solution z of the state equation is

differentiable with respect to design, how can the derivative of *G* with respect to design *u* be calculated?

To answer the first question, mathematical and technical aspects of existence of design derivatives should be considered. The basic calculus applying to sensitivity functions is the calculus of partial differentiation and calculus of variation. Basic design differentiability results for many structural problems have been proved by Haug et al. (1986). It is important to realize, however, that the delicate question of the existence of design derivatives should not be ignored. In our study, we will restrict our attention to classes of smooth functions and need not be concerned with the more general function spaces. For more mathematical details and studies for the differentiability of different fields with respect to design variables, reference is made to Haug and Rousselet (1980), Rousselet (1983) and Haug et al. (1986).

To answer the second question, the two analytical methods of design sensitivity are considered; the direct differentiation method and the adjoint variable method. Both methods start by differentiation of Eq. (3.2) using the chain rule of differentiation to obtain the total derivative of *G* with respect to design *u* as follows:

$$\frac{dG}{du} = \frac{\partial G}{\partial u} + \frac{\partial G}{\partial z}\frac{dz}{du}$$

(3.3)

in which *∂G /∂u and ∂G /∂z* are easy to compute since *G* is the explicitly given function of both its arguments *z* and *u*. The two analytical methods give two alternatives for the calculation of *dz/du*.

3.3.2.1 *Direct differentiation method (design space method)*

The direct analytical method is based on differentiating the equations that describe the system with respect to the desired parameters and the solution of these sensitivity

46

equations. This method is also denoted as the design space method (Arora and Haug, 1979).

We differentiate the state Eq. (3.1) and re-order the terms to obtain:

$$K\frac{dz}{du} = \frac{\partial F}{\partial u} - \frac{dK}{du}z = C \tag{3.4}$$

Accordingly, Eq. (3.4) may be numerically solved for dz/du and substituted into Eq. (3.3) to obtain the sensitivity of the function G. It is seen that the method is insensitive to the number of performance (response/constraint) functions G. However, the above calculation should be performed for each design parameter independent of the others. For this reason, the method is costly when the number of design variables is large.

3.3.2.2 Adjoint variable method (state space method)

Adjoint methods define an adjoint physical system whose solution permits rapid evaluation of the desired sensitivities. This method is also denoted as the state space method (Arora and Haug, 1979). The method starts by defining an (n × 1) vector of adjoint variables, λ, that satisfies the equation

$$K\lambda = \left(\frac{\partial G}{\partial z}\right)^T \tag{3.5}$$

Taking transpose of both sides:

$$\lambda^T K^T = \left(\frac{\partial G}{\partial z}\right) \tag{3.6}$$

Using the symmetry of the stiffness matrix ($K^T = K$) and substituting $\partial G/\partial z$ in Eq. (3.3) we obtain:

47

$$\frac{dG}{du} = \frac{\partial G}{\partial u} + \lambda^T K \frac{dz}{du}$$ (3.7)

Or using Eq. (3.4):

$$\frac{dG}{du} = \frac{\partial G}{\partial u} + \lambda^T \left(\frac{\partial F}{\partial u} - \frac{dK}{du} z \right) = \frac{\partial G}{\partial u} + \lambda^T C$$ (3.8)

Accordingly, Eq. (3.5) may be solved for the adjoint variable λ and substituted in Eq. (3.8) to obtain the sensitivity of G. It is seen that the solution of λ (Eq. 3.5) is insensitive to the number of design parameters. However, the above calculation should be performed for each performance function G. The method is therefore costly when the number of performance functions is large.

The adjoint method of sensitivity analysis will be used in obtaining sensitivities in the current study. Therefore, the adjoint method is treated in more detail in the following section.

3.4 ADJOINT METHOD OF SENSITIVITY ANALYSIS

The basic idea of the adjoint method of sensitivity analysis was introduced in the previous section for a linear discretized system. The discussion for this method will be extended in this section to include nonlinear and distributed parameter systems. In addition, different formulation techniques of the adjoint method are introduces for the calculation of sensitivity derivatives. The physical significance of the adjoint variable is discussed at the end of this section.

48

3.4.1 Adjoint method using a variational approach

A variational approach can be used to obtain similar results of design derivatives by the adjoint variable method as those obtained above (Section 3.3.2.2). This can be done in the frame work of the calculus of variation (Weinstock,1974, Gefland and Fomin, 1964, Akhiezer, 1962).

Arora and Haug (1979) followed a variational approach to derive the design derivative vector by the adjoint variable method. In this method, state variable vector z is first treated as an independent variable. An adjoint relationship is then introduced to express the effect of a variation in z in terms of the variation in design variables vector u. Hence, the method was also called a state space method.

A first variation of function $G(u, z)$, treating u and z as independent variables, is given as:

$$\delta G = \frac{\partial G(u,z)}{\partial u} \delta u + \frac{\partial G(u,z)}{\partial z} \delta z \qquad (3.9)$$

where δG is the first-order change in the function G, δu is a small change in u, and δz is the corresponding small change in z. In the adjoint variable (state space) method, the right hand side in Eq. (3.9) is expressed as a function of δu, such that the equation may be written as:

$$\delta G = \Lambda^T \delta u \qquad (3.10)$$

where Λ is the column vector of design derivatives, that is,

$$\Lambda = \frac{dG(u,z(u))}{du} \qquad (3.11)$$

49

In order to achieve the objective of eliminating the second term on the right hand side of Eq. (3.9), Eq. (3.1) is premultiplied by the transpose of an (n × 1) adjoint variable vector λ that is associated with the constraint G. Taking the first variation of the resulting equation, one obtains

$$\lambda^T K(u)\delta z = \lambda^T C \delta u \tag{3.12}$$

where the matrix C is given in Eq. (3.4) . Similar to Eq. (3.5) (Section (3.3.2.2)), the adjoint equation defines λ as the solution of

$$K\lambda = \left(\frac{\partial G}{\partial z}\right)^T \tag{3.13}$$

Accordingly, Eq.(3.12) becomes

$$\frac{\partial G(u,z)}{\partial z}\delta z = \lambda^T C \delta u \tag{3.14}$$

Substituting from Eq. (3.14) into Eq. (3.9) and comparing the result with Eq. (3.10), one obtains the following expression:

$$\Lambda = \frac{\partial G^T(u,z)}{\partial u} + C^T \lambda \tag{3.15}$$

where the adjoint variable vector λ is efficiently obtained from the adjoint Eq. (3.13) or (3.5), using the previously calculated factors of $K(u)$ in Eq. (3.1).

It is clear that the results given in Eq. (3.15) are the same as those given in Eq. (3.8). Thus, the adjoint method of sensitivity can be obtained by a variational approach (Eq. 3.15) as shown in this section or by a direct total derivative approach (Eq. 3.8) as shown in the previous section.

50

A special case of the adjoint variable (state space) method is the virtual load method mentioned in the literature (Arora and Haug, 1979). However it is only applicable if a special form of the constraint G is assumed. Whenever the virtual load method is applicable, it generates a sequence of operations for design derivative calculation that is identical to the one generated by the adjoint variable method.

3.4.2 Adjoint method for distributed parameter systems

In the distributed parameter approach, the state and design variables are functions (displacement field and material distribution) and the structural state equations are boundary-value problems of ordinary or partial differential equations. Thus displacement fields are used rather than nodal displacements. Instead of the vector of design parameters u and the state vector z one now must allow for a distributed design variable $u(x) = [u_1(x), u_2(x), ..., u_m(x)]^T$ and a state variable $z(x)$ where x is a space variable.

For distributed parameter systems, the performance measure is given in a form of functional rather than a function. For discrete systems, the functional takes the form of a scalar valued function G. Gelfand and Fomin (1964) defined a functional as follows: "by a functional, we mean a correspondence which assigns a definite (real) number to each function (or curve) belonging to some class. Thus, one might say that a functional is a kind of function, where the independent variable is itself a function."

For discretized systems, both the direct (matrix) and variational approaches are possible as indicated in the previous sections. However, in distributed parameter systems, only the variational approach is acceptable. Therefore, the variational, or energy-related, formulation of the given problem is needed. The state equations which are boundary-value problems can be reduced to the powerful variational formulation. This formulation provides the foundation for the rigorous and practical theory of finite element analysis (Cook et al., 2002, Bathe, 1996). The results of this formulation can be obtained from reducing the boundary value problem or, can be viewed as the principle of virtual work or may be obtained from the principle of minimum potential energy.

51

The variational formulation is obtained now as mentioned above for a bending of a beam as an example. The boundary-value of a clamped beam (Figure 3.2) with a normalized axial coordinate x, length l, subjected to a distributed lateral load $f(x)$ and with lateral displacement field z, is written formally as:

$$EIz'''' = f(x) \tag{3.16}$$

$$z(0) = z'(0) = z(l) = z'(l) = 0 \tag{3.17}$$

where the prime denotes the derivative with respect to x.

By multiplying both sides of Eq. (3.16) by an arbitrary function $\bar{z}(x)$ and integrating twice by parts then imposing the boundary conditions, we obtain the variational formulation (weak form of problem):
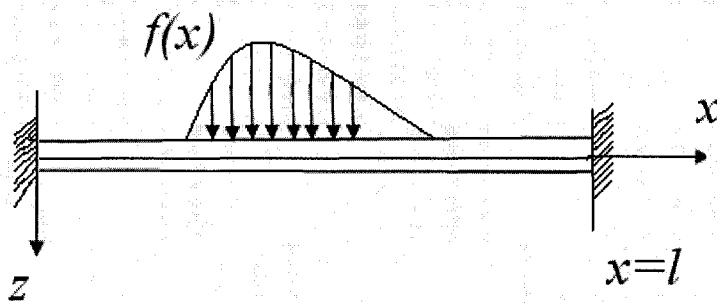
Figure 3.2 Clamped beam used as an example for the variational formulation

52

$$\int_0^l EIz''\bar{z}''dx = \int_0^l f\bar{z}dx \qquad \text{for all } z,\bar{z} \in Z \qquad (3.18)$$

where Z is the space of kinematically admissible displacements.

Define the energy bilinear form as:

$$a_u(z,\bar{z}) = \int_0^l EIz''\bar{z}''dx \qquad (3.19)$$

and define the load linear form as:

$$l_u(\bar{z}) = \int_0^l f\bar{z}dx \qquad (3.20)$$

Therefore, the variational formulation can be written as:

$$a_u(z,\bar{z}) = l_u(\bar{z}) \qquad \text{for all } \bar{z} \in Z \qquad (3.21)$$

where the subscripts u denotes dependence of energy bilinear and load linear forms on the design vector u.

Equation (3.18) or (3.21) can be written directly from the principle of virtual work by viewing $\bar{z}(x)$ as a virtual displacement. In addition, the same equation can be obtained from the minimum total potential energy characterization of beam bending. That is, the displacement $z(x)$ is to minimize the potential energy PE

$$PE = \int_0^l \left[\frac{1}{2} EI(z'')^2 - fz \right] dx \qquad (3.22)$$

53

Equating the first variation of *PE* to zero with the variation $\bar{z}(x)$ having two derivatives and satisfying the boundary conditions in Eq.(3.17), we obtain:

$$\delta PE = \int_0^l [EIz''\bar{z}'' - f\bar{z}]dx = 0 \qquad (3.23)$$

Equation (3.23) gives again the variational formulation in Eq. (3.21).

Differentiability of Energy bilinear forms and static solution

Basic design differentiability results for energy bilinear forms and the solution of the static structural equations were proved by Haug et al., 1986. Therefore,

$$\delta a_{\delta u} \equiv \frac{d}{d\tau}[a_{u+\tau\delta u}(\tilde{z},\bar{z})]\Big|_{\tau=0} = \frac{\partial}{\partial u}(a_u(\tilde{z},\bar{z}))\delta u \qquad (3.24)$$

exists, where $\tilde{z}$ denotes the state z with dependence on τ suppressed and $\bar{z}$ is independent of τ. The notation $\delta a_{\delta u}$ denotes the first variation of the calculus of variation with respect to explicit dependence of the energy bilinear form a_u on design u evaluated in the direction δu.

The load linear form is also differentiable with respect to design. That is,

$$\delta l_{\delta u} = \frac{d}{d\tau}[l_{u+\tau\delta u}(\bar{z})]\Big|_{\tau=0} = \frac{\partial}{\partial u}(l_u(\bar{z}))\delta u \qquad (3.25)$$

exists. The explicit inclusion of the argument δu in the energy bilinear and load linear forms is to emphasize dependence on design variation. In addition, the solution of the state equation (Eq. 3.21) is differentiable with respect to design. That is,

54

$$\delta z = \delta z(x;u,\delta u) \equiv \frac{d}{d\tau}z(x;u+\tau\delta u)\big|_{\tau=0} = \frac{dz}{du}\delta u \qquad (3.26)$$

exists and is the first variation of the solution of Eq. (3.21) at design u and in the direction δu of design change.

Using the chain rule of differentiation and using the definitions in Eqs. (3.24) and (3.26), one obtains:

$$\frac{d}{d\tau}[a_{u+\tau\delta u}(z(x;u+\tau\delta u),\bar{z})]\big|_{\tau=0} = \delta a_{\delta u}(z,\bar{z}) + a_u(\delta z,\bar{z}) \qquad (3.27)$$

Taking the total variation of both sides of Eq. (3.23), Eq. (3.27) is used to obtain:

$$a_u(\delta z,\bar{z}) = \delta l_{\delta u}(\bar{z}) - \delta a_{\delta u}(z,\bar{z}) \qquad (3.28)$$

Presuming that the state z is known as the solution of Eq. (3.21), Eq. (3.28) is a variational equation with the same energy bilinear form for the first variation δz.

Sensitivity analysis

The adjoint variable method for design sensitivity analysis presented by Haug et al. (1986) is followed below to obtain design sensitivity expressions of general functionals in terms of perturbations of design. However, the state variable $z(x)$ is taken as a function of one independent variable x (i.e. 1-D problem for simplicity). Consider now a measure of structural performance that may be written in the integral form as the functional G (defined over the space Ω):

$$G = \int_\Omega g(z,z',u)d\Omega \qquad (3.29)$$

where function g is continuously differentiable with respect to its arguments, z is the state (displacement) variable, z' is the gradient of z, $z' = \dfrac{\partial z}{\partial x}$, and u is the vector of design parameters, $u = \{u_1(x), u_2(x), ..., u_m(x)\}^T$.

Functionals of that form represent a wide variety of structural performance measures. For example, the volume of a structural element can be written with g depending on u, average stress over a subset of plane elastic solid can be written in terms of u and the gradient of z (defining stress), and the displacement at a point in a beam or plate can be written formally using the Dirac function times the displacement function in the integrand.

Taking the variation of the functional G gives

$$\delta G = \int_\Omega [\frac{\partial g}{\partial z}\delta z + \frac{\partial g}{\partial z'}\delta z' + \frac{\partial g}{\partial u}\delta u]d\Omega \tag{3.30}$$

the objective is to obtain an explicit expression for δG in terms of δu, which requires writing the first two terms under the integral on the right of Eq.(3.30) explicitly in terms of δu. Recall that the variations of the state fields (δz and $\delta z'$) depend implicitly on the design variations δu. The basic idea of the adjoint structure approach is to replace the implicit design variations of the state fields in Eq. (3.30) by the explicit design variations and the adjoint state fields.

For Eq. (3.30) to substitute the state fields' variations with the adjoint fields and design variables variations, an adjoint equation is introduced by replacing δz by a virtual displacement $\bar{\lambda}$ and equating terms involving $\bar{\lambda}$ in Eq. (3.30) to the energy bilinear form $a_u(\lambda, \bar{\lambda})$, yielding the adjoint equation for the adjoint variable λ

$$a_u(\lambda, \bar{\lambda}) = \int_\Omega [\frac{\partial g}{\partial z}\bar{\lambda} + \frac{\partial g}{\partial z'}\bar{\lambda}']d\Omega \qquad \text{for all } \bar{\lambda} \in Z \tag{3.31}$$

56

where a solution $\lambda \in Z$ is desired.

To take advantage of the adjoint equation, Eq.(3.31), may be evaluated at $\bar{\lambda} = \delta z$, since $\delta z \in Z$, to obtain

$$a_u(\lambda, \delta z) = \int_\Omega [\frac{\partial g}{\partial z} \delta z + \frac{\partial g}{\partial z'} \delta z'] d\Omega \qquad (3.32)$$

which is just the terms in Eq. (3.30) that it is desired to write explicitly in terms of δu. Similarly, the identity of Eq.(3.28) may be evaluated at $\bar{z} = \lambda$, since both are in Z, to obtain:

$$a_u(\delta z, \lambda) = \delta l_{\delta u}(\lambda) - \delta a_{\delta u}(z, \lambda) \qquad (3.33)$$

The energy bilinear form $a_u(.,.)$ is symmetric in its arguments, then the left sides of Eq. (3.32) and Eq. (3.33) are equal, yielding the desired result

$$\int_\Omega [\frac{\partial g}{\partial z} \delta z + \frac{\partial g}{\partial z'} \delta z'] d\Omega = \delta l_u(\lambda) - \delta a_{\delta u}(z, \lambda) \qquad (3.34)$$

where the right side is linear in δu and can be evaluated once the state z and adjoint variable λ are determined as the solutions of Eqs. (3.21) and (3.31), respectively. Substituting this result into Eq. (3.30) the explicit design sensitivity is obtained as:

$$\delta G = \int_\Omega \frac{\partial g}{\partial u} \delta u d\Omega + \delta l_u(\lambda) - \delta a_{\delta u}(z, \lambda) \qquad (3.35)$$

where the form of the last two terms on the right depend on the problem under investigation.

3.4.3 Adjoint method for nonlinear systems

Nonlinearities in structural systems can de due to large displacements, large strains, material behavior, and boundary conditions. Several theories were provided by researchers to treat these nonlinearities (Novizhilov, 1953, Eringen, 1962, Gadala et al., 1984, Bathe, 1996).

In the current study, the material nonlinearity is demonstrated in the p-y relationships of the soil-pile system. Equations of virtual work and stress-strain constitutive law are nonlinear. There are several methods for solving such a system of equations. The incremental/iterative procedure based on Newton methods is the most commonly used and effective procedure. It is assumed that the equilibrium is known at level t and it is desired at level $t + \Delta t$. The incremental form of the virtual work equation is written which is still nonlinear. The equation will then be linearized by assuming a linear increment of strain and a linear incremental stress-strain constitutive law. Since linear approximations are used, the equilibrium at $t + \Delta t$ will not be exactly satisfied. Therefore iterations within the load step are needed to satisfy the equilibrium exactly at $t + \Delta t$.

Similar to the linear case of the adjoint method, an adjoint system is introduced to obtain explicit design sensitivity expressions that relate variations in structural design (parameter variations) to variations of structural performance. The original (primary) system is a nonlinear system, however, a linear system is assumed for the adjoint one. The linearized equilibrium equation mentioned above is used to identify the adjoint system. Accordingly, the adjoint system is assumed to be linear with a linear stress-strain relation (constitutive law) and a linear adjoint strain field (Choi and Santos, 1987 and Cardosa and Arora, 1988).

58

3.4.4 Formulation techniques

There are a number of formulation techniques for adjoint sensitivity analysis. These are:

1. Formulations based on the Lagrange multiplier method (Belegundu, 1985, Belegundu and Arora 1985)

2. Formulations based on the virtual work principle

3. Formulations based on the stationary energy principle (Phelan et al.,1991)

In most cases, the various adjoint formulation techniques lead to identical sensitivity expressions under similar modeling assumptions. Thus, the choice of formulation method is to a large extent a matter of personal preference. These alternative sensitivity formulations are valuable as a collection, because they provide alternative mathematical and physical interpretations of the adjoint system. A brief discussion on these techniques is given below.

3.4.4.1 Formulations based on the Lagrange multiplier method

Belegundu (1985) developed a Lagrangian method to sensitivity analysis for structural, dynamic, distributed parameter, and shape optimal design problems. The method was based on forming the Lagrangian multiplier to insure satisfaction of the equilibrium equations, resulting in an expression for the sensitivity of the cost or constraint functional.

It was shown in this work that the adjoint variables referred to in the literature were simply the Lagrange multipliers and that the adjoint equations are the Euler-Lagrange equations. The method presented a unified and harmonious method for various categories of problems. As an example, the derivation of the formulation for structural systems and distributed parameter systems is given below.

59

In the finite element setting, consider a scalar valued function, $G(u,z)$ in which $u = $ a column vector of design parameters; and $z = $ a vector of nodal displacements. The state or equilibrium equations are

$$R(u, z) = K(u)z - F(u) = 0 \qquad (3.36)$$

in which $K = $ an n x n stiffness matrix; and $F = $ a load vector.

The first step is to form the Lagrangian L

$$L = G + \lambda^T R \qquad (3.37)$$

in which $\lambda = $ an (n x 1) Lagrange multiplier vector. Then

$$\delta G = \delta L = \frac{\partial L}{\partial u}\delta u + \frac{\partial L}{\partial z}\delta z \qquad (3.38)$$

To insure that the variation, δG, satisfies Eq. (3.36), choose λ such that

$$\partial L/\partial z = 0 \qquad (3.39)$$

The attractive feature of the Lagrangian approach is that the basis for choosing λ as in Eq. (3.39) is simply the classical approach used in the calculus of variation. Then, from Eq. (3.38)

$$\delta G = \frac{dG}{du}\delta u = \frac{\partial L}{\partial u}\delta u \qquad (3.40)$$

Using Eq. (3.36), Eq. (3.40) yields

$$\frac{dG}{du} = \frac{\partial G}{\partial u} + \lambda^T \frac{\partial}{\partial u}(K\tilde{z} - F) \tag{3.41}$$

In which $\tilde{z}$ means that z is treated as a constant while carrying out the partial differentiation, $\partial / \partial u$. This is done to avoid working with third order tensors. Eq. (3.39) reduces to

$$\frac{\partial G}{\partial z} + \lambda^T \frac{\partial}{\partial z}(Kz - F) = 0$$

or $\quad K\lambda = -\frac{\partial G}{\partial z}^T$ \hfill (3.42)

The components of λ, which are called the adjoint variables in Sections 3.3.2 and 3.4.1, are simply the Lagrange multipliers associated with the state equation in Eq. (3.36).

Distributed Parameter Systems

For distributed parameter sensitivity formulation using the Lagrange multipliers approach (Budkowska, 1997a, Belegundu, 1985), consider the scalar valued functional

$$G = \int_0^l g(z(x), z'(x), u(x))dx \tag{3.43}$$

where function g is continuously differentiable with respect to its arguments, z is the state variables vector, $z = \{z_1, z_2, ..., z_n\}^T$, z' is the gradient of z, $z' = \frac{\partial z}{\partial x}$, and u is the vector of design parameters, $u = \{u_1(x), u_2(x), ..., u_m(x)\}^T$.

61

The equilibrium equations for one-dimensional structural systems are described by set of first order differential equations which can have the form:

$$R(z,z',u) \equiv z' - F(z,u) = 0 \qquad (3.44)$$

where $F(z, u)$ is the vector which depends on the external load conditions , state variables vector z and design variables vector u as well. It is apparent that Eq. (3.44) is accompanied by a system of suitable boundary conditions.

The objective of the analysis is to find the first variation of the functional G, δG , due to the variation of the design variables vector u, δu. The first step is to form the Lagrangian L where:

$$L = g + \lambda^T R \qquad \text{or} \qquad L(z,z',u,\lambda) = g(z,z',u) + \lambda^T (z' - F(z,u)) \qquad (3.45)$$

where λ^T is the Lagrange multipliers vector given as:

$$\lambda^T = \{\lambda_1(x), \lambda_2(x), \dots, \lambda_n(x)\}^T \qquad (3.46)$$

The augmented functional G is represented as follows:

$$G(z,z',u,\lambda) = \int_0^l [g(z,z',u) + \lambda^T (z' - F(z,u))]dx \qquad (3.47)$$

Taking into account the constraints in Eq. (3.44), the first variation of the augmented functional must satisfy the following relationship:

$$\delta G = \int_0^l \delta L dx = \int_0^l \delta g dx \qquad (3.48)$$

62

However, based on the relationship in Eq. (3.45), the first variation of the augmented functional must also satisfy the following relationship:

$$\int_0^l \delta L \, dx = \int_0^l \frac{\partial L}{\partial u} \, \delta u \, dx + \int_0^l \left(\frac{\partial L}{\partial z} \delta z + \frac{\partial L}{\partial z'} \delta z' \right) dx \qquad (3.49)$$

Bearing in mind that the purpose of the analysis is the determination of δG due to the changes of δu, therefore the second integral on the right hand side of Eq. (3.49) must vanish. Thus:

$$\int_0^l \left(\frac{\partial L}{\partial z} \delta z + \frac{\partial L}{\partial z'} \delta z' \right) dx = 0 \qquad (3.50)$$

The integration by parts of the expression under integral (in order to get rid of the variation of the first derivative of the state variable vector z') gives:

$$\frac{\partial L}{\partial z'} \delta z \Big|_0^l + \int_0^l \left(\frac{\partial L}{\partial z} - \frac{d}{dx}\left(\frac{\partial L}{\partial z'} \right) \right) \delta z \, dx = 0 \qquad (3.51)$$

Equation (3.51), must be satisfied by arbitrary δz, therefore both terms associated with δz must vanish. This means the following equations (Euler-Lagrange equations) must be satisfied:

$$\frac{\partial L}{\partial z} - \frac{d}{dx}\left(\frac{\partial L}{\partial z'} \right) = 0 \qquad (3.52)$$

and the following boundary conditions:

$$\frac{\partial L}{\partial z'}(l)\delta z(l) = 0, \qquad \frac{\partial L}{\partial z'}(0)\delta z(0) = 0 \qquad (3.53)$$

63

Substituting for L given in Eq. (3.45) into Eq. (3.52) yields:

$$\frac{\partial}{\partial z}[g(z,z',u) + \lambda^T(z' - F(z,u))] - \frac{d}{dx}\left(\frac{\partial}{\partial z'}[g(z,z',u) + \lambda^T(z' - F(z,u))]\right) = 0 \qquad (3.54)$$

Performing in Eq. (3.54) the required differentiations and applying the operation of transposition, the following equation is reached:

$$\lambda' - \left[\frac{\partial g}{\partial z} - \frac{d}{dx}\left(\frac{\partial g}{\partial z'}\right)\right]^T - \left(\frac{\partial F}{\partial z}\right)^T \lambda = 0 \qquad (3.55)$$

Substituting for L in the boundary conditions (Eq.3.53) yields:

$$\frac{\partial}{\partial z'}[g(z,z',u) + \lambda^T(z' - F(z,u))]\big|_0 \, \delta z(0) = 0,$$

$$\frac{\partial}{\partial z'}[g(z,z',u) + \lambda^T(z' - F(z,u))]\big|_l \, \delta z(l) = 0 \qquad (3.56)$$

which can be abbreviated as:

$$\left[\frac{\partial g}{\partial z'}(0) + \lambda^T(0)\right]\delta z(0) = 0, \qquad \left[\frac{\partial g}{\partial z'}(l) + \lambda^T(l)\right]\delta z(l) = 0 \qquad (3.57)$$

Equation (3.55) together with the boundary conditions given in Eq. (3.57) represent the adjoint (conjugated) system of equations to the initial problem (Eq. (3.47)), which should be solved for unknown Lagrange multipliers vector $\lambda(x)$. After determination of $\lambda(x)$, the first variation of the functional G due to the variations of the design variables vector can be determined from Eq. (3.47). That is:

64

$$\delta G = \int_0^l \left(\frac{\partial g}{\partial u} \delta u - \lambda^T \frac{\partial F}{\partial u} \delta u \right) dx \qquad\qquad (3.58)$$

3.4.4.2 Formulations based on virtual work

Haug et al. (1986) used energy and load forms to obtain sensitivity expressions for linear systems. Their formulation was based on the variational formulation of the problem which can be regarded as the principle of virtual work as discussed above. Choi and Santos (1987) extended their work to nonlinear problems.

Dems and Mróz (1983) provided a systematic variational approach to sensitivity analysis based on the virtual work principle. Their study was limited to linear elastic systems in which they generated first and second variations using the adjoint concept for structures of fixed shape with varying material parameters. They supplemented their work (Dems and Mróz, 1985) by considering the variation of local stress, strain and displacement. In addition, they discretized the expressions for the first and second variations of an arbitrary functional assuming the structural behavior is modeled using the finite element method.

Haftka and Mróz (1986) used the principle of virtual work to find sensitivity derivatives of structural response with respect to stiffness parameters. They used both direct and adjoint approaches to calculate first and second order derivatives. However, their analysis was limited to structures with fixed configuration, small deformations, and nonlinear material properties.

Cardoso and Arora (1988) described a unified variational formula for the design sensitivity analysis of linear and nonlinear structures (geometric and material nonlinearities) and shape, nonshape, and material selection problems. The formulation was based on the principle of virtual work. In addition, the equations of continuum mechanics, concepts of reference volume and adjoint structures were used to develop the formula.

65

3.4.4.3 Formulations based on stationary energy principles

Phelan et al. (1991) presented an adjoint variable method for explicit design sensitivity analysis of geometrically and materially non-linear elastic systems. This method was an extension of the mutual Hu-Washizu energy method presented by Phelan and Haber (1989) for linear systems. The non-linearities considered by Phelan et al. (1991) were due to finite deformations and non-linear, hyperelastic constitutive models. Their method used the mutual Hu-Washizu energy principle to define the adjoint system and domain parameterization to treat shape design variations.

In the Hu-Washizu energy principle, the stationary conditions were applied on energy functionals to obtain the governing equations of the real and adjoint systems. The governing equation for the adjoint system was shown to be linear in the adjoint response variables. This linearization was a result of using the incremental, truncated form of an energy functional defined in the Hu-Washizu method used by the authors. They pointed out again that the cost of the sensitivity analysis in the numerical implementation is small since the adjoint system is linear.

3.4.5 Physical significance of adjoint variables

The sensitivity interpretation of the adjoint variable, which is also a Lagrange multiplier, is extremely useful and leads to some insights into the adjoint variable method. It also has implications in practical applications and numerical implementations of the method.

In the research work carried out (Belegundu, 1985 and Belegundu and Arora, 1985) a physical interpretation for the adjoint variable was introduced. This was accomplished by considering the structural system mentioned above in Section (3.4.4.1). By considering the force vector, F, as the design vector, u, i.e. let $F = u$. Then, Eq (3.40) yields

66

$$\delta G = \frac{\partial L}{\partial F} \delta F \qquad\qquad (3.59)$$

with $L = G + \lambda^T (Kz\text{-}F)$

Since the cost or constraint function, G, does not normally depend explicitly on F, and the stiffness matrix, K, does not depend on F, Eq. (3.59) reduces to

$$\delta G = - \lambda^T \delta F \qquad\qquad (3.60)$$

And since $\delta G = (dG/dF) \delta F$, then

$$\lambda = -\left(\frac{dG}{dF}\right)^T \qquad\qquad (3.61)$$

Equation (3.59) shows that the adjoint vector λ of Eq. (3.61) represents the gradient of G with respect to the load vector. The value of $- \lambda_i$ is the "influence coefficient" associated with G, i.e. $- \lambda_i$ is the value of G due to a unit load acting along the ith degree of freedom.

Cardoso and Arora (1988) used the continuum approach to derive the design sensitivity formulation. They pointed out that adjoint fields can be interpreted as sensitivities of the quantities related to the primary structure. These interpretations revealed in their formulation, provide further useful sensitivity information. For example, some terms in their formulation involving adjoint fields were used to determine implicit design variations of the considered functional with respect to the body force, with respect to the constitutive law and with respect to the specified surface tractions.

In the continuum approach, the sensitivity interpretation of adjoint displacements, stresses, and strains is readily available. With the discretized approach, the sensitivity interpretation of the adjoint displacements had to be discovered using the Lagrangian approach (Belegundu (1985) and Belegundu and Arora (1985)).

67

3.5 COMPARISON BETWEEN METHODS/APPROACHES OF SENSITIVITY ANALYSIS

3.5.1 Direct differentiation method and adjoint variable method

Sensitivity analysis can be carried out analytically by either of the two methods discussed in Section 3.3.2; the direct differentiation method (DDM) or the adjoint variable method (AVM). Formulations based on the direct differentiation method were developed by: Wu and Arora (1987), Ryu et al. (1985), Haug et al. (1986), Kleiber et al. (1997). Amongst the works based on the adjoint method are those by Choi and Santos (1987), Cardoso and Arora (1988), Ryu et al. (1985), Belegundu and Arora (1985), Belegundu (1985), Phelan et al. (1991), Dems and Mróz (1983), Dems and Mróz (1985) and Haug and Arora (1978).

To determine which of the two approaches is to be used for the sensitivity analysis, the number of equations to be solved for each approach should be compared. Denote the number of active constraints (G) to be considered by the designer by NC and the number of design variables by m and the number of loading conditions by NL. For linear systems, the same structural stiffness matrix is applicable to all loading conditions, but the structural equations yield different displacement vectors z associated with different applied force vectors. In the DDM, for each load condition, the number of equations to be solved is equal to the number of design variables m (Eq. 3.4). Therefore, the number of computations required is m x NL. However, for the AVM, the number of equations to be solved is equal to the number of constraints NC (Eq. 3.5). Therefore, if m x NL < NC, then the DDM is preferred while AVM is preferred when m x NL > NC.

Haug et al. (1986) concluded that the adjoint variable method is more efficient in structural optimization applications. This is because the number of active constraints NC must be no greater than the number of design variables m in structural optimization problems. Therefore, the adjoint variable approach will be most efficient even for a single loading. Haug and Arora (1978) showed that for linear systems, where direct numerical

68

comparisons are possible, the adjoint variable method is shown to be five to ten times faster than the direct differentiation method. Arora and Haug (1979) also stated that in iterative optimization process the AVM (state space method) is more efficient than the DDM (design space method) often by factors up to ten.

In addition, Haug and Arora (1979) pointed out that the adjoint variable technique of sensitivity analysis is in many respects better suited for mechanical and structural system design than for problems of optimal control. This is due to the fact that many of the equations governing mechanical and structural systems can be written in symmetric form, whereas the initial value problems of optimal control theory cannot.

For nonlinear systems, the structural stiffness matrices are no longer constant for different loading conditions. Thus m and NCI (number of constraints needed for the lth loading condition) should be compared for each loading condition. If m < NCI, then DDM is preferred while AVM is preferred when m > NCI.

Phelan et al. (1991) indicated through their analysis of the research work by Tsai and Arora (1989) that the direct differentiation method is more appropriate than any of the adjoint sensitivity analysis approaches for continuum problems involving path-dependent materials. Kleiber et al. (1997) also reached the same conclusion that there appears to be no way of making the AVM competitive against the DDM for solving path-dependent problems of nonlinear mechanics. They proved that the method is essentially useless for path-dependent applications, but by no means so for nonlinear elastic problems.

3.5.2 Distributed parameter (continuum) approach and discretized approach

As indicated above (Section 3.4.2), there is a principal distinction between the discretized (matrix) approach of analysis and the distributed parameter (continuum) approach. This lies in the fact that the distributed parameter approach uses displacement fields that satisfy boundary-value problems of elasticity to characterize structural deformation,

while the discretized approach uses nodal displacements that are determined by matrix equations.

The discretized approach was used to formulate the design sensitivity problem by many researchers. Among them are Wu and Arora (1987), Ryu et al. (1985), Arora and Haug (1979), Adelman and Haftka (1986) and Dems and Mróz (1985). Another group of researchers used the distributed parameter structural design sensitivity analysis approach (continuum approach). Among them are Cardoso and Arora (1988), Choi and Santos (1987), Phelan et al. (1991), Haftka and Mróz (1986) and Dems and Mróz (1983).

These two approaches are related since the discretized approach is considered as an approximation of the distributed parameter approach. However, each method has its advantages and disadvantages. There are two main advantages for the distributed parameter approach. First, a rigourous mathematical theory is obtained, without the uncertainity associated with the discretized approximation error. Second, explicit relations for design sensitivity are obtained in terms of physical quantities, rather than in terms of sum of derivatives of element matrices. However, the main disadvantage of the distributed parameter approach is the higher level of mathematical sophistication associated with this method from an engineers point of view.

The sensitivity analysis in discrete formulation provides a final value (in numerical terms) of the sensitivity of the performance of a chosen point when the design variables change in known places by a given amount. On the other hand, the sensitivity analysis with distributed (continuous) parameters allows conducting a sensitivity investigation of a performance of the system in such a way that besides final numerical value of sensitivity result, it also gives an opportunity to show precisely in spatial and numerical terms how, where and why the design variables affect the performance of a system the physical model of which is known. These features of the adjoint system method of distributed parameters turn out to have a significant appeal to all sorts of civil engineering applications.

70

The specified advantages of the distributed design variables approach of sensitivity analysis are the result of an opportunity to conduct all investigations explicitly under spatial integral, before integrating them with respect to the spatial variable. On the other hand, the engagement of finite element analysis in the adjoint system method of discrete design variable employs already integrated results through the fact that it uses the stiffness matrix that requires spatial integration of the investigated problem.

It was shown that the continuum approach presented by Cardoso and Arora (1988) is equivalent to the discrete approaches presented by Ryu et al. (1985) and Wu and Arora (1987) in numerical implementations. In addition, Dems and Mróz (1985) discretized the expressions for the first and second variations of an arbitrary functional that was obtained using the continuum approach in their previous work (Dems and Mróz, 1983) assuming the structure behavior is modeled by a finite element method.

However, the continuum approach offers some insights that are not apparent in the discretized model. For example, design sensitivity analysis with discretized models needs only adjoint displacements because stress and strains are expressed in terms of displacements. The adjoint stresses and strains are neither needed nor calculated. On the other hand, the continuum approach uses adjoint stresses and strains.

In addition, Cardoso and Arora (1988) pointed out another advantage of the continuum approach as mentioned in Section 3.4.5. That is that the sensitivity interpretation of adjoint displacements, stresses, and strains is readily available in the continuum approach. With the discretized approach, the sensitivity interpretation of the adjoint displacements had to be discovered using the Lagrangian approach.

3.5.3 Linear analysis and nonlinear analysis

The design sensitivity analysis for linear structural analysis has been thoroughly investigated. Some references for these linear investigations are: Adelman and Haftka (1986), Arora and Haug (1979), Haug and Arora (1979), Haug et al. (1986), Dems and

71

Mróz (1983), Dems and Mróz (1985) and Haug and Arora (1978). However, in the 1980s, an increasing attention to the use of nonlinear materials and the design requirements for structures to survive under extreme conditions urged the development of design sensitivity methods with nonlinear response. Design sensitivity analysis for nonlinear structural analysis has been investigated by Wu and Arora (1987), Ryu et al. (1985), Cardoso and Arora (1988), Kleiber et al. (1997), Phelan et al. (1991), Tsai and Arora (1989), Choi and Santos (1987) and Haftka and Mróz (1986).

Just as in linear formulation, there are two basic procedures of design sensitivity analysis for nonlinear response; direct differentiation method (DDM) and adjoint variable method (AVM). In addition, the considerations in selection of DDM and AVM are the same for nonlinear as for the linear case, however, each loading step has to be considered. For each loading step, if the number of design variables is more than the number of constraints to be considered in the sensitivity analysis, then the AVM is preferred. Otherwise DDM is preferred.

Haftka and Mroz (1986) applied first and second order sensitivity analysis to linear and nonlinear structures. However their analysis was limited to structures with fixed configuration, small deformations, and nonlinear material properties.

Regarding linear analysis using the adjoint sensitivity method of analysis, both the original (primary) and adjoint systems are linear. However, for nonlinear analysis, the original system is nonlinear while the adjoint system is linear as discussed above in Section 3.4.3. The computational considerations for such analysis are discussed below.

Computational (numerical) considerations for nonlinear systems:

Ryu et al. (1985) presented several procedures for design sensitivity analysis of nonlinear response. They developed different numerical procedures and strategies that can be used for implementation into large commercial programs (such as ADINA) for the design sensitivity analysis and optimization of nonlinear systems. They pointed out to some

72

basic differences between design sensitivity analysis for linear and nonlinear response. They showed that these differences are quite significant in the computational procedures. From these differences are that the coefficient (stiffness) matrix for the nonlinear response depends on the state variable so it is different for each loading condition while for the linear analysis it is not. They also showed that the tangent stiffness approach of nonlinear analysis is found to be more appropriate than the secant stiffness approach for design sensitivity analysis as the matrix at the final load level can be directly used.

Wu and Arora (1987) derived a design sensitivity analysis procedure for nonlinear structures using the incremental/ iterative solution procedure. In the numerical procedure, they showed that with a little additional computational effort, derivatives of response quantities can be calculated. This is because most of the computational effort is spent in the analysis phase. In particular, many quantities needed in sensitivity analysis (derivatives of internal forces, stresses, and strains with respect to the state variables) are already calculated in the analysis phase. In addition, nonlinear analysis of structures requires solution of nonlinear equations using load incrementation and iterations within it, whereas design sensitivity analysis requires the solution of linear equations.

In addition, they (Wu and Arora, 1987) suggested using a semi-analytical approach for obtaining sensitivities of nonlinear systems. In the design sensitivity analysis of nonlinear structural response most of the needed quantities are already calculated in the analysis phase. Specifically derivatives of internal forces, stresses, and strains with respect to the state variables are available without any additional calculations when incremental solution scheme is used. Therefore, only the total design derivatives of state variables (dz/du) and the partial design derivatives of stress, strain and internal force for each finite element are needed to complete sensitivity analysis. The computation of dz/du requires the solution of a linear system. The partial design derivatives are finite element related and require more computational and programming effort. Thus they suggested use of finite difference to compute these partial derivatives. In this approach, the original structure is analyzed; it is then modified by perturbing a design variable (keeping the state variable constant). Since this computation does not require reanalysis of the

73

structure (state variables are fixed while the design is perturbed), the design sensitivity coefficients of the nonlinear response can be calculated efficiently.

Phelan et al. (1991) showed that in numerical solutions, the final tangent coefficient matrix used to solve the nonlinear real system is the same matrix used to solve the adjoint system. Since this matrix is decomposed in the final iteration of the analysis of the real structure, solving the adjoint system requires only the assembly of the adjoint load vector and a single vector reduction/back substitution. In addition, since the adjoint system is linear the cost of the sensitivity analysis is small when compared to the cost of the response analysis for many nonlinear problems. Therefore, the sensitivity analysis can be an excellent investment of computational resources for non-linear problems, because it provides the analyst with useful design information at minimal additional cost.

Poldneff et al. (1993) implemented design sensitivity analysis into a general nonlinear finite element code, MARC. Nonlinear elastic solids with constraints and follower forces were included in the implementation. The constraints were implemented through Lagrange multipliers. They showed from the implementation that one of the most general and easy ways to implement design sensitivity analysis into a general finite element code without sacrificing accuracy is to use a semi-analytical method that uses the central difference scheme. They concluded that the implementation of sensitivity analysis for constrained nonlinear problems follows the same route as for unconstrained problems and that implementation of sensitivity analysis inside the code is preferred if the source code is available.

3.5.4 Method and approach used in the current study

The current study investigates the sensitivity of the performance of laterally loaded piles to changes in the design variables of the system. The performance of the pile is described by the lateral pile head deflection and pile head rotation. The design variables are the pile and soil parameters (8 parameters). Therefore, the adjoint variable method is preferred

74

over the direct differentiation method since the number of design variables is considerably larger than the number of performance measures investigated.

The distributed parameter approach is used in the current analysis rather than the discretized one since it allows for the spatial graphical presentation of the distribution of sensitivity operators along the pile length which shows how and where each design variable affects the system's performance as explained above in Section 3.5.2. This distribution of sensitivity operators provides a valuable knowledge on the behavior of the system if employed at the design stage or in an aging process and in general, in decision making process. It also gives basis for the quantification of the importance of the distributed design variables on the performance of the system.

The sensitivity analysis is applied to a nonlinear system (physically nonlinear) since the soil-pile interaction is modeled using nonlinear p-y curves, where p stands for soil reaction and y stands for lateral deflection. Accordingly, the current sensitivity analysis will be carried out using the adjoint variable method with a distributed parameter approach applied to the nonlinear pile-soil system.

3.6 APPLICATIONS OF SENSITIVITY ANALYSIS

The application of sensitivity analysis to different fields and different areas of engineering was shown in Figure 1.1. A literature review for the application of sensitivity analysis in the civil engineering field is discussed below.

3.6.1 Applications of sensitivity analysis in civil engineering problems

Lee and Lim (1997) presented an approach for extension of sensitivity methods to include the structural uncertainty with random parameters. Their formulation was based on the perturbation method. They derived a method of direct differentiation for calculating sensitivity coefficients in regards of the governing equation, the first-order

75

perturbed equation and the second-order perturbed equation. They applied their method to a 10-bar truss where the stiffness parameter and the load vector were considered as the random parameters. They verified their analysis by comparing the results with the probabilistic finite difference method.

In addition, Ghosh et al. (2001) performed a stochastic sensitivity analysis of structures under uncertain structural parameters. They used the perturbation method within the finite element framework for computation of response statistics. The primary objective of their study was to assess the effectiveness of perturbation method for sensitivity analysis of structures compared to that of the Monte Carlo simulation. A numerical example on static beam problems has been presented to elucidate their proposed method. They showed from their study that for the first-order perturbation, the models of stochastic finite element and stochastic design sensitivity are almost identical. The developed algorithm can be easily adopted to fit into existing finite element program. The sensitivity statistics obtained through first-order perturbation analysis is quite satisfactory compared to Monte Carlo results if the coefficient of variation of input random parameter is small. However, for higher coefficient of variation, the perturbation is not so effective. They recommended that for higher coefficient of variation of randomness, second-order terms in perturbation should be studied.

Kaminski (2001) investigated material sensitivity analysis in homogenization of linear elastic composites. The direct differentiation method (DDM) of sensitivity analysis was used in his study. The sensitivity analysis of effective material properties was presented in a general form for an n-components periodic composite, and was illustrated by examples of one-dimensional and two-dimensional heterogeneous structures. The sensitivity gradients were computed using a homogenization-oriented computer program, according to the DDM approach implementation. The composite design parameters were the Young's moduli and Poisson's ratios of the constituents. His results confirmed the usefulness of the homogenization method in computational analysis of composite materials. In addition, it was shown that for the Poisson's ratios values tending to their physical bounds, an uncontrolled increase of all the sensitivity gradients was observed.

76

Burg (2002) applied the discrete sensitivity analysis using the adjoint variable formulation to ground water analysis. The derivatives of a numerically approximated objective function with respect to a set of parameters were efficiently estimated at a fraction of the cost of using finite differences. Coupled with an optimization algorithm, this method was used to locate the optimal set of parameters for the objective function. The adjoint variable technique was applied to a time-dependent, two-dimensional groundwater code. It was shown that the derivatives agreed with finite difference derivatives to between 6 and 8 significant digits, at approximately 1/8 the computational cost.

Coa et al. (2002) developed an efficient numerical method for sensitivity computation of large-scale differential-algebraic systems based on the adjoint method. In their paper they addressed issues that are critical for the implementation. Complexity analysis and numerical results demonstrated that the adjoint sensitivity method is advantageous over the forward sensitivity method for applications with a large number of sensitivity parameters and few objective functions.

Sanders and Katopodes (2003) applied the sensitivity analysis to water wave control in river and estuarine systems. They used the adjoint method of sensitivity analysis. Their analysis was based on the shallow-water equations. They derived a new formulation for sensitivity of shallow-water flow to boundary changes in depth and discharge. In addition, they developed new adjoint boundary conditions for river estuarine forecasting models with open-water inflow and outflow sections.

Drewko and Hien (2005) applied a variational formulation to a sensitivity problem of beam systems in the context of deformable solids with cracks. They treated natural frequencies as state variables involved in the energy functional of the system, while the crack's length and position were treated as system parameters. They obtained first and second derivatives of the natural frequency functions with respect to the crack's length and position. An analytical procedure for calculations of the second-order sensitivities of natural frequencies was proposed for the non-symmetrical equation system operator.

77

Numerical algorithms were proposed and implemented computationally. They pointed out that for a fixed position of the crack the natural frequencies are more sensitive with respect to the crack's length (the larger the crack length is the more weakened is the beam). Also, they showed that there exist a few points –with zero or stationary values of bending moments– that are insensitive with respect to the crack length.

3.6.2 Applications of sensitivity analysis to geotechnical problems

As mentioned above, sensitivity analysis emerged as a fruitful area in the engineering field. However, its application still needs to be better established in the geotechnical field. It has been applied to few geotechnical problems such as soil consolidation (Arnod et al., 1996). Moreover, its application to the geotechnical field is of special importance due to the soil's nature associated with parameter uncertainties. The different sensitivity methods need to be applied to various geotechnical problems to make use of the beneficial important information that can be obtained form sensitivity results.

3.6.2.1 Application to raft foundations

Valliappan et al. (1997) applied the sensitivity analysis to raft foundations. They proposed an algorithm for the semi-analytical sensitivity method applied to non-linear analysis and a modification of the two-point constraint approximation, named bi-point constraint approximation. They analyzed a raft foundation on soil medium and compared their results to validate their proposed method. In 1999, Valliappan et al. applied a structural optimization combined with the finite element method for the optimal design of a raft-pile foundation system. The sensitivity analysis, for the optimization process, was carried out using the approximate semi-analytical method while the constraint approximation was obtained from the combination of extended Bi-point and Lagrangian polynomial approximation methods. The raft thickness, cross-section, length and number of piles were taken as the design variables. The cost of the foundation was selected as the objective function of the problem. The constraints were the maximum displacement and

78

differential displacement. It was shown that an optimum design of the raft-pile foundation was achieved efficiently and accurately using the proposed method.

3.6.2.2 *Application to pile foundations*

This section will be presenting sensitivity analysis applied to piles subjected to axial load and torsion. Laterally loaded piles will be discussed in a separate section since they are the focus of the research.

Piles subjected to axial load

Budkowska and Szymczak (1993a, 1994b) applied the sensitivity analysis to axially loaded piles. They derived the first variations of a vertical displacement and axial force of axially loaded piles due to changes of the design variables using the virtual work theorem. The pile and soil parameters were selected as the design parameters. A simple one-dimensional idealization of the pile in conjunction with the soil model consisting of a continuously distributed system of springs and a spring located on the pile toe or Winkler-type model of the soil behavior was assumed. Numerical examples were presented in their research that showed good performance of the accuracy of the approximation of the change of the design variables.

Budkowska and Szymczak (1995b) employed the same models of the pile and soil to perform the sensitivity analysis of axially loaded piles. However, the design variable was chosen as the location of the end-points of the piles. The numerical examples presented in their study showed that the accuracy of the approximation is good even for 30% change in the pile length.

Budkowska and Szymczak (1996, 1997) presented the first variation of the critical buckling load of a pile partially embedded in soil due to variation in design variables. The design variables were the pile material, soil properties and the location of pile ends. The accuracy of the approximation of the change of critical buckling load due to the change in

79

the design variables was investigated and showed that the first variation led to a good approximation.

Piles undergoing Torsion

Budkowska and Szymczak (1993b) derived first order variations of an angle of the pile twist and a torque at a specified cross-section of the pile due to design variable variations. The design variables were the cross-sectional dimensions and the parameters defining the pile material and the soil behavior. The study was restricted to the linear range of the structural behavior.

Budkowska and Szymczak (1994a) presented the sensitivity analysis of piles subjected to torsion, but a different design variable was considered. The design variable was taken as an increment of the pile length. The pile studied had a circular cross-section and was made of a linear elastic material. The considerations were based on the calculus of variations with moving boundaries. The sensitivity analysis enabled the calculation of changes in the quantities under consideration due to the pile end shifts without a full re-analysis of the pile. A detailed discussion of a pile embedded in multilayered soil was also presented in their study.

3.6.2.3   Application to laterally loaded piles

Laterally loaded piles are piles subjected to lateral loads and bending moments as pointed out in Chapter 2. Regarding laterally loaded piles, one of the important areas in the geotechnical field as mentioned in the previous chapter, a continuing research program has been started in the last few years at the University of Windsor. The work done in this field is reviewed below.

Budkowska and Szymczak (1992a, 1992b) conducted the sensitivity analysis of laterally loaded piles in soils using the adjoint method. They used the beam on elastic foundation approach combined with a one-dimensional pile idealization. The linear Winkler type

80

elastic foundation was used. The cases presented in the paper are the sensitivity of lateral displacement and angle of rotation at top of the pile due to the changes of the pile's bending stiffness (EI) and the foundation stiffness (k) for both a uniform and a linearly varying foundation stiffness k distribution. Numerical examples for many cases were covered and showed that the approximation of the changes of the state variables due to the changes of the design variables by means of their first variations were good. However, it was observed that there are significant differences in the sensitivity results between uniform and linearly varying foundation stiffness.

Budkowska and Szymczak (1995a) proposed an approximate procedure for calculation of changes of maximum values of an arbitrary displacement and an internal force of laterally loaded piles due to some increments of the pile cross-sectional dimensions, the pile material and the soil parameters. The pile was modeled as a one-dimensional beam element and the response of the soil was modeled as an elastic foundation of Winkler type. The adjoint method of analysis was used to obtain the first order variation of the maximum value of quantity under consideration. Because of the nature of the modeling of the pile-soil system the researchers suggested that the procedure could be applied to linear and nonlinear systems. Then constant variations of design variables EI and k have been injected to the system.

In addition, change in the flexural moment has been determined and graphically presented. The accuracy of the calculation of the changes of the maximum value of the flexural moment of the pile by means of its first variation was discussed. The results obtained in the numerical example using the formulation have been compared with the actual values calculated through finite element method. For the finite element method, the pile was discretized into twenty elements. The calculated value of change of maximum flexural moment, determined with the proposed formulation, was approximate and close to the actual value obtained by finite element method. Through the study of the values of the numerical example, the researchers found that the procedure works good for change of design variables up to 40% of initial values.

Budkowska and Cean (1995) presented the sensitivity analysis of short piles subjected to bending moment. First variations of the generalized lateral displacements and internal forces at the specified cross section were derived based on the adjoint method. The pile was modeled as a one dimensional beam element where the response of the soil was simulated by the Winkler type foundation. The behavior of the pile was obtained via the solution of differential equation of the problem with suitable boundary conditions. The distribution of the sensitivity coefficients of kinematic quantities at specified cross-sections was also presented.

Budkowska and Cean (1996) presented the theoretical formulation of sensitivity analysis of laterally loaded long piles embedded in homogeneous sandy soils subject to horizontal loads and bending moment. The same models and method of analysis were used and the design variables were taken as the pile's bending stiffness, EI, and the subgrade reaction of the soil, k. A comparative analysis for the two different types of loading was performed. The effects of changes of the design variables on the components of kinematic field for the pile due to both types of loadings had quantitatively the same value. They also performed the distribution of the sensitivity operators that can be used for engineering practice in design/redesign/rehabilitation of the shape of the pile structure (sensitivity due to EI) and the information on the most effective and rational improvement of the soil (sensitivity due to k).

Budkowska (1997a) derived a general formulation of the distributed parameter sensitivity analysis of laterally loaded short piles embedded in a homogeneous soil medium. The adjoint method based on the principles of variational calculus was used. The central point of the analysis was connected with the concept of functional with constraints, which is then transformed into augmented functional without constraints, however dependent on the Lagrange multipliers vector. Thus the formulation technique used for the adjoint method of analysis was that based on the Lagrangian multiplier method.

Budkowska (1997b) performed a numerical investigation based on the theoretical formulation derived in the first part of the paper (Budkowska, 1997a). The pile structure

was embedded in a homogeneous sand and clayey soil modeled as a one-dimensional structural element supported by the Winkler type foundation. The type of pile-soil interaction was described by means of the modulus of subgrade reaction. The design variables were taken as the bending stiffness of the pile structure and the modulus of subgrade reaction. The modulus of subgrade reaction was taken as a constant for the clay layer case while it was taken as linear with depth of pile in case of the homogenous sandy soil. Thus the analysis is a linear sensitivity analysis. Distributions of sensitivity operators showing the effect of the design variables on the deformation of the pile were presented and important conclusions were drawn for practicing engineers.

Budkowska (1998a) presented the sensitivity analysis of piles subject to bending moment due to variation of pile length. Again, the pile was modeled as a beam element and the soil as an elastic foundation of Winkler type. The functionals of bending and shear energy were defined in the scope of variational calculus based on the principle of virtual work employing the adjoint method. The first variations of the deformation and static field components were formulated using moving ends. The evaluation of changes of kinematic and static fields utilized Taylor's mean value theorem, as well as approximate values of variations of deformation field component not defined within the intervals of shift of soil support conditions. The final forms of the sensitivity equations were accompanied with set of equations defining the behavior of natural boundary conditions for primary and adjoint structure. The obtained sensitivity results were compared with exact solutions and accuracy of the results were examined from the error analysis standpoint. Budkowska (1998b) performed the sensitivity analysis of long piles embedded in homogeneous soil subjected to bending moments. The same previous method and models were employed but different design variables were considered.

In 1999, Budkowska et al. (Budkowska, 1999, Budkowska et al., 1999a) presented the theoretical formulation of sensitivity analysis of laterally loaded piles due to variable location of soil layer. The distributed parameter sensitivity was performed using the adjoint method. The same models for piles and soil were used. The sensitivity results enables one to analyze the effect of the changes of the internal forces and generalized

dispalacements of laterally loaded piles for various scenarios of changes of boundaries of the arbitrary soil layer resulting in expansion/shrinkage, as well as translation upwards or downwards. The numerical investigations (Budkowska et al., 1999b) were compared with the exact solutions obtained by means of reanalysis of the problem. The accuracy of the sensitivity outcomes was examined in the framework of the error analysis.

Priyanto (2002) conducted the sensitivity analysis of laterally loaded piles embedded in a homogeneous soft clay layer subjected to lateral cyclic loading. The distributed parameter sensitivity was performed using the adjoint method and the pile was modeled as a one-dimensional beam similar to the previous studies mentioned above. However, the soil-pile system was modeled using the p-y non-linear model for soft clay layer located below water table subjected to lateral cyclic loading. The design variables under investigation were the pile and soil parameters involved in the p-y relationship. The sensitivity analysis study included single piles (Budkowska and Priyanto, 2002a) and pile groups (Budkowska and Priyanto, 2002b).

Suwarno (2003) carried out the sensitivity analysis of laterally loaded piles using the same adjoint method however the piles were embedded in another homogeneous soil layer which is stiff clay below water table. In addition, the piles were subjected to static loads rather than cyclic ones. The soil was modeled using the nonlinear p-y model for stiff clay below water table subjected to cyclic loading. Both the theoretical formulations of the problem and the numerical investigations were conducted for single piles (Budkowska and Suwarno, 2002a) and pile groups (Budkowska and Suwarno, 2002b).

Following the same sensitivity analysis method but for piles embedded in different homogeneous types of soil and subjected to different types of loading, Lui and Budkowska (2004) presented the sensitivity analysis of laterally loaded piles embedded in stiff clay below water table subjected to cyclic loading. Abedin (2004) performed the sensitivity analysis of laterally loaded piles embedded in sand below water table subjected to static loading while Rahman (2004) performed the analysis for piles embedded in sand below water table subjected to cyclic loading. Mora (2006) performed

84

the sensitivity analysis for piles in soft clay below water table subjected to static loading. The different *p-y* models used for the above different homogeneous types of soils and loadings will be presented in Chapter 4.

3.6.3 Application of sensitivity analysis employed in the current study

As pointed out in the above section, Budkowska and coworkers (Budkowska and Szymczak, 1992a,b, 1995, Budkowska and Cean, 1995, 1996, Budkowska, 1997a,b, Budkowska, 1998a,b, Budkowska,1999 and Budkowska, Sekulovic and Saha, 1999a,b) presented the sensitivity analysis of laterally loaded piles embedded in homogeneous soils modeled using the linear Winkler model. Starting from the new millennium, Budkowska and coworkers (Budkowska and Priyanto, 2002a,b, Priyanto, 2002, Priyanto, 2002, Budkowska and Suwarno, 2002a, b, Suwarno 2003, Lui, 2004, Liu and Budkowska, 2004, Abedin, 2004, Rahman, 2004 and Mora, 2006) carried out studies on laterally loaded piles embedded in homogeneous soils modeled using the non-linear *p-y* models rather than linearly modeled soils.

The current study presents the sensitivity analysis of laterally loaded piles subjected to cyclic loading embedded in non-homogeneous soil rather than homogeneous soils (Hafez and Budkowska, 2004, 2005a, b, 2006a, b, c, d, 2007a and 2007b). The non-homogeneous soil stratification is a more general case especially in lowland areas where the soil profile starts with clay layers of variable thicknesses. The non-homogeneity will be considered in a layered fashion where a layer of soft clay overlies a layer of sand. The nonlinear *p-y* models obtained from experimental field tests on homogeneous soils will be used to model the soil behavior. However, application of the *p-y* methodology to stratified soils will require an appropriate modification of the *p-y* approach. The modeling used to describe the behavior of the non-homogeneous soil will be presented in Chapter 4.

The theoretical formulation of the sensitivity of the pile's performance to changes in the design parameters will be derived. The pile's performance is measured by the lateral head

85

deflection and pile's head rotation which are considered as important serviceability measures for the superstructure supported by the pile foundation. The non-homogeneous soil consists of soft clay overlying sand and the design parameters are those that define the pile and the adjacent clay and sand. The distributed parameter sensitivity analysis using the adjoint method for nonlinear systems will be used as mentioned above (Section 3.5.4) to derive the theoretical formulation of the problem. Three different formulation techniques for the adjoint method will be presented in Chapter 5. The formulation will include piles subjected to lateral forces and bending moments applied at the pile head.

The formulation results in obtaining sensitivity operators that can show along the pile length where and how the change of each parameter affects the change of the pile's performance. The formulation provides the basis for studying the effect of the thickness of the overlying clay on the sensitivity results. Numerical studies will be carried out for piles with different cases of head fixity, different lengths and for different cases of soil stratification. In addition, the study will be extending the sensitivity analysis for the above cases to pile groups rather than single piles in order to take into account the interactive group effect existing among the piles.

CHAPTER 4

MODELING OF NON-HOMOGENEOUS SOIL

4.1 INTRODUCTION

As mentioned in the literature review of laterally loaded piles, there are several approaches used to model the soil-pile interaction behavior in a laterally loaded pile. However, the most common and reliable approach of analysis is the *p-y* approach. These *p-y* curves, relating the soil reaction *p* to the pile deflection *y*, were developed in the seventies of the twentieth century for many kinds of homogeneous soils based on field experiments with full-sized piles. They were able to adequately model the nonlinear behavior of laterally loaded piles and were used over the years in a number of case studies showing good to excellent agreement with experimental results (Reese and Van Impe, 2001). This approach will be used in the current study to model the soil-pile behavior which is needed for the development of the sensitivity formulation.

Previous sensitivity investigations were all performed for laterally loaded piles embedded in homogeneous soils. The current study focuses on the sensitivity of laterally loaded piles embedded in non-homogeneous soil. The non-homogeneity considered is of layered type. The soil profile studied consists of a layer of soft clay overlaying a layer of sand. The non-homogeneity of the soil should be accounted for since the *p-y* curves were developed for homogeneous soils. The non-homogeneity will be accounted for by the use of the equivalent thickness method proposed by Georgiadis (1983).

The soil models used by previous researchers to describe the soil behavior in their sensitivity investigations are first presented. A description of the soil models used in the current study is then presented followed by the incorporation of the non-homogeneity of the soil profile in the *p-y* models.

87

4.2 SOIL MODELS USED IN PREVIOUS RESEARCH

4.2.1 Linear soil response

Budkowska and Szymczak (1992a, b) and Budkowska and Cean (1995 and 1996) studied the sensitivity of laterally loaded piles embedded in homogeneous soils modeled as Winkler type foundation. In a Winkler type foundation the pile-soil interaction is described by means of the modulus of subgrade reaction k. .

In the sensitivity analysis of laterally loaded piles performed by Budkowska (1997a and b), the type of pile-soil interaction was also described by means of the modulus of subgrade reaction. The analysis was performed for a case of a pile embedded in homogeneous clay and another for a pile embedded in sand. The modulus of subgrade reaction, k, was taken as a constant for the case of homogeneous clay layer, while it was taken as linear with depth of pile in case of the homogenous sandy soil. The geometry of the pile structure and the modeling of the soil support conditions embedded in both types of soil are shown in Figure 4.1. Thus the above mentioned analyses used a linear soil response in modeling the soil.
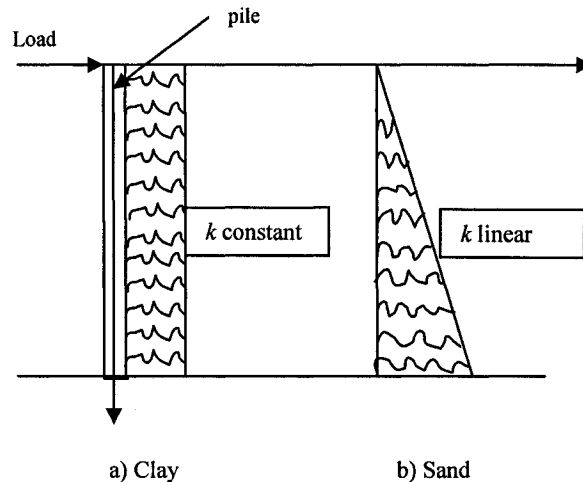
Figure 4.1 Soil modeling for piles embedded in a) clay, b) sand after Budkowska (1997b)

88

4.2.2 Nonlinear p-y curves for stiff clay below water table

Suwarno (2003) carried out the sensitivity analysis of laterally loaded piles and pile groups embedded in stiff clay below water table subjected to static loading. This research was based on the soil p-y model developed by Reese et al. (1975) shown in Figure 4.2.
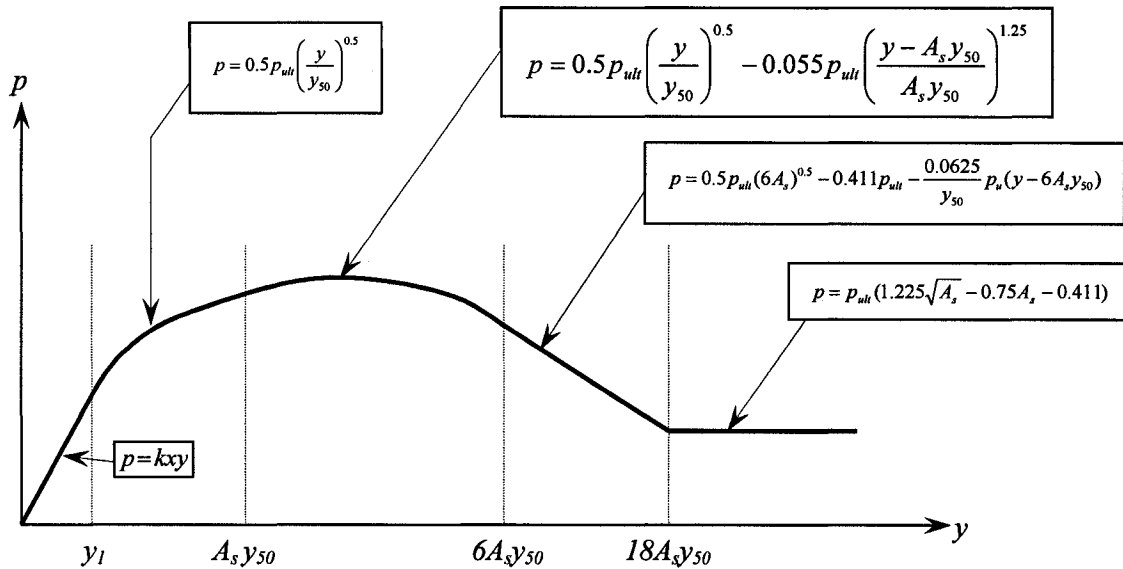
Figure 4.2 A typical p-y curve for stiff clay located below water table for an arbitrary depth x after Reese et al. (1975)

Reese et al. (1975) suggested the shown p-y curves based on full scale lateral load tests for piles driven in stiff clay below the water table at a sight near Manor, Texas . The p-y relationships for each part of the p-y curve are shown in Figure 4.2. The p -y consists of five segments corresponding to the linear elastic, the nonlinear elastic, the nonlinear softening, the linear softening, and the plastic flow phases. They are marked by y_l (point of intersection of first two equations) and some products of $A_s y_{50}$. A_s is a constant given by Reese et al. (1975) based on experiment and y_{50} is the deflection at one-half of that ultimate soil resistance. The deflection y_{50} is given as:

89

$$y_{50} = \varepsilon_{50}b \qquad (4.1)$$

where ε_{50} is the strain corresponding to one-half the compressive strength of clay and b is the width or diameter of the pile.

These p-y equations are given as a function of the ultimate soil resistance p_{ult} and y_{50}. For calculation of the ultimate soil resistance p_{ult}, it is important to consider depth of the reduced soil resistance, x_{rc}, where the ultimate soil resistance, p_{ult}, is a linear function above it but it is a constant below the depth x_{rc}. The ultimate soil resistance, p_{ult}, along the depth x above x_{rc}, is given by the following equation:

$$p_{ult} = 2c_ab + \gamma'_c bx + 2.83c_ax \qquad (4.2)$$

where c_a is the average undrained soil shear strength over the depth x, γ'_c is the effective unit weight of the clay and x is a spatial variable starting from the soil surface and directed downwards along the pile axis. The ultimate soil resistance, p_{ult}, below x_{rc} is given by:

$$p_{ult} = 11\,c\,b \qquad (4.3)$$

where c is the undrained shear strength or cohesion. The value of x_{rc} (depth of reduced soil resistance for clay) is calculated by equating the two values of p_{ult} given in Eqs. (4.2) and (4.3).

4.2.3 Nonlinear p-y curves for stiff clay above water table

Liu (2004) presented the sensitivity analysis of laterally loaded piles and pile groups embedded in stiff clay above water table subjected to cyclic loading. The soil model used is shown in Figure 4.3.
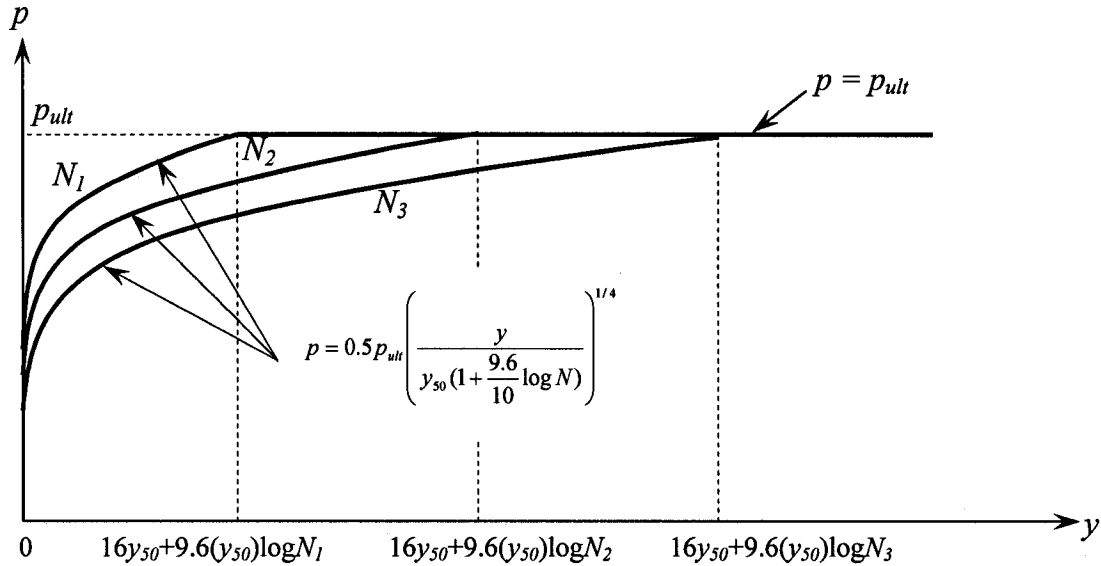
Figure 4.3 Typical *p-y* curves for stiff clay located above water table subjected to cyclic loading after Reese and Welch (1975)

The *p-y* curves are based on full scale tests of a bored pile performed in Houston, Texas (Reese and Welch, 1975 and Welch and Reese, 1972). The curves are given explicitly in terms of the number of cycles of loading, *N*. The *p-y* relation is formulated by means of two quantities: the ultimate soil resistance per unit length of the pile, p_{ult} and the deflection at one-half of that ultimate soil resistance, y_{50}. The deflection y_{50} is given as:

$$y_{50} = 2.5\varepsilon_{50}b \tag{4.4}$$

where ε_{50} is the strain corresponding to one-half the compressive strength of clay, and b is the diameter of the pile. The ultimate soil resistance, p_{ult}, is given as:

$$p_{ult} = \left(3 + \frac{\gamma'_c}{c}x + \frac{J}{b}x\right)cb \quad \text{for } x \leq x_{rc} \quad, \qquad p_{ult} = 9cb \quad \text{for } x \geq x_{rc} \tag{4.5}$$

91

where γ_c' is the effective unit weight of clay, c is the undrained cohesion, J is a model constant, and x is a spatial variable starting from the soil surface and directed downwards along the pile axis. The value of x_{rc} (depth of reduced soil resistance for clay) is calculated by equating the two values of p_{ult} given in Eq. (4.4) to maintain its continuity.

4.2.4 Nonlinear *p-y* curves for sand below and above water table

Abedin (2004) performed the sensitivity analysis of laterally loaded piles and pile groups embedded in sand below water table subjected to static loading while Rahman (2004) performed the analysis for piles embedded in sand below water table subjected to cyclic loading. The *p-y* curves are based on full scale tests on piles driven into sand at Mustang Island, Texas (Cox et al., 1974 and Reese et al., 1974).

The *p-y* curves are the same for sand above and below water table, however, the buoyant unit weight is used for sand below water table and total unit weight is used for sand above water table. The *p-y* model for sand subjected to cyclic loading will be discussed in detail in Section 4.3.1 since it is used in the present study. The curves for static loading are similar to those for cyclic loading, however, the values of coefficients $\tilde{A}_s$ and B_s used for static loading substitute those of $\tilde{A}_c$ and B_c used for cyclic loading.

4.2.5 Nonlinear *p-y* curves for soft clay below water table

Priyanto (2002) carried out the sensitivity analysis of laterally loaded piles embedded in soft clay below water table subjected to cyclic loading while Mora (2006) performed the sensitivity analysis for piles in soft clay below water table subjected to static loading. The *p-y* curve for static loading is shown in Figure 4.4. The values of y_{50} and p_{ult} are given in Eqs. (4.4) and (4.5), respectively. The *p-y* model for cyclic loading will be discussed in detail in Section 4.3.1 since it is used in the present study. Both curves (cyclic and static) were developed by Matlock (1970) based on full scale tests for piles driven into clays near Lake Austin, Texas.

92

$$\frac{p}{p_{ult}} = 0.5\left(\frac{y}{y_{50}}\right)^{1/3}$$
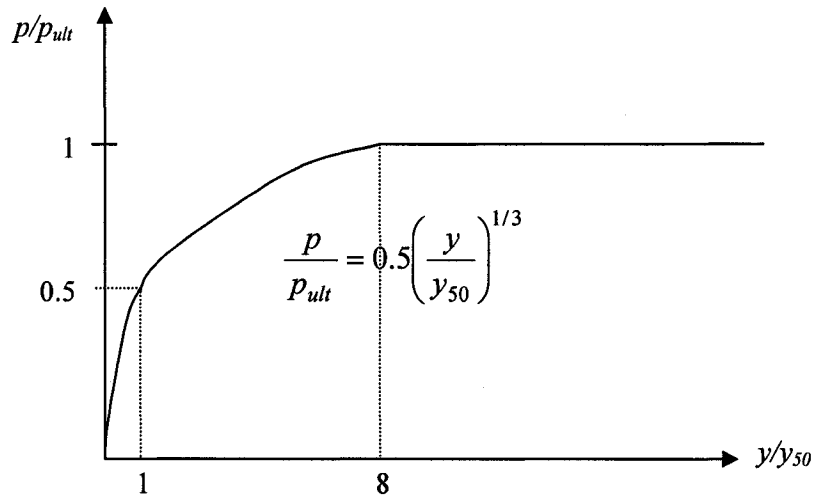
Figure 4.4 Nonlinear soil behavior of soft clay below water table subjected to static loading after Matlock (1970)

4.3 MODELING SOIL BEHAVIOR IN THE CURRENT RESEARCH

The soil profile consists of a layer of soft clay overlying a sand layer. The well-established p-y curves, relating the nonlinear soil reaction p to pile deflection y, are used to model the soil behavior of homogeneous layers of soft clay and sand (Matlock, 1970 and Reese et al., 1974). The cyclicity of the load is taken into account implicitly through the models used. Application of p-y methodology to stratified soils requires an appropriate modification of p-y approach. The two homogeneous p-y models for each type of soil are incorporated to the non-homogeneous soil profile by means of an equivalent thickness method. The soil behavior of each homogeneous layer is first presented followed by the incorporation of the non-homogeneity of the soil to the p-y models.

93

4.3.1 Soil behavior for homogeneous soil

The p-y curves proposed by Matlock (1970) for soft clay and those proposed by Reese et al. (1974) for sand are used in our study. Both models were for soils below water table and for a cyclic type of loading. The effect of the cyclic loading on the soil response when conducted explicitly is very complex. Thus the cyclicity of the load is included implicitly in the soil models by the use of a quasi-static approximation of a lower bound of soil resistance that corresponds to an infinitely large number of load cycles. This means that no matter how complex the cyclic loading is, it is possible to describe the soil behavior at an arbitrary depth by means of a simple p-y curve.

4.3.1.1 Soil model for soft clay

The p-y curves for soft clay were developed by Matlock (1970) based on full scale tests for piles driven into clays near Lake Austin, Texas. The soil behavior of soft clay below water table subjected to cyclic loading is described by three stages or two depending on the depth at which the p-y relationship is required. This behavior is shown in Figure 4.5. For a depth less than x_{rc}, where x_{rc} is the depth of reduced resistance, there are three stages given in Table 4.1. In the first stage, the soil behaves in a nonlinear elastic manner. In the second stage, the soil experiences softening while the third stage is a plastic flow stage. For a depth greater than x_{rc}, the soil experiences a nonlinear elastic behavior described by the same equation given in Table 4.1 (stage 1) followed directly by a plastic stage given as

$$p = 0.72 \, p_{ult} \tag{4.6}$$

The relationships in Table 4.1 are given in terms of two quantities: the ultimate soil resistance per unit length of the pile, p_{ult}, and the deflection at one-half of that ultimate soil resistance, y_{50}. The values of y_{50} and p_{ult} are given by Eqs. (4.4) and (4.5) respectively. The distribution of p_{ult} along the pile axis is shown in Figure 4.6.

94
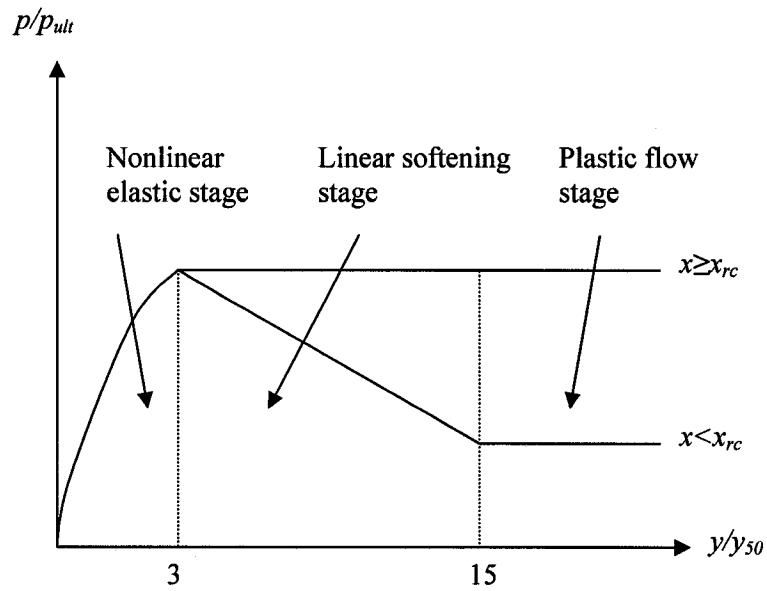
Figure 4.5 Nonlinear soil behavior of soft clay below water table subjected to cyclic loading after Matlock (1970)

Table 4.1 The p-y relationships for soft clay for depth $x < x_{rc}$ for the different soil stages

Soil Stage	Deflection Range	p-y Relationships
Nonlinear Elastic	$0 < y < 3y_{50}$	$\dfrac{p}{p_{ult}} = 0.5\left(\dfrac{y}{y_{50}}\right)^{1/3}$
Linear Softening	$3y_{50} < y < 15y_{50}$	$\dfrac{p}{p_{ult}} = \left(0.9 - 0.18\dfrac{x}{x_{rc}}\right) - 0.06\dfrac{y}{y_{50}}\left(1 - \dfrac{x}{x_{rc}}\right)$
Plastic Flow	$y > 15y_{50}$	$\dfrac{p}{p_{ult}} = 0.72\dfrac{x}{x_{rc}}$

95
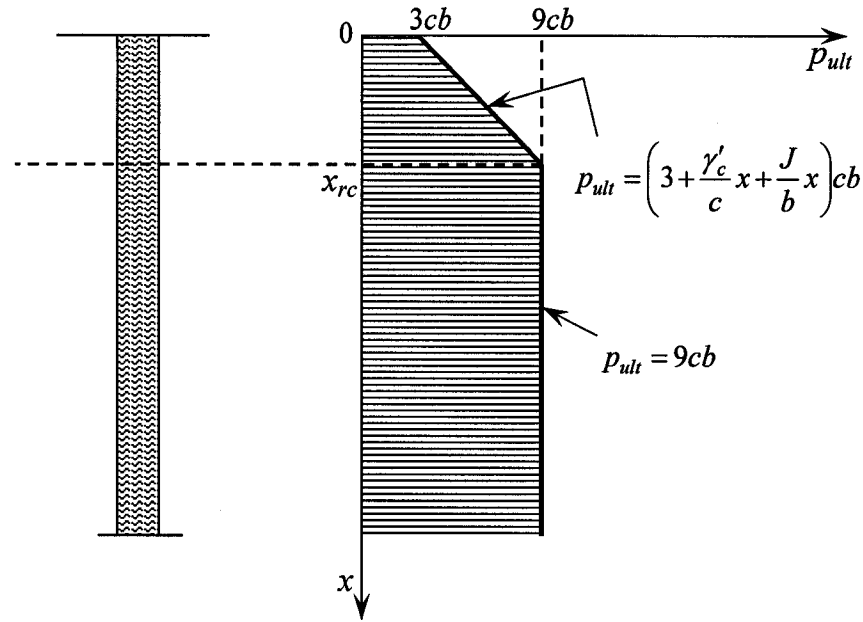
Figure 4.6 Distribution of ultimate soil resistance, p_{ult}, for soft clay below water table subjected to cyclic loading

As recommended by Matlock (1970), the proposed p-y models apply to submerged clay soils which are naturally consolidated or slightly overconsolidated. In addition, Matlock (1970) recommended the following tests in approximate order of preference for determining the undrained cohesion, c, of soft clay required in the p-y construction:

1. In-situ vane-shear tests with parallel sampling for soil identification

2. Unconsolidated-undrained triaxial compression tests having a confining stress equal to the overburden pressure with c being defined as one-half the total maximum principal-stress difference

3. Miniature vane tests of samples in tubes

4. Unconfined compression tests

4.3.1.2   Soil model for sand

The behavior of sand, employed in the sensitivity analysis, is modeled using the soil model developed by Reese et al. (1974). The p-y curves are based on full scale tests on piles driven into sand at Mustang Island, Texas (Cox et al., 1974 and Reese et al., 1974).

96

The nonlinear *p-y* relation of sand is described by four stages depending on the lateral deflection of the pile *y*. The first phase is a linear elastic stage ($0 < y < y_k$), the second is a parabolic nonlinear stage ($y_k < y < y_m$), the third is a linear hardening stage ($y_m < y < y_u$), and the fourth is a plastic flow stage ($y > y_u$). These four stages of the soil behavior are shown in Figure 4.7 and the corresponding *p-y* relationships are given in Table 4.2. In Table 4.2, *k* is a constant representing the modulus of subgrade reaction in the linear stage in the curve.

The different stages of the sand behavior depend on the deflection. There are four stages: a linear elastic stage, a parabolic nonlinear stage, a linear hardening stage and a plastic flow stage. The deflections differentiating between the different stages are y_k, y_m and y_u, where y_k is calculated by the intersection of the curves of the two stages while the values of y_m and y_u are shown in Figure 4.7. Their corresponding soil reactions p_m and p_u are given as:

$$p_m = B_c p_s ; \qquad p_u = \tilde{A}_c p_s \tag{4.7}$$

where $\tilde{A}_c$ and B_c are non-dimensional coefficients which are given in graphs as functions of (*x/b*) and p_s is the ultimate soil resistance per unit length of the pile.

The resistance p_s is denoted as p_{st} for the upper part of the pile-soil system ($x \leq x_{rs}$) and is given in Eq. (4.8). It is denoted as p_{sd} for the lower part of the pile soil system ($x \geq x_{rs}$) and is given in Eq. (4.9).

$$p_{st} = \gamma'_s x \left[\frac{0.4x \tan \phi \sin \beta}{\tan(\beta - \phi) \cos \alpha} + \frac{\tan \beta}{\tan(\beta - \phi)} (b + x \tan \beta \tan \alpha) + 0.4x \tan \beta (\tan \phi \sin \beta - \tan \alpha) - K_a b \right] \qquad \text{for } x \leq x_{rs} \tag{4.8}$$

$$p_{sd} = K_a b \gamma'_s x (\tan^8 \beta - 1) + (0.4 b \gamma_s x \tan \phi \tan^4 \beta) \qquad \text{for } x \geq x_{rs} \tag{4.9}$$

97

where ϕ is the friction angle of sand, $\alpha = \phi/2$, $\beta = 45 + \phi/2$, $K_a = \tan^2(45 - \phi/2)$ and γ_s' is the submerged unit weight of sand. The value of x_{rs} is the value of the depth of reduced resistance of sand and is calculated by the intersection of Eqs. (4.8) and (4.9).
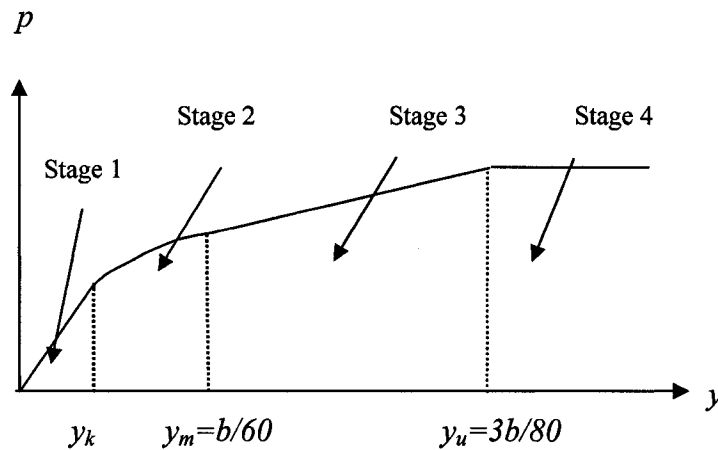
Figure 4.7 The nonlinear soil behavior of sand below water table subjected to cyclic loading after Reese et al. (1974).

Table 4.2 The p-y relationships for sand for the different soil stages

Soil Stage	Deflection range	p-y Relationships
Linear elastic	$0 < y < y_k$	$p = (kx)y$
Parabolic nonlinear	$y_k < y < y_m$	$p = \left(\dfrac{60}{b}y\right)^{0.8\left(\frac{A_c}{B_c}-1\right)} p_m$
Linear hardening	$y_m < y < y_u$	$p = p_s\left[B_c + \dfrac{48}{b}\left(y - \dfrac{b}{60}\right)(A_c - B_c)\right]$
Plastic flow	$y > y_u$	$p = p_u$

According to Reese et al. (1974), the sand is assumed to be cohesionless sand. Reese and Van Impe (2001) recommended that triaxial compression tests be performed to obtain the friction angle of sand. Confining pressures should be used which are close or equal to

98

those at the depths are being considered in the analysis. However, frequently the friction angle is estimated from results of some type of insitu test since it may be impossible to obtain undisturbed samples (Reese and Van Impe, 2001).

4.3.2   Soil behavior for non-homogeneous soil

Based on field experiments with full-sized piles, analytical expressions were developed for p-y curves for various types of homogeneous soil. The nonlinear p-y models of soft clay and sand for homogeneous soils presented above should now be treated differently since the soil is no longer homogeneous. The non-homogeneity can be incorporated in the p-y models using the equivalent thickness method proposed by Georgiadis (1983). This method is based on the continuity of ultimate lateral soil reaction resultant.

The present research focuses mainly on the sensitivity analysis of laterally loaded piles embedded in non-homogeneous soil of layered type. The soil stratification considered is a layer of clay overlaying a layer of sand. A pile of length l is embedded in soil consisting of an upper layer of soft clay of depth H_l overlaying an extended layer of sand where the depth of embedment of the pile in sand is H_2 as shown in Figure 4.8. The water surface is at the ground level and the pile is subjected to cyclic loading.

To develop the p-y curves for this case, the upper soft clay layer is treated as if the soil consists altogether of soft clay. However, when dealing with the lower sand layer, an equivalent depth of sand, h_2, corresponding to the upper layer should be determined in order to treat the sand layer as if it was a homogeneous layer of sand. The key factor in determination of this depth, h_2, is that the value of the sum of the ultimate soil resistance provided by the upper soft clay is equal to the ultimate soil resistance provided by the equivalent sand layer at the interface between the two layers.

This postulate allows for the determination of a local coordinate system of the lower layer of soil that is analyzed by means of the p-y model for homogeneous soil. The equivalent depth, h_2, at which the local coordinates of the sand start, is thus calculated by equating the forces F_l and F_2 given in the following equation:

99

$$F_1 = \int_0^{H_1} p_{ult} dx \qquad\qquad F_2 = \int_0^{h_2} p_s dx \qquad\qquad (4.10)$$

where F_1 is the sum of the ultimate soil resistance of the upper soft clay layer, F_2 is the sum of the ultimate soil resistance of the equivalent depth of sand. The values of p_{ult} for clay are computed according to Eq. (4.5) while those for sand are computed according to Eqs (4.8) and (4.9).

To employ the p-y models for soft clay and sand in the sensitivity analysis of the non-homogeneous soil, each layer is treated through its local coordinates. The local coordinates of the clay layer start at the ground surface (local coordinates x_1), while that of the sand layer starts from a depth h_2 from the interface between the two layers (local coordinates x_2). These local coordinates, shown in Figure 4.8, are used to determine the proper depth x used in the p-y relationships.
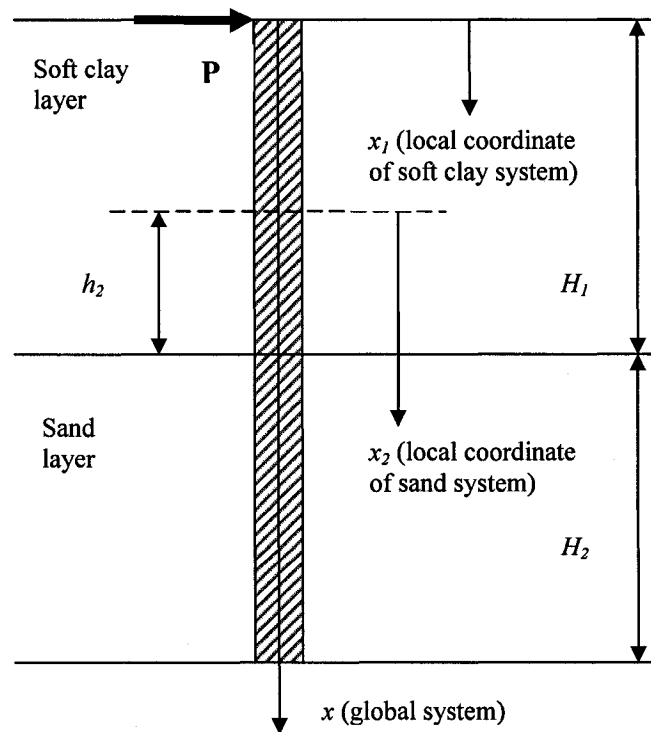
Figure 4.8 The coordinate systems for a pile embedded in non-homogeneous soil

100

CHAPTER 5

THEORETICAL FORMULATION

5.1 INTRODUCTION

In Chapter 3, it was concluded that sensitivity analysis is uniquely connected with the type of an investigated system and with the physical model employed in analysis of the structural system. Different methods of sensitivity analysis were presented. From the presentation, it was found that the most appropriate method for fulfilling the current research purpose is the adjoint variable method of nonlinear sensitivity analysis with a distributed parameter approach (Section 3.5.4).

The adjoint method is preferred over the direct differentiation method since the number of design variables in our study is considerably more than the number of performance measures needed to be investigated. The current research investigates the sensitivity of the performance of laterally loaded piles to the variation of the different design variables. The suitable indicators of a performance of laterally loaded piles are their maximum generalized deflections, i.e. the lateral pile-head deflection and pile-head rotation. These quantities are crucial serviceability measures for the behavior of the superstructure supported by the pile system. Good and safe performance of the piles will be achieved if these measures are satisfied.

The design variables studied are the pile and soil parameters involved in the p-y models. The models are highly nonlinear and require the involvement of various soil strength parameters as well as pile structure as described in Chapter 4. These mathematical p-y models for non-homogeneous soil (Section 4.3) will be used for the sensitivity analysis and serve basically for the determination of the kinematics and strength performance of the laterally loaded pile-soil systems.

101

The distributed parameter approach is used rather than the discretized one as pointed out in Section 3.5.4. This approach considers the material properties (in general terms) as the spatial functions. The sensitivity theory, through the fact of making the material parameters spatially dependent functions, is able to show where and how these material changes are distributed in the system investigated. The spatial functions determined in the scope of sensitivity analysis that allow assessing and localizing those parameters that affect the performance of the system are called the sensitivity operators or sensitivity integrands. Physically, they represent the potential material change that contributes to the changes in the performance of the system. The graphical presentation of those sensitivity operators is one form of the sensitivity results. Besides this form of results, another four important quantities are calculated. These sensitivity results are of key importance in the design stage, the assessment of the aging infrastructure system and in general, in decision making process.

In this chapter, the theoretical formulation of sensitivity for both single and pile groups are presented in Sections 5.2 and 5.3, respectively. For the single piles (Section 5.2), the adjoint variable method of sensitivity analysis will be used for obtaining the theoretical formulation of the sensitivity problem. The theoretical formulation for the sensitivity analysis is derived using three different formulation techniques associated with the adjoint variable method. These are the formulation based on the virtual work principle, the formulation using energy and load forms and the formulation based on Lagrange multipliers method. The derivation for each technique will then be presented followed by a comparison between the results obtained from the different techniques. Finally, the different forms of the sensitivity results are obtained. For the pile group (Section 5.3), the theoretical formulation for the single piles is extended to pile groups by applying suitable modification.

102

5.2 THEORETICAL FORMULATION FOR SINGLE PILES

5.2.1 Sign convention and pile modeling

The sign conventions which are commonly used for laterally loaded piles (Reese and Van Impe, 2001, Evans and Duncan, 1982 and Wang and Reese, 1993) are followed here in the dissertation. Figure 5.1 shows the sign conventions used in the derivation of the theoretical formulations. In Figure 5.1, y denotes the deflection, θ denotes the angle of rotation, M denotes the bending moment, V denotes the shear force and p denotes the soil reaction (p is taken positive when it is pointing from right to left since the equations of p-y are given as $p = +Ey$ rather than $p = -Ey$.)
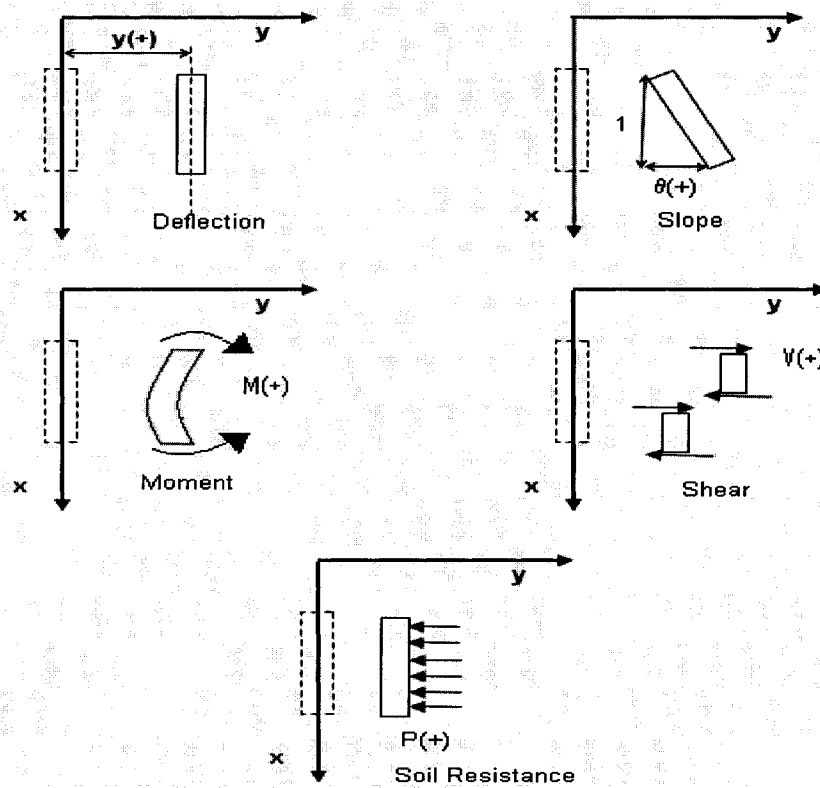
Figure 5.1 Sign conventions used in the derivation of the theoretical formulation

103

The laterally loaded pile is modeled as a one-dimensional beam on elastic foundation (Hetenyi, 1946 and VanImpe and Reese, 2001). For a laterally loaded pile subjected to a positive lateral load P_t and bending moment M_t as shown in Figure 5.2, the following equations describe the pile behavior:

$$\theta = y' \tag{5.1}$$

$$M = EIy'' \tag{5.2}$$

$$V = \frac{dM}{dx} = EI\frac{d^3 y}{dx^3} = EIy''' \tag{5.3}$$

$$p = -\frac{dV}{dx} = -EI\frac{d^4 y}{dx^4} = -EIy'''' \tag{5.4}$$
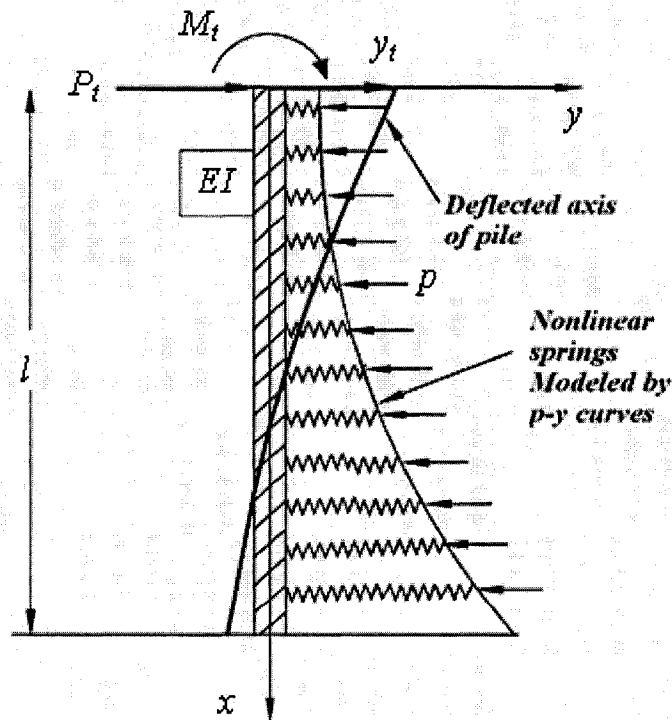
Figure 5.2 Laterally loaded pile subjected to a lateral load P_t or bending moment M_t

104

5.2.2 Formulation based on Virtual Work Principle

The lateral pile-head displacement occurring at the top of the pile y_t and the angle of rotation at the top of the pile θ_t are the performance measures subject to sensitivity analysis. Thus the first variation of these kinematic field components, considered as important serviceability measures, due to the variations in the design parameters is sought. The sensitivities of these performance measures are given in the following subsections, respectively. For each performance measure, two cases of loading of the pile are considered; the first is for piles subjected to lateral load applied at the pile head and the second is for piles subjected to bending moment also applied at the top of the pile.

5.2.2.1 Sensitivity of the lateral pile-head deflection

Consider a pile of length l embedded in a non-homogeneous soil medium of layered type. The non-homogeneous soil consists of a layer of soft clay overlying sand. The pile is subjected to a lateral force or a bending moment at the pile head as shown in Figure5.2. The behavior of the non-homogeneous soil is described by the nonlinear p-y models given in Chapter 4. The design variables considered for investigation are the pile's bending stiffness and the parameters defining the p-y relationships for the adjacent soil; soft clay and sand. The design variables are gathered in the following vector of design variables u:

$$u = \{EI, b, \gamma'_c, c, \varepsilon_{50}, \gamma'_s, \phi, k\}^T \tag{5.5}$$

where EI is the pile's bending stiffness and $\{\}^T$ denotes the transpose of the vector.

According to Eq. (5.5), the explored system forms an eight parameter sensitivity system. The maximum value of the lateral deflection is connected with the pile head, thus the maximum deflection occurs at the top of the pile and is denoted as y_t. It is considered as an indicator of serviceability of the supporting system that affects the serviceability of the superstructure. The critical notion that is postulated in this analysis is that change of

105

deflection is not associated with the change of load but with other factors that affect the deflection of the system in similar fashion as deformability when subjected to load.

As discussed previously, the distributed parameter sensitivity can be explored by means of an adjoint system method. The virtual displacement of the adjoint system, by definition, is measured from the equilibrium configuration of the primary structure (Malvern, 1969). It is worth noting that while the virtual displacement and associated strains and rotations are infinitesimal, no restrictions are placed on the magnitudes of the actual displacements from any reference configuration to the equilibrium configuration. The principle can therefore be used also in finite-displacement problems.

The determination of the change of maximum deflection δy_t can be obtained based on the virtual work principle employed in the virtual load method. Thus, it requires introducing the adjoint structure that defines state of deformation of the original structure. The original structure is called the primary structure and is subjected to a lateral load P_t or bending moment M_t. The change of lateral top deflection δy_t caused by the change of the design variables δu is obtained by subjecting the adjoint pile to a unit lateral load, 1_a, at the pile head in the positive direction of the pile deflection . Both the primary and adjoint piles for the two loading cases of the primary pile are shown in Figures 5.3 and 5.4.

Using the virtual load principle, δy_t is given as:

$$1_a \delta y_t = -(\int_0^l -M_a \delta y'' dx + \int_0^l -p_a \delta y dx) = \int_0^l M_a \delta y'' dx + \int_0^l p_a \delta y dx \qquad (5.6)$$

where M_a and p_a are the internal forces (bending moment and soil reaction) of the adjoint structure subjected to the unit lateral load 1_a, and $\delta y''$ and δy are the changes of the increment of angle of flexural rotation and deflection of primary structure (subjected to a lateral load P_t or bending moment M_t) caused by changes in the design variables, respectively.

106
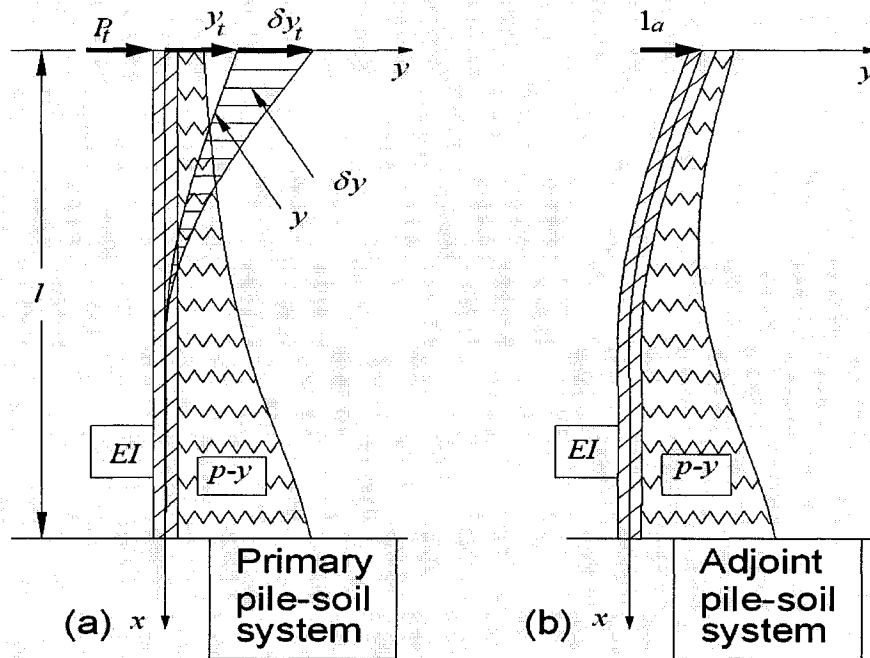
Figure 5.3 Primary and adjoint pile soil systems used for the sensitivity of lateral pile head deflection (a) primary pile subjected to lateral load P_t (b) adjoint pile subjected to a unit lateral load 1_a
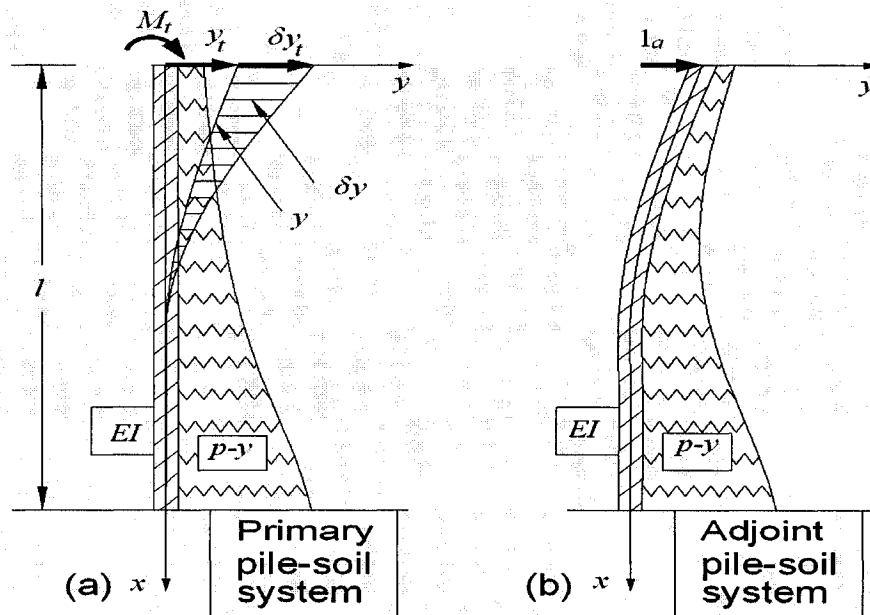
Figure 5.4 Primary and adjoint systems used for the sensitivity of lateral pile head deflection (a) primary pile subjected to bending moment M_t (b) adjoint pile subjected to a unit lateral load 1_a

107

It is worth noting that the minus sign in front of the integral of Eq. (5.6) means that an increase of δy_t requires the decrease of the design variables that represent the physical parameters of the system when the sustained load is constant (i.e. the increase in the deflection is because of the weakness of the material rather than an increase of load).

The interaction of two substructural materials such as the pile structure and the supporting soil system are defined in general terms as:

$$M = EIy'' = M(y, u). \tag{5.7}$$

$$p = p(y, u) \tag{5.8}$$

The increments of change of angle of flexural rotation $\delta y''$, and deflection δy of primary structure in the presence of constant load can be referred to increments of suitable internal forces of the primary structure as;

$$\delta M = \frac{\partial M}{\partial y''} \delta y'' + \frac{\partial M}{\partial u} \delta u \tag{5.9}$$

$$\delta p = \frac{\partial p}{\partial y} \delta y + \frac{\partial p}{\partial u} \delta u \tag{5.10}$$

It is worth noting that in Eqs. (5.7) and (5.9) the design variables vector u contains only one component that affects the pile material, that is EI, whereas Eqs. (5.8) and (5.10) have the remaining components of the design variables vector u that are associated with non-homogeneous soil.

Moreover, Eqs. (5.9) and (5.10) are characteristic equations of sensitivity analysis by the fact that they include the internal force-generalized displacement relationship and also the variability of the material parameters. This is considered as an intrinsic feature of sensitivity theory of distributed parameter. Equations (5.9) and (5.10) are given in

108

explicit fashion, which demonstrates simplicity of analysis and applicability to engineering practice.

Since the investigated primary system subjected to external load is in static equilibrium, therefore the increment of internal forces is not allowed to develop, thus they must vanish. This means that:

$$0 = \frac{\partial M}{\partial y''} \delta y'' + \frac{\partial M}{\partial u} \delta u \tag{5.11}$$

$$0 = \frac{\partial p}{\partial y} \delta y + \frac{\partial p}{\partial u} \delta u \tag{5.12}$$

Equations (5.11) and (5.12) provide basis for determination of the sought variation $\delta y''$ and δy. Thus these variations are obtained using Eq. (5.7) as:

$$\delta y'' = -\frac{\partial y''}{\partial M}\left(\frac{\partial M}{\partial u}\right)\delta u = -\left(\frac{\partial M}{\partial y''}\right)^{-1}\left(\frac{\partial M}{\partial u}\right)\delta u = -\frac{1}{EI}\left(\frac{\partial M}{\partial EI}\right)\delta EI = -\frac{1}{EI}y''\delta EI \tag{5.13}$$

$$\delta y = -\left(\frac{\partial p}{\partial y}\right)^{-1}\left(\frac{\partial p}{\partial u}\right)\delta u \tag{5.14}$$

then, substitution of Eqs. (5.13) and (5.14) into Eq. (5.6) gives the following outcome:

$$1_a \delta y_t = -\int_0^L \frac{M_a}{EI} y'' \delta EI dx - \int_0^L p_a \left(\frac{\partial p}{\partial y}\right)^{-1} \frac{\partial p}{\partial u} \delta u dx \tag{5.15}$$

where the adjoint pile is subjected to a positive lateral unit load and the primary pile is subjected to a lateral load P_t or bending moment M_t (Figures 5.3 and 5.4).

109

5.2.2.2 Sensitivity of the pile-head rotation

Based on the virtual work principle (the virtual load method), the change of lateral top rotation caused by the change of the design variables δu is obtained by introducing an adjoint pile, which defines state of deformation of the original pile subjected to a lateral load or bending moment, and subjecting this adjoint pile to a suitable loading. The adjoint pile should be subjected to a unit load (moment), 1_a, at the same location and in the same direction of the sensitivity performance measure under consideration for sensitivity. According to the sign convention given in Figure 5.1, a negative unit load (moment) is in the direction of the positive counter-clockwise rotation.

If a positive counter-clockwise rotation at the pile head is considered as the performance measure then a negative counter-clockwise unit bending moment should be applied to the adjoint pile at the pile head according to the sign convention given in Figure 5.1. However, we will subject the adjoint pile to a positive unit load (clockwise bending moment at the pile head) and consider the performance measure θ_t as the negative clockwise rotation at the pile head.

Figures 5.5 and 5.6 show the primary and adjoint piles used for determination of the sensitivity of the clockwise rotation of the pile head for primary piles subjected to a lateral load P_t and a bending moment M_t, respectively. Using the virtual load principle, the change of clockwise top rotation $\delta\theta_t$ is given as:

$$1_a\delta\theta_t = \int_0^l M_a\delta y'' dx + \int_0^l p_a\delta y dx \qquad (5.16)$$

where M_a, p_a are the internal forces (bending moment and soil reaction) of the adjoint structure subjected to the clockwise unit bending moment 1_a, and $\delta y''$, δy are the changes of increment of angle of flexural rotation and deflection of primary structure

110

(subjected to a lateral load P_t or bending moment M_t) caused by changes in the design variables, respectively.

Following the same steps from Eq. (5.6) to (5.15), the following result is reached:

$$1_a \delta\theta_t = -\int_0^L \frac{M_a}{EI} y'' \delta EI dx - \int_0^L p_a \left(\frac{\partial p}{\partial y}\right)^{-1} \frac{\partial p}{\partial u} \delta u dx \tag{5.17}$$

where the adjoint pile is subjected to a positive unit clockwise bending moment and $\delta\theta_t$ is the change of clockwise top rotation. The primary pile is subjected to a lateral load P_t or bending moment M_t (Figures 5.5 and 5.6).
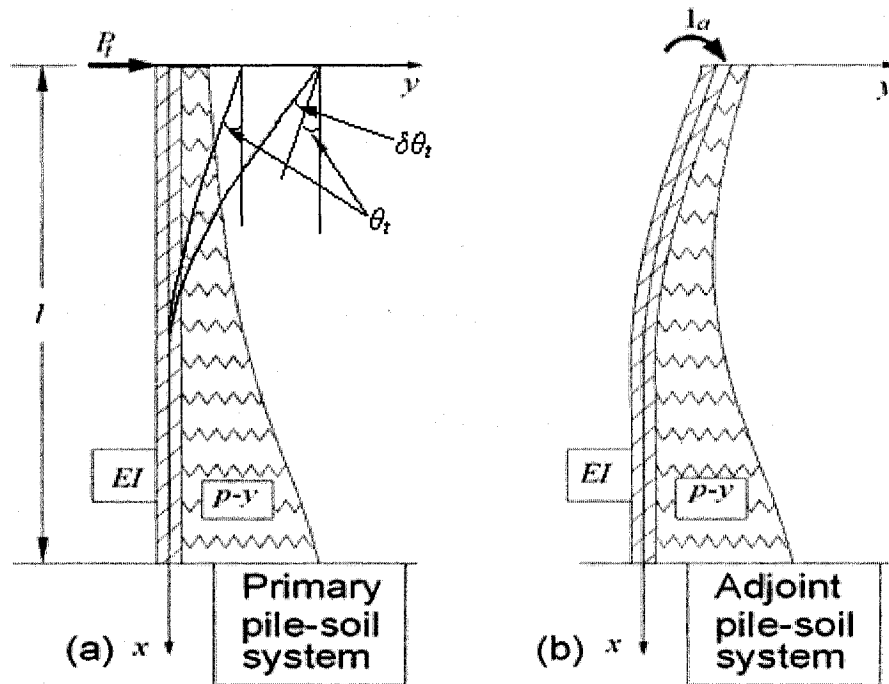
Figure 5.5 Primary and adjoint pile-soil systems used for the sensitivity of clockwise pile head rotation $\delta\theta_t$ (a) primary pile subjected to lateral load P_t (b) adjoint pile subjected to a unit bending moment 1_a

111
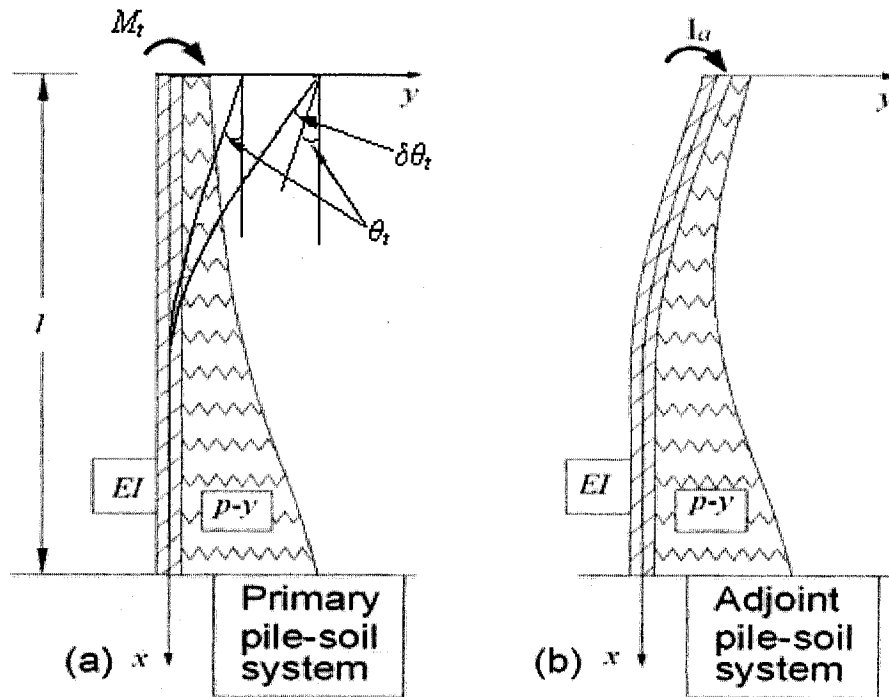
Figure 5.6 Primary and adjoint pile-soil systems used for the sensitivity of clockwise pile head rotation $\delta\theta_t$ (a) primary pile subjected to bending moment M_t (b) adjoint pile subjected to a unit bending moment 1_a

5.1.1   Formulation using energy and load forms

The formulation given in Chapter 3 for the adjoint method of sensitivity analysis for distributed parameter systems (Section 3.4.2) will be followed to derive the sensitivity of the pile's performance to changes in the design variables. The example of bending of a clamped beam with a normalized axial coordinate x, length l, subjected to a distributed lateral load $f(x)$ and with lateral displacement field z, was given in Section 3.4.2. While the previous analysis given in Chapter 3 has been carried out with the clamped-clamped beam, the same sensitivity results are valid for many other boundary conditions including the case of a cantilevered beam that has its own associated boundary conditions.

Since the laterally loaded pile is modeled in our study as a one-dimensional beam resting on p-y soil then the sensitivity results given in Section 3.4.2 are valid. The energy bilinear and load linear forms given are applicable for our cantilever studied case since the pile is subjected to a concentrated load or bending moment at the pile head as shown in Figure

112

5.2. The lateral displacement field is denoted as y in the figure however the derivation will proceed with the lateral displacement denoted as z to be consistent with derivation in Chapter 3.

Following the notations given in Chapter 3, the energy bilinear form is given as:

$$a_u(z,\bar{z}) = \int_0^l EIz''\bar{z}''dx \tag{5.18}$$

Accordingly, the variation $\delta a_{\delta u}$ given in Eq. (3.24) yields:

$$\delta a_{\delta u} \equiv \frac{d}{d\tau}[a_{u+\tau\delta u}(\tilde{z},\bar{z})]\big|_{\tau=0} = \frac{\partial}{\partial u}(a_u(\tilde{z},\bar{z}))\delta u \tag{5.19}$$

and since EI is the only component of u present in the energy bilinear form, then

$$\delta a_{\delta u} = \frac{\partial}{\partial EI}\left(\int_0^l EIz''\bar{z}''dx\right)\delta EI = \int_0^l (z''\bar{z}''\delta EI)dx \tag{5.20}$$

The load linear form is given as:

$$l_u(\bar{z}) = \int_0^l f\bar{z}dx \tag{5.21}$$

The distributed load f in our case is the soil reaction acting in the opposite direction of z which gives:

$$l_u(\bar{z}) = \int_0^l -p\bar{z}dx \tag{5.22}$$

113

Accordingly, the variation $\delta l_{\delta u}$ given in Eq. (3.25) yields:

$$\delta l_{\delta u} = \frac{d}{d\tau}[l_{u+\tau\delta u}(\bar{z})]\Big|_{\tau=0} = \frac{\partial}{\partial u}(l_u(\bar{z}))\delta u = \frac{\partial}{\partial u}\int_0^l(-p\bar{z}dx)\delta u = -\int_0^l(\frac{\partial p}{\partial u}\bar{z}\delta u)dx \qquad (5.23)$$

5.2.3.1 Sensitivity of the lateral pile head deflection

The first measure of the performance of the laterally loaded pile is the lateral deflection of the pile head (at the top of the pile), y_t. To obtain the required sensitivity of the pile lateral top deflection, the variation of a functional G_1, that defines the value of the displacement z (or y) at an isolated point $\hat{x}$, due to the variation in design variables is sought. The functional G_1 can be expressed as follows:

$$G_1 \equiv z(\hat{x}) = \int_0^l \hat{\delta}(x - \hat{x})z(x)dx \qquad (5.24)$$

where $\hat{\delta}(x)$ is the Dirac measure at zero.

The sought explicit design sensitivity is obtained from Eq. (3.35) as:

$$\delta G_1 = \int_0^l \frac{\partial g}{\partial u}\delta u dx + \delta l_u(\lambda) - \delta a_{\delta u}(z,\lambda) \qquad (5.25)$$

From Eqs. (5.24), (5.23) and (5.20) respectively, the three terms required for Eq. (5.25) are given as:

$$\int_0^l \frac{\partial g}{\partial u}\delta u dx = \int_0^l \frac{\partial}{\partial u}(\hat{\delta}(x - \hat{x})z(x))\delta u dx = 0 \qquad (5.26)$$

114

$$\delta l_u(\lambda) = -\int_0^l \frac{\partial p}{\partial u} \lambda dx \qquad (5.27)$$

$$\delta a_{\delta u}(z,\lambda) = \int_0^l (z''\lambda''\delta EI)dx \qquad (5.28)$$

Substituting the above three terms in Eq. (5.25) yields:

$$\delta G_1 = -\int_0^l \frac{\partial p}{\partial u}\lambda \delta u dx - \int_0^l z''\lambda''\delta EI dx \qquad (5.29)$$

where the adjoint variable λ is the solution of the adjoint equation of Eq. (3.31) given as:

$$a_u(\lambda, \bar{\lambda}) = \int_0^l [\frac{\partial g}{\partial z}\bar{\lambda} + \frac{\partial g}{\partial z'}\bar{\lambda}']dx = \int_0^l \hat{\delta}(x - \hat{x})\bar{\lambda}dx \qquad (5.30)$$

Interpreting the Dirac $\hat{\delta}$ function as a unit load applied at point $\hat{x}$, physical interpretation of λ is immediately obtained as the displacement of the beam (or pile) due to a positive unit load at $\hat{x}$. Thus the adjoint beam (or pile) in this case is just the original beam with a different load. Since the quantity under sensitivity investigation is the lateral deflection at the pile head, therefore $\hat{x}$ is equal to 0 and the adjoint pile is subjected to a unit load at the pile head. In addition, the system is nonlinear, therefore the unit load is applied to the adjoint structure which is in the state of deformation of the primary structure.

Denoting the lateral deflection as y instead of z and y_a as the solution of the adjoint pile subjected to unit lateral load instead of λ, δy_t is obtained from Eq. (5.29) as:

115

$$\delta y_t = -\int_0^l \frac{\partial p}{\partial u} y_a \delta u dx - \int_0^l y'' y_a'' \delta EI dx \tag{5.31}$$

or

$$\delta y_t = -\int_0^l y_a'' y'' \delta EI dx - \int_0^l y_a \frac{\partial p}{\partial u} \delta u dx \tag{5.32}$$

Figures 5.3 and 5.4 still represent the pile soil systems used in Eq. (5.32) where the adjoint pile is subjected to a unit lateral load and the primary pile is subjected to a lateral load P_t or bending moment M_t, respectively.

5.2.3.2 Sensitivity of the pile-head rotation

The second measure of the performance of the laterally loaded pile is the pile-head rotation (at the top of the pile), θ_t. The value of the rotation (or slope) at an isolated point $\hat{x}$ can be expressed as follows:

$$\theta(\hat{x}) = z'(\hat{x}) = \int_0^l \hat{\delta}(x - \hat{x}) z'(x) dx = -\int_0^l \hat{\delta}'(x - \hat{x}) z(x) dx \tag{5.33}$$

However, to be consistent with the derivation in Section 5.3, the performance measure under consideration is taken as the counter clockwise rotation at the pile head given as the performance functional G_2 in the following equation:

$$G_2 \equiv \theta_t = -\theta(\hat{x} = 0) = -z'(\hat{x}) = -\int_0^l \hat{\delta}(x - \hat{x}) z'(x) dx = \int_0^l \hat{\delta}'(x - \hat{x}) z(x) dx \tag{5.34}$$

The last equalities in Eqs. (5.33) and (5.34) represent an integration by parts that defines the derivative of the Dirac measure. In beam theory it is well known that the derivative of the Dirac measure is a point moment applied at the point $\hat{x}$. The preceding analysis

116

(Section 5.2.3.1) may now be directly repeated with $\hat{\delta}$ replaced by $\hat{\delta}'$, defining the adjoint equation

$$a_u(\lambda, \overline{\lambda}) = \int_0^l \hat{\delta}'(x - \hat{x})\overline{\lambda}dx \qquad (5.35)$$

Physically, λ is the displacement in an adjoint pile that is the original beam with a positive unit moment (clockwise) applied at the point $\hat{x}$.

As in the preceding, Eq. (5.25) is evaluated to obtain:

$$\delta G_2 = -\int_0^l \frac{\partial p}{\partial u} \lambda \delta u dx - \int_0^l z'' \lambda'' \delta EI dx \qquad (5.36)$$

Denoting the lateral deflection as y instead of z and y_a as the solution of the adjoint pile subjected to a positive clockwise unit moment at pile top instead of λ, the change in the lateral clockwise top rotation $\delta\theta_t$ is obtained from Eq. (5.36) as:

$$\delta\theta_t = -\int_0^l y_a'' y'' \delta EI dx - \int_0^l y_a \frac{\partial p}{\partial u} \delta u dx \qquad (5.37)$$

Figures 5.5 and 5.6 still represent the pile soil systems used in Eq. (5.37) where the adjoint pile is subjected to a positive clockwise unit bending moment and the primary pile is subjected to a lateral load P_t or bending moment M_t, respectively.

117

5.2.4 Formulation based on Lagrange Multipliers method

The Lagrange multipliers technique for distributed parameter systems presented in Section 3.4.4.1 is used in this section to derive the theoretical formulation of the adjoint sensitivity analysis.

5.2.4.1 Sensitivity of the lateral pile-head deflection

As mentioned in the previous section, the first measure of the performance of the laterally loaded pile is the lateral deflection of the pile head (at the top of the pile), y_t. The variation of a functional G_l, that defines the value of the lateral displacement y at an isolated point $\hat{x}$, due to the variation in design variables is sought. The functional G_l is expressed as follows:

$$G_1 \equiv y(\hat{x}) = \int_0^l \hat{\delta}(x - \hat{x}) y(x) dx \qquad (5.38)$$

The first variation of the functional G_1 due to the variations of the design variables vector can be determined based on the Lagrange method presented in Chapter 3 from Eq. (3.58). That is:

$$\delta G = \int_0^l \left(\frac{\partial g}{\partial u} \delta u + \lambda^T \frac{\partial F}{\partial u} \delta u \right) dx \qquad (5.39)$$

where u is the design variables vector given in Eq. (5.5), and g is defined from Eq. (5.38) as follows:

$$g = \hat{\delta}(x - \hat{x}) y(x) \qquad (5.40)$$

Accordingly,

$$\frac{\partial g}{\partial u} = 0 \tag{5.41}$$

From the equilibrium equation given in Eq. (3.44) the vector F which depends on the external load conditions, state variables vector z and design variables vector u as well is defined as:

$$F(z,u) = z' \tag{5.42}$$

where z' is the gradient of the state variables vector z which contains the following components:

$$z = \begin{Bmatrix} y \\ \theta \\ M \\ V \end{Bmatrix} \tag{5.43}$$

where y is the lateral deflection, θ is the angle of rotation, M is the bending moment and V stands for the shear force.

Using the relationships given in Eqs. (5.1) to (5.4), Eq.(5.42) gives:

$$F = \begin{Bmatrix} \theta \\ \dfrac{M}{EI} \\ V \\ -p \end{Bmatrix} \tag{5.44}$$

Differentiating with respect to the design variables vector u given in Eq. (5.5) with its appropriate corresponding components results in:

119

$$\frac{\partial F}{\partial u} = \begin{Bmatrix} 0 \\ \dfrac{\partial}{\partial u}\left(\dfrac{M}{EI}\right) \\ 0 \\ -\dfrac{\partial p}{\partial u} \end{Bmatrix} = \begin{Bmatrix} 0 \\ -\dfrac{M}{EI^2} \\ 0 \\ -\dfrac{\partial p}{\partial u} \end{Bmatrix} \qquad (5.45)$$

The components of the vector of Lagrange multipliers λ which describes the conjugated (adjoint) structure are denoted by a subscript a where λ is defined as:

$$\lambda = \begin{Bmatrix} V_a \\ M_a \\ \theta_a \\ y_a \end{Bmatrix} \qquad (5.46)$$

and should satisfy Eq.(3.55) given in Chapter 3 that describes the behavior of the adjoint system and is repeated below as:

$$\lambda' + \left(\frac{\partial F}{\partial z}\right)^T \lambda + \left[\frac{\partial g}{\partial z} - \frac{d}{dx}\left(\frac{\partial g}{\partial z'}\right)\right]^T = 0 \qquad (5.47)$$

The explicit form of each of the terms of Eq. (5.47) is as follows:

$$\frac{\partial F}{\partial z} = \left[\frac{\partial F}{\partial y}, \frac{\partial F}{\partial \theta}, \frac{\partial F}{\partial M}, \frac{\partial F}{\partial V}\right] = \begin{bmatrix} 0 & 1 & 0 & 0 \\ 0 & 0 & \dfrac{1}{EI} & 0 \\ 0 & 0 & 0 & 1 \\ -\dfrac{\partial p}{\partial y} & 0 & 0 & 0 \end{bmatrix} \qquad (5.48)$$

120

$$\left(\frac{\partial F}{\partial z}\right)^{T} = \begin{bmatrix} 0 & 0 & 0 & -\dfrac{\partial p}{\partial y} \\ 1 & 0 & 0 & 0 \\ 0 & \dfrac{1}{EI} & 0 & 0 \\ 0 & 0 & 1 & 0 \end{bmatrix} \tag{5.49}$$

$$\frac{\partial g}{\partial z} = [\hat{\delta}(x - \hat{x}), \ 0, \ 0, \ 0] \tag{5.50}$$

$$\frac{\partial g}{\partial z'} = [0, \ 0, \ 0, \ 0] \tag{5.51}$$

Taking into account definition (5.46), the final form for Eq.(5.47) is:

$$\frac{d}{dx} \begin{Bmatrix} V_a \\ M_a \\ \theta_a \\ y_a \end{Bmatrix} + \begin{bmatrix} 0 & 0 & 0 & -\dfrac{\partial p}{\partial y} \\ 1 & 0 & 0 & 0 \\ 0 & \dfrac{1}{EI} & 0 & 0 \\ 0 & 0 & 1 & 0 \end{bmatrix} \begin{Bmatrix} V_a \\ M_a \\ \theta_a \\ y_a \end{Bmatrix} + \begin{Bmatrix} \delta(x - \hat{x}) \\ 0 \\ 0 \\ 0 \end{Bmatrix} = \begin{Bmatrix} 0 \\ 0 \\ 0 \\ 0 \end{Bmatrix} \tag{5.52}$$

Performing the required operations in Eq.(5.52), the following system of equations define the adjoint pile system:

$$\frac{dV_a}{dx} = -\delta(x - \hat{x}) + \frac{\partial p}{\partial y} y_a \tag{5.53}$$

$$\frac{dM_a}{dx} = -V_a \tag{5.54}$$

$$\frac{d\theta_a}{dx} = -\frac{M_a}{EI} \tag{5.55}$$

121

$$\frac{dy_a}{dx} = -\theta_a \qquad (5.56)$$

These equations indicate that the adjoint structure is made of the same material as the primary structure and has the same type of support however the y axis is pointing to the right and the positive direction of the different quantities is shown in Figure 5.7. According to sign conventions in Figure 5.7, Eq. (5.53) shows that the soil reaction (distributed load in the positive direction of the soil reaction) of the system shown in Figure 5.7 is given as:

$$p_a = \frac{dV_a}{dx} = -\delta(x - \hat{x}) + \frac{\partial p}{\partial y} y_a \qquad (5.57)$$

Bearing in mind the properties of the Dirac delta function, Eq. (5.57) indicates that the adjoint structure shown in Figure 5.7 is subjected at the cross section $x = \hat{x}$ to a concentrated unit force in the positive direction of the y axis. Since the quantity under sensitivity investigation is the lateral deflection at the pile head, therefore $\hat{x}$ is equal to 0 and the adjoint pile is subjected to a positive unit load (in the positive direction of the y axis) applied at the pile head.

Physically, the above mentioned system for the adjoint pile is the same system for the primary pile shown in Figure 5.2 with the same sign conventions of Figure 5.1 (y axis pointing to the right) and with same governing Eqs. (5.1) to (5.4) given for the adjoint pile as:

$$\theta_a = y_a' \qquad (5.58)$$

$$M_a = EI y_a'' \qquad (5.59)$$

$$V_a = \frac{dM_a}{dx} = EI \frac{d^3 y_a}{dx^3} = EI y_a''' \qquad (5.60)$$

122

$$p_a = -\frac{dV_a}{dx} = -\delta(x - \hat{x}) + \frac{\partial p}{\partial y} y_a \qquad (5.61)$$

This adjoint system is subjected to a positive unit load applied at the pile head in the positive direction of the y axis. Thus Figures (5.3) and (5.4) still represent the adjoint and primary systems used in the analysis.
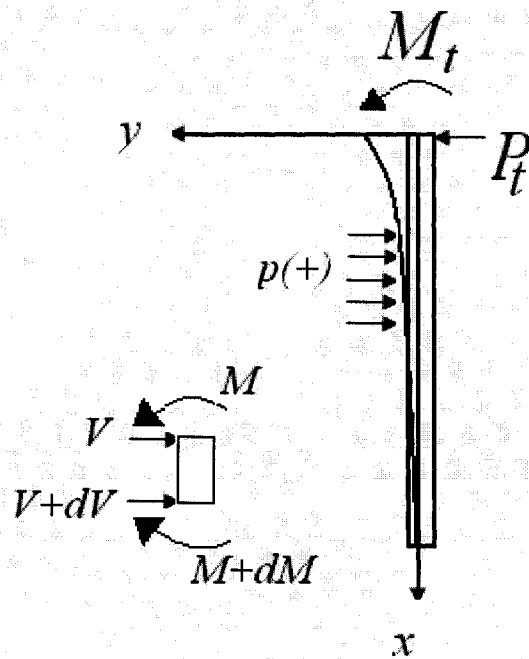
Figure 5.7 Adjoint pile structure defined by Equations (5.53) to (5.57)

Substituting Eqs. (5.41), (5.45) and (5.46) into Eq. (5.39) results in the first variation of the quantity required:

123

$$\delta G_1 = \int_0^l 0 + [V_a \quad M_a \quad \theta_a \quad y_a] \begin{Bmatrix} 0 \\ -\dfrac{M}{EI^2} \\ 0 \\ -\dfrac{\partial p}{\partial y} \end{Bmatrix} \delta u dx \qquad (5.62)$$

Denoting the functional G_1 as the lateral top deflection y_t and the vector λ as the solution of the adjoint pile subjected to a positive unit lateral load, δy_t is obtained from as:

$$\delta y_t = -\int_0^l \frac{M_a}{EI}\frac{M}{EI}\delta u dx - \int_0^l y_a \frac{\partial p}{\partial u}\delta u dx \qquad (5.63)$$

Using Eqs. (5.2) and (5.59), the result is given as:

$$\delta y_t = -\int_0^l y_a'' y'' \delta EI dx - \int_0^l y_a \frac{\partial p}{\partial u}\delta u dx \qquad (5.64)$$

Figures 5.3 and 5.4 represent the primary and adjoint pile-soil systems associated with Eq. (5.64).

5.2.4.2 Sensitivity of the pile-head rotation

As mentioned in the previous sections (Section 5.2.2.2 and 5.2.3.2), the performance measure under consideration is taken as the counter clockwise rotation at the pile head given as the performance functional G_2 in the following equation:

$$G_2 \equiv \theta_t = -\theta(\hat{x} = 0) = -z'(\hat{x}) = -\int_0^l \hat{\delta}(x - \hat{x})z'(x)dx = \int_0^l \hat{\delta}'(x - \hat{x})z(x)dx \qquad (5.65)$$

124

In beam theory it is well known that the derivative of the Dirac measure is a point moment applied at the point $\hat{x}$. The preceding analysis (Section 5.2.4.1) may now be directly repeated with $\hat{\delta}$ replaced by $\hat{\delta}'$ in Eq. (5.50) as:

$$\frac{\partial g}{\partial z} = [\hat{\delta}'(x - \hat{x}), \quad 0, \quad 0, \quad 0] \tag{5.66}$$

Accordingly Eq. (5.61) defining the adjoint system is given as

$$p_a = -\frac{dV_a}{dx} = -\hat{\delta}'(x - \hat{x}) + \frac{\partial p}{\partial y} y_a \quad \text{or} \quad \frac{dV_a}{dx} = \hat{\delta}'(x - \hat{x}) - \frac{\partial p}{\partial y} y_a \tag{5.67}$$

This adjoint system is subjected to a positive unit moment (clockwise) applied at the pile head. Thus Figures (5.5) and (5.6) still represent the adjoint and primary systems used in the analysis.

As in the preceding, Eq. (5.39) is evaluated to obtain:

$$\delta\theta_t = -\int_0^l y_a'' y'' \delta EI dx - \int_0^l y_a \frac{\partial p}{\partial u} \delta u dx \tag{5.68}$$

where $\delta\theta_t$ is the change of clockwise top rotation and y_a and y_a'' result from the solution of the adjoint pile subjected to a positive clockwise unit moment at the pile top as shown in Figures (5.5) and (5.6).

125

5.2.5 Comparison between formulations

Three different formulation techniques of the adjoint method (which are the technique based on the virtual work principle, the technique using energy and load forms and that based on Lagrange multipliers method) were used to derive the sensitivity formulations for the lateral pile head deflection and pile head rotation performance measures in Sections 5.2.2, 5.2.3 and 5.2,4, respectively. The results of the formulation for the sensitivity of the lateral pile head deflection were given in Eqs. (5.15), (5.32) and (5.63) for these methods, respectively while those for the sensitivity of the pile head rotation were given in Eqs. (5.17), (5.37) and (5.68), respectively.

The three equations for each performance measure have the same reference figures. Equations (5.15), (5.32) and (5.63) giving the first variation of lateral pile head deflection δy_t refer to Figures 5.3 and 5.4 where the adjoint pile is subjected to a unit load at the pile head and M_a, p_a, y_a, and y_a'' are obtained from the solution of that adjoint pile. These equations are repeated below:

$$1_a \delta y_t = -\int_0^L \frac{M_a}{EI} y'' \delta EI dx - \int_0^L p_a \left(\frac{\partial p}{\partial y} \right)^{-1} \frac{\partial p}{\partial u} \delta u dx \qquad (5.69)$$

$$\delta y_t = -\int_0^l y_a'' y'' \delta EI dx - \int_0^l y_a \frac{\partial p}{\partial u} \delta u dx \qquad (5.70)$$

$$\delta y_t = -\int_0^l y_a'' y'' \delta EI dx - \int_0^l y_a \frac{\partial p}{\partial u} \delta u dx \qquad (5.71)$$

Equations (5.17), (5.37) and (5.68) giving the first variation of the clockwise pile head rotation refer to Figures 5.5 and 5.6 where the adjoint pile is subjected to a unit positive

126

clockwise bending moment at the pile head and M_a, p_a, y_a, and y_a'' are obtained from the solution of that adjoint pile. These equations are repeated below for convenience.

$$1_a \delta\theta_t = -\int_0^L \frac{M_a}{EI} y'' \delta EI dx - \int_0^L p_a \left(\frac{\partial p}{\partial y}\right)^{-1} \frac{\partial p}{\partial u} \delta u dx \qquad (5.72)$$

$$\delta\theta_t = -\int_0^l y_a'' y'' \delta EI dx - \int_0^l y_a \frac{\partial p}{\partial u} \delta u dx \qquad (5.73)$$

$$\delta\theta_t = -\int_0^l y_a'' y'' \delta EI dx - \int_0^l y_a \frac{\partial p}{\partial u} \delta u dx \qquad (5.74)$$

From the first set of equations (Eqs. (5.69), (5.70) and (5.71)) it is clear that Eqs. (5.70) and (5.71) have the same final form while Eq. (5.69) is different from them. The terms on the right hand side of Eq. (5.69) are in terms of the generalized internal forces (soil reaction and bending moment) of the adjoint pile while for Eqs. (5.70) and (5.71) they are in terms of the generalized displacements (lateral deflection and change of angle of rotation) of the adjoint pile.

Accordingly, the relationship for the adjoint structure has to be postulated. The adjoint structure is considered as an incremental structure. This means that it deforms almost "infinitesimally" since the load applied is very small from the state of deformation of the primary structure. Thus, we can say that from the point of view of primary structure it is described by increment of generalized deformation. This unknown physical relationship of the adjoint structure is defined by Taylor's Linearization method of constitutive physical law. This means that the physical relationships for the primary structure (given in Eqs. (5.7 and 5.8) as $M = M(y'', u) = EIy''$ and $p=p(y, u)$ for bending moment and soil reaction, respectively) can be given in general terms in an incremental form by means of Taylor's expansion series as:

127

$$\delta M = \frac{\partial M}{\partial y''} \delta y'' \ , \qquad \delta p = \frac{\partial p}{\partial y} \delta y \qquad\qquad (5.75)$$

These increments are identified with the adjoint structure, thus application of Eq. (5.75) to the adjoint structure that is deformed in the vicinity of the applied load of primary structure and subjected to almost infinitesimal load 1_a gives:

$$M_a = \frac{\partial M}{\partial y''}\bigg|_{y^o} y_a'' \ , \qquad p_a = \frac{\partial p}{\partial y}\bigg|_{y^o} y_a \qquad\qquad (5.76)$$

where $\big|_{y^o}$ means that the partial differentiation is calculated at the vicinity of the applied load where the deflection of the primary structure is y^o.

Substitution of Eq. (5.76) into Eq. (5.69) results in:

$$
\begin{aligned}
1_a \delta y_t &= -\int_0^L \frac{M_a}{EI} y'' \delta EI dx - \int_0^L p_a \left(\frac{\partial p}{\partial y}\right)^{-1} \frac{\partial p}{\partial u} \delta u dx = \\
&= -\int_0^l \frac{EI}{EI} y_a'' y'' \delta EI dx - \int_0^l \frac{\partial p}{\partial y} y_a \left(\frac{\partial p}{\partial y}\right)^{-1} \frac{\partial p}{\partial u} \delta u dx \\
&= -\int_0^l y_a'' y'' \delta EI dx - \int_0^l y_a \frac{\partial p}{\partial u} \delta u dx
\end{aligned}
\qquad (5.77)
$$

Equation (5.77) shows that Eq. (5.69) and Eqs. (5.70 and 5.71) are the same. However, Eq. (5.69) requires differentiation to be conducted twice, whereas Eqs. (5.70 and 5.71) need the differentiation of the soil part to be conducted only once. Thus for one differentiation the round off errors are small. Accordingly the equation to be used in the analysis is Eq. (5.71) (or 5.70) since it is easy to conduct and the possibility of making numerical errors (and round off errors) is smaller.

128

The same discussion given above applies to the second set of equations (Eqs. (5.72), (5.73) and (5.74)) obtained from the different techniques for the sensitivity of the pile head rotation. The terms on right hand side of the three equations are similar to those of the first set of equations (Eqs. (5.69), (5.70) and (5.71)) except that M_a, p_a, y_a, and y_a'' are obtained from the solution of the adjoint pile that is now subjected to a unit bending moment instead of a unit lateral load. Therefore, for the same reasons mentioned above Eq. (5.74) will be used for the sensitivity analysis of the pile head rotation.

It is worth noting that the incremental approach (linearization of constitutive relationships) shown above for the adjoint structure provided consistent treatment for pile material and the soil medium. It is also noted that these postulated adjoint relationships (Eq. (5.76)) can be confirmed through the literature where the adjoint system for nonlinear structures is assumed to be linear as presented by Cardoso and Arora (1988), Choi and Santos (1987), and Haftka and Mroz (1986). In these references, the stress-strain relationship of the adjoint system is given with the following constitutive law:

$$\sigma_a = \frac{\partial \tilde{s}}{\partial \varepsilon} \varepsilon_a \qquad \qquad (\text{or } p_a = \frac{\partial p}{\partial y} y_a) \qquad \qquad (5.78)$$

where σ_a is the stress in the adjoint structure, $\tilde{s}$ denotes the nonlinear stress-strain relationship and ε_a is the strain in the adjoint structure.

In addition, it is also noticed that the same adjoint relationships appear in view of the Lagrange multipliers formulation where the adjoint relationships are given explicitly in Eqs. (5.58) to (5.61). Equations (5.59) and (5.61) are similar to the adjoint relationships given in Eq. (5.78).

From the above, it is concluded that Eq. (5.71) associated with Figures 5.3 and 5.4 will be used to obtain the sensitivity of the lateral pile head deflection while Eq. (5.74) associated with Figures 5.5 and 5.6 will be used to obtain the sensitivity of the pile head rotation. The different forms of sensitivity results will be derived in the following section.

129

5.2.6 Forms of sensitivity results

The sensitivity formulations resulted in Eq. (5.71) for sensitivity of lateral pile deflection and (5.74) for sensitivity of pile head rotation as mentioned above. The final results of the formulation to be practically used by the engineer are given in five forms. These are the sensitivity operators (S), the sensitivity factors (A), the percent change ratio (PCR), the total relative sensitivity factors (TF) and the group relative sensitivity factors (GF). These forms are explained below. These forms are derived for the lateral pile head deflection performance measure (Eq. (5.71)) then they will be generalized for the pile head rotation with different cases of loading of primary and adjoint piles in the last section.

5.2.6.1 Sensitivity operators /integrands S

Equation (5.71) for sensitivity of lateral pile head deflection is given as:

$$\delta y_t = -\int_0^l y_a'' y'' \delta EI dx - \int_0^l y_a \frac{\partial p}{\partial u} \delta u dx \qquad (5.79)$$

The soil consists of soft clay overlying sand and the parameters describing these two soils given in the p-y clay and sand relationships (Chapter 4) along with the pile's bending stiffness are the design variables. The design variables are given in vector u shown in Eq. (5.5). The suitable components of the design variables vector u are appropriately assigned to Eq. (5.79).

In addition the proper local coordinate systems are used for both clay and sand as derived in Chapter 4 and shown in Figure 4.8. From Figure 4.8 the local coordinates for each layer (x_1 and x_2) are used to determine the proper depth used in the p-y relationships at a certain location along the pile global axis x. For example; for the location at the top of the clay layer, the local axis x_1 used to substitute in the p-y clay relationships is equal to zero since the local coordinate x_1 and global coordinate x start from the same position at the ground surface. However, for the sand layer, the sand layer is considered to start virtually

130

at a level h_2 above the real interface between clay and sand to account for the presence of the top clay layer. Therefore at the real interface between the two layers (which is according to the global axis x at depth H_1 from the ground surface) the value of the depth x_2 (local axis) that is used to substitute in the p-y sand relationships is equal to h_2 as seen from the figure.

However when it comes to integration, the layers are integrated over their real lengths. The actual layer of sand doesn't start except at depth H_1 from the ground surface which is at depth h_2 from the local sand coordinate system. The integration is conducted for each layer according to its local coordinate system.

Taking the above into consideration, from Eq. (5.79) it is arrived at:

$$
\begin{aligned}
\delta y_t = & -\int_0^{H_1} y_a'' y'' \delta EI dx_1 - \int_0^{H_1} y_a [\frac{\partial p}{\partial b} \delta b + \frac{\partial p}{\partial \gamma_c'} \delta \gamma_c' + \frac{\partial p}{\partial \varepsilon_{50}} \delta \varepsilon_{50} + \frac{\partial p}{\partial c} \delta c] dx_1 \\
& -\int_{h_2}^{h_2 + H_2} y_a'' y'' \delta EI dx_2 - \int_{h_2}^{h_2 + H_2} y_a [\frac{\partial p}{\partial b} \delta b + \frac{\partial p}{\partial \gamma_s'} \delta \gamma_s' + \frac{\partial p}{\partial \phi} \delta \phi + \frac{\partial p}{\partial k} \delta k] dx_2
\end{aligned}
\tag{5.80}
$$

The review of Eq. (5.80) shows that terms under integrals associated with different design variables have different units. This fact makes assessment of sensitivity integrands inconvenient when comparison of various terms is required. The high nonlinearity of the system does not allow for normalization of changes of the performance with respect to the load values. Therefore, the applied load is considered in a discrete fashion and a normalization process for the variations of the design variables with respect to their initial values is performed. The normalization of variations of the design variables with respect to their initial values has two advantages. First, it allows expressing all the variations of the design variables in unitless form. Second, all resulting integrands have the same unit, which is unit of force.

131

Performing the normalization process Equation (5.80) can be written as:

$$\delta y_t = \int_0^{H_1} [-y_a'' y'' EI] \left[\frac{\delta EI}{EI} \right] dx_1 + \int_0^{H_1} [-y_a \frac{\partial p}{\partial b} b] \left[\frac{\delta b}{b} \right] dx_1 + \int_0^{H_1} [-y_a \frac{\partial p}{\partial \gamma_c'} \gamma_c'] \left[\frac{\delta \gamma_c'}{\gamma_c'} \right] dx_1$$

$$\int_0^{H_1} [-y_a \frac{\partial p}{\partial c} c] \left[\frac{\delta c}{c} \right] dx_1 + \int_0^{H_1} [-y_a \frac{\partial p}{\partial \varepsilon_{50}} \varepsilon_{50}] \left[\frac{\delta \varepsilon_{50}}{\varepsilon_{50}} \right] dx_1 + \int_{h_2}^{h_2+H_2} [-y_a'' y'' EI] \left[\frac{\delta EI}{EI} \right] dx_2 +$$

$$\int_{h_2}^{h_2+H_2} [-y_a \frac{\partial p}{\partial b} b] \left[\frac{\delta b}{b} \right] dx_2 + \int_{h_2}^{h_2+H_2} [-y_a \frac{\partial p}{\partial \gamma_s'} \gamma_s'] \left[\frac{\delta \gamma_s'}{\gamma_s'} \right] dx_2 +$$

$$\int_{h_2}^{h_2+H_2} [-y_a \frac{\partial p}{\partial \phi} \phi] \left[\frac{\delta \phi}{\phi} \right] dx_2 + \int_{h_2}^{h_2+H_2} [-y_a \frac{\partial p}{\partial k} k] \left[\frac{\delta k}{k} \right] dx$$

(5.81)

The expressions in small square brackets result in normalized sensitivity operators $S_{(.)}$ whereas the variations of design variables divided by their initial values give normalized variations of the design variables $\delta\, (..)_N$.

Thus Eq. (5.81) can be written as:

$$\delta y_t = \int_0^{H_1} S_{EI} (\delta EI_N) dx_1 + \int_0^{H_1} S_b (\delta b_N) dx_1 + \int_0^{H_1} S_{\gamma c} (\delta \gamma_{cN}') dx_1$$

$$+ \int_0^{H_1} S_c (\delta c_N) dx_1 + \int_0^{H_1} S_{\varepsilon 50} (\delta \varepsilon_{50N}) dx_1 + \int_{h_2}^{h_2+H_2} S_{EI} (\delta EI_N) dx_2 +$$

(5.82)

$$\int_{h_2}^{h_2+H_2} S_b (\delta b_N) dx_2 + \int_{h_2}^{h_2+H_2} S_{\gamma s} (\delta \gamma_{sN}') dx_2 + \int_{h_2}^{h_2+H_2} S_\phi (\delta \phi_N) dx_2 + \int_{h_2}^{h_2+H_2} S_k (\delta k_N) dx_2$$

where $S_{(.)}$ denotes the normalized sensitivity operators corresponding to each design variable $(.)$ which are given between [ ] in Eq. (5.81). The symbol $(\delta (..)_N)$ denotes the normalized variations of design variables corresponding to each design variable $(..)$, which are given between $\left[- \right]$ in Eq. (5.81).

132

The operators $S_{(.)}$ are spatial functions which when being integrated with respect to dx give final results in unit being product of force and length. (i.e. kN.m). Consequently, the left hand side of the equation has unit of work (i.e. kN.m) (note: the unit adjoint force 1_a (kN) was omitted from the left hand side) as the right hand side. The normalized variations of design variables denoted as $(\delta(..)_N)$ carry no units while the sensitivity operators carry a unit of force (kN).

The distributed parameter sensitivity analysis is conducted under a spatial integral, therefore, the sensitivity operators are called the sensitivity integrands. They are spatial functions that can be visualized graphically. The graphical presentation of these operators associated with each parameter along the pile length allows the engineer to detect the locations of maximum and minimum influence the change of that parameter has on the variation of the lateral pile head deflection.

Sensitivity operators/integrands for clay are plotted in the clay layer while those for sand are plotted in the sand layer. Sensitivity operators for the pile parameters b (pile diameter) and EI (pile's bending stiffness) appear in both clay and sand layers. It can be seen from Eqs. (5.81) and (5.82) that the sensitivity operator for the parameter b in the clay S_b has a different formula than that in sand since it depends on the p-y relationship which is different for clay and sand. Therefore, the sensitivity of lateral pile head deflection to change in the diameter b represented by the sensitivity operator S_b is plotted along both layers but has different formulae in clay and sand (Refer to Appendix A for details on values of S).

It is also seen from Eqs. (5.81) and (5.82) that the sensitivity operator for the parameter EI in clay has the same formula as that in sand since it doesn't depend on the p-y relationships. Therefore the sensitivity of lateral pile head deflection to change in the pile's bending stiffness EI represented by the sensitivity operator S_{EI} is plotted along both layers and has similar formulae in clay and sand.

133

More details about the different operators will be given in the numerical part when these operators are plotted for different cases. The graphical presentations of the sensitivity operators are presented for single piles and pile groups in Chapter 6. However a sketch of the results in that graphical form is given below in Figure 5.8 to demonstrate the physical meaning of these normalized sensitivity operators. In Figure 5.8, the normalized sensitivity operator/integrand $S_{(.)}$ is plotted against the location x on the pile. The value of $S_{(.)}$ indicates the influence the change of the design variable $_{(.)}$ has on the pile head lateral deflection. Thus the operators $S_{(.)}$ represent the influence line of the change of pile head lateral deflection caused by the moving variation of the design variable $(\delta(..)_N)$ equal to unit.

The location along the pile axis x with a greater value of $S_{(.)}$ indicates that there is more influence on the pile head deflection when this parameter changes at this location than for another location with a smaller value of $S_{(.)}$. Accordingly from Figure 5.8 the change of the parameter at point (a) has more influence on the change in the lateral pile head deflection than point (b), whereas there is no effect on the lateral pile head deflection when changing the parameter at point (c).

For each parameter, the normalized sensitivity operators have different expressions depending on the location along the pile and the lateral deflection of the pile. The different expressions for the sensitivity operators S for the eight studied parameters are given in Appendix A.

134
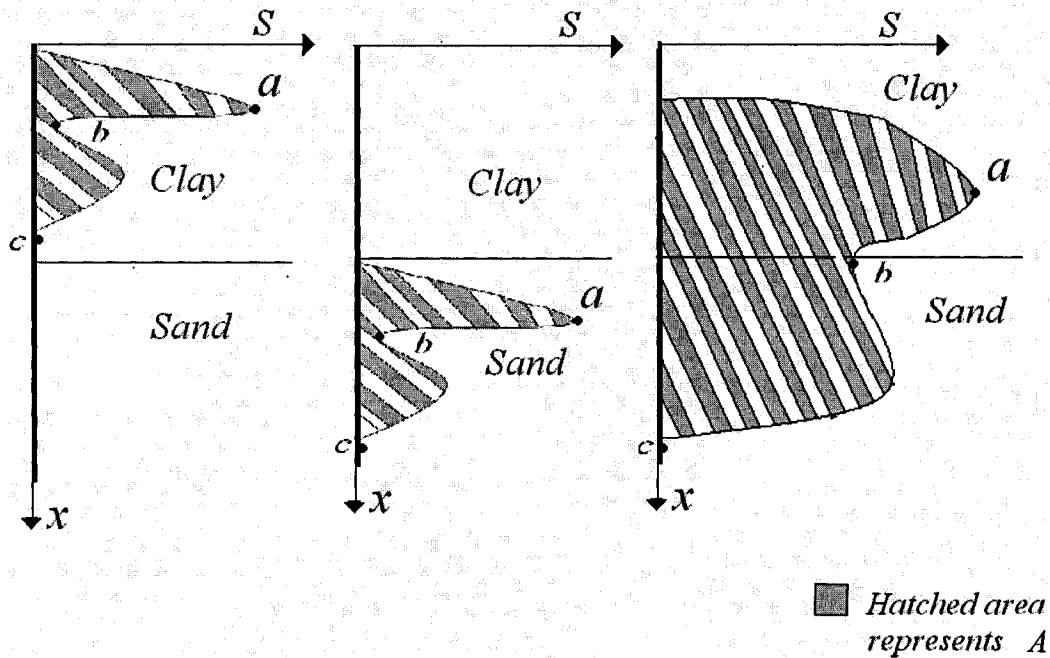
Figure 5.8 Sketch of the graphical form of sensitivity operators, S, and sensitivity factors, A, showing their physical meaning (a) for clay parameters, (b) for sand parameters and (c) for pile parameters

The importance of this form of results given in the graphical presentations of the sensitivity operators lie in the following:

1. allowing the engineer to detect the locations of maximum and minimum influence of each parameter on the performance of the system

2. giving the engineer more insight to the system behavior

3. allowing to visualize the soil-pile system transparently and revealing the black box behavior of the system that is not accessible.

4. based on the graphical presentations, sensors for measuring change in parameters can be located in proper positions

5. based on the graphical presentations, decisions by the engineer can be made in the design stage of the pile system or in the rehabilitation stage.

6. in soil exploration programs, the depths at which the sampling of soil properties is of particular importance can be estimated. Sensitivity analysis for every system provides rationale for economic and effective sampling.

135

5.2.6.2 Sensitivity factors A

The normalized variations of the design vectors denoted as $(\delta(..)_N)$ corresponding to each design variable $(..)$ are given between $\begin{bmatrix} - \end{bmatrix}$ in Eq. (5.81)

as $\left[\dfrac{\delta EI}{EI}\right], \left[\dfrac{\delta\gamma_c'}{\gamma_c'}\right], \left[\dfrac{\delta c}{c}\right], \left[\dfrac{\delta\varepsilon_{50}}{\varepsilon_{50}}\right], \left[\dfrac{\delta b}{b}\right], \left[\dfrac{\delta\gamma_s'}{\gamma_s'}\right], \left[\dfrac{\delta\phi}{\phi}\right] and \left[\dfrac{\delta k}{k}\right]$. These quantities can be taken out of the integral in Eq. (5.82) since they are constants resulting in the following equation:

$$
\begin{aligned}
\delta y_t = & (\delta EI_N)\int_0^{H_1} S_{EI}dx_1 + (\delta b_N)\int_0^{H_1} S_b dx_1 + (\delta\gamma_{cN}')\int_0^{H_1} S_{\gamma c}dx_1 \\
& + (\delta c_N)\int_0^{H_1} S_c dx_1 + (\delta\varepsilon_{50N})\int_0^{H_1} S_{\varepsilon 50}dx_1 + (\delta EI_N)\int_{h_2}^{h_2+H_2} S_{EI}dx_2 + \\
& (\delta b_N)\int_{h_2}^{h_2+H_2} S_b dx_2 + (\delta\gamma_{sN}')\int_{h_2}^{h_2+H_2} S_{ys}dx_2 + (\delta\phi_N)\int_{h_2}^{h_2+H_2} S_\phi dx_2 + (\delta k_N)\int_{h_2}^{h_2+H_2} S_k dx_2
\end{aligned}
\tag{5.83}
$$

Denoting the integral of the sensitivity operators introduced in Eq. (5.83) as the sensitivity factors $A_{(.)}$ the following equation is reached:

$$
\begin{aligned}
1_a\,\delta y_t = & (\delta EI_N)A_{EI} + (\delta b_N)A_b + (\delta\gamma_{cN}')A_{yc} + (\delta c_N)A_c + (\delta\varepsilon_{50N})A_{\varepsilon 50} + (\delta\gamma_{sN}')A_{ys} \\
& + (\delta\phi_N)A_\phi + (\delta k_N)A_k
\end{aligned}
\tag{5.84}
$$

These sensitivity factors that represent the integration of each sensitivity integrand with respect to spatial variables give the numerical value of the change of quantity of interest due to the change of the corresponding design variables. They carry unit of bending moment (kN.m). The numerical value of A gives the change of the top lateral deflection δy_t in meters when multiplied by the percent change in the parameter due to changing that parameter along the whole length of the pile with that certain percent. The sensitivity factors for clay parameters A_{yc}, A_c and $A_{\varepsilon 50}$ are the integration of sensitivity operators that appear in the clay while those for sand parameters A_{ys}, A_ϕ and A_k are the integration of

136

sensitivity operators that appear in sand. The sensitivity factors for the pile parameters A_{EI} and A_b are the integration of sensitivity operators that appear in both clay and sand. They are given as:

$$A_{EI} = \int_0^{H_1} S_{EI} dx_1 + \int_{h_2}^{h_2+H_2} S_{EI} dx_2 = \int_0^l S_{EI} dx = \int_0^l -y_a'' y'' EI dx \qquad (5.85)$$

$$A_b = \int_0^{H_1} S_b dx_1 + \int_{h_2}^{h_2+H_2} S_b dx_2 \qquad (5.86)$$

The physical meaning of the sensitivity factors $A_{(.)}$ can be demonstrated from Figure 5.8 in which the hatched area represents the sensitivity factors. The value of A for a given design variable represents the magnitude of the influence of that design variable on the pile head lateral displacement. The greater the value of A the more effective is the design variable on the variation of the lateral head displacement.

5.2.6.3 Percent Change Ratio PCR

The percent change ratio is the ratio between the percent change in the lateral top deflection (or top rotation) and the percent change in the variable. In other words, it answers the following question: if the parameter changes along the entire pile length with a certain percent what will be the percent change in the lateral deflection (or rotation) at the pile head?

If the change in y_t is required due to the change in only one parameter (c for example), then from Eq. (5.83) and (5.84):

$$\delta y_t = \int_0^{H_1} S_c (\delta c_N) dx_1 = A_c (\delta c_N) = A_c \left(\frac{\delta c}{c}\right) \qquad (5.87)$$

137

Dividing both sides of Eq. (5.89) by the lateral top deflection y_t to obtain the percent change in lateral top deflection $\left(\dfrac{\delta y_t}{y_t} \right)$ gives:

$$\frac{\delta y_t}{y_t} = \frac{A_c}{y_t} \left(\frac{\delta c}{c} \right) = PCR_c \left(\frac{\delta c}{c} \right) \tag{5.88}$$

Therefore,

$$PCR_c = \frac{A_c}{y_t} = \left. \left(\frac{\delta y_t}{y_t} \right) \middle/ \left(\frac{\delta c}{c} \right) \right. \tag{5.89}$$

Accordingly, *PCR* can be calculated directly from the value of A ($PCR=A/y_t$ or $PCR=A/\theta_t$). The numerical value of *PCR* gives the ratio between the % change in the top lateral deflection $(\delta y_t/y_t)$ and the percent change in the variable. i.e. if the variable c changes by a certain percent (10% for example), there will be a change in the lateral top deflection by a percent equal to $PCR*10$.

5.2.6.4 Total Relative sensitivity factors TF

The total relative sensitivity factor denoted by *TF* compares the influence of each design variable to all the design variables in the study given in vector u in Eq. (5.5). To measure the total relative sensitivity factor, the summation of the absolute values of all the sensitivity factors is first calculated as:

$$A_{tot} = \left| A_{\gamma c} \right| + \left| A_c \right| + \left| A_{\varepsilon 50} \right| + \left| A_{\gamma s} \right| + \left| A_{\phi} \right| + \left| A_k \right| + \left| A_{EI} \right| + \left| A_b \right| \tag{5.90}$$

The second step is to divide the sensitivity factor for each design variable by A_{tot} to obtain the total relative sensitivity factors *TF* as:

138

$$TF_{\gamma c} = \frac{\left|A_{\gamma c}\right|}{A_{tot}} \qquad (5.91)$$

$$TF_{c} = \frac{\left|A_{c}\right|}{A_{tot}} \qquad (5.92)$$

$$TF_{\varepsilon_{50}} = \frac{\left|A_{\varepsilon_{50}}\right|}{A_{tot}} \qquad (5.93)$$

$$TF_{\gamma s} = \frac{\left|A_{\gamma s}\right|}{A_{tot}} \qquad (5.94)$$

$$TF_{\phi} = \frac{\left|A_{\phi}\right|}{A_{tot}} \qquad (5.95)$$

$$TF_{k} = \frac{\left|A_{k}\right|}{A_{tot}} \qquad (5.96)$$

$$TF_{b} = \frac{\left|A_{b}\right|}{A_{tot}} \qquad (5.97)$$

$$TF_{EI} = \frac{\left|A_{EI}\right|}{A_{tot}} \qquad (5.98)$$

139

5.2.6.5   Group relative sensitivity factors GF

In the group relative sensitivity factor denoted by *GF* each design variable is compared with the design variables in its group. The parameters are divided into three groups; clay parameters, sand parameters and pile parameters. Accordingly the summation of the sensitivity factors is calculated for each group as follows:

$$A_{gc} = \left| A_{\gamma c} \right| + \left| A_c \right| + \left| A_{\varepsilon 50} \right|$$
(5.99)

$$A_{gs} = \left| A_{\gamma s} \right| + \left| A_{\phi} \right| + \left| A_k \right|$$
(5.100)

$$A_{gp} = \left| A_{EI} \right| + \left| A_b \right|$$
(5.101)

Then each design variable is compared with its group to get the group relative sensitivity factor for each parameter as:

$$GF_{\gamma c} = \frac{\left| A_{\gamma c} \right|}{A_{gc}}$$
(5.102)

$$GF_c = \frac{\left| A_c \right|}{A_{gc}}$$
(5.103)

$$GF_{\varepsilon 50} = \frac{\left| A_{\varepsilon 50} \right|}{A_{gc}}$$
(5.104)

$$GF_{\gamma s} = \frac{\left| A_{\gamma s} \right|}{A_{gs}}$$
(5.105)

$$GF_{\phi} = \frac{\left| A_{\phi} \right|}{A_{gs}}$$
(5.106)

$$GF_k = \frac{|A_k|}{A_{gs}} \tag{5.107}$$

$$GF_b = \frac{|A_b|}{A_{gp}} \tag{5.108}$$

$$GF_{EI} = \frac{|A_{EI}|}{A_{gp}} \tag{5.109}$$

5.2.7 Notations of results for different cases of primary and adjoint piles

All the above forms of the sensitivity results were derived for the sensitivity of the lateral pile head deflection. The same expressions given in the above results apply to the sensitivity of the pile head rotation since Eqs. (5.71) and (5.74) have similar terms on the right hand side of the equation except that y_a and y_a'' in Eq. (5.74) are obtained from the solution of the adjoint pile that is subjected to a unit bending moment instead of a unit lateral load. In addition, Eq. (5.71) for the sensitivity of the lateral pile head deflection is associated with Figures 5.3 and 5.4 while Eq. (5.74) for the sensitivity of the lateral pile head deflection is associated with Figures 5.5 and 5.6.

To differentiate between the different cases of loading of the primary and adjoint pile given in Figures 5.3 to 5.6, the notation to be used for the sensitivity operators S, sensitivity factors A, percent change ratio PCR, total relative sensitivity factors TF and group relative sensitivity factors GF corresponding to these figures is given in Figure 5.9.

141

Load type applied to the primary
structure,"M" for bendig moment,"P"
for lateral load

The studied pile response affected by
the changes of design variables,"y" for
lateral deflection, "θ" for rotation

X X

X

$(\bullet\bullet)$

Form of result S, A, PCR, TF or GF

The studied parameter, EI, b, γ'_c, c,
ε_{50}, γ'_s, ϕ or k
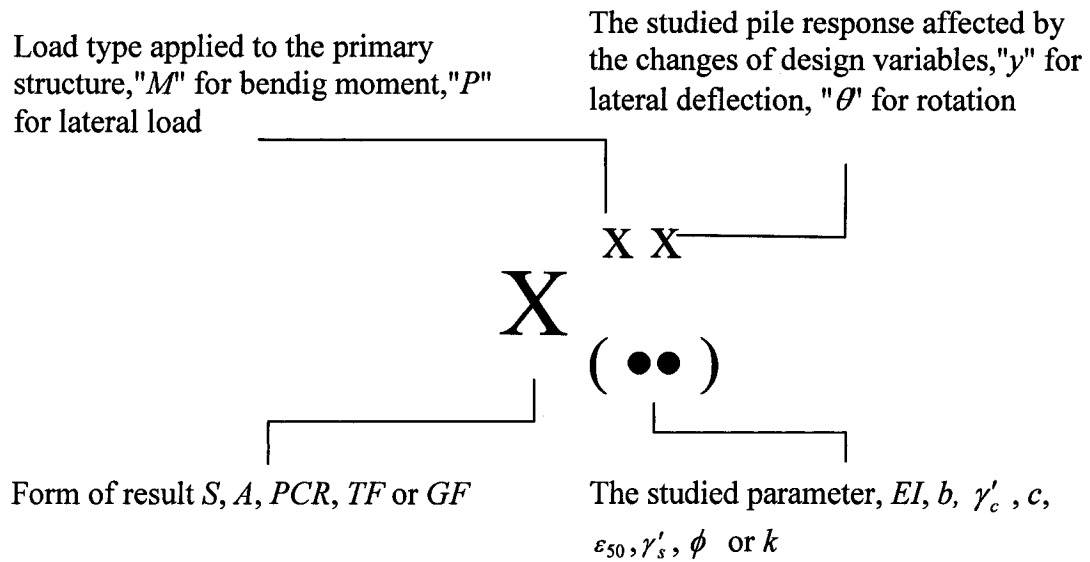
Figure 5.9 Notation used for different loading of primary and adjoint pile for the different forms of the sensitivity results

5.3 THEORETICAL FORMULATION FOR PILE GROUPS

5.3.1 Pile group arrangement

A typical view of the 3 x 3 pile group structure that will be considered in this study is shown in Figure 5.10. The nomenclature used for describing the locations of piles in the pile group is presented in Figure 5.11. The spacing between two adjacent piles in a row (denoted as s) or line (denoted as s') is described by the center to center (c/c) distance. The leading row is the first row on the right where the lateral load acts from left to right. The rows following the leading row are labeled as 1st trailing row, 2nd trailing row and so on.

142
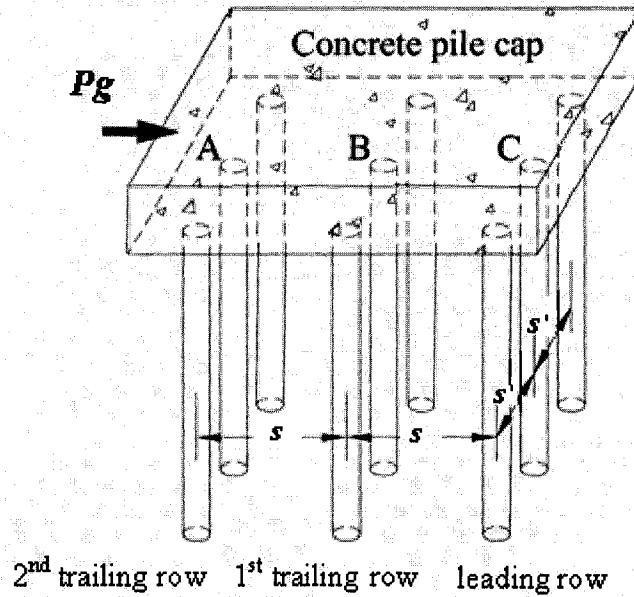
Figure 5.10 A typical view of the pile group system under a lateral load *Pg*
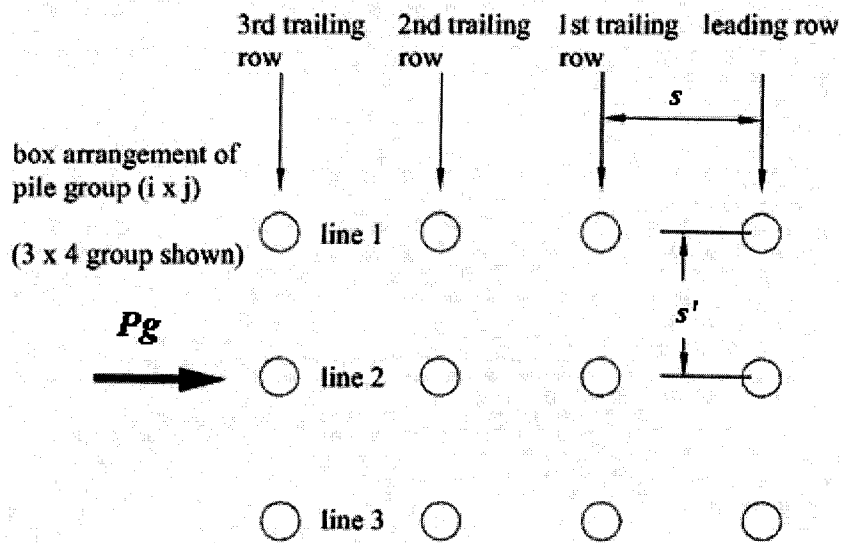
s = c/c spacing in direction of load (spacing between "rows" of piles)
s' = c/c spacing perpendicular to direction of load (spacing between "lines" of piles)
i = number of lines oriented parallel to direction of loading
j = number of rows oriented perpendicular to direction of loading
Pg = horizontal load applied to pile group

Figure 5.11 Nomenclature used to describe pile group arrangements

143

5.3.2 Difference in formulation between a single pile and a pile group

The theoretical formulation for a pile group is based on the formulation for the single pile given above in Section 5.2. The main difference between the formulations is that for the pile groups it is necessary to apply some modifications to the p-y relationships to account for the group effect. The concept of the p-multipliers presented by Mokwa and Duncan (2001b) is used in the current study to account for the group effect as pointed out in Section 2.3.2.7.

Mokwa and Duncan (2001b) formulated equations and proposed design curves for the p-multiplier, f_m, for all kinds of soil based on the analysis of the state-of-the-art soil values. They are used in the design of laterally loaded pile groups to account for the shadowing effect that describe the overlap of zones of resistance, and the consequential reduction of lateral soil resistance for piles in a group. To analyze a pile in a pile group, the lateral load resistance (p_{group}) of a pile in the group is equal to the lateral load resistance of a single pile (p_{single}) multiplied by a p-multiplier (f_m):

$$p_{goup} = f_m \, p_{single} \qquad\qquad (5.110)$$

Mokwa and Duncan (2001b) presented a chart (given in Figure 5.12) that shows p-multipliers as functions of pile spacing s (s is normalized by the diameter of the pile D) and pile location in a useful way for engineering design practice.

Brown and Reese (1985), Morrison and Reese (1986) and McVay et al. (1955) found that little variation exists among the response of piles in a given row. For this reason, the current state of practice is to associate the value of the p-multiplier (f_m) with the row and to use the value of f_m for all piles in the same row. It is generally assumed that p-multipliers are constant with depth, even when there are variations in the soil properties with depth. Another important observation with respect to the bending moments and shear forces is that for the corner piles in the leading row, the bending moment should be adjusted when the piles are spaced ($s<3D$) very closely as shown in Figure 5.12.

144

Pile Distance s (D)
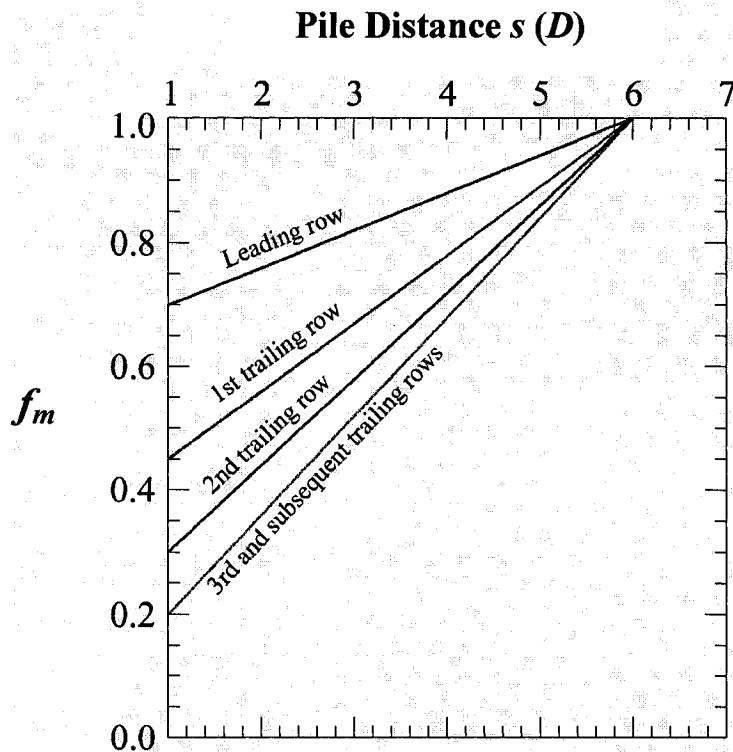
Notes:
Bending moments and shear forces computed for the
leading row corner piles should be adjusted as follows:

Side by side spacing	Corner pile factor
3D	1.0
2D	1.2
1D	1.6

Figure 5.12 The p-multiplier design curves proposed by Mokwa and Duncan (2001b)

5.3.3 Forms of the sensitivity results for pile groups

The five forms of the sensitivity results for pile groups are similar to those for single piles given in Section 5.2.6. The main difference is in the incorporation of the p-multiplier in the p-y relationship as pointed above and accordingly on the expressions of the sensitivity operators S and the other forms of results. The expressions for S given in Appendix A will thus be multiplied by f_m for all parameters except for EI which doesn't depend on p-y. The numerical study is presented for the pile groups in Chapter 6 (Section 6.3).

145

CHAPTER 6

NUMERICAL SENSITIVITY ANALYSIS

6.1 INTRODUCTION

The theoretical formulation of sensitivity analysis was presented in Chapter 5. In this chapter, numerical studies will be performed based on the obtained theoretical formulation. The different forms of sensitivity results given in Section 5.2.6 will be numerically calculated, graphically presented, analyzed and verified for both single piles and pile groups. The sensitivity results for single piles are presented in Section 6.2 while those for pile groups are presented in Section 6.3.

6.2 NUMERICAL ANALYSIS FOR SINGLE PILES

The input data used for the numerical study, scope of the analysis, programs used, modeling, analysis and discussion of the results and verification of the results are presented in the following subsections, respectively. In the analysis of the results, the effect of the nonlinearity of the system, the effect of non-homogeneity of the soil, the effect of the pile's boundary condition, the effect of the type of load and the effect of soil response studied are investigated.

6.2.1 Input data (Data used in the numerical analysis)

6.2.1.1 Design parameters

Initial values of the design variables are needed to perform the numerical sensitivity investigations since the sensitivity results are determined for constant initial values of the design variables. Obtaining clay, sand and pile parameters should be performed in a stage prior to performing the sensitivity analysis. Initial design parameters should be obtained

146

first by the designer using the *p-y* methodology and from conducting laboratory or field tests to obtain clay and sand parameters. After the initial design, parameter variations may be thought of as a result of

1. An imaginary experiment on the part of the analyst who may want to know the direction of change in system performance in order to possibly come up with an improved (optimized design). Accordingly, for example, the designer might chose to improve the soil rather than increase the pile's stiffness. Not only that but using the distributed parameter type of sensitivity will allow the designer to detect where the improvement is required exactly along the pile length or to what depth.

2. Unavoidable imperfections or uncertainties in the material properties (due to errors in testing for example), the effect of which have to be analyzed.

3. Deterioration of parameters that can occur by time where its effect has to be analyzed.

The design variables under investigation were given in Chapter 5 (design variables vector u in Eq. 5.5). In the dissertation, typical values of clay and sand parameters were chosen within the range that can be modeled using the soft clay and sand *p-y* criteria. These parameters would practically depend on the site investigated. Typical values of the design parameters were used as an example to show the results of sensitivity analysis and to perform the numerical investigations.

For soft clay, typical values of unconfined compressive strength for soft clay range from 20 to 40 kN/m^2 (Craig, 1978) or from 24 to 48 kN/m^2 as reported by Das (1997) and Brown (2001). A value of 36 kN/m^2 was chosen for the unconfined compressive strength, i.e. the undrained cohesion c was chosen to be equal to 18 kN/m^2. Wang and Reese (1993) suggested that a typical value of 0.02 can be used for ε_{50} (strain corresponding to one-half the compressive strength of clay) if no stress-strain curves are available. This value was chosen for the numerical analysis. A typical value of the submerged unit weight, γ_c', of soft clay was chosen as 7.5 kN/m^3 as reported by Terzaghi and Peck (1967) (Fellenius (1999) gave a range for γ_c' of 3 to 8 kN/m^3).

147

For sand, a medium dense sand that is rounded and uniform was chosen for the numerical investigation with angle of internal friction, ϕ, equal to $33°$ (Typical range of ϕ for that sand is given as 27.5 to $34°$ (Terzaghi and Peck, 1967) or 32 to $34°$ (Perloff and Baron, 1967)). A value of 10 kN/m^3 was chosen for the submerged unit weight of sand γ_s' (Das, 1997 and Perloff and Baron, 1967). Wang and Reese (1993) recommended a value of 16,286 kN/m^3 for the modulus of subgrade reaction, k. Accordingly, the following typical values are used in the current numerical study:

Design parameters for the soft clay layer: γ_c' = 7.5 kN/m^2; c = 18 kN/m^2; ε_{50} = 0.02

Design parameters for the sand layer: γ_s' = 10 kN/m^2; ϕ = $33°$; k = 16,286 kN/m^3

The pile used in this study is a standard hollow steel pile HSS 406x13 defined by "Hollow Structural Sections to ASTM A 500 Grade C" and issued by Canadian Institute of Steel Construction 2000. The section properties of the pile are presented in Figure 6. 1. Accordingly, the following design parameters for the pile are given as:

Design parameters for the pile: EI = 55,400 kN.m^2, b = 0.406m,

Pile Properties	
Type	ASTM A500 HSS 406
Mass	123 kg/m
b (outer diameter)	406 mm
nominal wall thickness	12.7 mm
design wall thickness	11.43 mm
$I_x = I_y$ (moment of inertia)	277 x10^6 mm^4
F_y (yield stress)	317 MPa
Modulus of elasticity E	2 x 10^8 kPa
Stiffness EI	55400 kN.m^2
Yield moment	508 kN.m
Area	14,200 mm^2
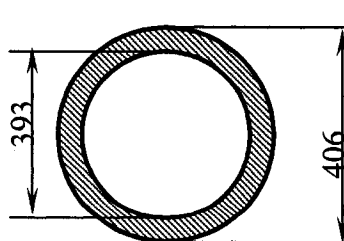
Figure 6.1 Pile's properties used in the sensitivity analysis

148

6.2.1.2 Soil stratification

To study the non-homogeneity of the soil consisting of soft clay overlying sand, 11 different cases of non-homogeneity (11 different soil stratifications) are studied. The soil stratifications cover different thicknesses of the upper clay layer which increases in an incremental fashion. These cases start from the special case of 0% of the pile's length embedded in clay and the rest of the pile embedded in sand, followed by 10%, 20%, 30%, 40%, 50%, 60%, 70%, 80%, 90% and finally reaches 100% of the pile's length embedded in clay.

The special case of 0% clay layer thickness means that the thickness of the upper soft clay layer is 0% of the pile's length and the thickness of the lower sand layer is 100% of the pile's length i.e the pile is embedded in a layer of homogeneous sand while the last case (100% clay layer thickness) is another special case where the pile is embedded in a homogeneous layer of clay. In the rest of the cases, soil is non-homogeneous with different thicknesses of the upper clay layer as a percent of the pile's length increasing by increments of 10 %.

6.2.1.3 Applied levels of load

The sensitivity analysis is developed in the vicinity of the applied load since we are dealing with a nonlinear behavior of the soil. Therefore the loading of the pile (horizontal force P_t or bending moment M_t) is applied in a discrete fashion. The loading is applied at the pile head (where the pile head is at the ground surface) in increments of 15 kN, 25 kN, 50 kN or 100 kN for horizontal force P_t and 50 kN.m or 100 kN.m for bending moment M_t depending on the pile's length and soil stratification.

For each case of non-homogeneity (soil stratification), the pile is loaded up to a load that causes the lateral deflection of the pile head to reach 0.305 m at the ground surface. This amount of deflection causes the clay at the ground surface to reach the plastic flow stage (refer to Figure 4.5). Accordingly, the various stages of soil deformability can be

149

investigated in the sensitivity analysis. For the case of 0% clay layer thickness, the lateral deflection of 0.305 m will fulfill that sand at the ground surface has also reached the plastic flow stage (where plastic flow in sand starts at deflection $y = 3b/80 = 0.015$ m as shown in Figure 4.7).

In some cases, the moment in the pile will exceed the allowable yield moment of the pile. In the results the level of load at which the yield moment is reached will be noted however the loading will continue until the allowable load criterion is satisfied. This is because we are interested more in the soil behavior and the yield moment for the pile can be easily increased if other types of piles were used.

6.2.1.4 Length of piles

The behavior of a laterally loaded pile depends on whether it is a long or a short pile. For long piles there is only small deflection at the bottom of long pile, so the long pile is considered as fixed at the bottom. The short pile keeps almost straight shape when the load is applied, and it rotates along a certain point located at the pile axis or can even translate laterally along the entire length if the pile head is fixed. A sketch for typical behavior (deformation) of long and short piles is shown in Figure 6.2.

(a)   (b)   (c)
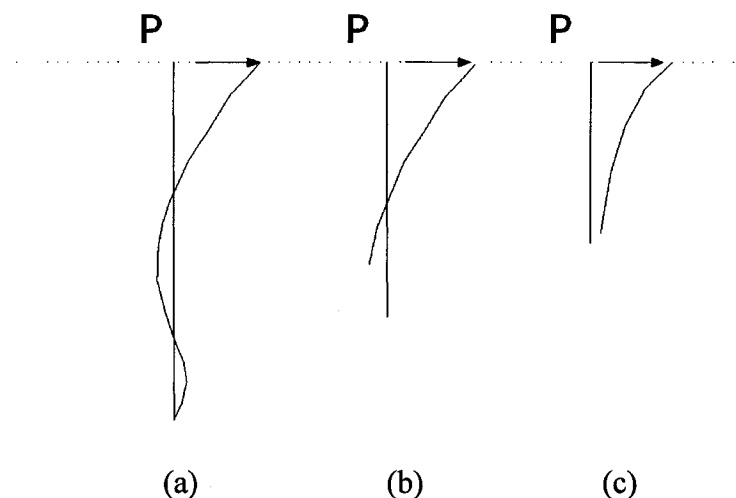
Figure 6.2 Sketch for (a) typical long pile behavior (b) typical short pile behavior (free head pile) (c) typical short pile behavior (fixed head pile)

150

For homogeneous soils described by the nonlinear *p-y* curves, the pile can be classified as long or short according to the characteristic load method (Evans and Duncan, 1982). Depending on a relative stiffness factor T, developed for homogeneous soil, the pile is classified into short for length $l < 4T$ and long for $l > 5T$. The relative stiffness factor T depends on the type of loading (horizontal force P_t or moment M_t), boundary conditions (free or fixed-head of pile), bending stiffness of the pile EI and the pile head horizontal displacement y_t.

The characteristic load method is used for homogeneous soils. However, the piles investigated in the current study are embedded in a non-homogeneous soil. To deal with such a case, the relative stiffness factor was calculated for a homogeneous layer of clay T_c and a homogeneous layer of sand T_s, both layers below water table and subjected to cyclic loading. An average value T_{av} $(T_{av}=(T_c+T_s)/2)$ was calculated based on average values of y_t/b found in the Evans and Duncan charts. This T_{av} is calculated for three different boundary conditions. Then according to numerical investigations using these T_{av} values, the pile is divided into long, short and intermediate for each boundary condition.

Since different values of load and different stratifications of soil for each boundary condition will be studied, using the average value T_{av} for each boundary condition, piles will be divided into long, short and intermediate for each of the three boundary conditions according to the following:

Long piles: All piles with a length greater than a certain value such that, starting from this length, piles will behave as a typical long pile for all cases of soil stratification (11 cases) and all cases of loading (or all values of applied load).

Short piles: All piles with length smaller than a certain value such that piles with smaller lengths will behave as a typical short pile for all cases of loading and all soil stratifications.

Intermediate piles: All piles in between the short and long piles such that they will behave as long or short depending on the soil stratification and the values of applied load.

151

For a long pile the critical case investigated to guarantee that all cases (for a length greater than or equal this length) will be long is the case with weakest soil stratification (special case of 100% clay layer thickness) and highest load. While for a short pile the critical case investigated to guarantee that all cases (for a length shorter than or equal this length) will be short is the case with strongest (stiffest) soil stratification (special case of 100% sand) and lowest applied load.

To calculate the values of T_{av} for each boundary condition, we have to calculate the relative stiffness factor for soft clay T_c and that for sand T_s for each boundary condition. The relative stiffness factor T depends on the type of loading (horizontal force P_t or moment M_t applied at the top of the pile), boundary conditions (free or fixed head pile), bending stiffness of the pile EI and the pile head horizontal displacement y_t. The relative stiffness factors T for the three boundary conditions are given as:

$$T = \sqrt[3]{\frac{y_t EI}{A_y P_t}} \quad \text{(For free or fixed head loading)} \tag{6.2}$$

$$T = \sqrt[2]{\frac{y_t EI}{B_y M_t}} \quad \text{(For pure moment loading)} \tag{6.3}$$

where $A_y = 2.43$ for a free head pile,

$\quad A_y = 0.93$ for fixed head pile, and

$\quad B_y = 1.62$.

Evans and Duncan (1982) presented charts to obtain the lateral load deflection y_t in terms of applied horizontal top load P_t or moment M_t. These charts are given in Figures 6.3 to 6.5 for the three boundary conditions of piles embedded in soft clay and in Figures 6.6 to 6.8 for the three boundary conditions of piles embedded in sand. The lateral deflection is given as a dimensionless parameter (y_t/b) where b is the pile's diameter. The applied loads P_t and M_t are given as dimensionless parameters (P_t/P_c) and (M_t/M_c) where P_c is the *characteristic shear load* and M_c is the *characteristic moment load*. The concept of the

152

characteristic shear load and *characteristic moment load* was developed by Evans and Duncan (1982) where they are expressed as follows:

$$P_c = \lambda b^2 ER_I \left(\frac{\sigma_p}{ER_I} \right)^m (\varepsilon_{50})^n \qquad (6.4)$$

$$M_c = \lambda b^2 ER_I \left(\frac{\sigma_p}{ER_I} \right)^m (\varepsilon_{50})^n \qquad (6.5)$$

where : P_c = characteristic shear load,

M_c = characteristic moment load,

b = diameter of the pile,

E = modulus of elasticity of pile (200GPa for steel),

m, n = exponents from Table 6.1,

λ = a dimensionless parameter on the soil's stress – strain behavior,

      where $\lambda = 1.00$ for plastic clay and sand

      $\lambda = (0.14)^n$ for brittle clay

R_I = characteristic moment of inertia given as:

$$R_I = \frac{I}{\pi b^4 / 64} \qquad (6.6)$$

where I = moment of inertia of pile,

      $R_I = 1.00$ for solid circular cross sections,

      $R_I = 1.70$ for square cross sections,

σ_p = representative passive pressure of soil , given as:

$$\sigma_p = 4.2 s_u \qquad \text{for cohesive soil} \qquad (6.7)$$

$$\sigma_p = 2C_{p\phi}\gamma\, b\, \tan^2(45° + \frac{\phi}{2}) \qquad \text{for cohesionless soil} \qquad (6.8)$$

153

where s_u = undrained shear strength of soil, in this study, $s_u = c$,

$C_{p\phi}$ = passive pressure factor = $\phi/20$

ϕ = angle of friction of soil (degree) from ground surface to a depth of 8 pile diameter

Table 6.1 Values of exponents m and n (Evans and Duncan, 1982)

Soil Type	For P_c		For M_c	
	m	n	m	n
Cohesive	0.683	- 0.22	0.46	- 0.15
Non Cohesive	0.57	- 0.22	0.40	- 0.15
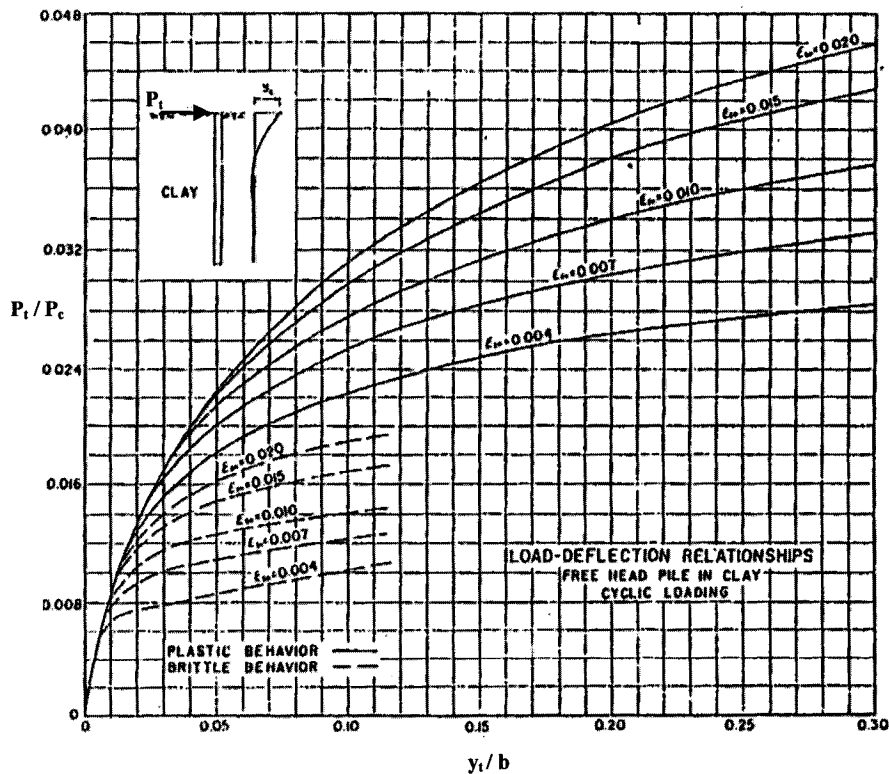
Figure 6.3 Load-deflection curves for free head pile in clay-cyclic (Evans and Duncan, 1982)

154
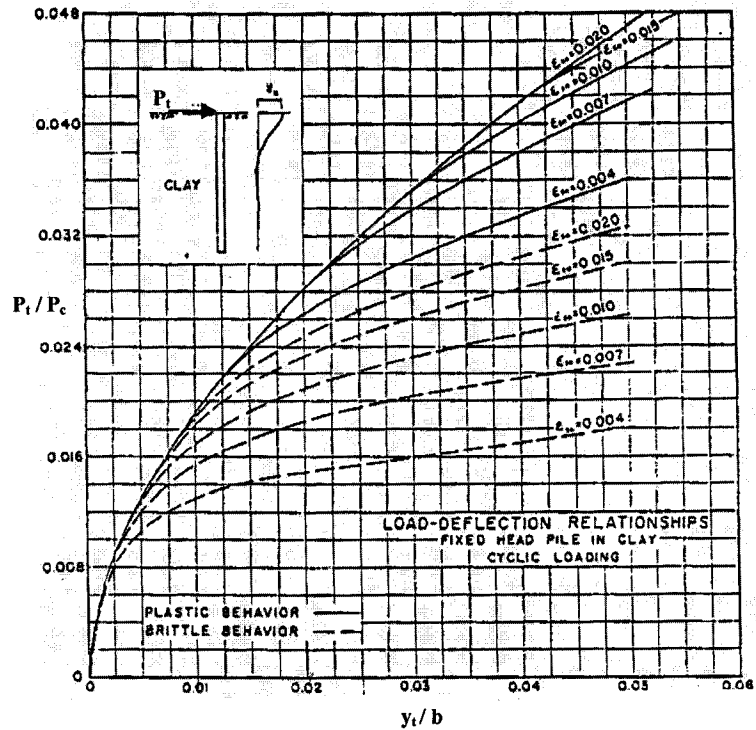
Figure 6.4 Load-deflection curves for fixed head pile in clay-cyclic (Evans and Duncan, 1982)
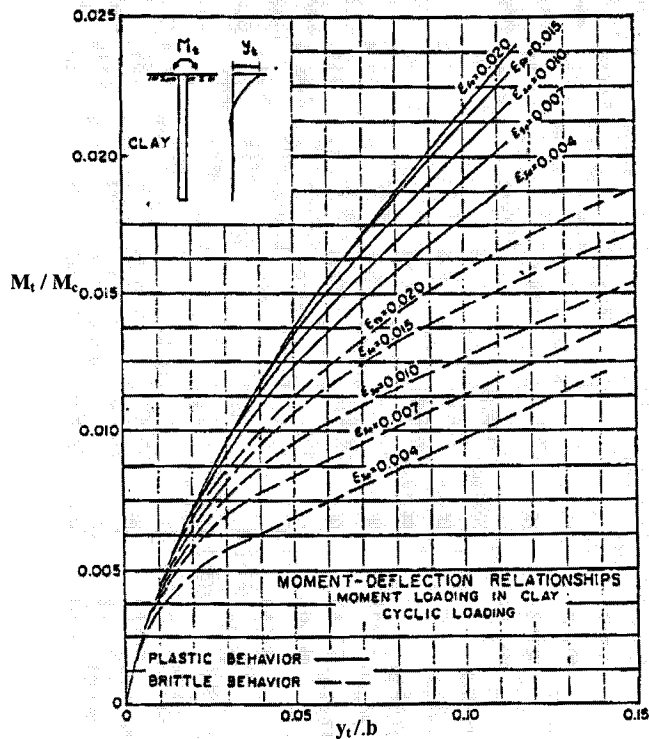
Figure 6.5 Moment-deflection curves for free head pile subjected to moment loading in clay-cyclic (Evans and Duncan, 1982)

155
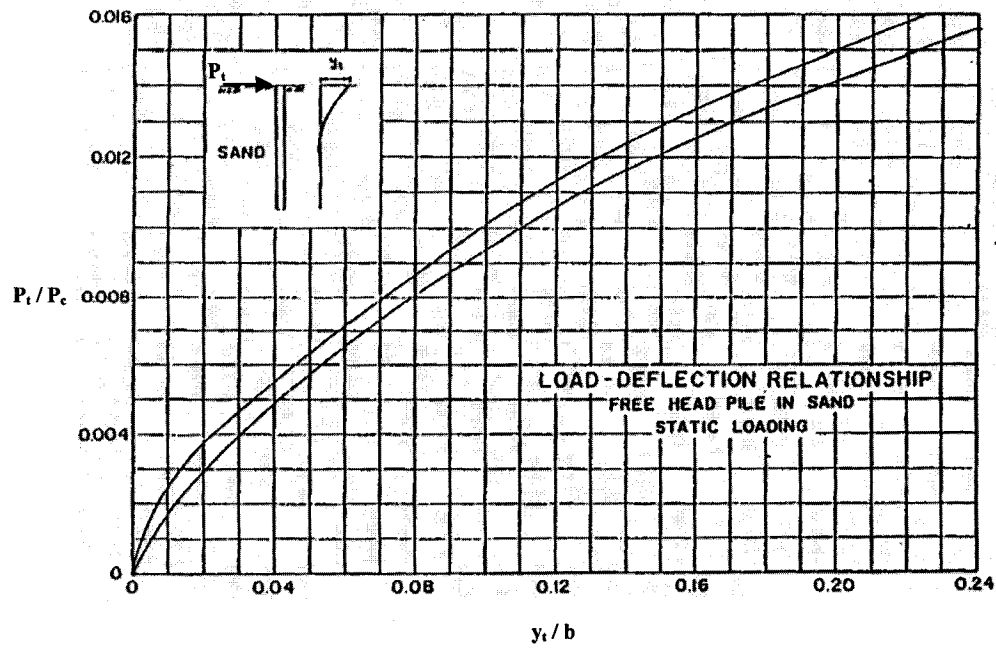
Figure 6.6 Load-deflection curves for free head pile in sand-static (Evans and Duncan, 1982)
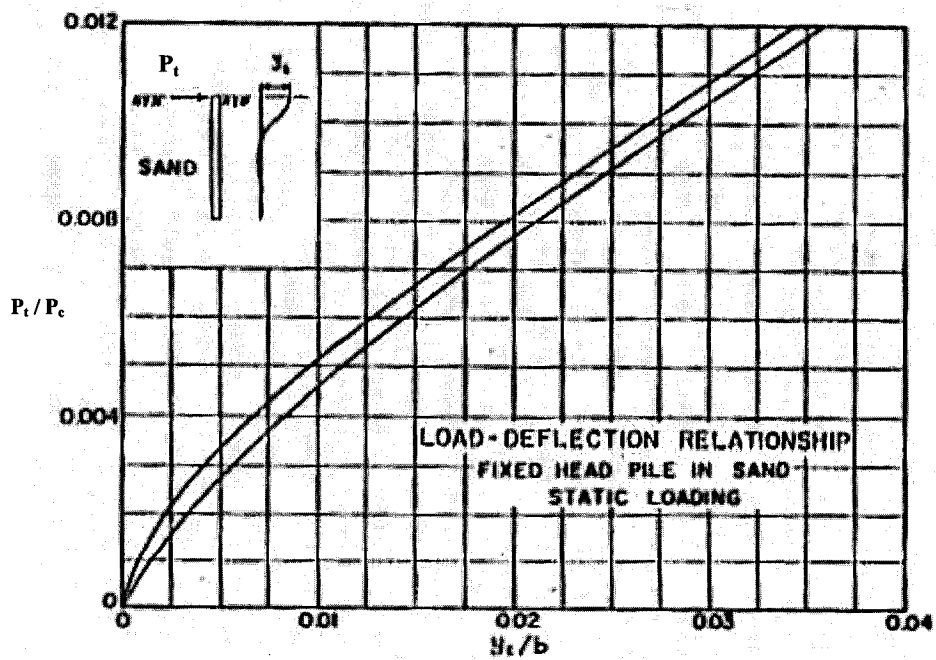
Figure 6.7 Load-deflection curves for fixed head pile in sand-static (Evans and Duncan, 1982)

156
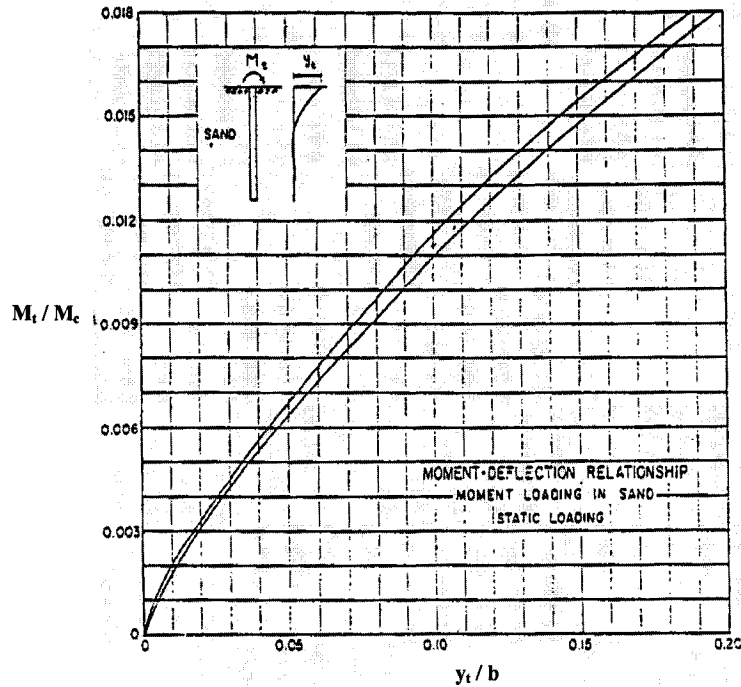
Figure 6.8 Moment-deflection curves for free head pile subjected to moment loading in sand-static (Evans and Duncan, 1982)

Using Figures 6.3 to 6.5 for soft clay (p-y cyclic curves show brittle behavior and using the average value of y_t/b available in the charts), the relative stiffness factors for clay T_c are calculated and shown in Table 6.2. Figures 6.6 to 6.8 are developed for piles embedded in sand subjected to a static load. For a pile embedded in sand subjected to cyclic loading Evans and Duncan proposed the increase in the values of the deflections calculated from the figures to account for cyclic loading as given in Table 6.3. The average value of y_t/b was increased by the ratios given in Table 6.3 and the relative stiffness factors for sand T_s were calculated as given in Table 6.4

Table 6.2 Values of relative stiffness factor for piles in soft clay subjected to cyclic loading, T_c

Boundary condition	y_t/b	P_t/P_c or M_t/M_c (Figs. 6.3-6.5)	P_c or M_c (Eqs. 6.4-6.5)	P_t or M_t (kN, kN.m)	T_c (m) (Eqs. 6.2-6.3)
Free head pile (P_t)	0.055	0.0168	2990.792	50.25	**2.0930**
Fixed head pile(P_t)	0.025	0.0265	2990.792	79.26	**1.9656**
Free head pile (M_t)	0.075	0.0138	15328.47	211.53	**2.2136**

157

Table 6.3 Increase in deflection for sand due to cyclic loading

Boundary condition	Increase in Deflection
Free head pile under lateral force P_t	<9%
Fixed head pile under lateral force P_t	No change
Free head pile under bending moment M_t	<7%

Table 6.4 Values of relative stiffness factor for piles in sand subjected to cyclic loading, T_s.

Boundary condition	y_t/b	P_t/P_c or M_t/M_c (Figs. 6.6-6.8)	P_c or M_c (Eqs. 6.4-6.5)	P_t or M_t (kN, kN.m)	T_c (m) (Eqs. 6.2-6.3)
Free head pile (P_t)	0.131	0.0116	15931.65	184.807	**1.8683**
Fixed head pile(P_t)	0.02	0.008	15931.65	127.45	**1.5574**
Free head pile(M_t)	0.107	0.0118	38344.28	452.46	**1.8078**

The value of T_{av} used for the non-homogeneous soil is calculated and shown in Table 6.5. The average value of T_{av} will be denoted as T in the rest of the dissertation. Performing numerical investigations using the values of T given in Table 6.5, the piles can be classified into long, short and intermediate based on the criterion mentioned above. The classification is given in Table 6.6.

Table 6.5 The relative stiffness factor T (or T_{av}) for different boundary conditions

Boundary condition	T_c	T_s	$T = T_{av} = (T_c+T_s)/2$
Free head pile under lateral force P_t	2.0930	1.8683	1.98 ≈ **2 m**
Fixed head pile under lateral force P_t	1.9656	1.5574	1.76 ≈ **1.8 m**
Free head pile under bending moment M_t	2.2136	1.8078	2.01 ≈ **2 m**

Table 6.6 Classification of piles into long, short and intermediate

Boundary condition & loading	long	short	intermediate
Free head pile subjected to lateral force P_t	≥ 8T (16 m)	≤ 3T (6 m)	4T-7T
Fixed head pile subjected to lateral force P_t	≥ 7T (12.6 m)	≤ 3T (5.4 m)	4T-6T
Free head pile subjected to moment M_t	≥ 7T (14 m)	≤ 2T (4 m)	3T-6T

158

6.2.2 Scope of analysis

The scope of sensitivity analysis for single piles will include the three boundary conditions and loadings mentioned above. Each case will be named by a support type. The sensitivity of the lateral top deflection, δy_t, and the lateral top rotation, $\delta \theta_t$, to changes in the design variables are investigated for the support types 1 and 3 (free head piles) while the sensitivity of the lateral top deflection, δy_t, to changes in the design variables are investigated for support type 2 (fixed head) as shown in Table 6.7.

Table 6.7 The types of responses under sensitivity investigation for the different support types

Support Type	Boundary condition & loading	Type of responses under investigation
1	Free head pile subjected to lateral force P_t	δy_t , $\delta \theta_t$
2	Fixed head pile subjected to lateral force P_t	δy_t
3	Free head pile subjected to moment M_t	δy_t , $\delta \theta_t$

For each support type, the sensitivities of the responses are investigated by calculating and plotting the different forms of the sensitivity results given in Section 5.2.6. For each support type, 9 cases of pile lengths are investigated ($2T$-$3T$-$4T$-$5T$-$6T$-$7T$-$8T$-$9T$-$10T$) and for each pile length, 11 cases of non-homogeneity are investigated (0% clay layer thickness-10% clay layer thickness- 20% clay layer thickness- 30%-40%-50%-60%-70%-80%-90% and 100% clay layer thickness) resulting in 99 cases investigated for each support type as shown in Table 6.8.

A total number of 297 cases are investigated for the three support types. For each case, the 5 forms of sensitivity results are calculated and plotted at different levels of applied loads at the pile head. The maximum load applied satisfies the criterion of the allowable deflection as discussed in Section *6.2.1.3*. The load increments (steps) are chosen such that a reasonable number of curves would be plotted in each figure. The load increments applied for the different cases are shown in Table 6.9.

159

Table 6.8 The number of cases investigated for single piles

Support type	Pile Length		Soil stratification		No. of cases
1	9 cases	2T	11 cases	% clay layer thickness	99 cases
				0%	
				10%	
				20%	
				30%	
				40%	
				50%	
				60%	
				70%	
				80%	
				90%	
				100%	
		3T	11 cases		
		4T	11 cases		
		5T	11 cases		
		6T	11 cases		
		7T	11 cases		
		8T	11 cases		
		9T	11 cases		
		10T	11 cases		
2	9 cases		11 cases		99 cases
3	9 cases		11 cases		99 cases

Table 6.9 Increments of loads for the different cases

Support Type	Pile Length	% clay layer thickness	Increments of force
1	2T (4 m)	0 to 100%	15 kN
	3T to 10T	0 to 50%	50 kN
		60% to 100%	25 kN
2	2T (3.6 m)	0 to 50%	50 kN
		60% to 100%	25 kN
	3T to 10T	0 to 50%	100 kN
		60% to 100%	50 kN
3	2T (4 m)	0 to 50%	50 kN.m
		60% to 100%	25 kN.m
	3T to 10T	0 to 100%	100 kN.m

160

6.2.3 Programs used

Two computer programs were used to obtain the sensitivity results. The first is the software program COM624P (Version 2) developed by Wang and Reese (1993) for the analysis of stresses and deflection of piles or drilled shafts under lateral loads. The basic program presented by the authors was developed for the purpose of highway construction and that required application of microcomputers. The program solves the equations giving pile deflection, rotation, bending moment, and shear by using iterative procedures because of nonlinearity of the p-y soil response. The beam-column-soil equations are solved by the finite difference method. In addition, the program uses the method proposed by Georgiadis (1983) in dealing with non-homogeneous soil. In the current research, COM624P is used to numerically analyze the piles to obtain the deflections and moments of the laterally loaded piles required for the sensitivity analysis.

The second program is MATLAB (version 7) where programs were developed to calculate and plot the different forms of the sensitivity results. The programs developed are based on previous program files developed by Lui (2004) for sensitivity of homogeneous soil. However, the programs developed in the current research are for non-homogeneous soils, model the adjoint pile in a different way and include different forms of the sensitivity results. The details of the programs developed in the current study are given in Appendix B. The developed programs mainly do the following:

1. Run the program COM624P for the different cases to obtain the deflections and moments of both the primary and adjoint piles.

2. Calculate the different expressions of the sensitivity results using the deflections and moments of the primary and adjoint piles.

3. Plot the sensitivity results as shown in the proceeding sections.

6.2.4 Modeling of the primary and adjoint piles

The primary pile is the original pile subjected to a horizontal load P_t (for support types 1 and 2) or a bending moment M_t (for support type 3). The adjoint pile is a pile in the state

161

of deformation of the primary pile subjected to a unit lateral horizontal force at the pile's head for obtaining δy_t or subjected to a unit moment at the pile's head for obtaining $\delta\theta_t$ as discussed in Chapter 5. To model such a case, the deflection and the moment of the adjoint pile was obtained by subtracting the deflection and the moment of pile 1 from pile 2 as given in Tables 6.10 and 6.11.

Table 6.10 Primary and adjoint piles for obtaining δy_t

Support type	Primary pile subjected to	Pile1 Subjected to	Pile 2 subjected to	Adjoint pile = Pile1 – Pile 2
1 (free head)	→P_t	→(P_t+1_a)	→P_t	→1_a
2 (fixed head)	→P_t	→(P_t+1_a)	→P_t	→1_a
3 (free head)	↷M_t	↷M_t+ →1_a	↷M_t	→1_a

Table 6.11 Primary and adjoint piles for obtaining $\delta\theta_t$

Support type	Primary pile subjected to	Pile1 Subjected to	Pile 2 subjected to	Adjoint pile = Pile1 – Pile 2
1 (free head)	→P_t	→P_t+ ↷1_a	→P_t	↷1_a
3 (free head)	↷M_t	↷(M_t+1_a)	↷M_t	↷1_a

6.2.5 Analysis of results

The results of the 297 cases mentioned above are given in the attached CD. The details of the contents of the CD and how to get the numerical values of the five forms of results (S, A, PCR, TF and GF) and their graphical presentation are given in Appendix C. In the current section, a sample of the results is presented and discussed and the effect of the different conditions on the sensitivity results is studied.

6.2.5.1 Sample of results and discussion

All the forms of the results required to study the sensitivity of the lateral top deflection y_t to changes in the design variables of the system are given, as a sample, for a pile with case of support type = 1 (free head pile subjected to lateral load P_t), with length = $9T$ =

162

18 m (long pile) and soil stratification (non-homogeneity) of 20% clay thickness, i.e. the thickness of the upper clay layer is equal to 3.6 m (20% of the length) and the rest of the pile (14.4 m) is embedded in sand. For this case, forces were applied in increments of 50 kN at the pile head and the maximum force reached was 250 kN. This maximum force satisfies the maximum lateral deflection criterion as explained in Section 6.2.1.3 (maximum allowable moment was reached at $P_t = 200$ kN). The superscript in the results for this sample is Py where P denotes that the primary pile is subjected to lateral force while y denotes that the lateral deflection is the response measure under investigation.

6.2.5.1.1 Sensitivity operator S

The first and very important form of the results is the sensitivity operator denoted by S. The sensitivity operators were discussed in detail in Section 5.2.6.1. The values of the sensitivity operators are calculated at very close discrete points along the pile length. (for all the piles, there are 301 nodes (points) along the pile length which is the maximum number of nodes allowed in the program COM624P). The values of the sensitivity operators are plotted along the pile length to show the locations of the critical points that have maximum and minimum effect of the change of the parameter on the change of the soil response. The sensitivity operators for the eight studied parameters are plotted at each load for the clay parameters (c, γ_c' and ε_{50}), sand parameters (k, γ_s' and ϕ) and pile parameters (EI and b) in Figures 6.9 (a, b, c and d) and 6.10 (a, b, c and d), respectively.

For the clay parameters (Figure 6.9 a, b and c), the distribution of sensitivity operators S_c, $S_{\gamma c}$, and $S_{\varepsilon 50}$ present the changes of pile-head lateral deflection δy_t caused by the change of design variables c, γ_c' and ε_{50}, respectively. These variables are connected to the clay layer only. At low levels of the applied load ($P_t = 50$ kN and 100 kN), the soft clay at the ground surface is in the nonlinear elastic stage. Since the deflection decreases with depth, the entire clay layer experiences a nonlinear elastic behavior (Figure 4.5). As the load P_t increases, the soil at the ground surface becomes in the linear softening stage. Therefore the entire clay layer is in the linear softening stage or the linear softening stage followed by the nonlinear elastic stage depending on the level of load applied.

163
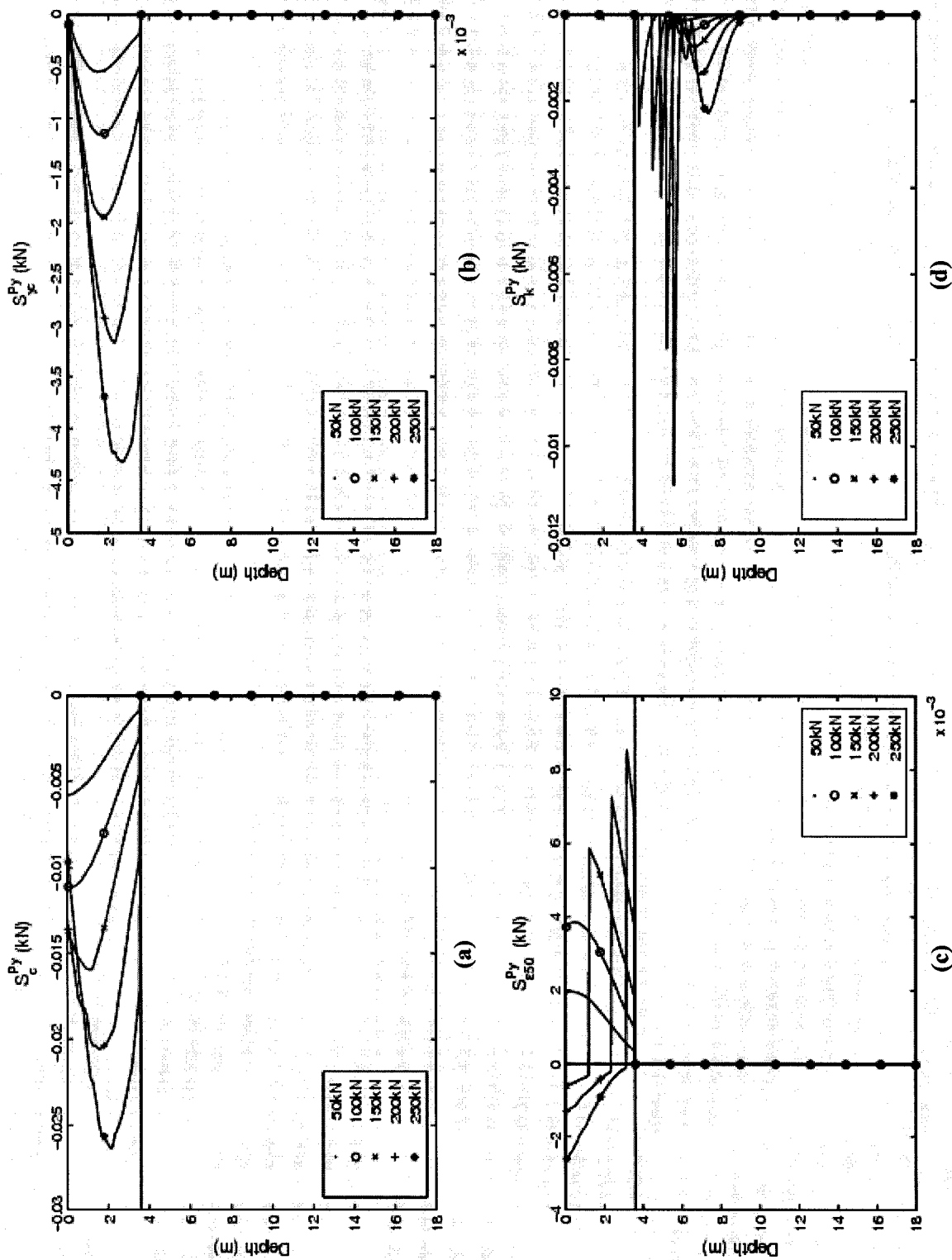
Figure 6.9 Sensitivity operators for 18 m long free head pile with 20% clay layer thickness
(a) S_c^{Py}, (b) $S_{\gamma c}^{Py}$, (c) $S_{\epsilon 50}^{Py}$ and (d) S_k^{Py}

164
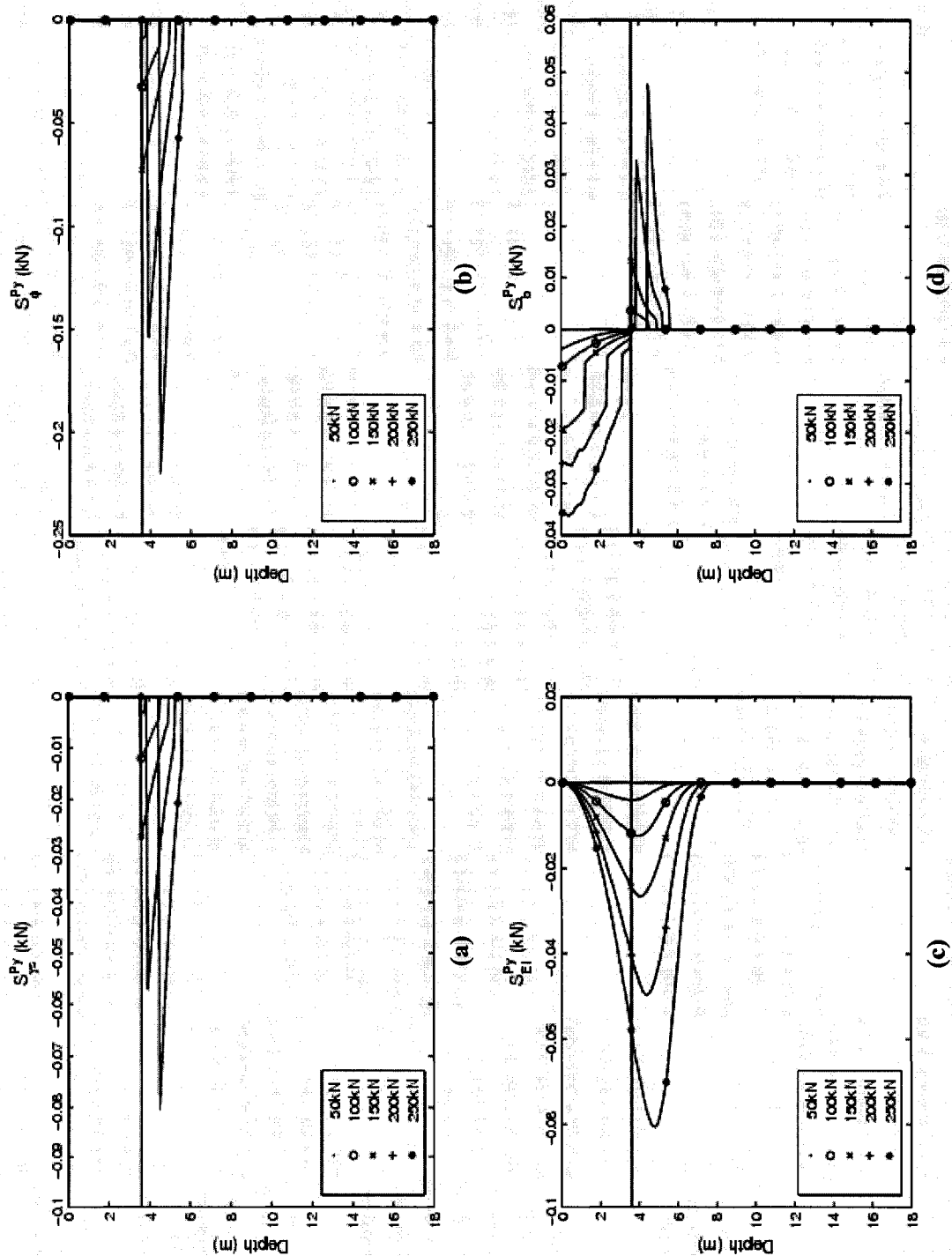
Figure 6.10 Sensitivity operators for 18 m long free head pile with 20% clay layer thickness (a) $S_{\gamma s}^{Py}$, (b) S_{ϕ}^{Py}, (c) S_{EI}^{Py} and (d) S_{b}^{Py}

165

For the distribution of the c operator S_c (Figure 6.9a), it starts with a high value at the surface and decreases with depth when the soft clay is in the nonlinear elastic stage at the ground surface (P_t =50 kN and 100 kN). However, when the soft clay at the ground surface is in the linear softening stage, the values increase with depth then decrease. The distribution of $S_{\gamma c}$ (Figure 6.9b) that presents the changes of δy_t caused by changes of the submerged unit weight of soft clay, γ'_c, shows zero values at the ground surface that increase with depth then decrease.

It is worth noting that, there is no effect for the change of γ'_c on δy_t below the depth $x = x_{rc}$. The depth of reduced resistance of clay x_{rc} is equal to 3.64 m for the initial design variables used. For 10 % and 20% clay layer thickness (clay thickness = 1.8 m and 3.6 m respectively), the clay thickness is less than x_{rc} thus values of $S_{\gamma c}$ are obtained in the entire clay thickness. This will be clearer when different thicknesses of clay are compared in the next section. In addition, it is observed that the numerical values of S_c are much higher than those of $S_{\gamma c}$. This indicates that the effect of the change of the cohesion c on the change in y_t is in general higher than that of the submerged unit weight γ'_c.

The distribution of sensitivity operator $S_{\varepsilon 50}$ shows a positive value of the operator (Figure 6.9c). The positive sign is expected since ε_{50} is a measure of deformability (opposite to the other variables), i.e. the increase of ε_{50} causes an increase in the lateral deflection. However, the values are positive only for ε_{50} when the soil is experiencing the nonlinear elastic stage (P_t = 50 kN and 100 kN). The sign is negative when the soil experiences the linear softening stage. The soil is in the linear softening stage at P_t =150, 200 and 250 kN at the ground surface and as we go deeper the soil stage is changed from linear softening to linear elastic and the values of $S_{\varepsilon 50}$ become positive again.

The sand operators (Figures 6.9d, 6.10 a, and 6.10b) appear in the sand layer only. The value of S_k depends directly on the deflection of the primary pile y and that of the adjoint pile y_a since the expression for S_k is given as follows (Appendix A):

166

$$S_k = xyy_a \qquad (6.9)$$

Therefore, the distribution of S_k has a similar pattern to that of the deflection. The values of S_k appear only when the deflection is less than y_k, i.e. the sand behavior is in the linear elastic stage (Stage 1 in Figure 4.7).

The operators $S_{\gamma s}$ and S_ϕ affect the soil behavior when the soil is in stages 2 and 3 only, i.e. when deflection y of the pile is $y_k < y < y_m$ and $y_m < y < y_u$ as shown in Figure 4.7. As the deflection decreases to $y < y_k$, the values of the sensitivity operator $S_{\gamma s}$ and S_ϕ become equal to zero. Therefore the effect of k appears at deeper levels below the zone of effect of γ_s' and ϕ. For $S_{\gamma s}$ and S_ϕ, as the load P_t increases the maximum values of the operators increase and is obtained at a greater depth from ground surface. The distribution for $S_{\gamma s}$ and S_ϕ have a similar pattern, however, the numerical values of S_ϕ are higher than those for $S_{\gamma s}$ indicating that the change in the parameter ϕ has a higher effect on the change of the lateral top deflection.

The sensitivity operators that affect the changes of the pile-head lateral deflection δy_t due to the changes of the normalized design variables EI and b appear in both the clay and sand (Figures 6.10c and 6.10d). The pile diameter b is considered as a design parameter involved in the p-y relationship of clay and also in the p-y sand relationship. The operators for the variable b are different for clay and sand since they depend on the p-y relationships (the expression for S_b in the clay layer is different than that in the sand layer). However, the sensitivity operators for the design variable EI are defined in the same fashion for clay and sand since they are connected with the pile material. The distribution of S_{EI} (Figure 6.10c) depends on the moment distribution therefore it has a similar pattern as that of the moment and is continuous along the pile length.

The distribution of S_b is given in Figure 6.10d. As seen there are values for S_b in both clay and sand. However, the value of S_b is negative in the clay layer and positive in sand. This implies that an increase in the pile diameter in the clay layer will cause a decrease in the

167

lateral pile head deflection while an increase in the pile diameter in the sand layer will cause an increase in the lateral pile head deflection. It was not possible to obtain this information by simply looking at the p-y relationships due to the complexity of the nonlinear p-y models. However it was possible to visualize it using the distributed parameter sensitivity analysis.

6.2.5.1.2 Sensitivity factor A

The second form of results is the sensitivity factor A discussed in Section 5.2.6.2. The sensitivity factors A for each variable are calculated at each level of applied load (Table 6.12) and are plotted in the form of a bar chart in Figure 6.11 (a, b, c and d) and Figure 6.12 (a, b, c and d) for the clay parameters $(c, \gamma_c'$ and $\varepsilon_{50})$, sand parameters $(k, \gamma_s',$ and $\phi)$ and pile parameters $(EI$ and $b)$, respectively. Each figure is for a design variable and the values in the figure represent A at the different levels of load.

The numerical value of A gives the change of the top lateral deflection δy_t in meters when multiplying it (A) by the percent change in the variable due to changing that parameter along the whole length of the pile with that certain percent. For example, at $P_t = 50$ kN, if the cohesion c in the entire clay layer increases by 10% $(\delta c/c=0.1)$, the lateral top deflection will decrease by 0.0013 m $(\delta y_t = A_c \times \delta c/c = -0.013 \times 0.1 = -0.0013$ m$)$.

Table 6.12 Values of sensitivity factors A for each variable at different load levels

	$P_t = 50$ kN	$P_t = 100$ kN	$P_t = 150$ kN	$P_t = 200$ kN	$P_t = 250$ kN
A_c^{Py}	-0.013	-0.027	-0.043	-0.061	-0.076
$A_{\gamma c}^{Py}$	-0.001	-0.003	-0.005	-0.008	-0.011
$A_{\varepsilon 50}^{Py}$	0.005	0.010	0.009	0.005	-0.000
A_k^{Py}	-0.001	-0.001	-0.002	-0.004	-0.005
$A_{\gamma s}^{Py}$	-0.001	-0.008	-0.021	-0.042	-0.049
A_ϕ^{Py}	-0.002	-0.021	-0.057	-0.115	-0.135
A_{EI}^{Py}	-0.012	-0.038	-0.082	-0.155	-0.261
A_b^{Py}	-0.005	-0.009	-0.021	-0.036	-0.065

168
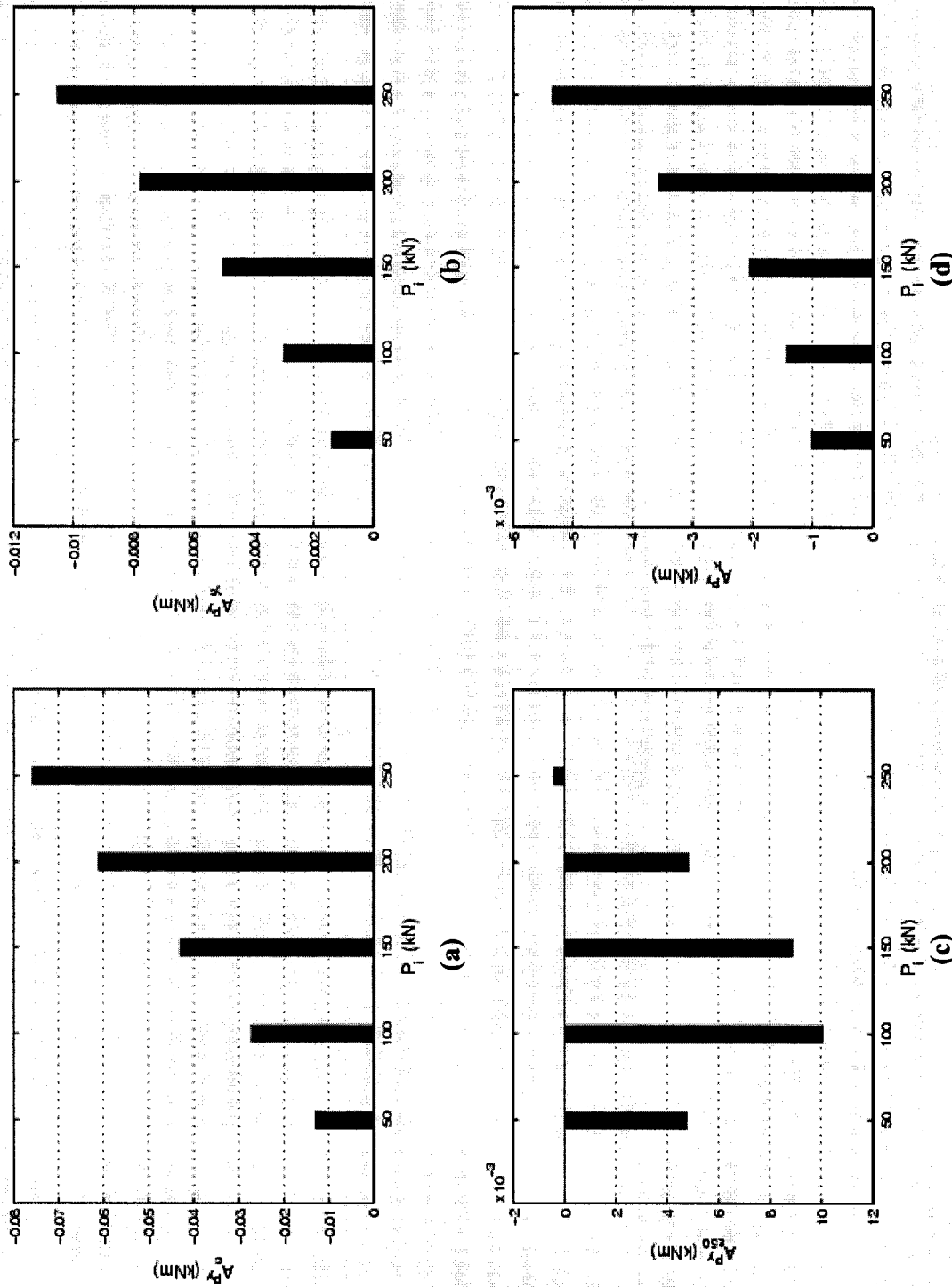
Figure 6.11 Sensitivity factors for 18 m long free head pile with 20% clay layer thickness (a) A_c^{Py}, (b) A_κ^{Py}, (c) $A_{\varepsilon50}^{Py}$ and (d) A_k^{Py}

169
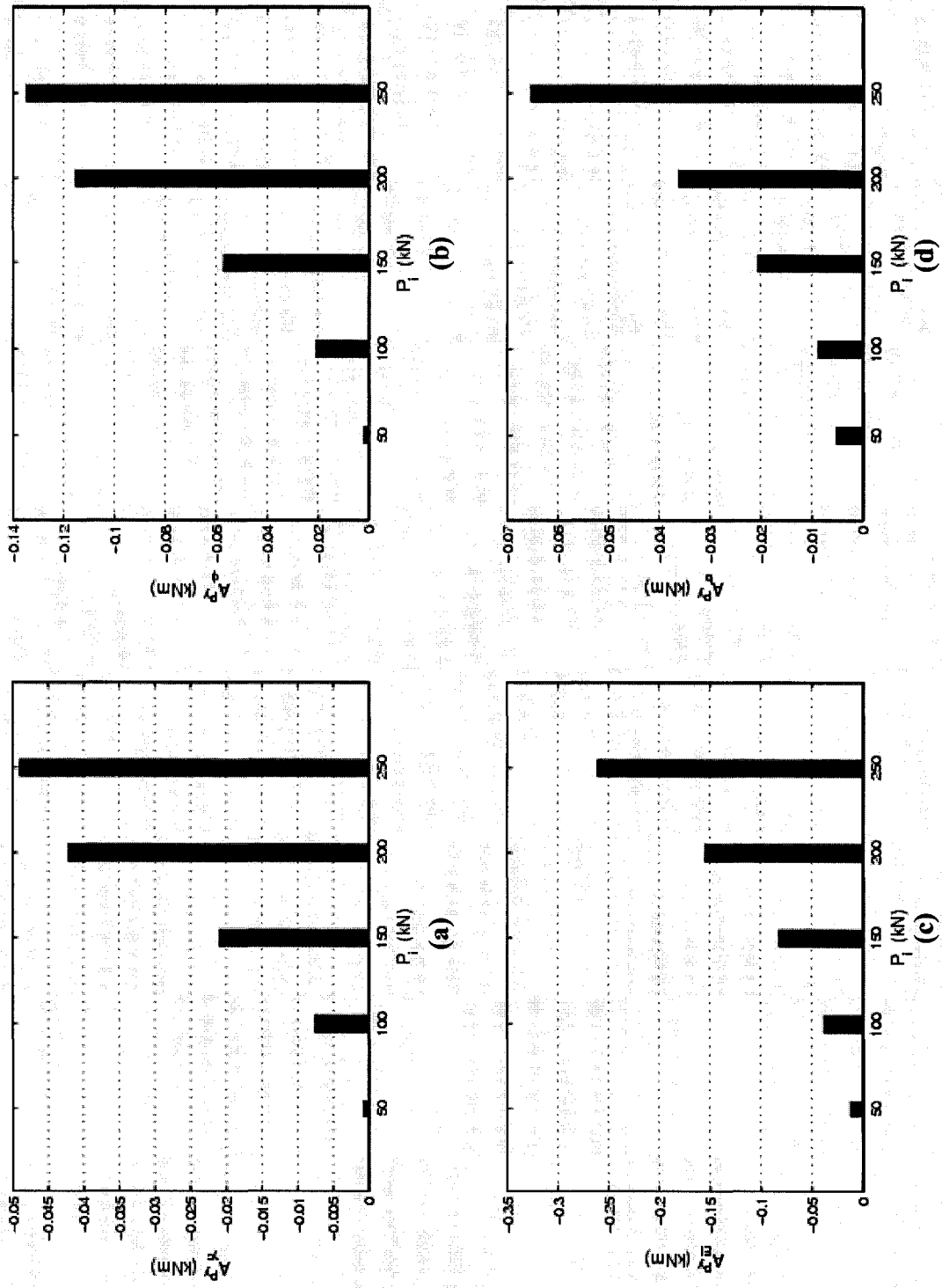
Figure 6.12 Sensitivity factors for 18 m long free head pile with 20% clay layer thickness (a) $A_{\gamma s}^{Py}$, (b) A_{ϕ}^{Py}, (c) A_{EI}^{Py} and (d) A_{b}^{Py}

170

6.2.5.1.3 Percent change ratio *PCR*

The third form of results is the percent change ratio (*PCR*) discussed in Section 5.2.6.3. The values of percent change ratio (*PCR*) for each design variable are calculated at each level of applied load (Table 6.13) and are plotted in Figure 6.13 (a, b, c and d) and Figure 6.14 (a, b, c and d) for the clay parameters (c, γ'_c and ε_{50}), sand parameters (k, γ'_s and ϕ) and pile parameters (*EI* and b), respectively. The value of *PCR* depends on the value of *A* ($PCR = A/y_t$).

The numerical value of *PCR* gives the ratio between the percent change in the top lateral deflection ($\delta y_t/y_t$) and the percent change in the design variable, i.e. if the design variable c changes by a certain percent cp, there will be a change in the lateral top deflection by a percent equal to $PCR*$cp. For example, at $P_t= 50$ kN, if the cohesion c in the entire clay layer increases by 10%, the lateral top deflection will decrease by 7.4% (δy_t (in%)= *PCR* x δc(in %) = -0.74x10= -7.4%)

Total relative sensitivity factor *TF*

The fourth form of results is the total relative sensitivity factor (*TF*) discussed in Section 5.2.6.4. The total relative sensitivity factors (*TF*), given in percent, for each variable are calculated at each level of applied load (Table 6.14) and are plotted in the form of bar charts in Figure 6.15 (a, b, c and d) and Figure 6.16 (a, b, c and d) for the clay parameters (c, γ'_c and ε_{50}), sand parameters (k, γ'_s and ϕ) and pile parameters (*EI* and b), respectively. The value *TF* gives the relative effect in percent of each design variable compared to all studied design variables.

At a given load, the addition of *TF* for all parameters should add up to 100%. In addition, the parameter that has the highest *TF* has the highest effect on the change in the lateral top deflection. For example, at load $P_t = 50$ kN, the parameters are arranged as follows from highest to lowest effect: c, *EI*, b, ε_{50}, ϕ, γ'_c, k, γ'_s. At load P_t =250 kN, the parameters

are arranged as follows from highest to lowest effect: $EI, \phi, \; c, \; b, \gamma_s', \gamma_c', \; k, \varepsilon_{50}$. It is clear that the order of parameters depend on the level of applied load. At low levels of load the pile deflection in sand is small and accordingly the effect of the sand parameters is low.

Table 6.13 Values of PCR for each variable at different load levels

	$P_t = 50$ kN	$P_t = 100$ kN	$P_t = 150$ kN	$P_t = 200$ kN	$P_t = 250$ kN
PCR_c^{Py}	-0.74	-0.54	-0.46	-0.40	-0.33
$PCR_{\gamma c}^{Py}$	-0.08	-0.06	-0.05	-0.05	-0.05
$PCR_{\varepsilon 50}^{Py}$	0.27	0.20	0.09	0.03	-0.00
PCR_k^{Py}	-0.06	-0.03	-0.02	-0.02	-0.02
$PCR_{\gamma s}^{Py}$	-0.04	-0.15	-0.23	-0.28	-0.21
PCR_ϕ^{Py}	-0.11	-0.41	-0.61	-0.76	-0.58
PCR_{EI}^{Py}	-0.71	-0.76	-0.88	-1.03	-1.14
PCR_b^{Py}	-0.30	-0.17	-0.22	-0.24	-0.29

Table 6.14 Values of TF (in %) for each variable at different load levels

	$P_t = 50$ kN	$P_t = 100$ kN	$P_t = 150$ kN	$P_t = 200$ kN	$P_t = 250$ kN
TF_c^{Py}	31.99	23.21	17.89	14.32	12.59
$TF_{\gamma c}^{Py}$	3.42	2.58	2.10	1.83	1.75
$TF_{\varepsilon 50}^{Py}$	11.80	8.59	3.70	1.14	0.07
TF_k^{Py}	2.53	1.22	0.85	0.84	0.89
$TF_{\gamma s}^{Py}$	1.83	6.53	8.78	9.90	8.13
TF_ϕ^{Py}	4.91	17.70	23.83	27.02	22.36
TF_{EI}^{Py}	30.59	32.71	34.24	36.46	43.36
TF_b^{Py}	12.91	7.44	8.62	8.49	10.85

Group relative sensitivity factor *GF*

The fifth form of results is the group relative sensitivity factor (*GF*) discussed in Section 5.2.6.5. The group relative sensitivity factors (*GF*), given in %, for each design variable are calculated at each level of applied load (Table 6.15) and are plotted in the form of bar charts in Figure 6.17 (a, b, c and d) and Figure 6.18 (a, b, c and d) for the clay

172
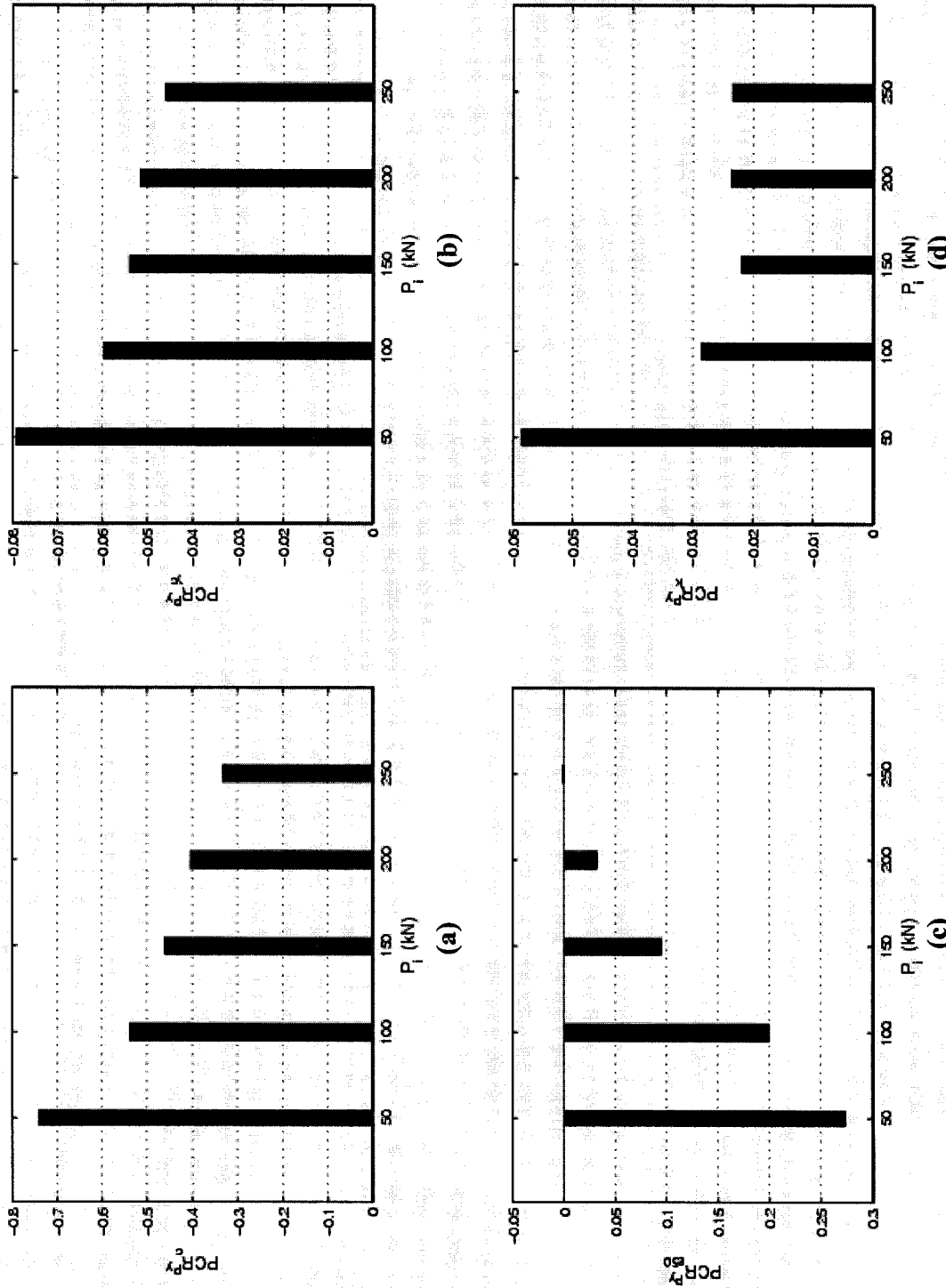
Figure 6.13 Percent change ratio for 18 m long free head pile with 20% clay layer thickness (a) PCR_c^{Py} **, (b)** $PCR_{\gamma c}^{Py}$ **, (c)** $PCR_{\varepsilon 50}^{Py}$ **and (d)** PCR_k^{Py}

173
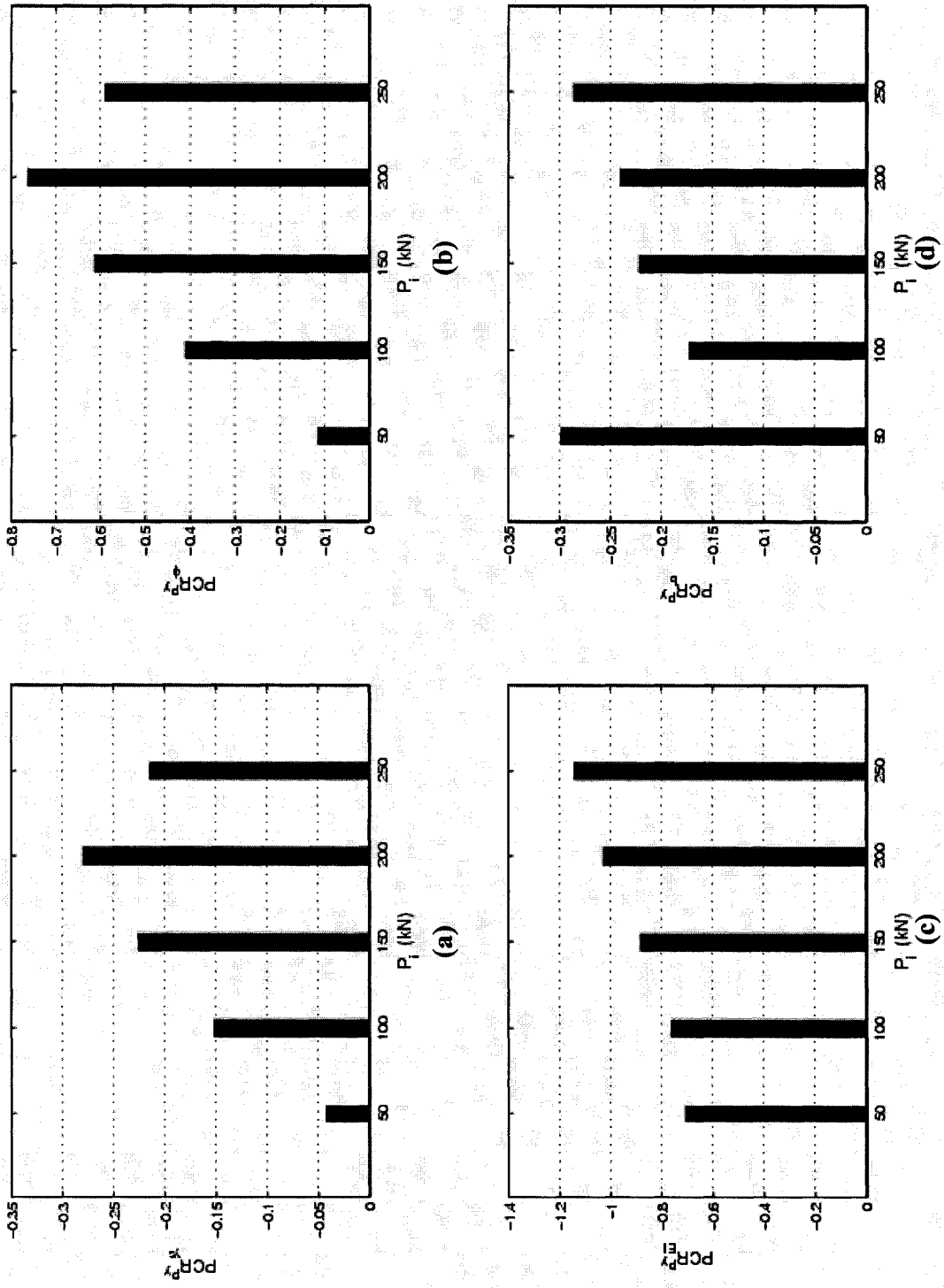
Figure 6.14 Percent change ratio for 18 m long free head pile with 20% clay layer thickness (a) PCR_{ys}^{Py} **, (b)** PCR_{ϕ}^{Py} **, (c)** PCR_{EI}^{Py} **and (d)** PCR_{b}^{Py}

174
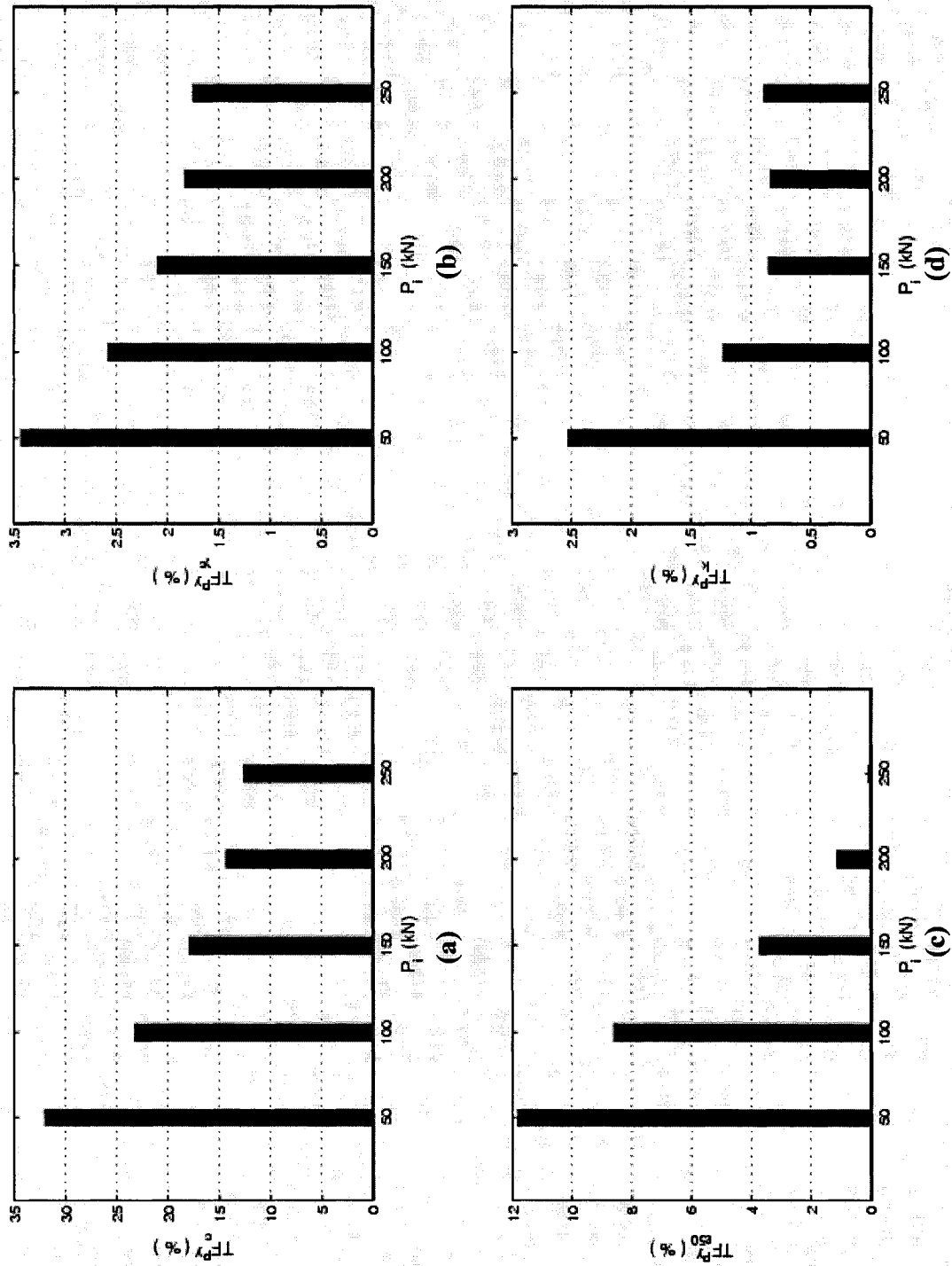
Figure 6.15 Total relative sensitivity factors for 18 m long free head pile with 20% clay layer thickness
(a) TF_c^{Py} , (b) TF_γ^{Py} , (c) $TF_{\varepsilon50}^{Py}$ and (d) TF_k^{Py}

175
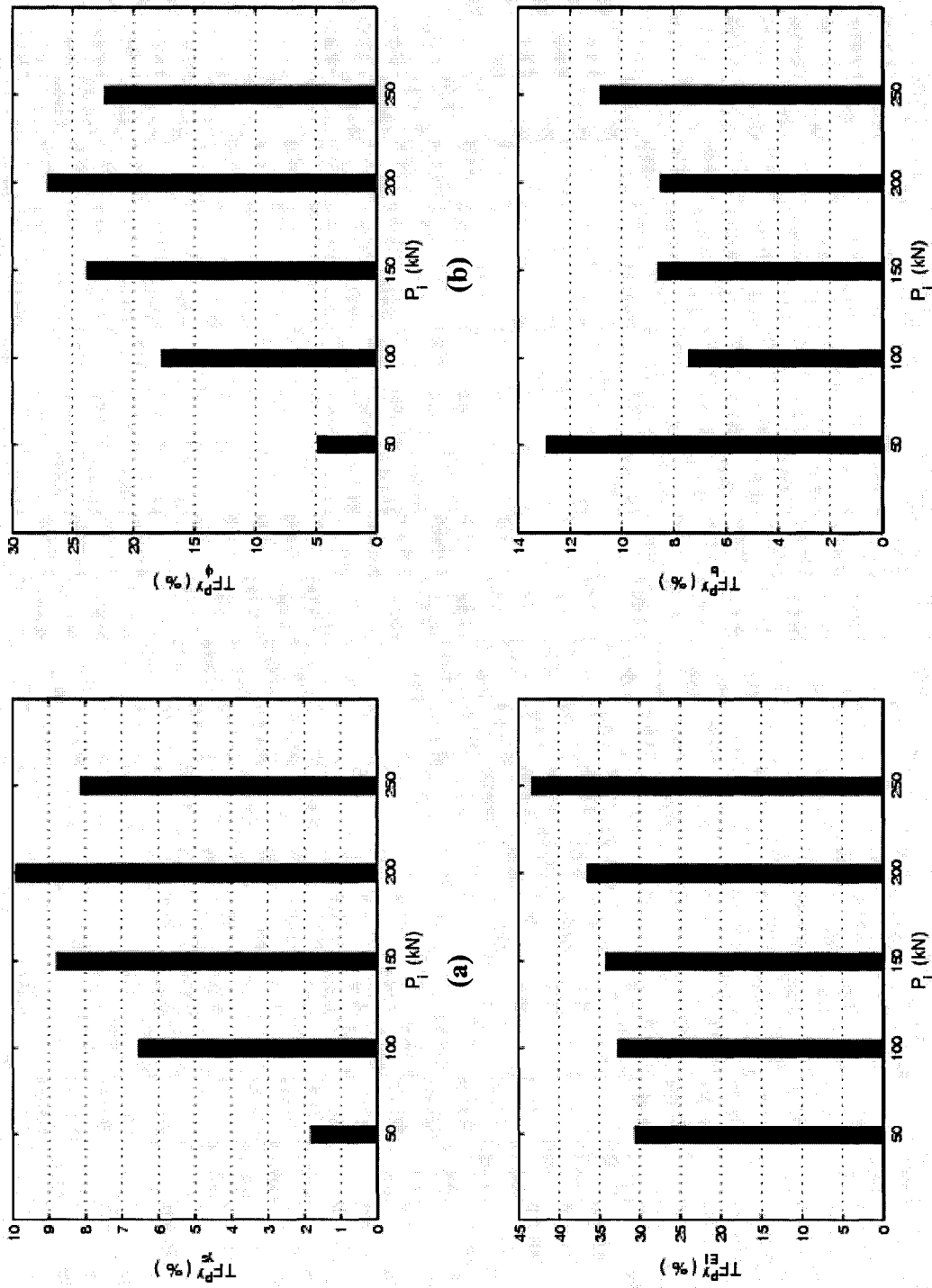
Figure 6.16 Total relative sensitivity factors for 18 m long free head pile with 20% clay layer thickness (a) $TF_{\gamma_s}^{Py}$, **(b)** TF_{ϕ}^{Py} , **(c)** TF_{EI}^{Py} **and (d)** TF_{b}^{Py}

176

parameters (c, γ'_c, and ε_{50}), sand parameters (k, γ'_s, and ϕ) and pile parameters (EI and b), respectively. The value GF gives the relative effect in percent of each variable compared to the variables of its group (pile, sand or clay).

At a given load, the addition of GF for the parameters in a material group (clay, sand or pile) should add up to 100%. In addition, the parameter that has the highest GF in its group has the highest effect on the change in the lateral top deflection. For example, at load P_t =50kN, the best clay parameter to improve and will have highest effect on the lateral top deflection is the cohesion c followed by ε_{50} followed by γ'_c. The best sand parameter to improve and will have highest effect on the lateral top deflection is the angle of friction ϕ followed by k followed by γ'_s. The best pile parameter to improve and will have highest effect on the lateral top deflection is the bending stiffness EI followed by b.

As the load increases, c remains the best clay parameter however ε_{50} comes after γ'_c due to the involvement of positive and negative values that appear in the distribution of operator $S_{\varepsilon50}$. The angle of friction ϕ remains the best sand parameter however k comes after γ'_s due to the increase of the influence of γ'_s associated with the increase in deflection as the load increases. The bending stiffness EI remains the best pile parameter followed by b at all levels of applied load.

Table 6.15 Values of GF for each variable at different load levels

	$P_t = 50$ kN	$P_t = 100$ kN	$P_t = 150$ kN	$P_t = 200$ kN	$P_t = 250$ kN
GF_c^{Py}	67.74	67.51	75.53	82.82	87.40
$GF_{\gamma c}^{Py}$	7.25	7.49	8.85	10.60	12.15
$GF_{\varepsilon50}^{Py}$	25.00	25.00	15.61	6.59	0.46
GF_k^{Py}	27.30	4.82	2.54	2.21	2.83
$GF_{\gamma s}^{Py}$	19.68	25.66	26.23	26.22	25.91
GF_ϕ^{Py}	53.01	69.52	71.22	71.56	71.27
GF_{EI}^{Py}	70.31	81.46	79.90	81.11	79.98
GF_b^{Py}	29.69	18.53	20.10	18.90	20.02

177
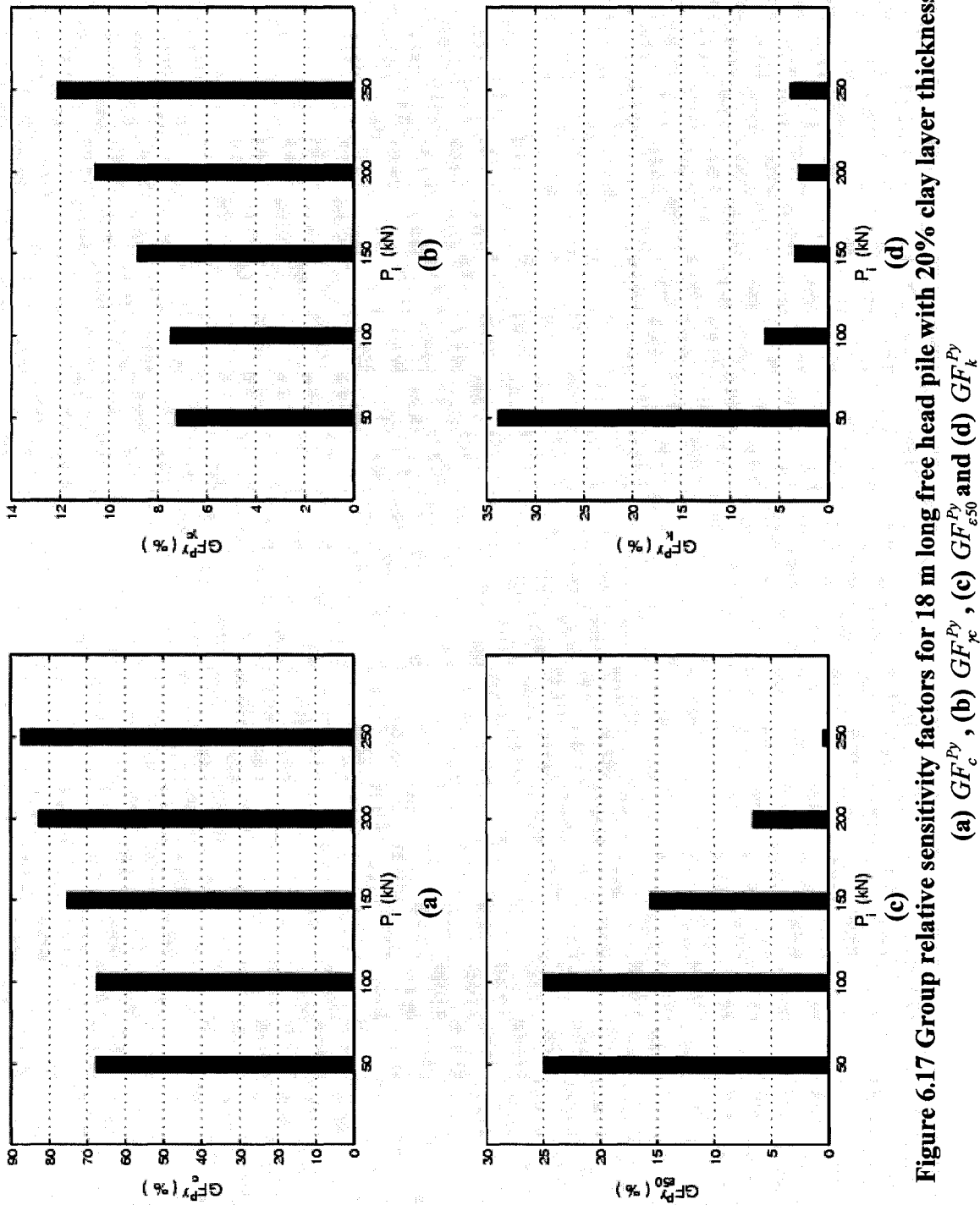
Figure 6.17 Group relative sensitivity factors for 18 m long free head pile with 20% clay layer thickness
(a) GF_c^{Py}, (b) GF_κ^{Py}, (c) $GF_{\varepsilon 50}^{Py}$ and (d) GF_k^{Py}

178
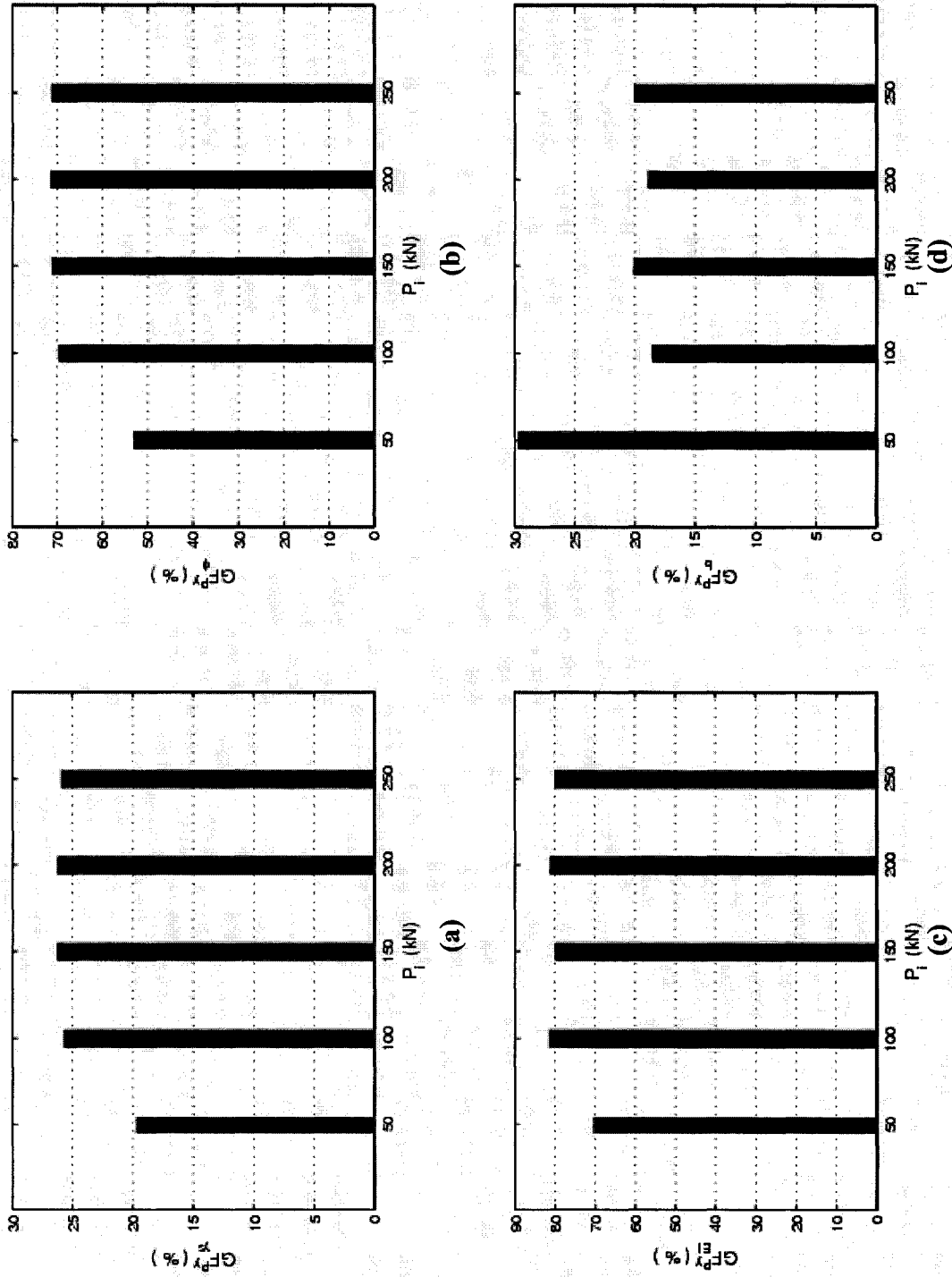
Figure 6.18 Group relative sensitivity factors for 18 m long free head pile with 20% clay layer thickness (a) $GF_{\gamma s}^{Py}$, (b) GF_{ϕ}^{Py}, (c) GF_{EI}^{Py} and (d) GF_{b}^{Py}

179

6.2.5.2 Effect of nonlinearity

For assessment of the nonlinearity of the pile-soil system subjected to a lateral load it is appropriate to utilize the load-deflection relationship. The pile head deflection y_t versus the lateral force P_t applied at the top of the pile for the sample case given above (a free head pile subjected to lateral loads P_t with length equal to 18 m embedded in soil with 20% clay layer thickness) is shown in Figure 6.19 to give a brief idea about the nonlinearity of the pile-soil system.

From the figures presented in the previous section, it is observed that as the lateral force P_t increases, the maximum value of the sensitivity operators for all variables increases in general. However, this increase is not linear. In addition, the nonlinearity is observed from the bar charts given for A, PCR, TF and GF (Figures 6.11 to 6.18).
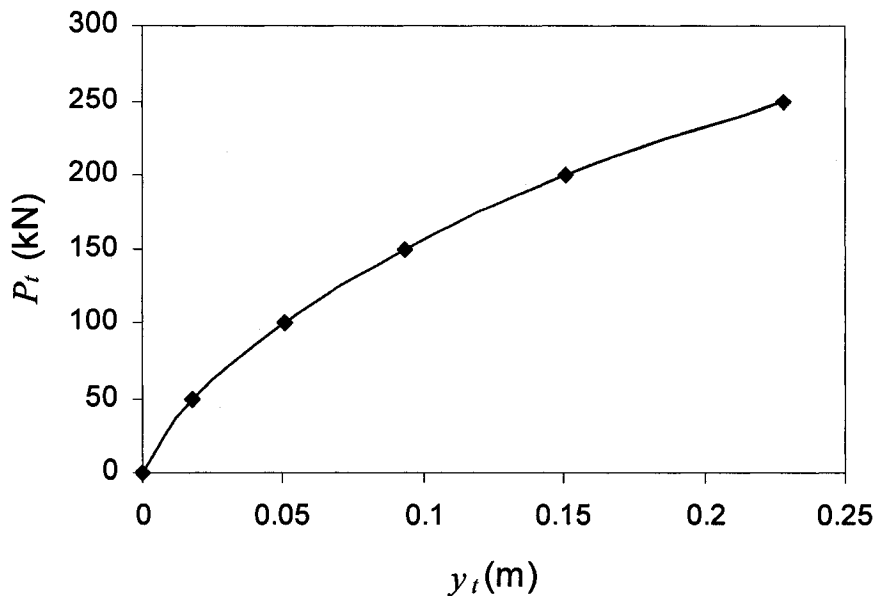
Figure 6.19 Pile head deflection y_t versus lateral force P_t applied to the top of the pile head for a free head 18 m long pile (20% clay layer thickness).

180

6.2.5.3 Effect of non-homogeneity

To study the effect of thickness of clay layer on the sensitivity results two approaches are taken. The first approach is to compare the sensitivity results for different thicknesses while the load is kept constant, i.e. load-based comparison. The second approach is to compare the sensitivity results for different thicknesses of clay while the deflection of the pile at the ground surface is kept constant, i.e. deflection-based comparison.

6.2.5.3.1 Load-based comparison

Effect of non-homogeneity on sensitivity operators

For the first approach, the sensitivity operators S are plotted in Figure 6.20 (a, b, c and d) and Figure 6.21 (a, b, c and d) for the clay parameters (c, γ_c' and ε_{50}), the sand parameters (k, γ_s' and ϕ) and pile parameters (EI and b), respectively, for different thicknesses of clay when the pile is subjected to a constant load. The constant load was taken equal to 100kN so that the two phases of the clay behavior will be included in the comparison.

For the clay parameters, at a constant load, as the thickness of clay increases, the deflection of the pile increases because the soil that supports the pile becomes weaker. This causes the sensitivity of the lateral pile-head deflection to changes in the clay parameters (Figure 6.20 a, b and c) to increase, i.e. the sensitivity increases in general.

For the sand parameters, at a constant load, as the thickness of clay increases, the deflection of the pile increases because the soil becomes weaker and accordingly the sensitivity increases in general. However, since sand starts at a deeper level as clay thickness increases, the sensitivity value for S_k (Figure 6.20 d) (which develops for $y<y_k$) can decrease when the deflection becomes very small at deep levels in the sand (as seen for thickness of clay greater than or equal to 40%).

181

Figure 6.20 Sensitivity operators for 18 m long free head pile at different thicknesses of clay at $P_t = 100$ kN (load-based comparison) (a) S_c^{Py}, (b) $S_{\gamma c}^{Py}$, (c) $S_{\varepsilon 50}^{Py}$ and (d) S_k^{Py}

182

Figure 6.21 Sensitivity operators for 18 m long free head pile at different thicknesses of clay at P_t =100 kN (load-based comparison) (a) S_{ys}^{Py} , (b) S_{ϕ}^{Py} , (c) S_{EI}^{Py} and (d) S_b^{Py}

183

In addition, since sand starts at a deeper level as clay thickness increases, the sensitivity value for S_{ys} and S_ϕ (Figure 6.21 a and b) can decrease if the load is not high enough to cause the sand to experience the third stage of the sand behavior. Accordingly, the sensitivity of S_{ys} decreases if deflection in sand starts at $y_k < y < y_m$ (as the case of load P_t =100 kN and clay thickness = 30%) or completely vanishes if $y < y_k$ (as seen for thickness of clay greater than or equal to 40%).

For the pile parameters (S_{EI} shown in Figure 6.21c and S_b shown in Figure 6.21d), the increase in the values of the S_{EI} operator are associated with the increase in the bending moment. However, for S_b the increase in the values of S_b along the pile length are associated with the increase of the deflection as the thickness increases at a constant load.

Effect of non-homogeneity on A and PCR

The values of the sensitivity factors A and the percent change ratio PCR for all the parameters are given in Table 6.16 and Table 6.17, respectively, for the different thicknesses of clay at a constant load (P_t =100 kN). The sensitivity factors A are the integrations of the sensitivity operators S and PCR is the sensitivity factor divided by the lateral top deflection ($PCR=A/y_t$). For the clay operators, as the thickness of clay increases, the integration of the sensitivity operators results in a higher value of the sensitivity factors A and the value of PCR.

For the sand operators, as the thickness of clay increases (from 0% to 100%), the sand operators start at a deeper level and the values of A and PCR for the sand parameters decrease. After a certain clay thickness, the values of A_k and PCR_k become negligible while those for γ_s' and ϕ become equal to zero when the deflection at the top of the sand layer is less than the value of y_k (i.e. $y < y_k$) .

For the parameter EI, A_{EI} and PCR_{EI} increases as the thicknesses of the clay increase (from 0% to 100%).   For the pile diameter b, A_b and PCR_b have positive values for 0% and 10% clay layer thickness since the values of S_b are negative in clay and positive in

184

sand. As the clay layer thickness increases, the integration along the pile length shows that the negative values in clay dominate resulting in a negative value of A_b and PCR_b.

Table 6.16 Values of A (in kN.m) for each variable at different thicknesses of clay for load P_t=100 kN (load-based comparison)

Clay layer thickness	0%	10%	20%	30%	40%	50%	60%	70%	80%	90%	100%
A_c^{Py}	0.0000	-0.0070	-0.0272	-0.0687	-0.0966	-0.0933	-0.0971	-0.0986	-0.0993	-0.0993	-0.0994
$A_{\gamma c}^{Py}$	0.0000	-0.0005	-0.0030	-0.0072	-0.0097	-0.0094	-0.0098	-0.0099	-0.0099	-0.0099	-0.0099
$A_{\varepsilon 50}^{Py}$	0.0000	0.0025	0.0101	0.0218	0.0289	0.0278	0.0290	0.0295	0.0297	0.0297	0.0297
A_k^{Py}	-0.0009	-0.0011	-0.0014	-0.0018	-0.0003	-0.0003	-0.0001	0.0000	0.0000	0.0000	0.0000
$A_{\gamma s}^{Py}$	-0.0159	-0.0132	-0.0077	-0.0017	0.0000	0.0000	0.0000	0.0000	0.0000	0.0000	0.0000
A_{ϕ}^{Py}	-0.0406	-0.0352	-0.0207	-0.0047	0.0000	0.0000	0.0000	0.0000	0.0000	0.0000	0.0000
A_{EI}^{Py}	-0.0152	-0.0207	-0.0383	-0.0515	-0.0523	-0.0523	-0.0537	-0.0531	-0.0532	-0.0532	-0.0532
A_b^{Py}	0.0026	0.0010	-0.0087	-0.0344	-0.0529	-0.0511	-0.0533	-0.0542	-0.0545	-0.0545	-0.0545

Table 6.17 Values of PCR (dimensionless) for each variable at different thicknesses of clay for load P_t=100 kN (load-based comparison)

Clay layer thickness	0%	10%	20%	30%	40%	50%	60%	70%	80%	90%	100%
PCR_c^{Py}	0.0000	-0.2447	-0.5386	-0.9986	-1.3226	-1.2739	-1.3165	-1.3350	-1.3435	-1.3436	-1.3453
$PCR_{\gamma c}^{Py}$	0.0000	-0.0190	-0.0598	-0.1044	-0.1331	-0.1285	-0.1325	-0.1335	-0.1344	-0.1345	-0.1346
$PCR_{\varepsilon 50}^{Py}$	0.0000	0.0879	0.1995	0.3174	0.3950	0.3797	0.3928	0.3988	0.4016	0.4016	0.4023
PCR_k^{Py}	-0.0413	-0.0382	-0.0285	-0.0266	-0.0048	-0.0042	-0.0015	-0.0001	0.0000	0.0000	0.0000
$PCR_{\gamma s}^{Py}$	-0.7415	-0.4598	-0.1516	-0.0251	0.0000	0.0000	0.0000	0.0000	0.0000	0.0000	0.0000
PCR_{ϕ}^{Py}	-1.8995	-1.2299	-0.4108	-0.0684	0.0000	0.0000	0.0000	0.0000	0.0000	0.0000	0.0000
PCR_{EI}^{Py}	-0.7109	-0.7239	-0.7592	-0.7478	-0.7155	-0.7140	-0.7275	-0.7193	-0.7199	-0.7197	-0.7196
PCR_b^{Py}	0.1230	0.0345	-0.1727	-0.5004	-0.7245	-0.6985	-0.7223	-0.7333	-0.7374	-0.7374	-0.7382

Effect of non-homogeneity on relative sensitivity factors TF and GF

The values of the total relative sensitivity factors *TF* for all the parameters are given in Table 6.18 for the different thicknesses of clay (0% to 100%) at a constant load equal to 100 kN. The total relative sensitivity factors *TF* for the clay parameters (c, γ_c' and ε_{50}) are

185

equal to zero at 0% clay layer thickness and increase until 40% clay layer thickness and becomes almost steady for higher thicknesses. On the other hand, the sand parameters start with a maximum value at 0% clay layer thickness and decrease till it reaches zero (or negligible values for the parameter k) for clay layer thickness greater than or equal 40%. For the pile parameters, the value of TF_{EI} increases then decreases until it reaches a steady percent of effect (almost 22%) at 40% clay layer thickness while TF_b decreases then increases until it reaches the same percent of effect (22%) at the same thickness.

In general, the values of the total relative sensitivity factors (i.e. effect in percent relative to all variables) for the different variables depend on the percent of clay and sand. For example, the most effective parameter relative to all variables is the angle of friction ϕ at 0% and 10% clay layer thickness while it is the bending stiffness EI at 20% clay layer thickness. The cohesion c is the most effective parameter at clay layer thickness equal to or greater than 30%.

The values of the group relative sensitivity factors GF for all the parameters are given in Table 6.19 for the different thicknesses of clay (0% to 100%) at a constant load =100 kN. The group relative sensitivity factors GF for the clay parameters start to appear at 10% clay layer thickness and it is noticed that c has the highest effect relative to its group (clay parameters), followed by ε_{50} then γ_c' regardless of the percent of clay, i.e. the values of GF do not change significantly with the increase in the thickness of clay.

For the sand parameters, the angle of friction ϕ has the highest effect relative to its group (sand parameters) followed by γ_s' then k. However, at percent clay = 40%, the effect of ϕ and γ_s' vanishes completely (since deflection in sand y becomes less than y_k) causing the effect of k to be 100% and that for ϕ and γ_s' to be 0%. For the pile parameters, the value of GF_{EI} increases then decreases until it reaches a steady percent of effect relative to the group (pile parameters) (almost 50%) at 40% clay layer thickness while GF_b decreases then increases until it reaches the same percent of effect (almost 50%) at 40% clay layer thickness.

186

Table 6.18 Values of TF (in %) for each variable at different thicknesses of clay for load P_t=100 kN (load-based comparison)

Clay layer thickness	0%	10%	20%	30%	40%	50%	60%	70%	80%	90%	100%
TF_c^{Py}	0.00	8.62	23.21	35.80	40.13	39.82	39.98	40.21	40.26	40.27	40.28
$TF_{\gamma c}^{Py}$	0.00	0.67	2.57	3.74	4.04	4.02	4.02	4.02	4.03	4.03	4.03
$TF_{\varepsilon 50}^{Py}$	0.00	3.10	8.60	11.38	11.99	11.87	11.93	12.01	12.03	12.04	12.04
TF_k^{Py}	1.18	1.35	1.23	0.96	0.15	0.13	0.05	0.00	0.00	0.00	0.00
$TF_{\gamma s}^{Py}$	21.09	16.20	6.53	0.90	0.00	0.00	0.00	0.00	0.00	0.00	0.00
TF_ϕ^{Py}	54.02	43.34	17.70	2.45	0.00	0.00	0.00	0.00	0.00	0.00	0.00
TF_{EI}^{Py}	20.22	25.51	32.71	26.81	21.71	22.32	22.09	21.67	21.57	21.57	21.55
TF_b^{Py}	3.50	1.21	7.44	17.94	21.99	21.84	21.93	22.09	22.10	22.10	22.10

Table 6.19 Values of GF (in %) for each variable at different thicknesses of clay for load P_t=100 kN (load-based comparison)

Clay layer thickness	0%	10%	20%	30%	40%	50%	60%	70%	80%	90%	100%
GF_c^{Py}	-	69.60	67.51	70.31	71.47	71.48	71.47	71.49	71.48	71.48	71.477
$GF_{\gamma c}^{Py}$	-	5.40	7.49	7.35	7.19	7.21	7.19	7.15	7.15	7.15	7.151
$GF_{\varepsilon 50}^{Py}$	-	25.00	25.00	22.34	21.34	21.31	21.33	21.36	21.37	21.37	21.372
GF_k^{Py}	1.54	2.21	4.82	22.17	100.00	100.00	100.00	100.00	100.00	100.00	-
$GF_{\gamma s}^{Py}$	27.65	26.61	25.66	20.89	0.00	0.00	0.00	0.00	0.00	0.00	-
GF_ϕ^{Py}	70.82	71.18	69.52	56.94	0.00	0.00	0.00	0.00	0.00	0.00	-
GF_{EI}^{Py}	85.25	95.45	81.47	59.91	49.69	50.55	50.18	49.52	49.40	49.39	49.362
GF_b^{Py}	14.74	4.55	18.53	40.09	50.31	49.45	49.82	50.48	50.60	50.61	50.638

Effect of non-homogeneity in general

For all the design parameters, the increase in the clay thickness has a minor effect on all the sensitivity results starting from 40% clay layer thickness (thickness of clay layer =7.2 m in the studied case of 18 m long pile). Although at the same level of applied load (100 kN), as the thickness of clay layer increases the soil becomes weaker and the deflection should increase, this increase in deflection starts to become negligible after a certain clay layer thickness (40% in this sample case) as the clay thickness increases for the long piles.

187

6.2.5.3.2 Deflection-based comparison

Effect of non-homogeneity on sensitivity operators

The second approach taken to study the effect of the thickness of overlaying clay layer on the sensitivity results is to investigate this effect while the deflection at the pile head is almost equal for the different cases of non-homogeneity (clay thickness). The sensitivity operators S are plotted in Figure 6.22 (a, b, c and d) and Figure 6.23 (a, b, c and d) for the clay parameters (c, γ_c' and ε_{50}), sand parameters (k, γ_s' and ϕ) and pile parameters (EI and b), respectively, for different thicknesses of clay when the pile has almost the same deflection at the pile head.

Table 6.20 shows the pile head deflections (almost equal) and the corresponding loads for the different cases of clay thickness. It is seen from the table that as the thickness of clay increases, the soil becomes weaker and requires the pile to be subjected to a smaller load to obtain the same deflection at the pile head.

Table 6.20 Values of P_t and corresponding y_t used in the deflection-based comparison approach

Clay Layer thickness	0%	10%	20%	30%	40%	50%	60%	70%	80%	90%	100%
y_t (m)	0.076	0.077	0.070	0.069	0.073	0.073	0.074	0.074	0.074	0.074	0.074
P_t (kN)	225	200	125	100	100	100	100	100	100	100	100

The distribution of sensitivity operators for clay $S_{\varepsilon_{50}}$, S_{γ_c}, S_c (Figure 6.22 a, b and c) based on the constant pile head deflection criterion show that the maximum values of the operators increase as the thickness of clay increase. Although the deflection of the primary pile y is almost equal for the different cases of non-homogeneity (different soil profiles), the operators are functions of both the deflection of the primary pile y and the adjoint pile deflection y_a. Therefore the increase in the maximum values of the operators can be explained in reference to the deflection curves for both the primary pile y and the adjoint pile y_a shown in Figures 6.24 a and 6.24b, respectively.

188

Although the deflection of the primary pile is almost the same for the primary pile at different thicknesses of clay (Figure 6.24a), the deflection of the adjoint pile y_a increases as the thickness of clay increases. This is due to the fact that as the thickness of clay increases, the soil becomes weaker and the load required to obtain the same deflection at ground surface decreases. The deflection of the adjoint pile y_a is obtained by applying a unit load to the adjoint pile which is in the state of deformation of the primary pile subjected to a given load. The value of y_a is obtained numerically by subtracting the deflection of a pile subjected to load P_t from the deflection of a pile subjected to load P_t+1. Therefore as P_t decreases y_a increases (for example a difference between the deflection of a pile subjected to load 2001 kN and 2000 kN will be less than the difference between piles subjected to loads 2 kN and 1 kN).

For the sand parameters (Figures 6.22d, 6.23a and 6.23b), at a constant top deflection, as the thickness of clay increases sand starts at a deeper level causing the maximum value of the operators to decrease. However, for 0% and 10% clay layer thickness, the effect of the operators start at the same depth and the maximum value is close in both cases (since all operators have zero value when $y>y_u$). The maximum value for S_k at soil profile with 30% clay layer thickness shows an increase in the operator rather than a decrease opposite to what is expected. This is because the change in the geometry of soil profile leads to the difference in the deflection along the pile length for the different soil profiles although the top deflection is almost equal. This difference caused an increase in deflection at 30% clay thickness in the zone at which S_k is developed (Figure 6.24a).

The sensitivity operators for the pile parameter EI are plotted in Figure 6.23c. It is obvious that the pile structure when embedded in sand with small thickness of clay layer is more rigid than in the case when the top clay layer increases its thickness. This means that increase of thickness of soft clay layer is equivalent to the weakening of pile support in the proximity of the soil surface. The association of constant pile deflection criterion means that the constant value of top displacement of rigid pile results in larger bending moment of pile structure that is developed at smaller depth of the pile. (i.e. as thickness increases, pile is subjected to a smaller load therefore bending moment in pile decreases). The bending moments for the different thicknesses of clay are plotted in Figure 6.25.
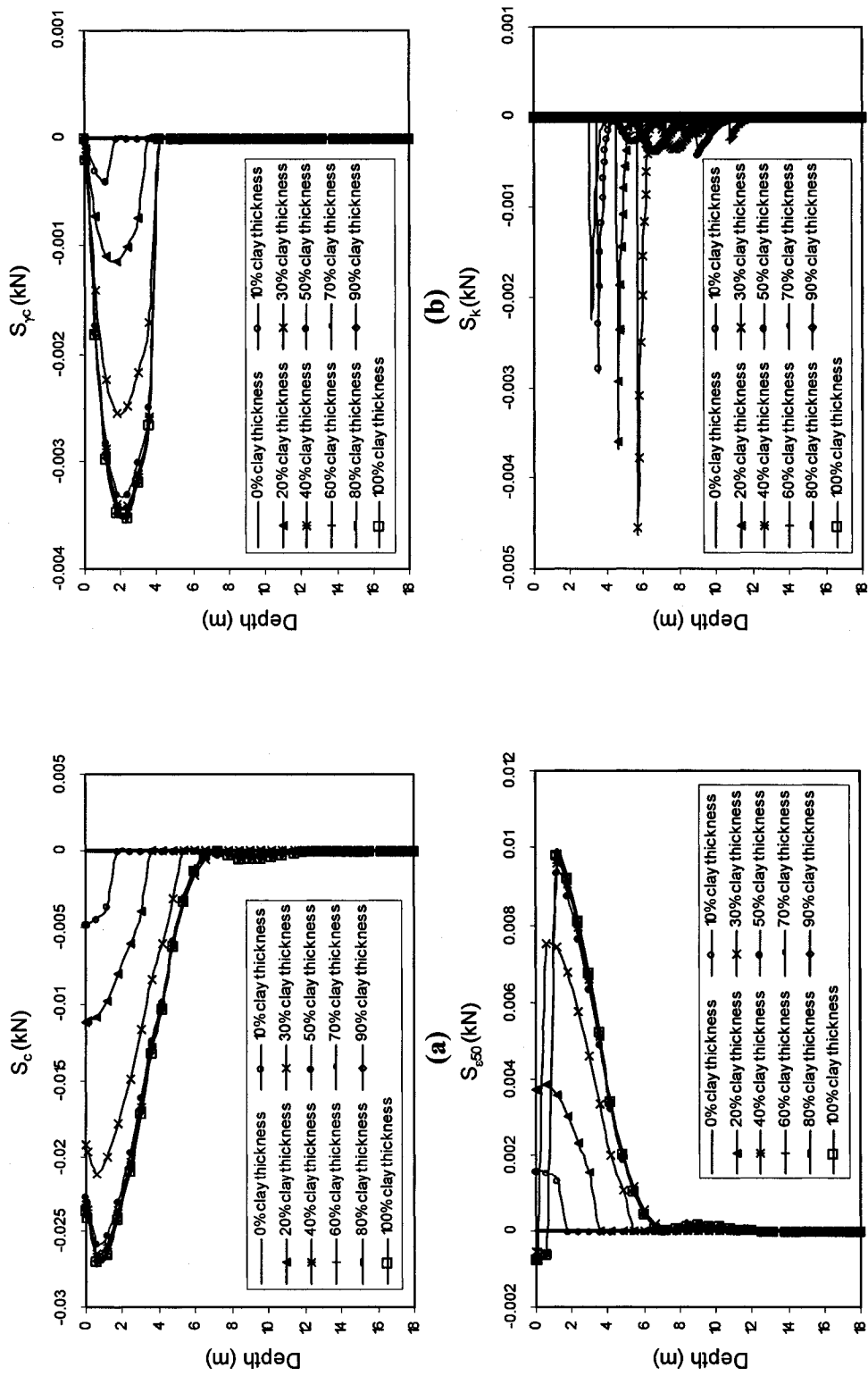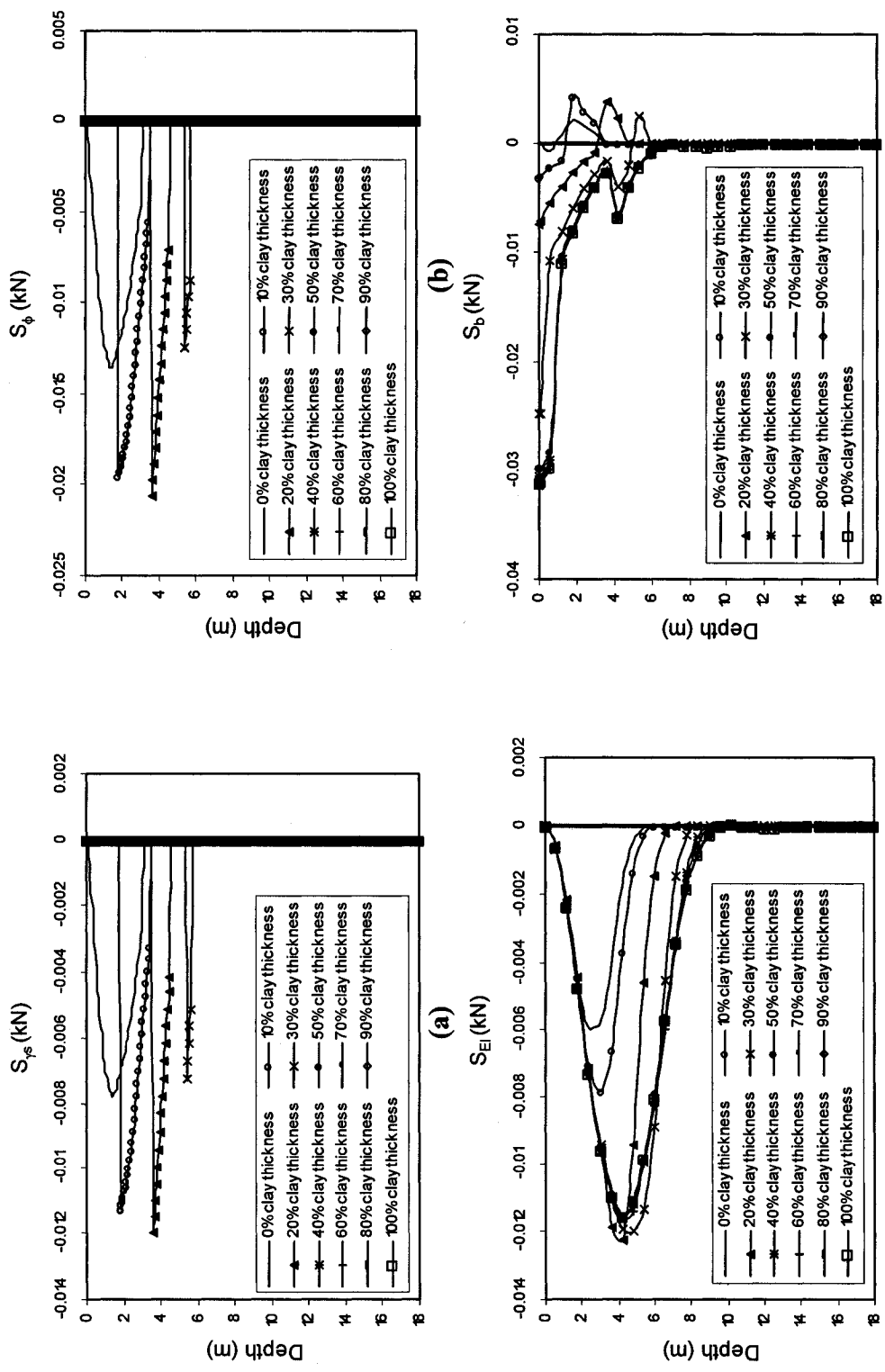
189
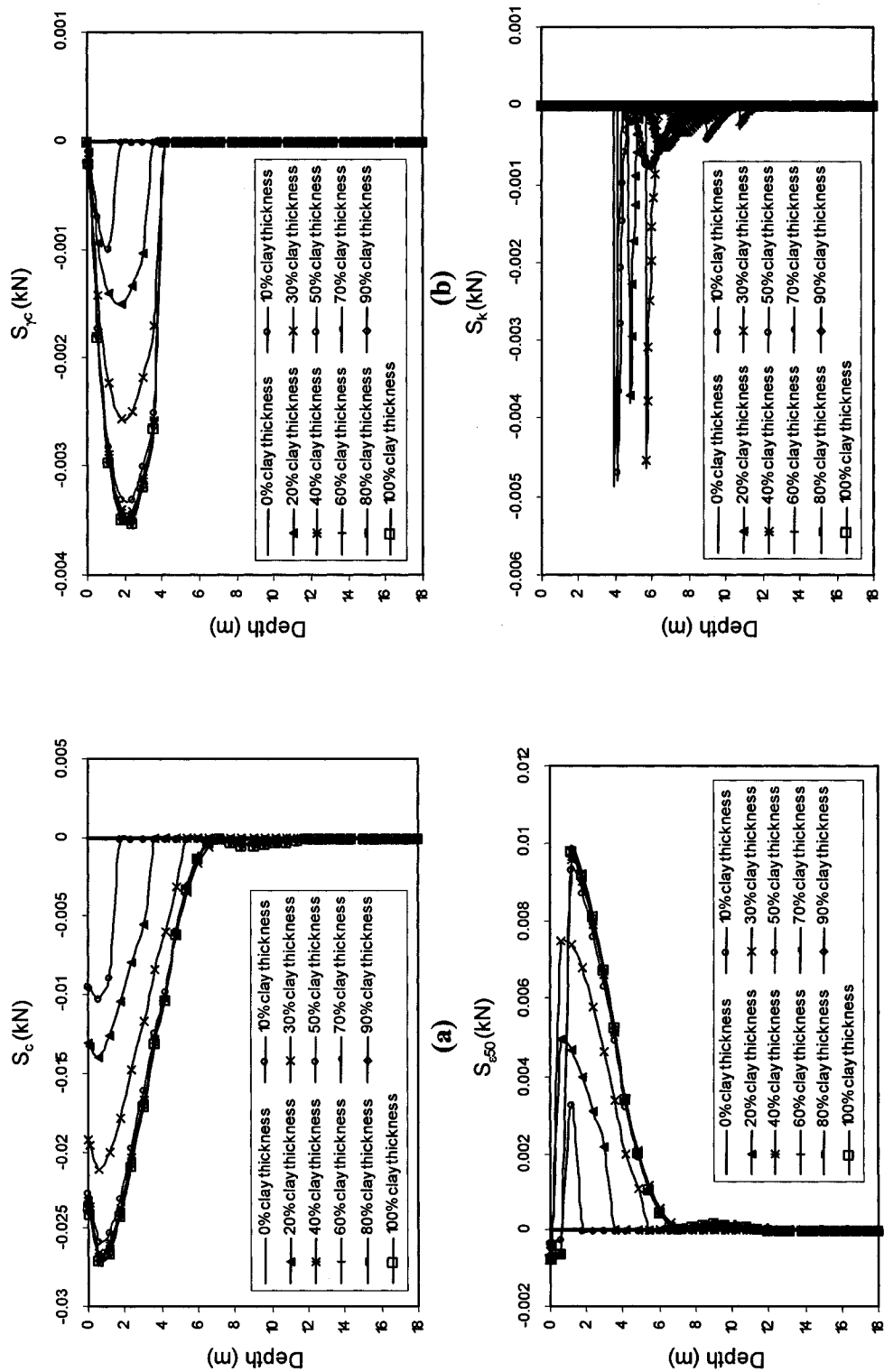
Figure 6.22 Sensitivity operators for 18 m long free head pile at different thicknesses of clay (deflection-based comparison) (a) S_c^{Py}, (b) $S_{\gamma c}^{Py}$, (c) $S_{\varepsilon 50}^{Py}$ and (d) S_k^{Py}

190
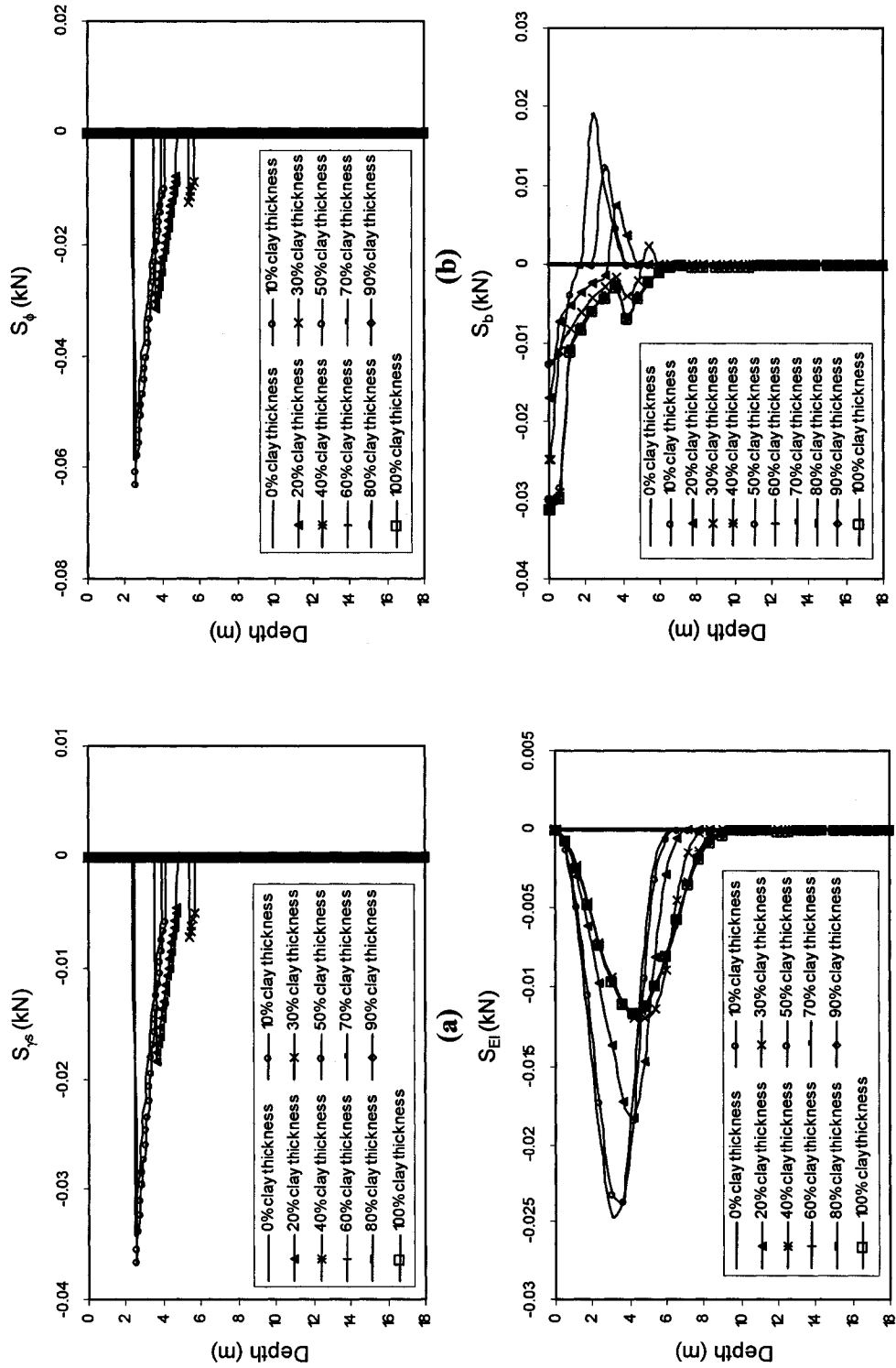
Figure 6.23 Sensitivity operators for 18 m long free head pile at different thicknesses of clay (deflection-based comparison) a) S_{ps}^{Py}, (b) S_{ϕ}^{Py}, (c) S_{EI}^{Py} and (d) S_{b}^{Py}

191
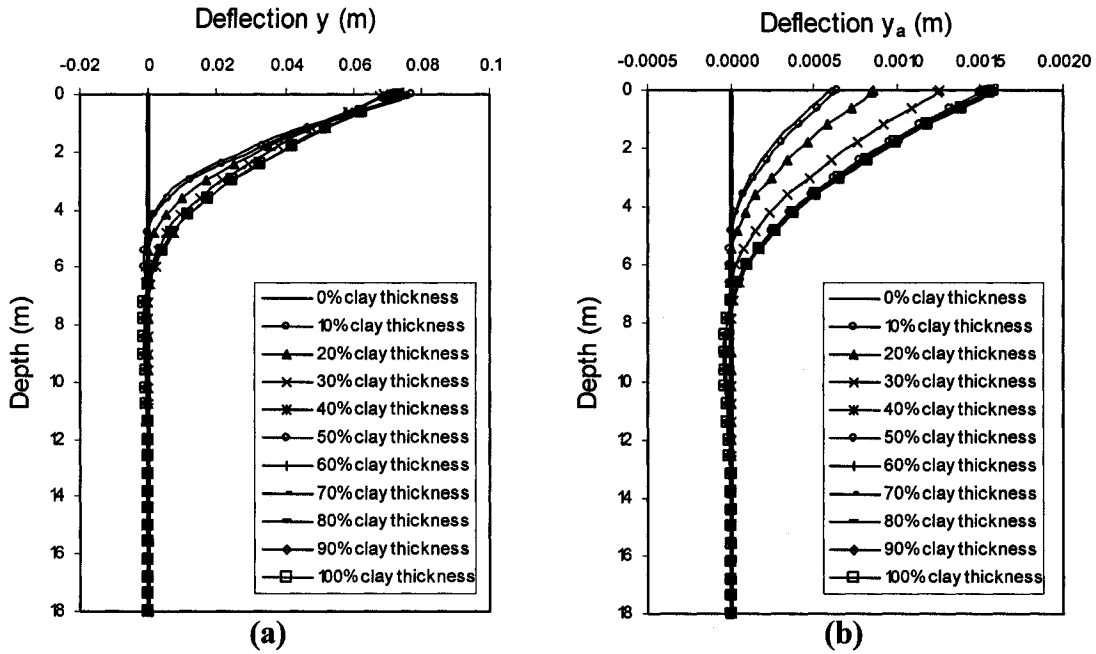
Figure 6.24 Deflections at different thicknesses of clay for (a) primary pile _y_, (b) adjoint pile _y_a (deflection-based criterion)
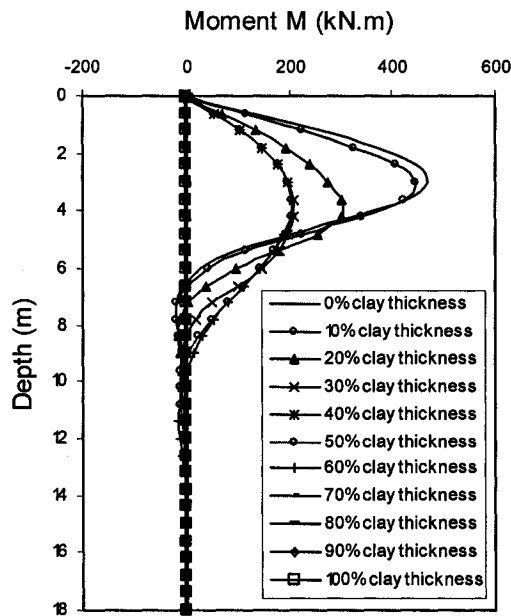
Figure 6.25 Bending moment of primary pile for different thicknesses of clay (deflection-based criterion)

This logic explains why the S_{EI} operators have higher values when the thicknesses of soft clay layer are small than when the thicknesses of clay layer are large. Moreover, Figure 6.23c shows that variability of S_{EI} for small values of thickness of clay layer is spread to

192

smaller depth than for the thicker clay layer. It is shown in the figure that as the thickness increases the maximum value of the operator S_{EI} decreases opposite to the behavior observed for the load-based comparison.

The sensitivity operators for the pile diameter b are given in Figure 6.23d. As the thickness of clay increases, the maximum values of S_b increase in the clay layer while they decrease in the sand layer. This is consistent with the observations given above for the clay and sand parameters.

Effect of non-homogeneity on A and PCR

The values of the sensitivity factors A and the percent change ratio PCR for all the parameters are given in Table 6.21 and Table 6.22, respectively, for the different thicknesses of clay for the deflection-based criterion. For the clay operators, as the thickness of clay increases, the integration of the sensitivity operators results in a higher value of the sensitivity factors A and the value of PCR.

For the sand operators, as the thickness of clay increases (from 0% to 100%), the sand operators start at a deeper level and the values of A and PCR for the sand parameters decrease except for 0% and 10% clay layer thickness since the values for A and PCR are close based on their S distribution. After a certain clay thickness, the values of A_k and PCR_k become negligible while those for γ_s' and ϕ become equal to zero when the deflection at the top of the sand layer is less than the value of y_k (i.e. $y<y_k$).

For the parameter EI, A_{EI} and PCR_{EI} decrease as the thicknesses of the clay increase (from 0% to 100%). For the pile diameter b, A_b and PCR_b have positive values for 0% and 10% clay layer thickness since the values of S are negative in clay and positive in sand. As the clay thickness increases, the integration along the pile length results shows that negative values of the clay dominates and results in a negative value of A_b and PCR_b.

193

Table 6.21 Values of A (in kN.m) for each variable at different thicknesses of clay (deflection-based criterion)

Clay layer thickness	0%	10%	20%	30%	40%	50%	60%	70%	80%	90%	100%
A_c^{Py}	0.0000	-0.0163	-0.0353	-0.0687	-0.0966	-0.0933	-0.0971	-0.0986	-0.0993	-0.0993	-0.0994
$A_{\gamma c}^{Py}$	0.0000	-0.0013	-0.0040	-0.0072	-0.0097	-0.0094	-0.0098	-0.0099	-0.0099	-0.0099	-0.0099
$A_{\varepsilon 50}^{Py}$	0.0000	0.0036	0.0108	0.0218	0.0289	0.0278	0.0290	0.0295	0.0297	0.0297	0.0297
A_k^{Py}	-0.0021	-0.0022	-0.0016	-0.0018	-0.0003	-0.0003	-0.0001	0.0000	0.0000	0.0000	0.0000
$A_{\gamma s}^{Py}$	-0.0291	-0.0319	-0.0133	-0.0017	0.0000	0.0000	0.0000	0.0000	0.0000	0.0000	0.0000
A_ϕ^{Py}	-0.0790	-0.0866	-0.0360	-0.0047	0.0000	0.0000	0.0000	0.0000	0.0000	0.0000	0.0000
A_{EI}^{Py}	-0.0679	-0.0673	-0.0571	-0.0515	-0.0523	-0.0523	-0.0537	-0.0531	-0.0532	-0.0532	-0.0532
A_b^{Py}	0.0133	0.0030	-0.0135	-0.0344	-0.0529	-0.0511	-0.0533	-0.0542	-0.0545	-0.0545	-0.0545

Table 6.22 Values of PCR (dimensionless) for each variable at different thicknesses of clay

Clay Layer thickness	0%	10%	20%	30%	40%	50%	60%	70%	80%	90%	100%
PCR_c^{Py}	0.000	-0.211	-0.502	-0.9986	-1.323	-1.274	-1.317	-1.335	-1.343	-1.344	-1.345
$PCR_{\gamma c}^{Py}$	0.000	-0.017	-0.057	-0.1044	-0.133	-0.129	-0.133	-0.134	-0.134	-0.134	-0.135
$PCR_{\varepsilon 50}^{Py}$	0.000	0.046	0.153	0.3174	0.395	0.380	0.393	0.399	0.402	0.402	0.402
PCR_k^{Py}	-0.028	-0.028	-0.023	-0.0266	-0.005	-0.004	-0.001	0.000	0.000	0.000	0.000
$PCR_{\gamma s}^{Py}$	-0.382	-0.412	-0.189	-0.0251	0.000	0.000	0.000	0.000	0.000	0.000	0.000
PCR_ϕ^{Py}	-1.039	-1.120	-0.512	-0.0684	0.000	0.000	0.000	0.000	0.000	0.000	0.000
PCR_{EI}^{Py}	-0.893	-0.870	-0.813	-0.7478	-0.716	-0.714	-0.727	-0.719	-0.720	-0.720	-0.720
PCR_b^{Py}	0.175	0.039	-0.193	-0.5004	-0.725	-0.699	-0.722	-0.733	-0.737	-0.737	-0.738

Effect of non-homogeneity on relative sensitivity factors TF and GF

The values of the total and group relative sensitivity factors (*TF* and *GF*) for all the parameters are given in Tables 6.23 and 6.24, respectively, for the different thicknesses of clay (0% to 100%) based on the deflection-based criterion. In general, the values of the *TF* (i.e. effect in percent relative to all variables) for the different variables depend on the percent of clay and sand. For the group relative sensitivity factors, the values of *GF* for the clay parameters do not change significantly with the increase in the thickness.

194

For the sand parameters, the values of *GF* are very close at 0% and 10% clay layer thickness as explained above. The angle of friction ϕ has the highest effect relative to the sand parameters as the percent clay increases up to percent clay equal to 40% where its effect become 0%(since deflection in sand y becomes less than y_k). For the pile parameters, the value of GF_{EI} decreases as percent clay increases while that for b increases except for 0% and 10% clay layer thickness.

Table 6.23 Values of TF (in %) for each variable at different thicknesses of clay

%clay	0%	10%	20%	30%	40%	50%	60%	70%	80%	90%	100%
TF_c^{Py}	0.00	7.69	20.58	35.807	40.13	39.82	39.98	40.21	40.26	40.27	40.28
$TF_{\gamma c}^{Py}$	0.00	0.62	2.32	3.742	4.04	4.02	4.02	4.02	4.03	4.03	4.03
$TF_{\varepsilon 50}^{Py}$	0.00	1.69	6.28	11.381	11.98	11.87	11.93	12.01	12.04	12.04	12.04
TF_k^{Py}	1.12	1.02	0.94	0.955	0.15	0.13	0.05	0.00	0.00	0.00	0.00
$TF_{\gamma s}^{Py}$	15.19	15.02	7.73	0.900	0.00	0.00	0.00	0.00	0.00	0.00	0.00
TF_ϕ^{Py}	41.26	40.81	20.98	2.453	0.00	0.00	0.00	0.00	0.00	0.00	0.00
TF_{EI}^{Py}	35.46	31.72	33.29	26.817	21.71	22.32	22.09	21.67	21.57	21.57	21.55
TF_b^{Py}	6.97	1.42	7.89	17.944	21.98	21.84	21.93	22.09	22.10	22.10	22.10

Table 6.24 Values of GF (in %) for each variable at different thicknesses of clay

%clay	0%	10%	20%	30%	40%	50%	60%	70%	80%	90%	100%
GF_c^{Py}	-	76.83	70.53	70.306	71.47	71.48	71.48	71.49	71.48	71.48	71.48
$GF_{\gamma c}^{Py}$	-	6.24	7.95	7.348	7.19	7.21	7.19	7.15	7.15	7.15	7.15
$GF_{\varepsilon 50}^{Py}$	-	16.93	21.53	22.346	21.34	21.31	21.33	21.36	21.37	21.37	21.37
GF_k^{Py}	1.94	1.80	3.16	22.167	100.00	100.00	100.00	100.00	100.00	100.00	-
$GF_{\gamma s}^{Py}$	26.39	26.41	26.08	20.893	0.00	0.00	0.00	0.00	0.00	0.00	-
GF_ϕ^{Py}	71.67	71.79	70.76	56.940	0.00	0.00	0.00	0.00	0.00	0.00	-
GF_{EI}^{Py}	83.58	95.71	80.84	59.911	49.69	50.55	50.18	49.52	49.40	49.39	49.36
GF_b^{Py}	16.42	4.29	19.16	40.089	50.31	49.45	49.82	50.48	50.60	50.61	50.64

195

6.2.5.4 Effect of boundary condition

To study the effect of the pile boundary condition on the sensitivity results, two piles with a free and fixed head will be compared. A fixed head pile will be compared with the sample of free head pile presented in Section 6.2.5.1. Both piles have the same length of 18 m (free head pile with length = $9T$ =18 m and fixed head pile with length = $10T$ =18 m) and same percent of clay thickness which is 20% (i.e. upper 3.6 m of the pile is embedded in soft clay). The sensitivity operators S for the fixed head pile are plotted in Figure 6.26 (a, b, c and d) and Figure 6.27 (a, b, c and d) for the clay parameters (c, γ'_c and ε_{50}), sand parameters (k, γ'_s and ϕ) and pile parameters (EI and b), respectively.

6.2.5.4.1 Effect of boundary condition on sensitivity operators S

To study the effect of the boundary condition on the sensitivity results, a comparison is made between the results of the free head pile and the fixed head one by comparing the results given in Figures 6.9 and 6.10 with results given in Figures 6.26 and 6.27. Comparison can be deflection-based or load-based. In deflection-based comparison, we compare free and fixed head piles having almost the same deflection at the pile head, i.e. we compare between piles that are subjected to loads causing the soil to be in the same soil stage. In the load-based comparison we compare the behavior of the free and fixed head piles when they are both subjected to the same load. The deflection and moments of both the studied free and fixed head piles are given in Figures 6.28 and 6.29, respectively.

For deflection-based comparison, we can compare load P_t = 150 kN for a free head pile (results in y_f= 0.093 m) with P = 400 kN for a fixed head pile (results in y_t = 0.090 m) since they cause almost the same deflection and cause the soil to be in the same stage. As noticed, it requires 2.67 (almost 3) times the applied load for the fixed head pile to cause the same deflection as for a free head pile. From Figures 6.9, 6.10, 6.26 and 6.27, it can be observed that, in general, distributions differ slightly between fixed and free head piles for all operators (does not differ in shape of distribution but in numerical value) except for EI where there is a major difference in the distribution of S_{EI} between the two piles.

196
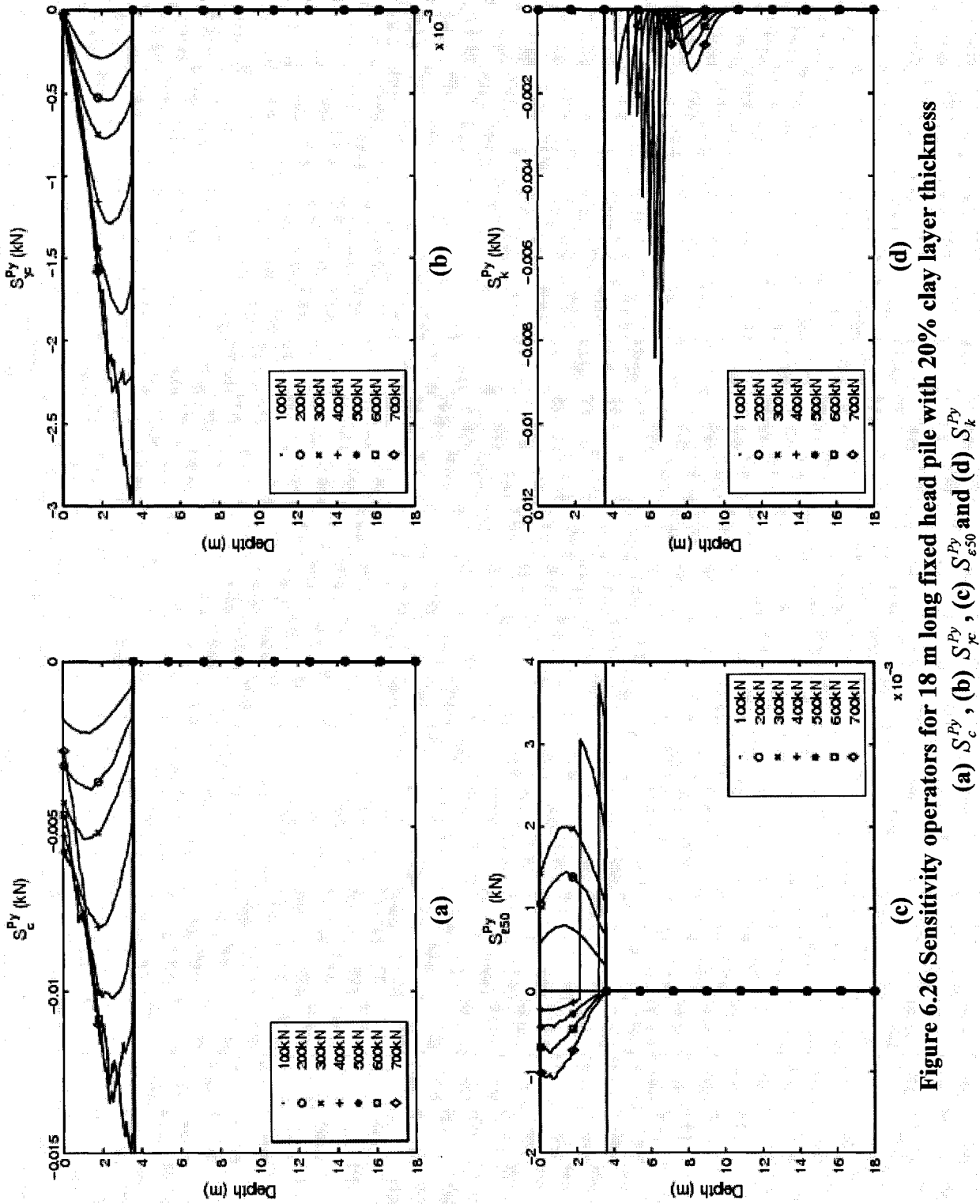
Figure 6.26 Sensitivity operators for 18 m long fixed head pile with 20% clay layer thickness (a) S_c^{Py} **, (b)** $S_{\gamma c}^{Py}$ **, (c)** $S_{\epsilon 50}^{Py}$ **and (d)** S_k^{Py}

197
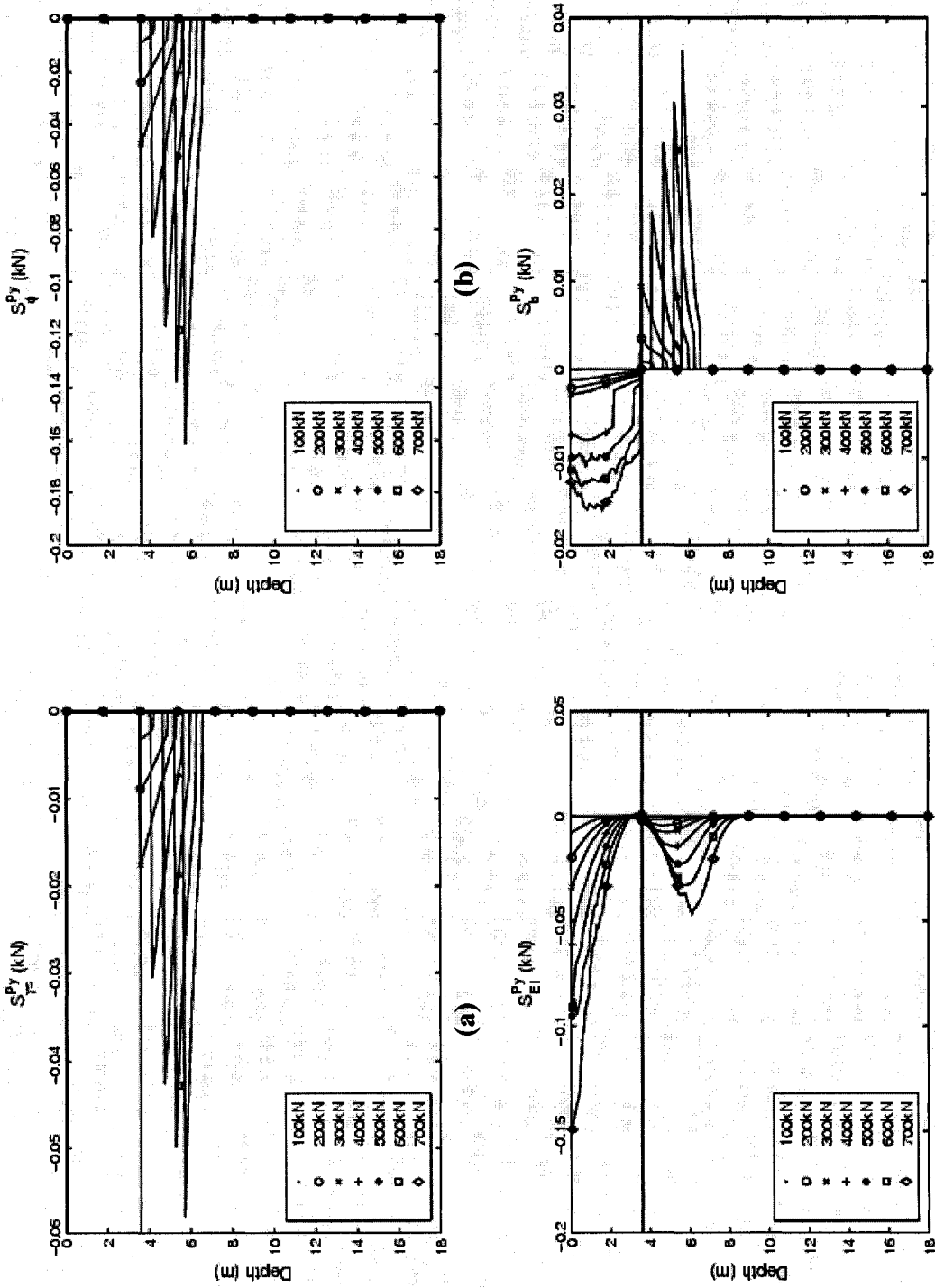
Figure 6.27 Sensitivity operators for 18 m long fixed head pile with 20% clay layer thickness
(a) S_{rs}^{Py} , (b) S_{ϕ}^{Py} , (c) S_{EI}^{Py} and (d) S_{b}^{Py}

198
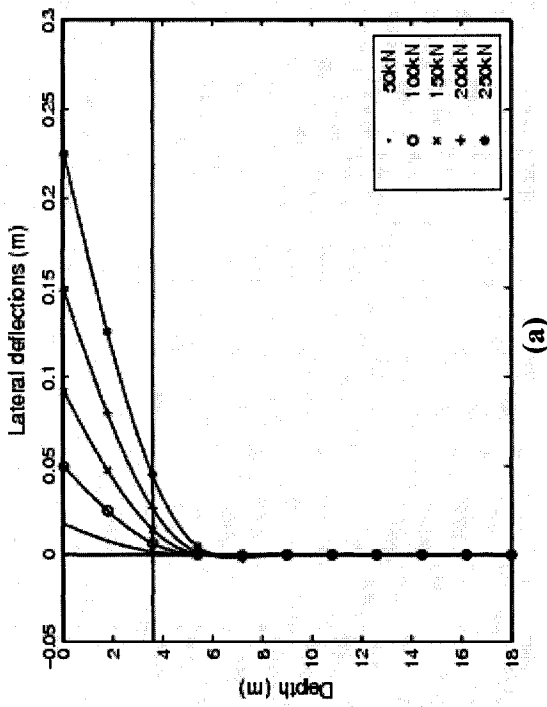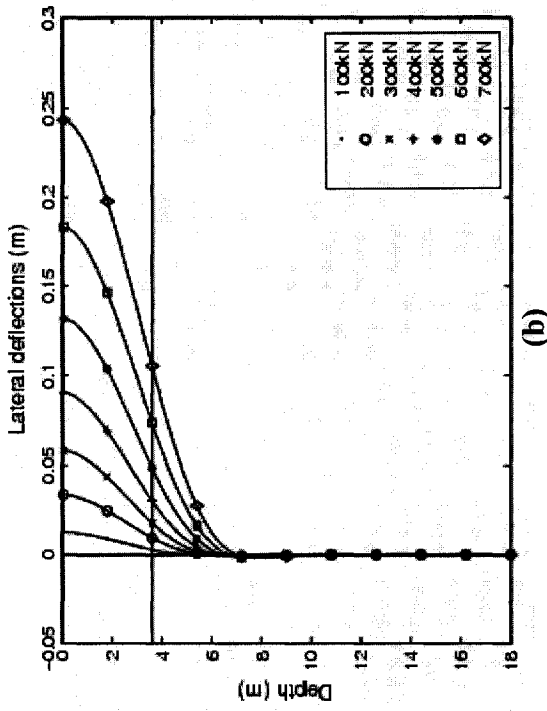
Figure 6.28 Deflections of primary pile for 18 m long pile with 20% clay layer thickness (a) free head pile (b) fixed head pile
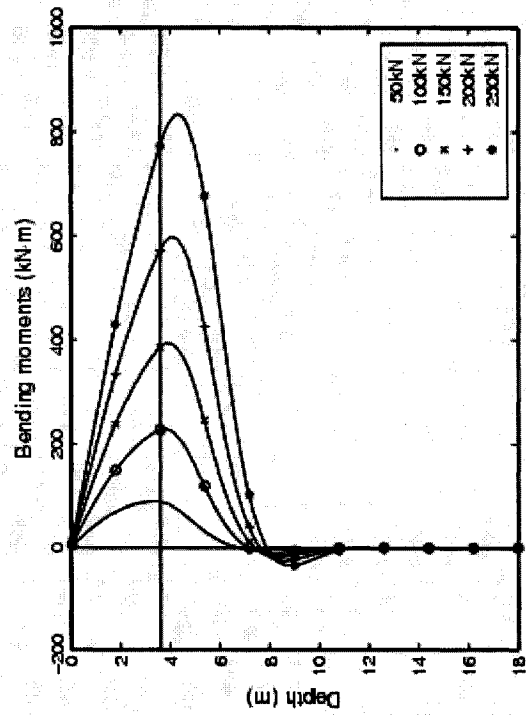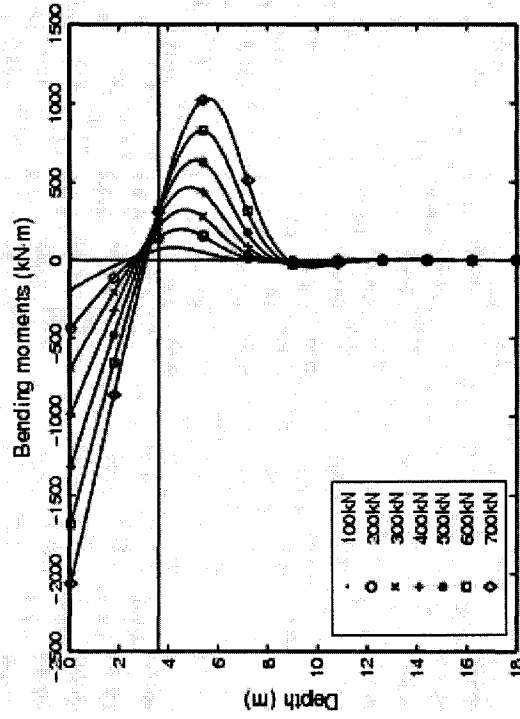
Figure 6.29 Bending moments of primary pile for 18 m long pile with 20% clay layer thickness (a) free head pile (b) fixed head pile

199

The graphical presentation of S_{EI} for a fixed and free head pile shows that for a free head pile variation of EI at the ground surface will not affect the pile head deflection δy_t while variation of EI at the ground surface will cause a considerable variation in the pile head deflection δy_t for a fixed head pile. The negative sign for both cases shows that increase in EI causes a decrease in δy_t as expected.

This uniqueness of S_{EI} can be attributed to the dependence of S_{EI} on the moments of the adjoint and primary piles and its independence on the p-y relationships (expression for S_{EI} in clay equals that in sand) (refer to Appendix A). The other operators do not depend on moment distribution and depend on the p-y relationships and accordingly on the deflection (refer to Appendix A). As shown in Figures 6.28 and 6.29, the moment differs considerably between free and fixed head piles while the deflection pattern doesn't differ considerably between the two cases (except for the slope at the ground surface).

If comparison is load-based, then for the same load, the deflection of the fixed head pile will be less than that of the free head pile (for example compare the piles when they are both subjected to load = 200 kN). The soil for the fixed-head pile will be in an earlier stage of soil behavior and the numerical values of the operators S will be less in general. Therefore we can say that sensitivity of top deflection to change in parameters is less for a fixed head pile than for a free head one in general for load-based comparison. However, there are two exceptions. The first is S_{EI} where the distribution pattern between free and fixed head piles is completely different. The second is the distribution of $S_{\varepsilon 50}$ where there are different signs of $S_{\varepsilon 50}$ for different stages of soil.

For example, if we compare $S_{\varepsilon 50}$ at load P = 200 kN, then the soft clay soil at the surface will be in a nonlinear elastic stage for the fixed head pile while it will be in the linear softening stage for the free head pile. As shown in Figures 6.9c and 6.26c, the sign of the operator is positive for the fixed head pile while it is negative for the free head one at the ground surface. Thus an increase in ε_{50} at the surface will cause an increase in the top deflection for the fixed head pile while it will cause a decrease in the top deflection for the free head one.

200

6.2.5.4.2 Effect of boundary condition on sensitivity results *A*, *PCR*, *TF* and *GF*

The values for the different sensitivity results are compared for free and fixed head piles in Table 6.25 (deflection-based comparison and load-based comparison). For deflection-based comparison, the values of the sensitivity *A*, *PCR*, *TF* and *GF* for the two boundary conditions (free and fixed head) are close since they are based on the distribution of sensitivity operators except for ε_{50} and *b* since they involve positive and negative values in the integration. Although the distribution of S_{EI} is different for the two boundary conditions, the results of integration of S_{EI} for both boundaries were coincidently close.

For the load-based comparison, we notice that the values of *A* for the fixed head pile are smaller than those for the free head pile as explained above for the sensitivity operators. However, since *PCR*= A/y_t and both *A* and y_t decrease in the case of fixed head pile, the values of *PCR* are close for both boundary conditions. Although the sensitivity operators *S* and sensitivity factors *A* have smaller values for the fixed head pile than for the free head pile, however, the relative sensitivity factors (*TF* and *GF*) are very close for both boundary conditions and are not affected by the difference in deflection between the two boundary conditions. From the values of *GF*, the key parameters are found to be *EI* for the pile, ϕ for the sand and *c* for the clay while *EI* is shown to be the most effective parameter from the values of *TF*. (Note that the parameters *EI*, *b* and ε_{50} still remain an exception for all the sensitivity results since *EI* has a completely different distribution of *S* while ε_{50} and *b* involve positive and negative values in the distribution of *S*.

Table 6.25 Values of A, PCR, TF and GF for different boundary conditions (deflection-based comparison and load-based comparison)

	Deflection-based comparison			Load-based comparison	
	P_t=150 kN (free head)	P_t= 400 kN (fixed head)		P_t= 200 kN (free head)	P_t= 200 kN (fixed head)
A_c^{Py}	-0.043	-0.024		-0.061	-0.011
$A_{\gamma c}^{Py}$	-0.005	-0.003		-0.008	-0.001
$A_{\varepsilon 50}^{Py}$	0.009	0.003		0.005	0.004
A_k^{Py}	-0.002	-0.002		-0.004	-9.07E-04

201

Table 6.25 Values of A, PCR, TF and GF for different boundary conditions (deflection-based comparison and load-based comparison)(continued)

	Deflection-based comparison			Load-based comparison	
	$P_t = 150$ kN (free head)	$P_t = 400$ kN (fixed head)		$P_t = 200$ kN (free head)	$P_t = 200$ kN (fixed head)
A_{ys}^{Py}	-0.021	-0.025		-0.042	-0.008
A_{ϕ}^{Py}	-0.057	-0.070		-0.115	-0.022
A_{EI}^{Py}	-0.082	-0.088		-0.155	-0.027
A_{b}^{Py}	-0.021	-0.006		-0.036	-0.002
PCR_{c}^{Py}	-0.46	-0.27		-0.40	-0.34
PCR_{yc}^{Py}	-0.05	-0.04		-0.05	-0.04
$PCR_{\varepsilon 50}^{Py}$	0.10	0.04		0.03	0.13
PCR_{k}^{Py}	-0.02	-0.02		-0.02	-0.027
PCR_{ys}^{Py}	-0.23	-0.28		-0.28	-0.23
PCR_{ϕ}^{Py}	-0.61	-0.77		-0.76	-0.64
PCR_{EI}^{Py}	-0.88	-0.97		-1.03	-0.79
PCR_{b}^{Py}	-0.22	-0.07		-0.24	-0.05
TF_{c}^{Py}	17.89	11.11		14.32	15.06
TF_{yc}^{Py}	2.10	1.47		1.83	1.87
$TF_{\varepsilon 50}^{Py}$	3.70	1.47		1.13	5.64
TF_{k}^{Py}	0.85	0.74		0.84	1.20
TF_{ys}^{Py}	8.78	11.46		9.90	10.46
TF_{ϕ}^{Py}	23.83	31.42		27.02	28.43
TF_{EI}^{Py}	34.24	39.59		36.46	35.24
TF_{b}^{Py}	8.61	2.745		8.49	2.10
GF_{c}^{Py}	75.53	79.11		82.82	66.73
GF_{yc}^{Py}	8.85	10.44		10.60	8.27
$GF_{\varepsilon 50}^{Py}$	15.61	10.44		6.59	25
GF_{k}^{Py}	2.541	1.71		2.21	2.99
GF_{ys}^{Py}	26.23	26.27		26.22	26.10
GF_{ϕ}^{Py}	71.22	72.02		71.56	70.91
GF_{EI}^{Py}	79.90	93.51		81.10	94.38
GF_{b}^{Py}	20.10	6.49		18.89	5.62

202

6.2.5.5 Effect of type of load

To study the effect of type of load on the sensitivity results, two piles with the same boundary condition, length, and percent clay are compared. A pile with support type 3 (free head subjected to bending moment M_t) is compared with the sample given in Section 6.2.5.1 (support type 1; free head pile subjected to lateral load P_t). Both piles are 18 m in length and the thickness of the upper layer of soft clay is 3.6m.

The sensitivity operators for the free head pile subjected to moment M_t for all the parameters are given in Figures 6.30 and 6.31. Since the types of load are different, only the deflection based comparison will be appropriate. The results are therefore compared at loads that give the same deflection at the pile head. The pile subjected to lateral load $P_t = 200$ kN (Figures 6.9 and 6.10) is compared with the pile subjected to bending moment $M_t = 800$ kN.m (Figures 6.30 and 6.31).

From the figures it is observed that patterns (distribution) of the sensitivity operators for both types of load are similar and distributed along the same length of the pile. However, the maximum values of sensitivity operators for the pile subjected to M_t are slightly lower than those for the pile subjected to P_t.

The results A, PCR, TF and GF are given in Table 6.26 to compare between the two types of load. Based on the observations regarding the distributions of the sensitivity operators S, the sensitivity factors A (integration of S) are slightly lower for the pile subjected to bending moment. However, since the distribution of ε_{50} involves positive and negative values, the value of $A_{\varepsilon 50}$ is not always lower for the pile subjected to bending moment M_t. Since y_t is equal for both types of load, the comments for sensitivity factors A apply for PCR ($PCR=A/y_t$).

The total relative sensitivity factors TF for both types of load show that results are very close. Based on the values of TF, the most to least effective parameters are given as : EI, ϕ, c, γ_s', b, γ_c', ε_{50} , k for the pile subjected to lateral load P_t while they are ordered from

203

most to least effective as: EI, ϕ, c, b, γ'_s, $\gamma'_c, \varepsilon_{50}$, k for the pile subjected to bending moment M_t.

Similarly, the group relative sensitivity factors GF for both types of load show that the results are very close. However, the order of the parameters within its group is similar for both cases of load type. They are given as follows from most effective to least:

c, $\gamma'_c, \varepsilon_{50}$ (for clay parameters group)

ϕ, γ'_s, k (for sand parameters group)

EI, b (for pile parameters group)

6.2.5.6   Effect of soil response studied (under investigation)

In the current study, two responses of the pile are under sensitivity investigations. The first is the lateral pile head deflection and the second is the lateral pile head rotation. Two cases are included to study the difference in the sensitivity results of both responses. The first case is for a primary pile subjected to lateral force P_t and the second is for a primary pile subjected to bending moment M_t. In both cases, adjoint pile is subjected to a unit lateral load I_a at pile head to obtain δy_t while it is subjected to a unit bending moment I_a at the pile head to obtain delta $\delta \theta_t$.

For the first case, the sample of results for sensitivity of lateral top deflection given in Section 6.2.5.1 for a primary pile of length 18 m and 3.6m deep clay layer with support type =1 (free head subjected to lateral load P_t) is compared with the sensitivity results of the lateral top rotation for the same pile. The sensitivity operators S for the lateral top rotation are given in Figures 6.32 and 6.33 for all the parameters. Comparing these figures with Figures 6.9 and 6.10 it is observed that the sensitivity operators have the same pattern for both sensitivity responses. However, the numerical values of the sensitivity operators S^{Py} for the lateral top deflection are higher (almost with 1 order of magnitude) than those for the lateral top rotation $S^{P\theta}$, i.e. 10% change in the parameter will produce δy_t in meters higher than $\delta \theta_t$ in radians.

204
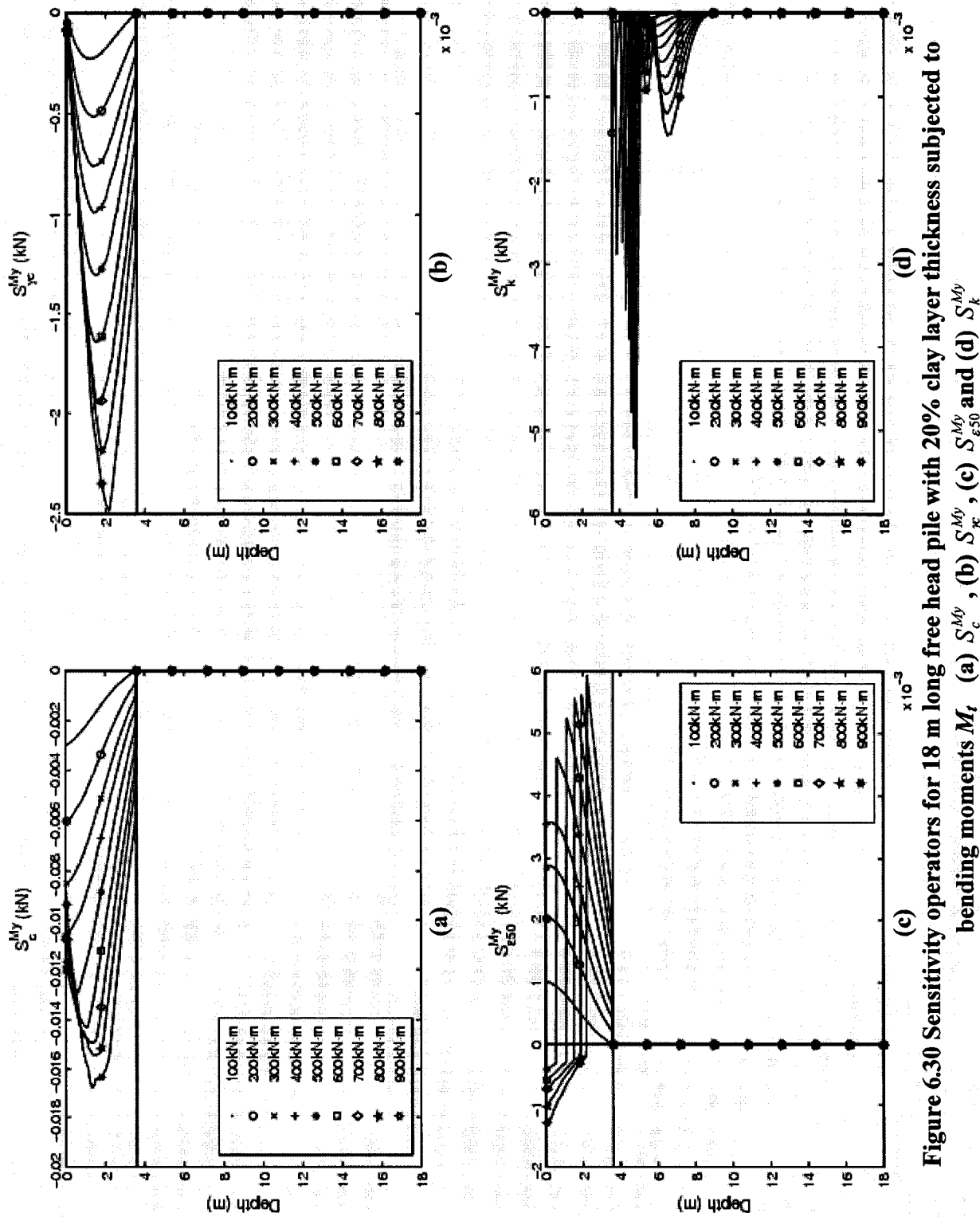
Figure 6.30 Sensitivity operators for 18 m long free head pile with 20% clay layer thickness subjected to bending moments M_t (a) S_c^{My}, (b) S_κ^{My}, (c) $S_{\varepsilon 50}^{My}$ and (d) S_k^{My}

205

Figure 6.31 Sensitivity operators for 18 m long free head pile with 20% clay layer thickness subjected to bending moments M_t (a) $S_{\gamma s}^{My}$, (b) S_{ϕ}^{My} , (c) S_{EI}^{My} and (d) S_{b}^{My}

206
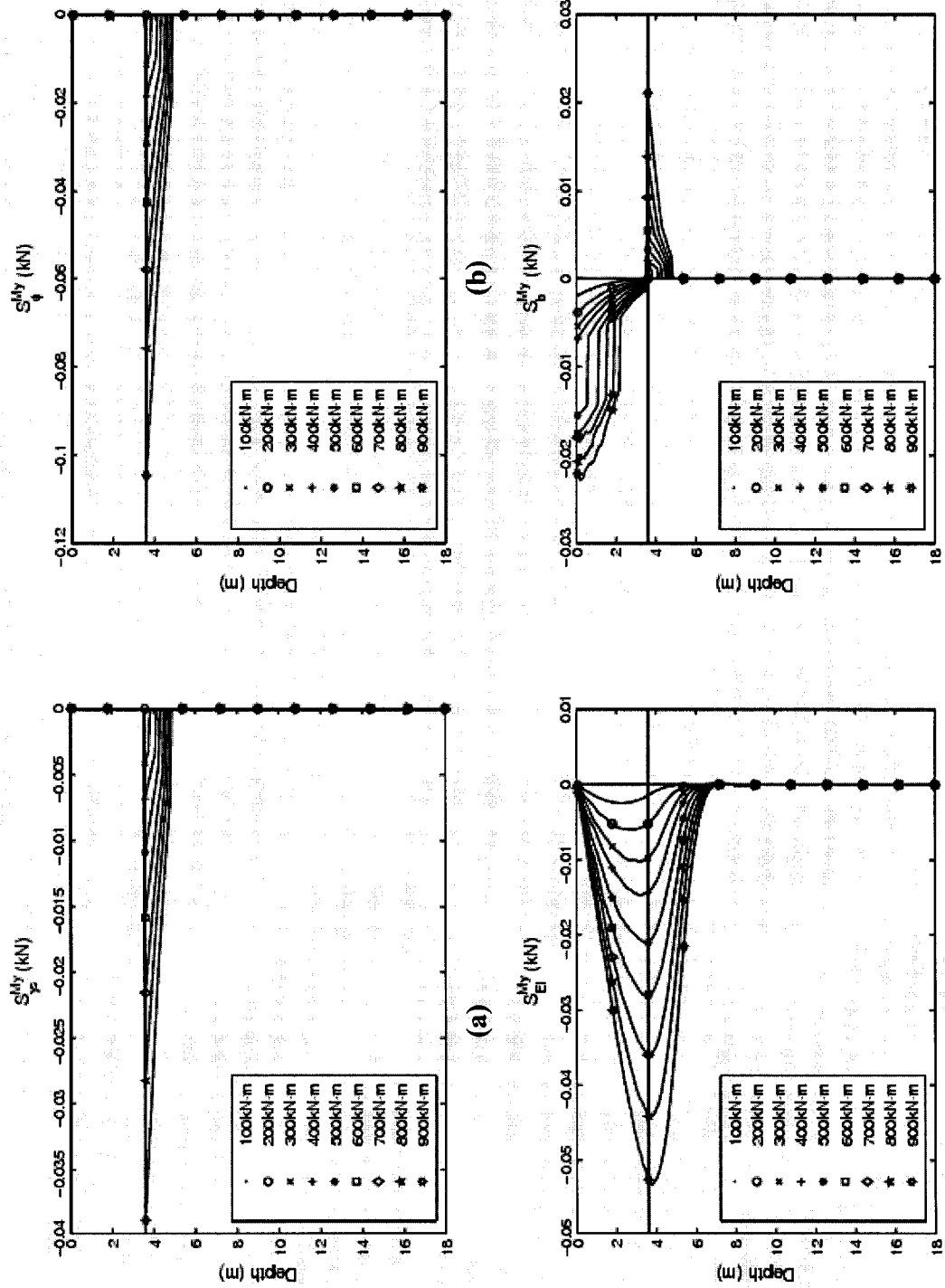
Table 6.26 Comparisons of A, PCR, TF and GF for different types of load

	Pile subjected to lateral load P_t $()^{Py}$	Pile subjected to moment M_t $()^{My}$
	$P_t = 200$ kN $(y_t = 0.151$ m) (Soil response studied $= y_t$)	$M_t = 800$ kN.m $(y_t = 0.154$ m) (Soil response studied $= y_t$)
A_c	-0.061	-0.043
A_{yc}	-0.008	-0.005
$A_{\varepsilon 50}$	0.005	0.005
A_k	-0.003	-0.003
A_{ys}	-0.042	-0.018
A_ϕ	-0.115	-0.050
A_{EI}	-0.155	-0.159
A_b	-0.036	-0.03
PCR_c	-0.40	-0.28
PCR_{yc}	-0.05	-0.03
$PCR_{\varepsilon 50}$	0.03	0.03
PCR_k	-0.02	-0.02
PCR_{ys}	-0.28	-0.12
PCR_ϕ	-0.76	-0.32
PCR_{EI}	-1.03	-1.03
PCR_b	-0.24	-0.19
TF_c	14.32	13.62
TF_{yc}	1.83	1.67
$TF_{\varepsilon 50}$	1.139	1.63
TF_k	0.84	0.94
TF_{ys}	9.90	5.89
TF_ϕ	27.02	15.95
TF_{EI}	36.46	50.72
TF_b	8.49	9.57
GF_c	82.82	80.49
GF_{yc}	10.60	9.86
$GF_{\varepsilon 50}$	6.59	9.64
GF_k	2.21	4.11
GF_{ys}	26.22	25.84
GF_ϕ	71.56	70.05
GF_{EI}	81.11	84.12
GF_b	18.89	15.88

207

The results for A, PCR, TF and GF are given in Table 6.27. As expected, the values of A for the lateral top deflection are higher than those for the lateral top rotation because of their dependence on S. However, since PCR gives a ratio relative to the original response ($\delta y_t/y_t$ or $\delta\theta_t/\theta_t$), it is found that the values of PCR for both responses are close (or $PCR^{P\theta}$ is slightly lower than PCR^{Py}).

Accordingly, the change in any parameter causes almost the same effect for the change in y_t (δy_t) and θ_t ($\delta\theta_t$) relative to the original response (y_t and θ_t), i.e. if EI for example, changes (increases) by 1 % , y_t will change (decrease) by 1.02% while θ_t will change (decrease) by 1.08%. In addition, the values of TF and GF are close for the two responses, i.e. the effect of each parameter relative to the other parameters (whether total (relative to all parameters) or group (relative to its group)) is very close for the two responses.

For the second case, the sample of results for sensitivity of lateral top rotation given in Section 6.2.5.5 (Figures 6.30 and 6.31) for a pile of length 18 m and 3.6m deep clay layer with support type =3 (free head subjected to bending moment M_t) is compared with the sensitivity results of the lateral top rotation for the same pile. The sensitivity operators S for the lateral top rotation are given in Figures 6.34 and 6.35.

Comparing Figures 6.34 and 6.35 with Figures 6.30 and 6.31, the same comments on the results given above for the first case (support type 1 free head pile subjected to P_t) apply to the second studied case (support type 3 free head pile subjected to M_t) with one exception which is for the parameter EI. It is observed that the distribution of the sensitivity operator S_{EI}^{My} (Figure 6.31c) is completely different than $S_{EI}^{M\theta}$ (Figure 6.35c).

Table 6.27 Comparisons of A, PCR, TF and GF for different soil response

	Soil response studied $= y_t$ $()^{Py}$	Soil response studied $= \theta_t$ $()^{P\theta}$
	$P_t = 200$ kN $(y_t = 0.151$ m$)$ (subjected to lateral load P_t)	$P_t = 200$ kN.m $(y_t = 0.151$ m$)$ (subjected to lateral load P_t)
A_c	-0.061	-0.013
A_{yc}	-0.008	-0.002
$A_{\varepsilon 50}$	0.005	9.03E-04
A_k	-0.004	-6.72E-04
A_{ys}	-0.042	-0.007
A_{ϕ}	-0.115	-0.020
A_{EI}	-0.155	-0.044
A_b	-0.036	-0.009
PCR_c	-0.40	-0.32
PCR_{yc}	-0.05	-0.04
$PCR_{\varepsilon 50}$	0.03	0.02
PCR_k	-0.02	-0.02
PCR_{ys}	-0.28	-0.18
PCR_{ϕ}	-0.76	-0.49
PCR_{EI}	-1.03	-1.08
PCR_b	-0.24	-0.22
TF_c	14.32	13.53
TF_{yc}	1.83	1.69
$TF_{\varepsilon 50}$	1.14	0.94
TF_k	0.84	0.70
TF_{ys}	9.90	7.56
TF_{ϕ}	27.02	20.64
TF_{EI}	36.46	45.66
TF_b	8.49	9.29
GF_c	82.82	83.76
GF_{yc}	10.60	10.45
$GF_{\varepsilon 50}$	6.59	5.80
GF_k	2.21	2.41
GF_{ys}	26.22	26.17
GF_{ϕ}	71.56	71.42
GF_{EI}	81.11	83.10
GF_b	18.89	16.90

209
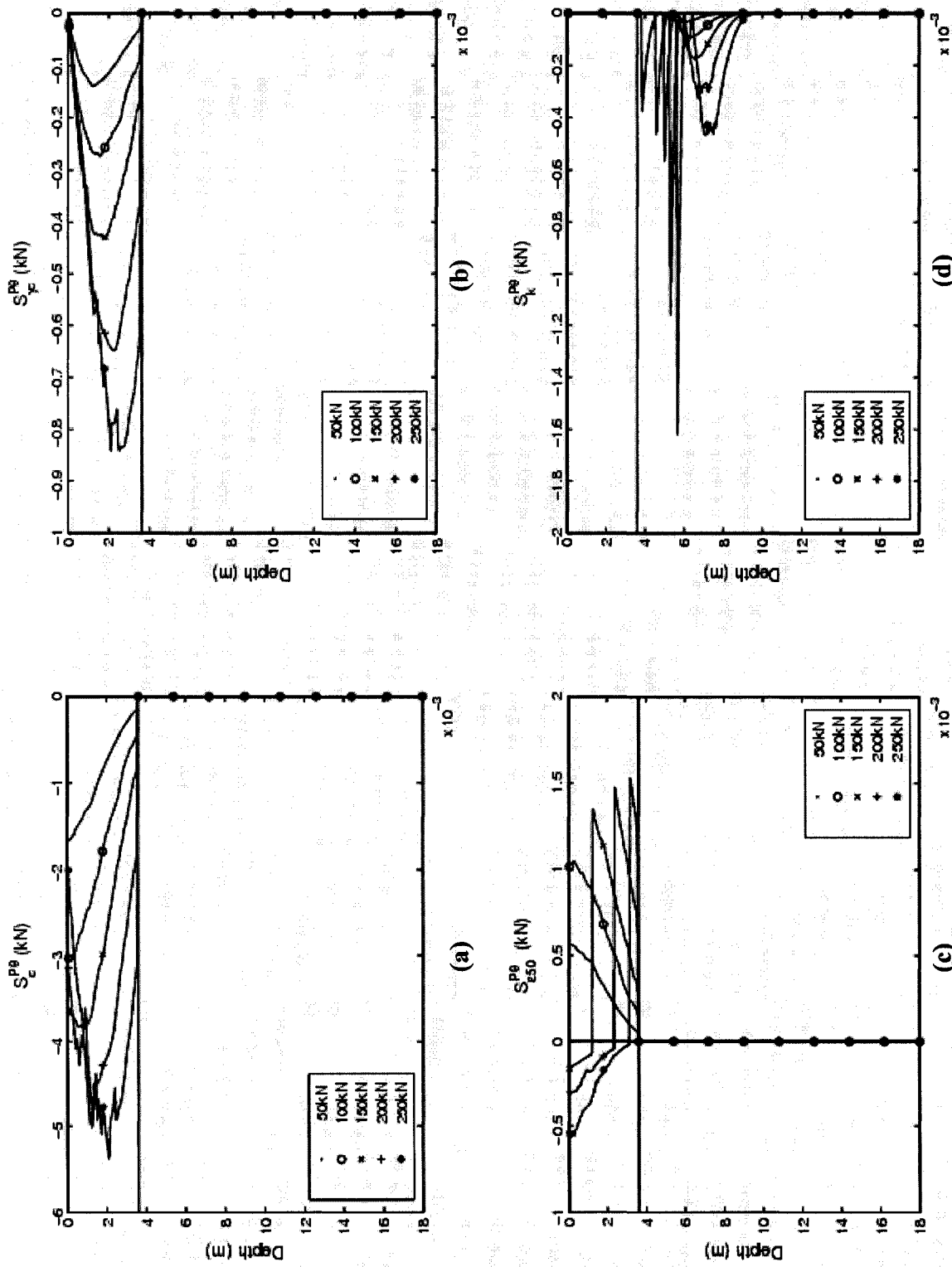
Figure 6.32 Sensitivity operators investigating $\delta\theta_t$ for 18 m long free head pile with 20% clay layer thickness subjected to lateral load P_t (a) $S_c^{P\theta}$, (b) $S_\kappa^{P\theta}$, (c) $S_{\varepsilon 50}^{P\theta}$ and (d) $S_k^{P\theta}$

210
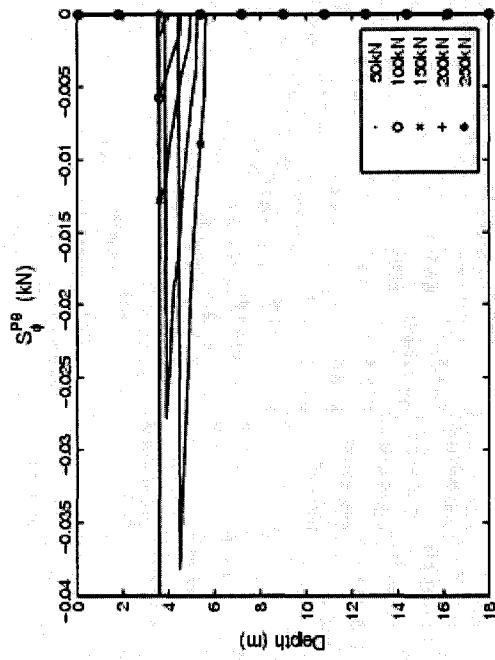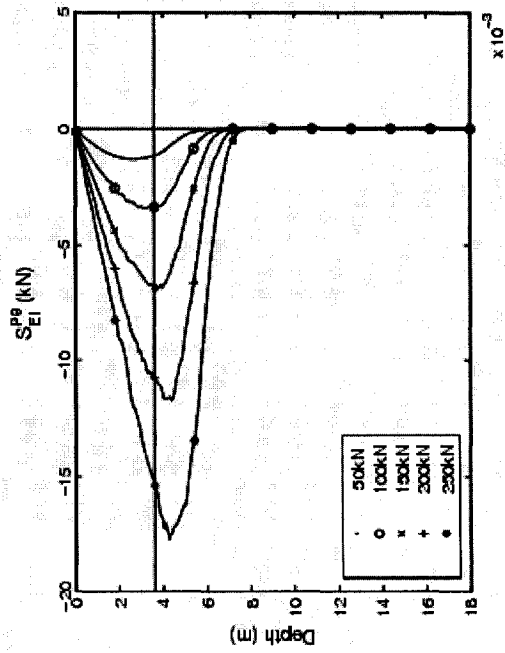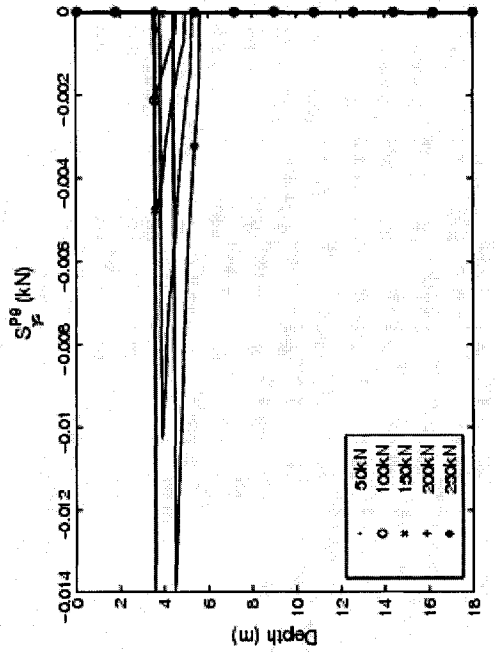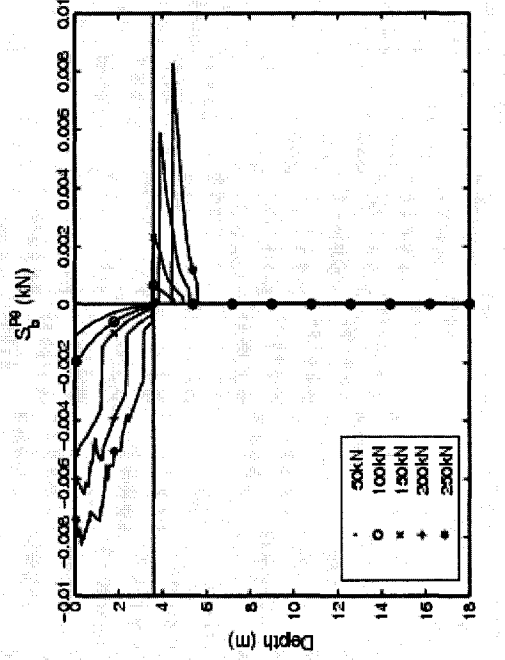
Figure 6.33 Sensitivity operators investigating $\delta\theta_t$ for 18 m long free head pile with 20% clay layer thickness subjected to lateral load P_t (a) $S_{\gamma s}^{P\theta}$, (b) $S_{\phi}^{P\theta}$, (c) $S_{EI}^{P\theta}$ and (d) $S_{b}^{P\theta}$

211

This can be explained in view of the bending moment diagrams for both primary and adjoint piles for both responses for each of the studied cases above since the sensitivity of EI depends on the moment distribution rather than the deflection distribution of both piles. For the second case (free head pile subjected to M_t), the moment of the primary pile, adjoint pile subjected to a unit lateral load (used for obtaining δy_t) and adjoint pile subjected to unit moment (used for obtaining $\delta\theta_t$) are given in Figure 6.36a, b and c.

The multiplication of moment of the primary pile (Figure 6.36a) by the moment of the adjoint pile for y_t (Figure 6.36b) results in a completely different distribution from the one that results from the multiplication of moment of the primary pile (Figure 6.36a) by the moment of the adjoint pile for θ_t (Figure 6.36c).

However, for the first case (free head pile subjected to P_t), the moment of the primary pile, adjoint pile subjected to a unit lateral load (used for obtaining δy_t) and adjoint pile subjected to unit moment (used for obtaining $\delta\theta_t$) are given in Figures 6.37a, b and c. The multiplication of moment of the primary pile (Figure 6.37a) by the moment of the adjoint pile for y_t (Figure 6.37b) results in a slightly different distribution from the one that results from the multiplication of moment of the primary pile (Figure 6.37a) by the moment of the adjoint pile for θ_t (Figure 6.37c). This is because the moment of the primary pile for case 1 (support type 1; free head subjected to P_t) has a zero value at the top of the pile (Figure 6.37a) while for case 2 (support type 2; free head subjected to M_t) there s a value for the moment at top of the primary pile (Figure 6.36a).

From the above discussion, the following can be concluded:
When the investigated pile is subjected to M_t the distribution of S_{EI} will be completely different in its pattern for the two responses (Figures 6.31c and 6.35c), while it will be slightly different in its pattern for the two responses when the pile is subjected to P_t (Figures 6.10c and 6.33c).

212
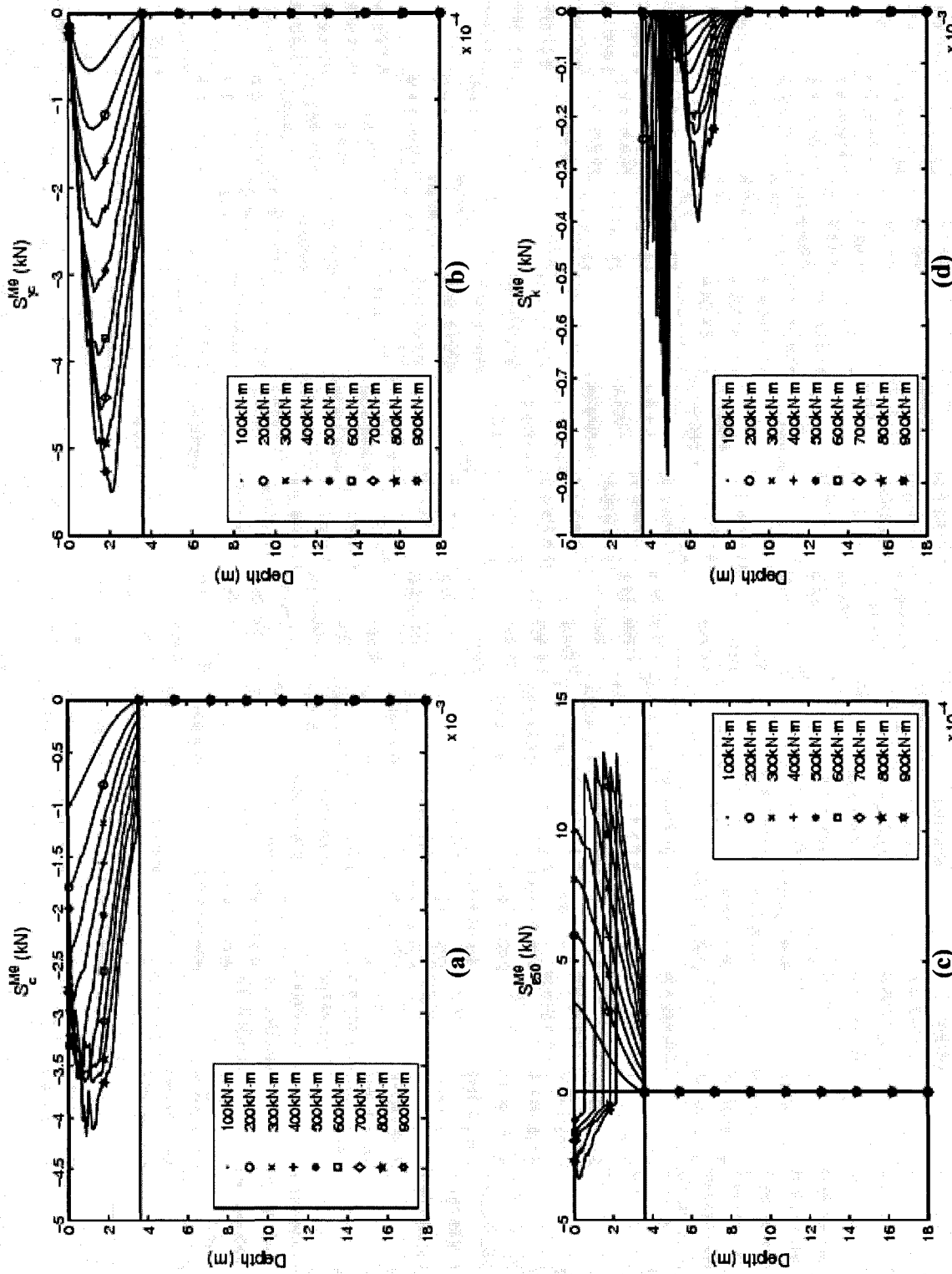
Figure 6.34 Sensitivity operators investigating $\delta\theta_t$ for 18 m long free head pile with 20% clay layer thickness subjected to bending moment M_t (a) $S_c^{M\theta}$, (b) $S_{\gamma c}^{M\theta}$, (c) $S_{\varepsilon 50}^{M\theta}$ and (d) $S_k^{M\theta}$

213
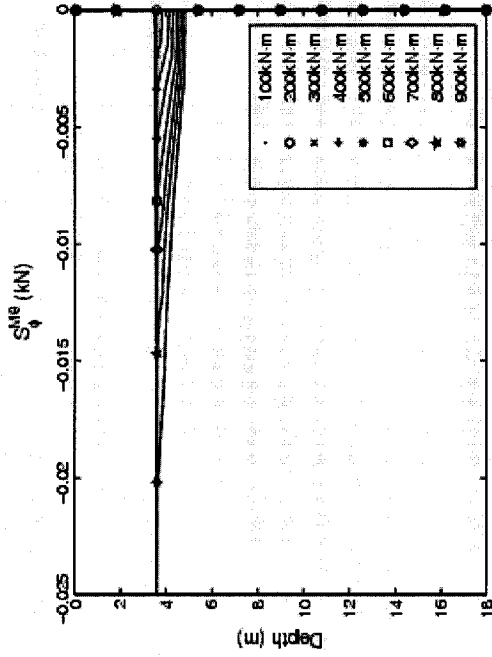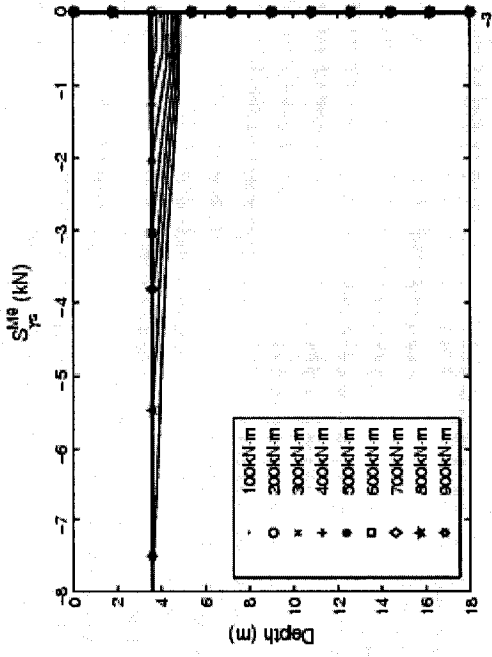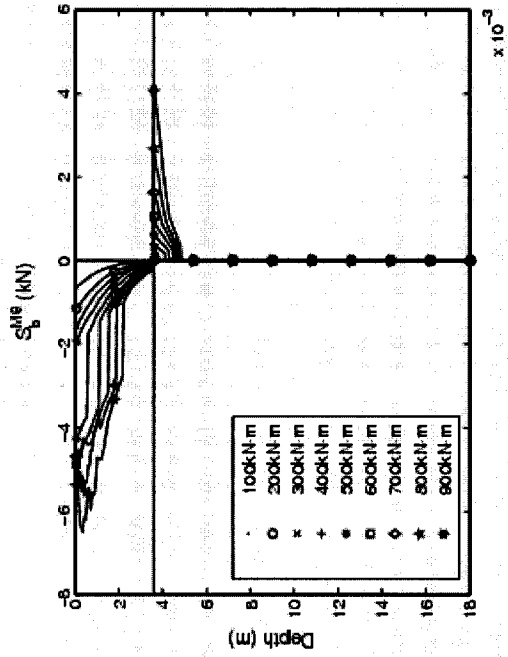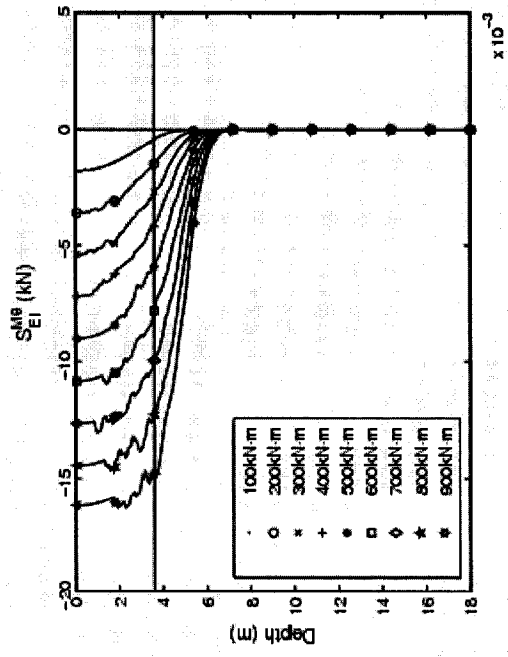
Figure 6.35 Sensitivity operators investigating $\delta\theta_t$ for 18 m long free head pile with 20% clay layer thickness subjected to bending moment M_t (a) $S_{ps}^{M\theta}$, (b) $S_{\phi}^{M\theta}$, (c) $S_{EI}^{M\theta}$ and (d) $S_b^{M\theta}$

214
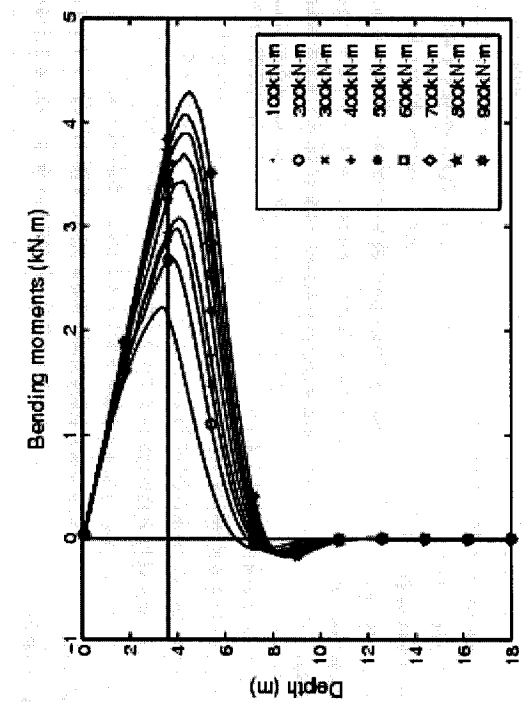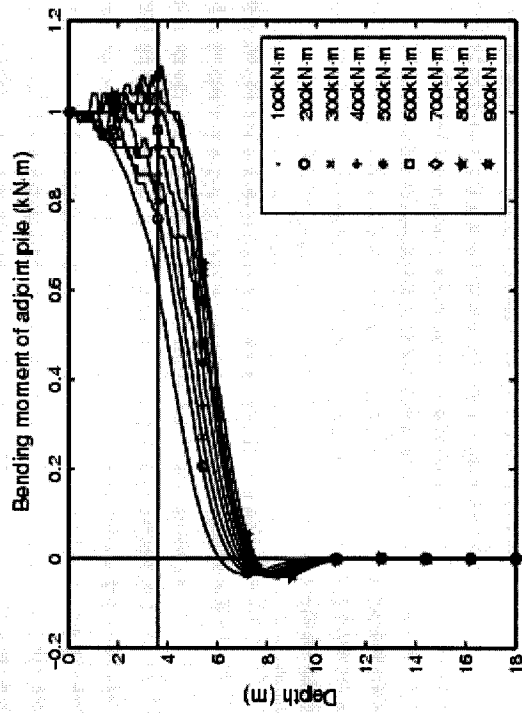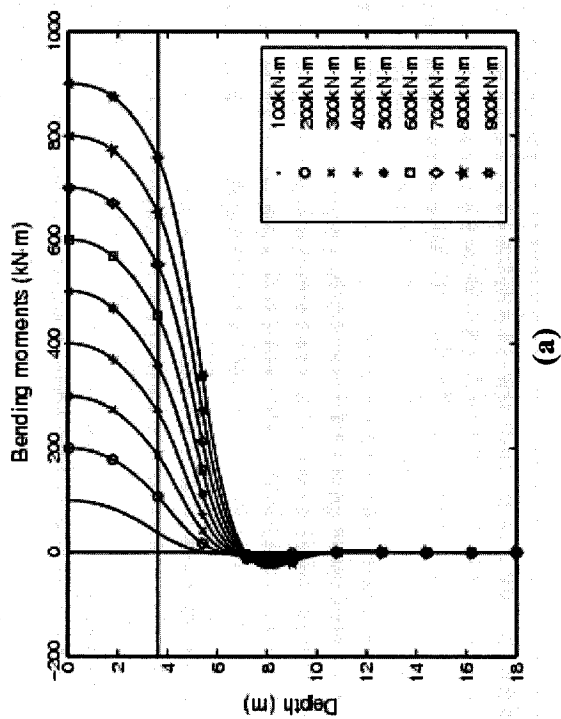
Figure 6.36 Bending moment for (a) primary pile subjected to M_t
(b) adjoint pile subjected to unit lateral load used for obtaining δy_t
(c) adjoint pile subjected to unit bending moment used for obtaining $\delta \theta_t$

215
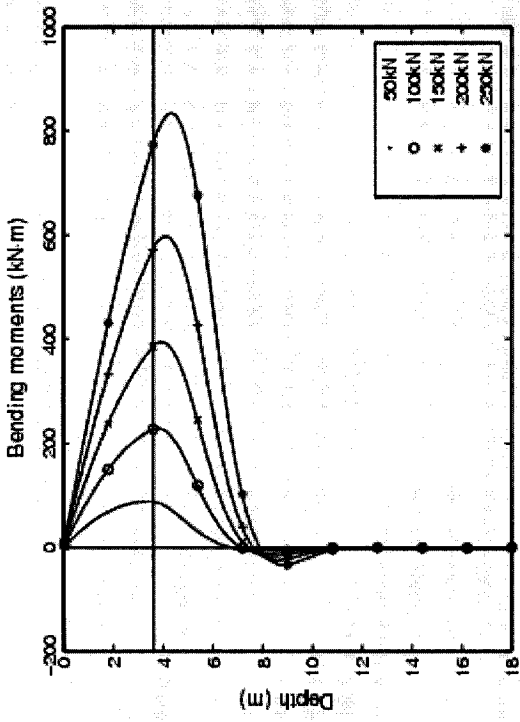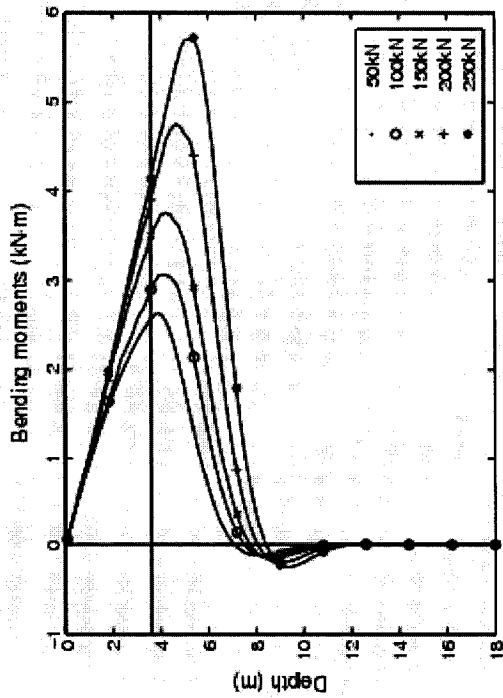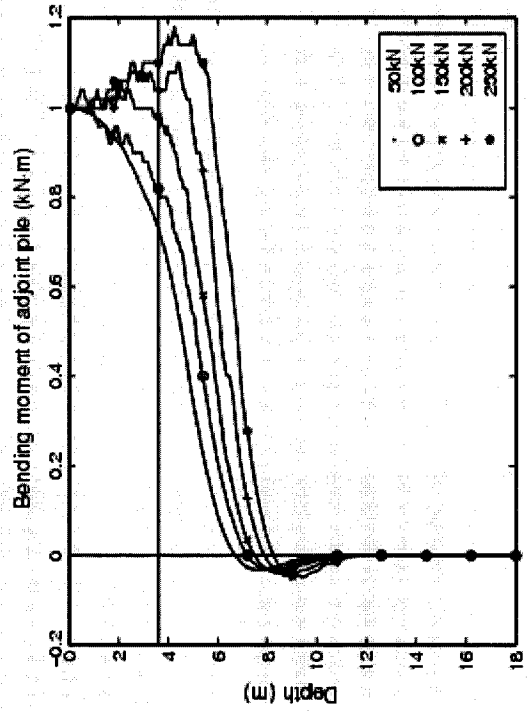
Figure 6.37 Bending moments for (a) primary pile subjected to P_t
(b) adjoint pile subjected to unit lateral load used for obtaining δy_t
(c) adjoint pile subjected to unit bending moment used for obtaining $\delta \theta_t$

216

6.2.5.7 Effect of pile length

The sensitivity results of a short and long pile are compared to study the effect of the pile length. The results for the long pile presented in Section 6.2.5.1 (Figures 6.9 and 6.10) are compared with those of a short pile with the same boundary condition (free head), the same type of load (subjected to P_t) and the same percent clay (20%). The short pile is 6m long (3T). The sensitivity operators for the short pile are given in Figures 6.38 and 6.39.

Comparing the distribution of sensitivity operators for the long pile (Figures 6.9 and 6.10) with those for the short pile (Figures 6.38 and 6.39), it is noticed that the clay operators have the same pattern. However, the sand and pile operators have different patterns. This is due to the difference in the deflection and moment patterns of the primary pile between the short and long piles especially at deep levels. Therefore the clay operators are not much affected. The deflections and bending moments for the short and long piles are compared in Figures 6.40 and 6.41, respectively.

The sand operators and the pile diameter b operators are affected by the deflection while the bending stiffness EI operators are affected by the bending moment. The deflections for the long pile are negligible and reaches zero at the end of the pile while the short pile deflects as a rigid body around a pivot and has negative values of deflection at its end. Similarly, the bending moment distribution for long piles is distributed along the upper part of the pile while it is distributed along the entire length of the pile for the short pile. Accordingly, the sand operators and the pile operators extend to the end of the pile as seen in Figures 6.38d, 6.39a, b, c and d.

It is also noticed from the deflections of the long and short piles (Figure 6.39) that although the short pile has a shorter length, it can sustain more load, i.e. at the same load a lower deflection is reached for the short pile. This shows that the thickness of the clay layer has a significant effect on the deflection and weakens the system considerably. The thickness of clay is a percent of the pile length, i.e. clay thickness for short pile is 1.2 m while it is 3.6 m for the long pile.

217
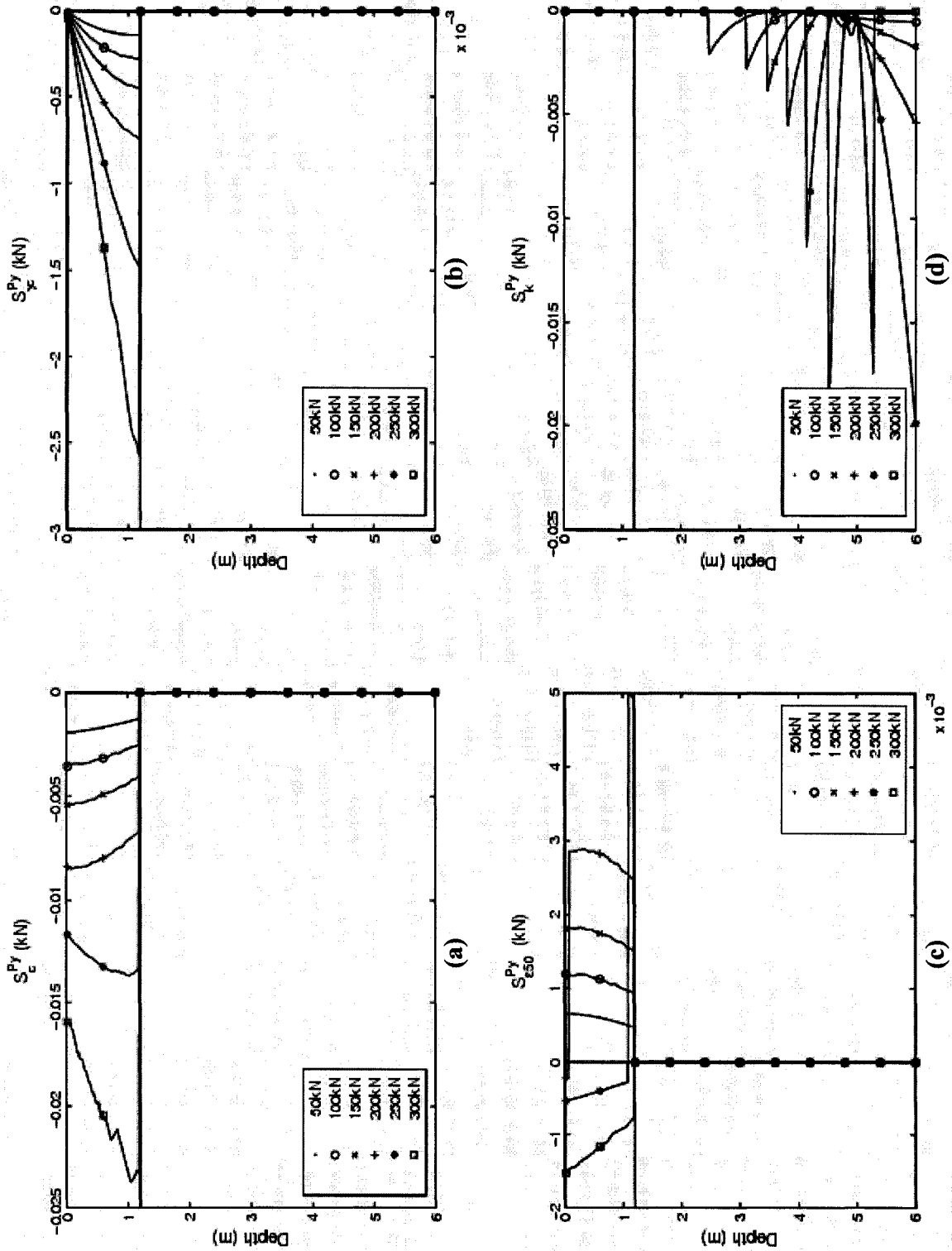
Figure 6.38 Sensitivity operators investigating δy_t for a short free head pile (6 m long) with 20% clay layer thickness subjected to lateral load P_t (a) S_c^{Py}, (b) S_κ^{Py}, (c) $S_{\epsilon 50}^{Py}$ and (d) S_k^{Py}

218
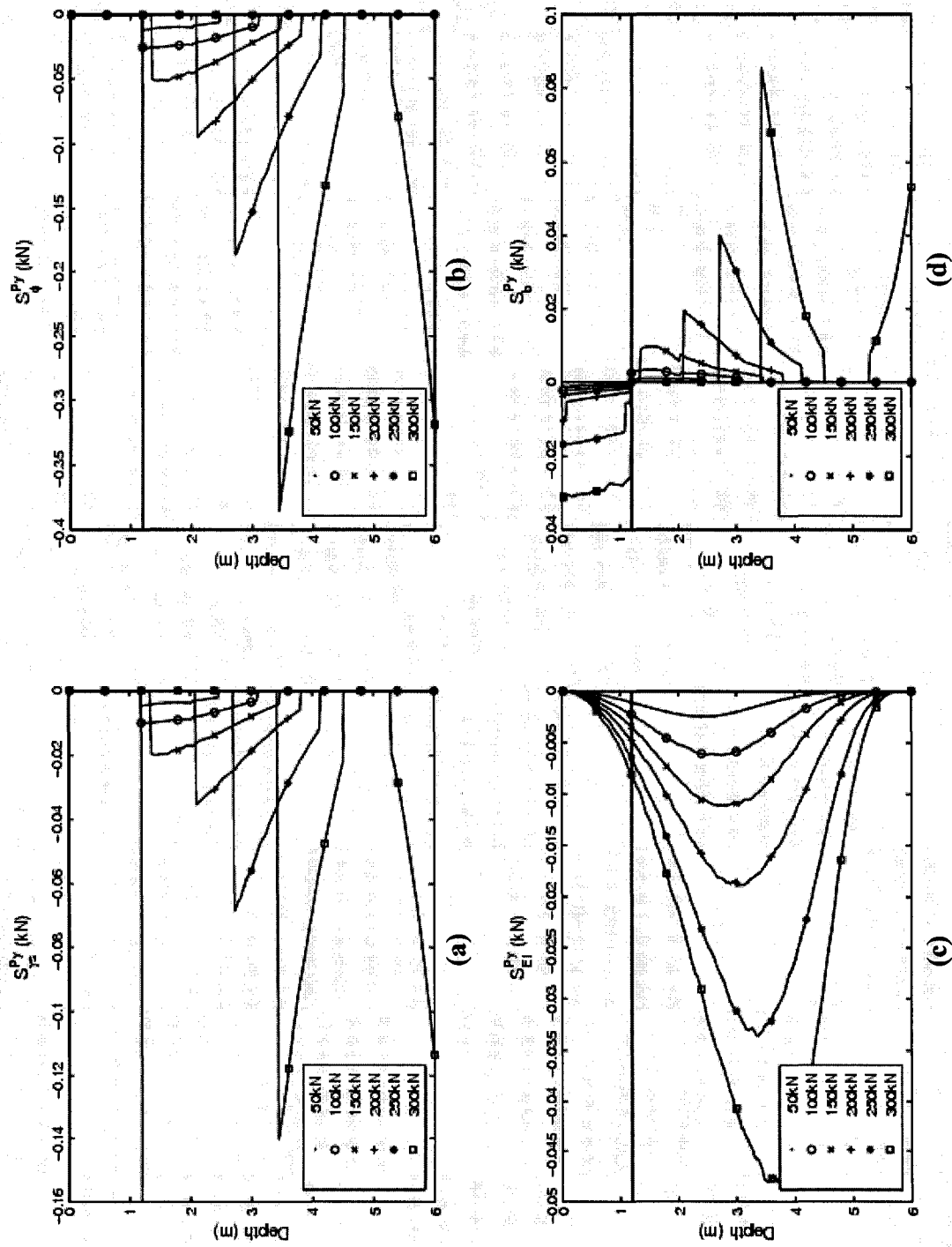
Figure 6.39 Sensitivity operators investigating δy_t for a short free head pile (6 m long) with 20% clay layer thickness subjected to lateral load P_t (a) S_{rs}^{Py}, (b) S_{ϕ}^{Py}, (c) S_{EI}^{Py} and (d) S_b^{Py}

219
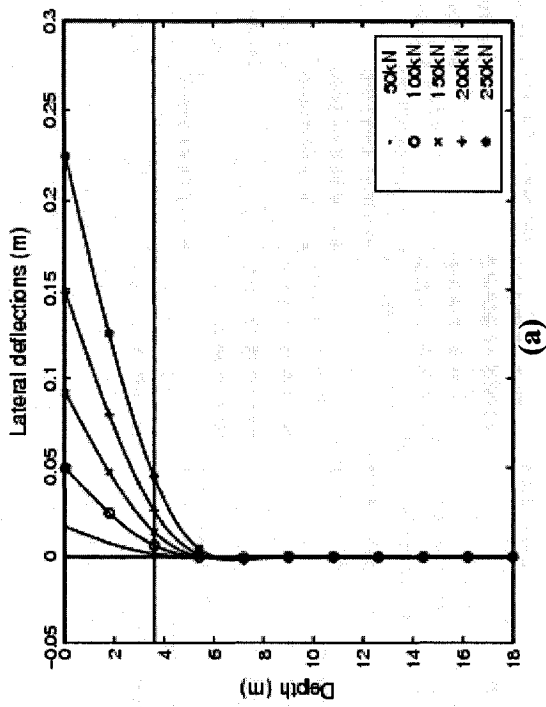
Figure 6.40 Deflections of primary pile subjected to lateral loads P_t with 20% clay layer thickness (a) long free head pile (18 m) and (b) short free head pile (6 m)
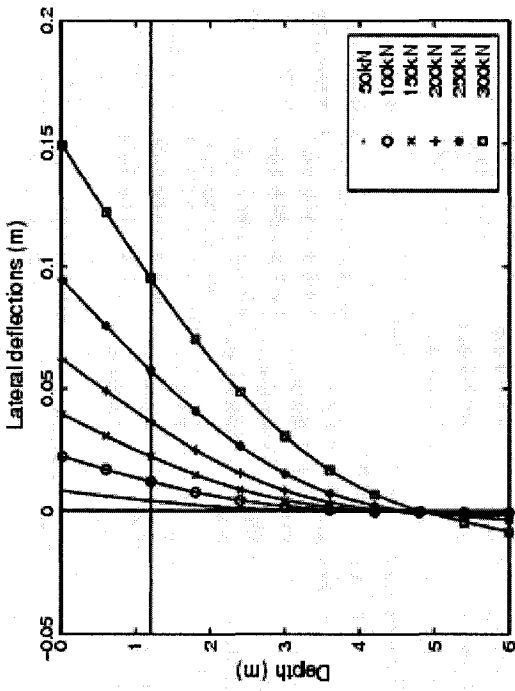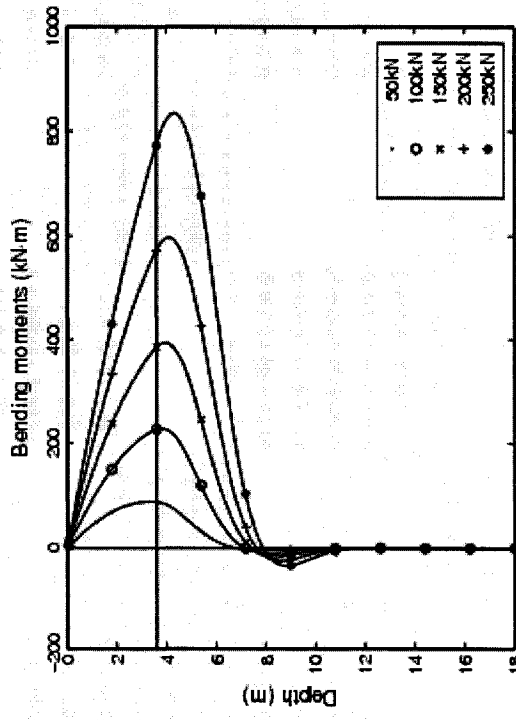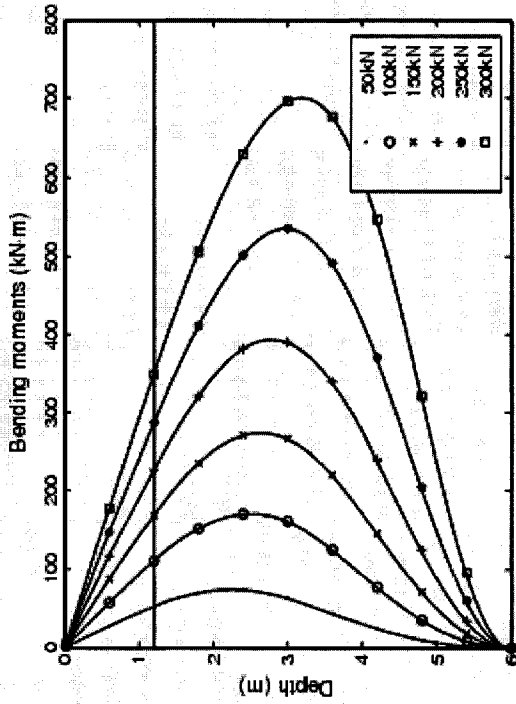
Figure 6.41 Bending moments of primary pile subjected to lateral loads P_t with 20% clay layer thickness (a) long free head pile (18 m), (b) short free head pile (6 m)

220

The sensitivity results for *A*, *PCR*, *TF* and *GF* are compared in Table 6.28. Both the deflection-based and the load-based comparisons are conducted.

Table 6.28 Values of A, PCR, TF and GF for different pile lengths (deflection-based comparison and load-based comparison)

	Deflection-based comparison		Load-based comparison	
	$P_t = 200$ kN ($y_t = 0.151$ m) (long pile)	$P_t = 300$ kN ($y_t = 0.1503$ m) (short pile)	$P_t = 200$ kN ($y_t = 0.151$ m) (long pile)	$P_t = 200$ kN ($y_t = 0.0627$ m) (short pile)
A_c^{Py}	-0.061	-0.024	-0.061	-0.009
$A_{\gamma c}^{Py}$	-0.008	-0.002	-0.008	-0.001
$A_{\varepsilon 50}^{Py}$	0.005	-0.001	0.005	0.003
A_k^{Py}	-0.004	-0.005	-0.004	-0.004
$A_{\gamma s}^{Py}$	-0.042	-0.122	-0.042	-0.034
A_ϕ^{Py}	-0.115	-0.340	-0.115	-0.093
A_{EI}^{Py}	-0.155	-0.122	-0.155	-0.048
A_b^{Py}	-0.036	0.024	-0.036	0.011
PCR_c^{Py}	-0.40	-0.16	-0.40	-0.15
$PCR_{\gamma c}^{Py}$	-0.05	-0.01	-0.05	-0.01
$PCR_{\varepsilon 50}^{Py}$	0.03	-0.01	0.03	0.05
PCR_k^{Py}	-0.02	-0.03	-0.02	-0.07
$PCR_{\gamma s}^{Py}$	-0.30	-0.82	-0.28	-0.55
PCR_ϕ^{Py}	-0.76	-2.26	-0.76	-1.49
PCR_{EI}^{Py}	-1.02	-0.82	-1.03	-0.76
PCR_b^{Py}	-0.24	0.16	-0.24	0.17
TF_c^{Py}	14.32	3.76	14.32	4.60
$TF_{\gamma c}^{Py}$	1.83	0.25	1.83	0.28
$TF_{\varepsilon 50}^{Py}$	1.14	0.22	1.14	1.52
TF_k^{Py}	0.84	0.73	0.84	2.03
$TF_{\gamma s}^{Py}$	9.90	19.11	9.90	16.94
TF_ϕ^{Py}	27.02	53.042	27.02	45.96
TF_{EI}^{Py}	36.46	19.11	36.46	23.50

221

Table 6.28 Values of A, PCR, TF and GF for different pile lengths (deflection-based comparison and load-based comparison)(continued)

	Deflection-based comparison			Load-based comparison	
	$P_t = 200$ kN (long pile)	$P_t = 300$ kN (short pile)		$P_t = 200$ kN (long pile)	$P_t = 200$ kN (short pile)
TF_b^{Py}	8.49	3.78		8.49	5.17
GF_c^{Py}	82.81	88.96		82.81	71.90
$GF_{\gamma c}^{Py}$	10.60	5.93		10.60	4.38
$GF_{\varepsilon 50}^{Py}$	6.59	5.10		6.59	23.72
GF_k^{Py}	2.21	1.00		2.21	3.12
$GF_{\gamma s}^{Py}$	26.22	26.22		26.22	26.09
GF_ϕ^{Py}	71.56	72.78		71.56	70.79
GF_{EI}^{Py}	81.11	83.45		81.11	81.96
GF_b^{Py}	18.90	16.55		18.90	18.04

6.2.5.7.1 Deflection-based comparison

A deflection-based comparison between the short and the long pile is conducted where the two piles produce the same deflection at the pile head. However the deflection pattern along the pile is different as explained above (Figure6.40).

For the clay parameters, since the thickness of the clay layer for the short pile becomes smaller (1.2 m rather than 3.6 m), the integration of the sensitivity operators results in lower values of A for the short pile compared to the long pile. In addition, the positive values for $S_{\varepsilon 50}$ that develop when the clay experiences the linear elastic behavior at small deflections are only developed along a very short length of the pile since the clay layer stops at 1.2 m depth (Figure 6.38c). Therefore, the value of $A_{\varepsilon 50}$ is negative for the short pile while it is positive for the long pile.

For the sand parameters, although the depth of the sand layer surrounding the pile is shorter for the short pile (4.8 m) compared to the long pile (14.4 m), the values of the

222

sensitivity factors A for the sand parameters (k, γ'_s and ϕ) are higher for the short pile compared to the long pile. This is because the operators extend along the entire pile length for the short pile (Figures 6.38d, 6.39a and 6.39b) while they extend along a short distance of the pile length for the long pile (Figure 6.9d, 6.10a, and 6.10b).

For the pile parameters (EI and b), the values of A_{EI} for the short pile are smaller than those for the long pile since the sensitivity operators S_{EI} for the long pile (Figure 6.10c) extend to a deeper level than for the short pile (Figure 6.39c). The values of A_b are positive for the short pile showing that the positive values of S_b in sand dominate over the negative values of S_b in clay (Figure 6.39d). However, the values of A_b are negative for the long pile showing that the negative values of S_b in clay dominate over the positive values of S_b in the sand (Figure 6.10d). This implies that an increase in the pile diameter along the entire length of the pile will cause the pile head deflection to increase for the short pile while it will cause the pile head deflection to decrease for the long pile.

The same observations for A apply to PCR since the comparison is deflection based (y_t is the equal for both piles and $PCR= A/y_t$). From Table 6.28, it is shown that the length of pile affects the order of parameters from most effective to least effective for TF when each parameter is compared to all the parameters (sand parameters have more effect for the short pile) while it doesn't affect the order of the parameter within its group (refer to values of GF in Table 6.28).

6.2.5.7.2 Load-based comparison

For the load-based comparison, since the same load causes the deflection to be smaller for the short pile, therefore the values of A for all parameters are smaller for the short pile. The values of $A_{\varepsilon 50}$ for both piles are positive (it is positive for short pile since the deflection is small and the linear elastic stage is developed resulting in a positive value (Figure 6.38c)). The value of A_b is positive for the short pile showing that the positive values of S_b in the sand layer are still dominating even at a smaller deflection of the short pile compared to the long pile deflection.

223

Since the pile head deflection y_t for the short pile is smaller than that for the long pile, the values of PCR ($PCR = A/y_t$) show higher values for the sand parameters for the short pile compared to the long one. In addition, the values of $PCR_{\varepsilon50}$ are higher for the short pile since the values of $S_{\varepsilon50}$ are mostly positive for the short pile leading to a high value of $A_{\varepsilon50}$ (still smaller than $A_{\varepsilon50}$ for the long pile) but when it is compared to y_t it results in a higher value of $PCR_{\varepsilon50}$ for the short pile compared to the long one.

Similarly, the total relative sensitivity factors TF show a higher value for the short piles for the sand parameters and ε_{50}. For the group relative sensitivity factors GF, the order of the parameters regarding the most and least effective is similar for the short and long piles, except for ε_{50} in the clay group due to the reason explained above.

6.2.6 Verification of results

The sensitivity analysis conducted is based on the soil models (p-y curves) used for defining the system behavior. The soil models used are not the interest of verification since they have been used over the years and have shown good to excellent agreement with field studies and are well established. However, the sensitivity results based on these models are the domain of interest of verification. This will be achieved by comparing the results obtained from the sensitivity study by results obtained from computer programs that use the p-y curves for the pile analysis.

Sensitivity operators S

The distribution of sensitivity operators along the pile length show how and where the change in each parameter affects the lateral top head deflection y_t or the lateral head rotation θ_t. The computer program COM624P was used to check the results of the sensitivity operators obtained from the sensitivity study. The sensitivity response that will be used to check the distribution of the sensitivity operators S is the lateral top deflection

224

since the computer program COM624P gives only the values of the lateral deflection of the pile and its output doesn't include the slope (or rotation) of the pile. The distribution of the sensitivity operators along the pile showed negative values for all the operators except for the clay parameter ε_{50} and the pile parameter b.

For the parameter ε_{50}, the positive and negative results were checked numerically using the computer code COM624P. The value of the lateral top deflection obtained by using the initial design variables was compared to the lateral top deflection obtained by increasing the value of ε_{50} as an input to COM624P and keeping the initial values of all the other parameters to study the effect of increasing ε_{50} on y_t. The value of ε_{50} was increased in the zone that gave positive values of $S_{\varepsilon 50}$ from the sensitivity results one time and another time it was increased only in the zone of negative values obtained from the distribution of $S_{\varepsilon 50}$. It was found that when ε_{50} is increased in the area where the operator has a positive value, the deflection at the pile head increases while it decreases in the area where the operator has a negative value when ε_{50} is increased verifying the sensitivity results obtained.

Also the correctness of the results obtained for the pile diameter b were checked using the computer program COM624P with suitably modified input data required for the checking procedure. Specifically, it was done by using different values of pile diameter in the clay and sand zones as an input to the program and detecting how this change of diameter values will affect the pile-head deflection results. By increasing the value of b in the clay layer a smaller deflection in the pile head was obtained and by increasing the diameter in the sand a larger value of deflection was obtained at the pile head. This is consistent with the sensitivity results obtained that show a negative value of S_b in the clay layer and a positive value of S_b in the sand layer.

For all the other parameters the negative values were checked and verified. Each parameter was increased by a certain percent as an input to the computer program and the effect of this increase on the value of the lateral pile head deflection y_t (soil response

225

under investigation) was observed. It was found that the increase in the parameters caused a decrease in the lateral top deflection verifying the negative sign obtained from the sensitivity study. In addition, the locations of the zero values obtained from the sensitivity results were checked by increasing the value of the parameter in the zone of zero values and obtaining no (zero) change in the lateral top deflection as a result from the computer program COM624P verifying the sensitivity results obtained.

In addition, the locations of maximum values of the sensitivity operators were checked by changing the value of the parameter as an input to COM624P at different zones and achieving the maximum change of the lateral deflection at the zone that showed highest values for S.

Sensitivity results A, PCR, TF and GF

By verifying the results of the sensitivity factors A, the other forms of results (*PCR, TF* and *GF*) will be accordingly verified since they depend on the sensitivity factors A (see Sections 5.2.6.3. to 5.2.6.5). The sensitivity factor A, when multiplied by the percent change in the parameter, gives the value of change in y_t (or θ_t) if the parameter is changed along the entire length of the pile.

To verify the results of the sensitivity factors an assessment of the error of the lateral top deflection and top rotation is conducted. This error analysis is based on comparing the approximate lateral top deflection and top rotation predicted by the sensitivity analysis to the exact top deflection and top rotation. This is achieved by developing a MATLAB program for checking the error using the computer program FB-Pier (that is used for pile groups (Section 6.3.)) since its output includes both the deflection and slope (rotation) of the pile.

The approximate top deflection predicted by the sensitivity analysis due to the change of the parameter (cohesion c taken as an example) is calculated as follows:

226

$$y_t(predicted) = y_t\big|_c + \delta y_t = y_t\big|_c + A_c\left(\frac{\delta c}{c}\right) \tag{6.10}$$

where

y_t (predicted) = the predicted new lateral deflection due to change in the parameter c,

$y_t\big|_c$ = the exact lateral deflection calculated from FB-Pier program when the cohesion is equal to the initial value of c,

δy_t = change in y_t due to change in c predicted by the sensitivity analysis,

A_c = the sensitivity factor calculated from the sensitivity analysis (A for y_t (i.e. A^{Py} or A^{My})),

$\left(\dfrac{\delta c}{c}\right)$ = normalized variation of design variable c, where δc is the change in c and

c is the initial value of cohesion, i.e. if c changes by 10% then $\left(\dfrac{\delta c}{c}\right)=0.1$.

The exact lateral deflection, denoted as y_t (*exact*), due to change in the parameter (c for example) is determined by inputting the changed parameter ($c + \delta c$) into the input file of FB-Pier program and using the FB-Pier program to calculate the exact lateral deflection corresponding to that new changed parameter.

The error (in percent) of the predicted lateral pile head deflection is defined as:

$$Error = \frac{\left|y_t(predicted) - y_t(exact)\right|}{y_t(exact)} \times 100 \tag{6.11}$$

The error assessment process can be clarified by the use of Figure 6.42. In Figure 6.42, the predicted and exact lateral pile head deflections are plotted against the percent change in the parameter c. The figure is plotted at P_t=50 kN for the sample case given in Section 6.2.5.1 which is a free head 18 m long pile subjected to lateral loads embedded in 20% clay layer thickness.

227
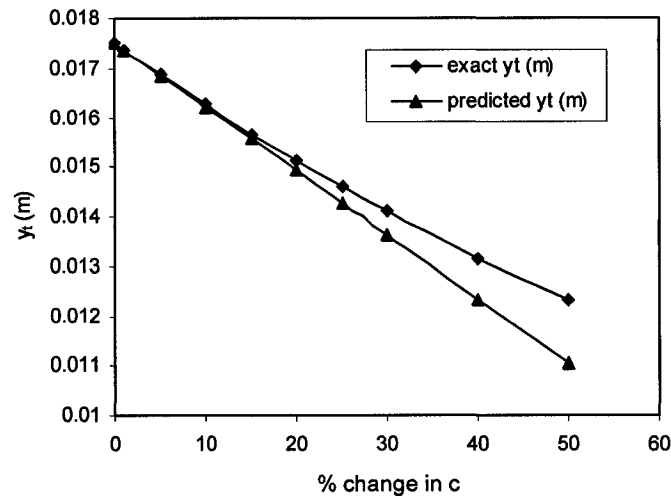
Figure 6.42 Exact and predicted pile deflection versus the percent change in c clarifying error assessment for a free head 18 m long pile with 20% clay layer thickness

Similarly, the error (in percent) of the predicted head rotation is defined with the use of the appropriate value of A for rotation (i.e. $A^{P\theta}$ or $A^{M\theta}$) as follows:

$$Error = \frac{\left|\theta_t(predicted) - \theta_t(exact)\right|}{\theta_t(exact)} \times 100 \qquad (6.12)$$

The calculated errors in y_t and θ_t using Eqs. 6.11 and 6.12 are given in Table 6.29 and Table 6.30 respectively for all parameters at the different levels of applied load for the sample case of free head 18 m long pile subjected to lateral loads embedded in a soil profile with 20% clay layer thickness. The error in the predicted pile response (y_t or θ_t) due to change in a given parameter (c for example) is denoted as $Error_{parameter}$ ($Error_c$ for example).

228

Table 6.29 Assessment of error (in %) in the predicted lateral top deflection y_t due to change in the eight studied parameters at different levels of applied load for free head 18 m long pile with 20% clay layer thickness

%change		1%	5%	10%	15%	20%	25%	30%	40%	50%
$Error_c$ (%)	P_f= 50 kN	0.016	0.016	0.491	0.430	1.221	2.235	3.451	6.244	10.354
	P_f= 100 kN	0.021	0.021	0.360	0.947	0.460	0.131	0.824	1.342	3.694
	P_f= 150 kN	0.020	0.020	0.282	1.858	1.516	1.111	0.632	1.329	0.375
	P_f= 200 kN	0.029	0.157	0.331	2.927	2.577	2.199	1.766	3.550	2.107
	P_f= 250 kN	0.034	0.165	0.323	4.208	3.972	3.724	3.459	7.057	6.228
$Error_{yc}$ (%)	P_f= 50 kN	0.002	0.009	0.021	0.037	0.057	0.083	0.115	0.193	0.287
	P_f= 100 kN	0.002	0.012	0.027	0.044	0.065	0.088	0.115	0.178	0.255
	P_f= 150 kN	0.002	0.012	0.025	0.040	0.059	0.082	0.107	0.166	0.239
	P_f= 200 kN	0.000	0.003	0.010	0.020	0.034	0.050	0.068	0.114	0.173
	P_f= 250 kN	0.005	0.024	0.048	0.068	0.085	0.099	0.111	0.123	0.124
$Error_{\varepsilon50}$ (%)	P_f= 50 kN	0.006	0.055	0.171	0.339	0.552	0.800	1.086	1.755	2.536
	P_f= 100 kN	0.008	0.059	0.166	0.312	0.493	0.709	0.954	1.524	2.184
	P_f= 150 kN	0.052	0.248	0.454	0.626	0.770	0.890	0.990	1.138	1.238
	P_f= 200 kN	0.093	0.440	0.817	1.142	1.421	1.661	1.864	2.184	2.401
	P_f= 250 kN	0.134	0.630	1.176	1.654	2.069	2.430	2.743	3.245	3.611
$Error_k$ (%)	P_f= 50 kN	0.001	0.000	0.045	0.107	0.205	0.315	0.452	0.764	1.123
	P_f= 100 kN	0.003	0.001	0.014	0.044	0.085	0.135	0.196	0.337	0.499
	P_f= 150 kN	0.000	0.002	0.013	0.036	0.064	0.104	0.146	0.250	0.369
	P_f= 200 kN	0.001	0.009	0.036	0.069	0.111	0.161	0.214	0.340	0.479
	P_f= 250 kN	0.001	0.015	0.042	0.073	0.119	0.167	0.221	0.348	0.488
$Error_{ys}$ (%)	P_f= 50 kN	0.002	0.027	0.927	0.990	1.085	1.205	1.367	2.427	2.815
	P_f= 100 kN	0.009	0.064	2.063	2.212	2.407	2.641	2.921	5.418	6.157
	P_f= 150 kN	0.013	0.106	2.887	3.111	3.403	3.759	4.173	7.676	8.776
	P_f= 200 kN	0.043	0.156	3.593	3.618	3.756	4.012	4.354	8.858	9.978
	P_f= 250 kN	0.225	1.073	2.941	2.134	1.461	0.911	0.477	4.703	4.418
$Error_{\phi}$ (%)	P_f= 50 kN	0.002	0.936	1.223	2.413	3.645	4.205	5.469	7.326	9.224
	P_f= 100 kN	0.013	2.019	2.304	4.630	7.120	7.934	10.727	15.037	20.008
	P_f= 150 kN	0.030	2.820	3.233	6.440	9.854	10.887	14.641	20.241	26.525
	P_f= 200 kN	0.127	3.274	3.125	7.019	11.187	12.100	16.730	23.402	31.144
	P_f= 250 kN	0.644	1.903	0.714	1.971	5.024	3.582	7.264	10.905	15.997
$Error_{EI}$ (%)	P_f= 50 kN	0.061	0.418	1.112	2.074	3.297	4.774	6.497	10.664	15.756
	P_f= 100 kN	0.072	0.486	1.284	2.388	3.788	5.479	7.454	12.234	18.084
	P_f= 150 kN	0.095	0.645	1.721	3.218	5.120	7.417	10.095	16.561	24.435
	P_f= 200 kN	0.135	0.899	2.338	4.341	6.863	9.915	13.464	22.041	32.504
	P_f= 250 kN	0.163	1.074	2.818	5.209	8.248	11.909	16.193	26.569	39.296
$Error_b$ (%)	P_f= 50 kN	0.005	0.033	0.091	0.175	0.288	0.432	0.622	1.141	1.106
	P_f= 100 kN	0.005	0.019	0.031	0.042	0.049	0.056	0.068	0.123	1.415
	P_f= 150 kN	0.012	0.071	0.184	0.354	0.581	0.878	1.240	2.195	1.351
	P_f= 200 kN	0.041	0.208	0.341	0.397	0.375	0.276	0.109	0.432	1.235
	P_f= 250 kN	0.034	0.156	0.260	0.307	0.291	0.212	0.077	0.378	2.399

229

Table 6.30 Assessment of error (in %) in the predicted top rotation θ_t due to change in the eight studied parameters at different levels of applied load for free head 18 m long pile with 20% clay layer thickness

%change		1%	5%	10%	15%	20%	25%	30%	40%	50%
Error_c (%)	P_t= 50 kN	0.007	0.017	0.150	0.132	0.549	1.102	1.778	3.392	5.721
	P_t= 100 kN	0.013	0.087	0.237	0.415	0.089	0.306	0.768	1.293	2.822
	P_t= 150 kN	0.008	0.050	0.131	1.158	0.956	0.713	0.421	0.761	0.315
	P_t= 200 kN	0.017	0.088	0.181	1.914	1.714	1.500	1.256	2.432	1.611
	P_t= 250 kN	0.017	0.080	0.149	2.867	2.762	2.655	2.544	5.011	4.649
Error_γc (%)	P_t= 50 kN	0.001	0.003	0.005	0.005	0.001	0.005	0.015	0.042	0.079
	P_t= 100 kN	0.001	0.007	0.014	0.024	0.036	0.050	0.066	0.103	0.149
	P_t= 150 kN	0.001	0.003	0.008	0.014	0.022	0.032	0.044	0.074	0.114
	P_t= 200 kN	0.001	0.002	0.001	0.002	0.007	0.014	0.022	0.045	0.077
	P_t= 250 kN	0.005	0.026	0.052	0.076	0.098	0.117	0.135	0.163	0.184
Error_ε50 (%)	P_t= 50 kN	0.003	0.009	0.064	0.163	0.297	0.462	0.657	1.129	1.692
	P_t= 100 kN	0.005	0.040	0.118	0.229	0.369	0.536	0.728	1.176	1.698
	P_t= 150 kN	0.043	0.203	0.369	0.503	0.611	0.696	0.762	0.841	0.869
	P_t= 200 kN	0.078	0.369	0.686	0.960	1.195	1.397	1.569	1.839	2.022
	P_t= 250 kN	0.110	0.519	0.970	1.366	1.710	2.010	2.272	2.695	3.009
Error_k (%)	P_t= 50 kN	0.003	0.010	0.000	0.019	0.056	0.098	0.153	0.281	0.432
	P_t= 100 kN	0.002	0.006	0.003	0.008	0.024	0.046	0.073	0.139	0.216
	P_t= 150 kN	0.001	0.003	0.000	0.009	0.023	0.043	0.065	0.122	0.189
	P_t= 200 kN	0.000	0.002	0.015	0.032	0.056	0.085	0.116	0.192	0.277
	P_t= 250 kN	0.001	0.004	0.015	0.031	0.055	0.082	0.113	0.188	0.273
Error_γs (%)	P_t= 50 kN	0.002	0.006	0.441	0.466	0.506	0.558	0.631	1.141	1.322
	P_t= 100 kN	0.003	0.024	1.112	1.179	1.268	1.378	1.510	2.861	3.218
	P_t= 150 kN	0.010	0.069	1.776	1.911	2.084	2.292	2.533	4.679	5.312
	P_t= 200 kN	0.031	0.122	2.283	2.265	2.314	2.436	2.608	5.463	6.061
	P_t= 250 kN	0.153	0.731	1.909	1.338	0.856	0.453	0.125	2.851	2.547
Error_φ (%)	P_t= 50 kN	0.003	0.441	0.564	1.133	1.725	1.988	2.597	3.490	4.407
	P_t= 100 kN	0.001	1.076	1.179	2.408	3.732	4.085	5.580	7.827	10.493
	P_t= 150 kN	0.021	1.733	1.963	3.901	5.967	6.496	8.756	12.006	15.671
	P_t= 200 kN	0.093	2.052	1.840	4.235	6.806	7.147	9.982	13.791	18.249
	P_t= 250 kN	0.437	1.196	0.633	1.022	2.912	1.750	4.005	5.909	8.681
Error_EI (%)	P_t= 50 kN	0.061	0.446	1.233	2.356	3.807	5.581	7.671	12.783	19.104
	P_t= 100 kN	0.069	0.497	1.363	2.592	4.177	6.114	8.397	13.981	20.893
	P_t= 150 kN	0.095	0.665	1.809	3.424	5.498	8.024	10.989	18.212	27.097
	P_t= 200 kN	0.121	0.833	2.226	4.196	6.711	9.780	13.380	22.163	32.996
	P_t= 250 kN	0.143	0.972	2.598	4.865	7.772	11.303	15.458	25.601	38.148
Error_b (%)	P_t= 50 kN	0.004	0.011	0.000	0.032	0.088	0.168	0.280	0.596	0.701
	P_t= 100 kN	0.004	0.020	0.039	0.062	0.088	0.118	0.156	0.262	0.441
	P_t= 150 kN	0.007	0.047	0.139	0.288	0.496	0.772	1.113	2.020	2.014
	P_t= 200 kN	0.028	0.136	0.217	0.240	0.203	0.108	0.041	0.503	0.308
	P_t= 250 kN	0.025	0.116	0.198	0.240	0.238	0.192	0.107	0.194	1.548

230

From Tables 6.29 and 6.30 it the following can be observed:

1. The values of the error are small verifying the sensitivity results obtained from the study

2. The maximum error obtained is for the design variables EI and the minimum error obtained is for the submerged unit weight of clay γ_c'.

3. The error in predicting the top rotation is less than the error in predicting the lateral top deflection in general (except for the parameter EI)

4. To achieve an error in predicting y_t less than 5%, the range of change in the parameter can be taken up to 25% except for EI and ϕ where error reached almost 12% for both parameters.

5. To achieve an error in predicting θ_t less than 5%, the range of change in the parameter can be taken up to 30% except for EI and ϕ where the error reached 15.5% and 10%, respectively.

6. For all the parameters, the change of the parameter up to 50%, gave an error in predicting y_t less than 15% (except for EI and ϕ, maximum error reached =39% and 31%, respectively) and an error in predicting θ_t less than 10% (except for EI and ϕ, maximum error reached =38% and 18%, respectively)

7. The range of applicability of the first variation of lateral top deflection and top rotation obtained from the study depends on the tolerable percent of error.

The error in predicting the lateral top deflection and rotation of all the studied cases for single piles (297 cases) are given in the attached CD (see Appendix C for contents of CD). In addition, the order of the parameters from most effective to least effective on the lateral top deflection was checked for several cases. It was found that the order of parameters obtained by the sensitivity analysis study is similar to that obtained by using COM624P directly.

231

6.3   NUMERICAL ANALYSIS FOR PILE GROUPS

The theoretical formulation of the pile groups was presented in Chapter 5 (Section 5.3). In the current section, a numerical sensitivity investigation is carried out for pile groups. The input data and scope of analysis are first presented followed by the programs used and the modeling of the primary and adjoint piles. The sensitivity results are then analyzed where the pile group results are compared to those of the single pile and the effects of pile location and pile spacing are studied. Finally, the results are verified.

6.3.1   Data used and scope of analysis

The input data used for the single piles is used for the pile groups. The initial values of the design parameters and the soil stratifications studied for the pile groups are similar to those of the single pile (Section 6.2.1). The pile lengths are taken equal to 18 m long piles ($l = 9T$ for support type 1 and 3 and $l = 10T$ for support type 2). The levels of applied load are taken equal to loads that produce the same deflection similar to the deflection produced by the single pile to be able to compare single and pile groups. This will be more clarified in Section 6.3.3.

The scope of analysis will include the sensitivity of the lateral top deflection (serviceability measure of interest in pile groups) for long piles (with length $l = 18$ m) with the following three support types for piles in the group:

1. Support type 1: piles pinned to cap and cap subjected to lateral concentrated force
2. Support type 2: piles fixed to cap and cap subjected to lateral concentrated force
3. Support type 3: piles pinned to cap and piles subjected to bending moment at pile head

The piles in the group are arranged in a 3x 3 pile arrangement as shown in Figure 6.43. The analysis will include different spacing s between the piles taken as $2D$, $3D$, $4D$ and $5D$ where D denotes the diameter of the pile (i.e. $D = b$).   In addition, the analysis is carried out for the piles located in the center of the second trailing row, first trailing row

232

and leading row (piles A, B and C in Figure 6.43). The values of the f_m multipliers used to account for the group effect are given in Table 6.31 based on Figure 5.12 (Section 5.3.2)

The number of cases studied for the pile groups are given in Table 6.32. For each of the support types given above, there are 132 cases investigated as shown in the table. A total number of 396 cases are investigated for the three support types. For each case, the 5 forms of sensitivity results are calculated and plotted at different levels of applied loads.
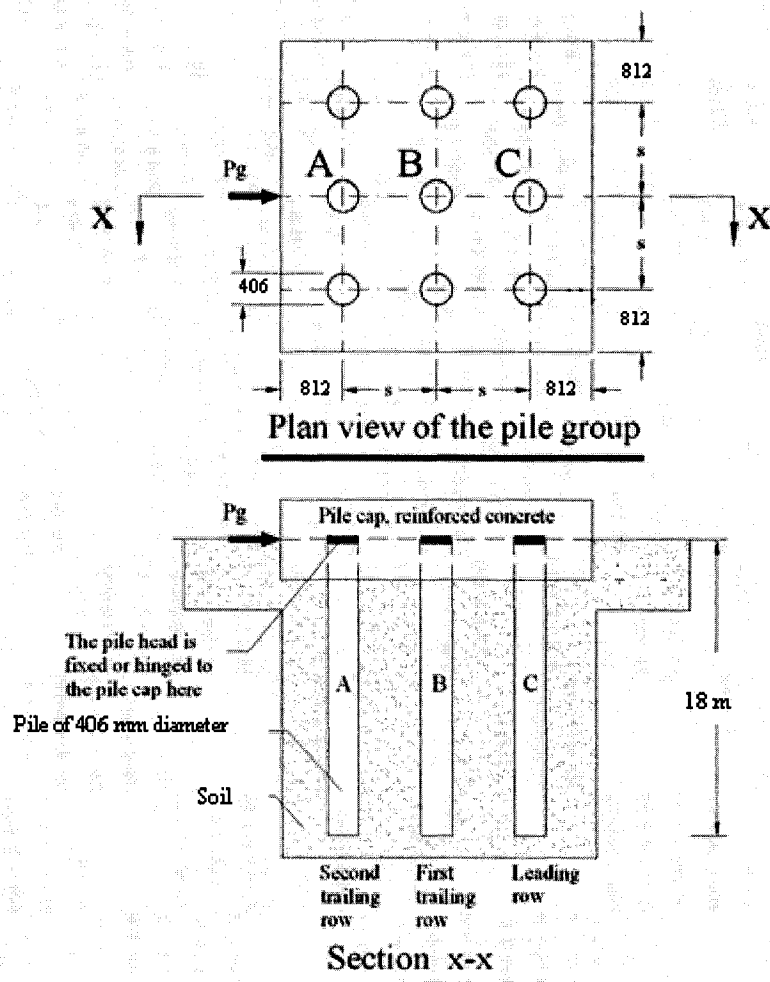
Figure 6.43 Pile group geometry used in the pile group analysis

233

Table 6.31 The values of f_m multipliers used for pile groups

Pile spacing	Pile location		Value of f_m multiplier
2D	Pile A	(2nd trailing row)	0.44
	Pile B	(1st trailing row)	0.56
	Pile C	(leading row)	0.76
3D	Pile A	(2nd trailing row)	0.58
	Pile B	(1st trailing row)	0.67
	Pile C	(leading row)	0.82
4D	Pile A	(2nd trailing row)	0.72
	Pile B	(1st trailing row)	0.78
	Pile C	(leading row)	0.88
5D	Pile A	(2nd trailing row)	0.86
	Pile B	(1st trailing row)	0.89
	Pile C	(leading row)	0.94

Table 6.32 The number of cases investigated for pile groups

Support type	Pile spacing s	Pile location		Soil stratification		No. of cases
				% clay layer thickness		
1	4 cases	2D	3 cases	Pile A	0%	132 cases
					10%	
					20%	
					30%	
				11 cases	40%	
					50%	
					60%	
					70%	
					80%	
					90%	
					100%	
			Pile B	11 cases		
			Pile C	11 cases		
	3D	3 cases	11 cases			
	4D	3 cases	11 cases			
	5D	3 cases	11 cases			
2	4 cases	3 cases	11 cases			132 cases
3	4 cases	3 cases	11 cases			132 cases

234

6.3.2 Programs used

Two computer programs were used to obtain the sensitivity results. The first is the software program FB-Pier (2001) developed by the bridge Software Institute (BSI), University of Florida, with the support of the Florida Department of Transportation and the Federal Highway Administration. The program has the capability to analyze and design single and pile groups. It employs the *p-y* method of analysis and the f_m multipliers required for the analysis of pile groups can be introduced to the program manually. The program uses the non-linear finite element analysis. In the current research, FB-Pier is used to numerically analyze the piles to obtain the deflections and moments of the laterally loaded piles required for the sensitivity analysis.

The second program is MATLAB (version 7) where programs were developed to calculate and plot the different forms of the sensitivity results for pile groups. The programs developed are based on previous program files developed by Lui (2004) for sensitivity of homogeneous soil. However, programs developed in the current research are for non-homogeneous soils, model the adjoint pile in a different way and include different forms of the sensitivity results. The details of the program developed in the current study are given in Appendix B. The developed programs mainly do the following:

1. Prepare input data for FB-Pier
2. Run the program FB-Pier for the different cases to obtain the deflections and moments of both the primary and adjoint piles.
3. Calculate the different expressions of the sensitivity results using the deflections and moments of the primary and adjoint piles.
4. Plot the sensitivity results as shown in the proceeding sections.

6.3.3 Modeling of the primary and adjoint piles

6.3.3.1 Modeling of primary and adjoint piles for support types 1 and 2 (subjected to lateral load)

To model the primary pile group, the lateral force Pg applied to the cap of a primary pile group needs to be determined. The basic concept used to obtain the force Pg is based on the principle that the pile group will produce the same deflection under the force Pg as the single pile under lateral force P_t. This concept is incorporated in order to compare the sensitivity results of single piles with those of the piles in a group.

To be able to determine the force Pg, the output values already calculated for single piles were used. A MATLAB program is developed to call the deflections of single piles already obtained from COM624P and plot it against the load P_t, run the FB-Pier program for the pile groups to obtain lateral load versus deflection for pile groups, and finally plot the results of lateral loads versus lateral deflections for both the single and pile groups together. Accordingly, the force Pg required for the pile group to produce the same deflection produced by the force P_t employed in the analysis of the single piles can be determined.

The method of obtaining Pg for pile groups is clarified in Figure 6.44 (as an example) for a single free head pile (18 m long with 20% clay layer thickness) subjected to lateral concentrated force P_t applied to the pile head, and the piles in the pile group are pinned to the pile cap (18 m long with 20% clay layer thickness). The pile group is subjected to lateral concentrated force Pg at the pile cap. In the figure, the ordinate values represents the external force Pg that the pile group is subjected to, and also the external lateral force P_t applied to the pile head of the single pile. The values represented by the abscissa correspond to the lateral deflections produced by the application of external force Pg or P_t.

236
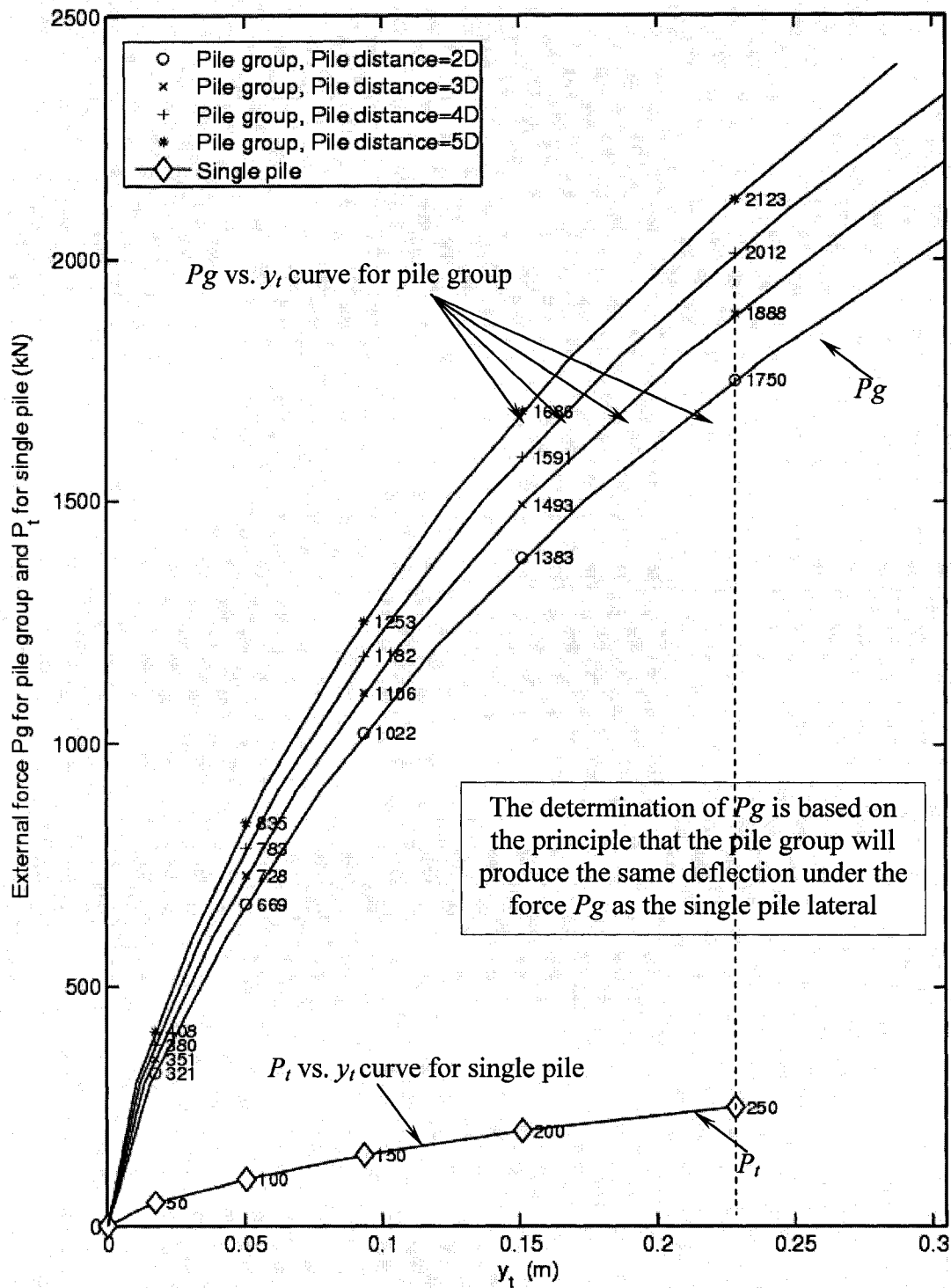
Figure 6.44 Determination of the force *Pg* applied to the cap of the 18 m long piles pinned to the cap (20% clay layer thickness) for different pile group spacing (*s* = 2*D*, 3*D*, 4*D* and 5*D*)

237

In order to perform numerical investigations and further sensitivity analysis on the piles inside of a group, an adjoint pile should be used. The concept is very close to the model adopted in the analysis of the single piles previously presented in this study. Once the force Pg is determined as explained above, the system for the primary structure is completely determined. However, the system requires an analysis of adjoint structure, and to carry out this analysis it is imperative that we determine the values of lateral forces Pg_1 applied at the pile cap that will result in application of the unit force to the pile member under investigation.

The distribution of the load applied to the cap to the pile members is not even, which means that the values of Pg_1 will vary according to location of the pile in the group (leading or trailing row). The utilization of the f_m multipliers, already described in Chapter 5, will be applied in the analysis. The unit lateral force Pg_1 related to the pile member under study (A, B or C), is the force applied to the pile cap that will result in a shear force reaction equal to unit force 1_a at the head of the pile under investigation.

Figure 6.45 presents the model adopted for both the primary and adjoint piles. After the application of the force Pg, shear forces will develop at the pile head indicated in Figure 6.45(b) as V_1-V_9. Accordingly, the following equation is valid for the shear forces:

$$Pg = \sum_{i=1}^{9} V_i \tag{6.13}$$

As an example to demonstrate the understanding of the model, the pile number 5 inside the shaded area in Figure 6.45(c) is used. It is required to find a force Pg_1 applied to the pile cap of the adjoint structure that will produce unit shear force at the pile head of the shaded pile. In that case the force Pg_1 can be calculated as follows:

$$Pg_1 = \frac{\sum_{i=1}^{9} V_i}{V_5} \bullet 1_a = \frac{Pg}{V_5} \bullet 1_a \tag{6.14}$$

238

where Pg_1 = the lateral force applied to the adjoint structure pile cap that will produce unit shear force at the pile head under analysis,

V_i = the shear force produced at the pile head number i by the application of the force Pg to the pile cap of the primary structure,

V_5 = the shear force produced at the head of the pile number 5 in the shaded area (Pile B) by the application of the force Pg to the pile cap of the primary structure.

To be able to perform the analysis of each pile, the force Pg_l applied to a pile subjected to analysis can be determined through the following equation:

$$(Pg_1)_j = \frac{\sum_{i=1}^{9} V_i}{V_j} \bullet 1_a = \frac{Pg}{V_j} \bullet 1_a \tag{6.15}$$

$$\frac{(Pg_1)_j}{1_a} = \frac{Pg}{V_j} \tag{6.16}$$

where $(Pg_1)_j$ = the lateral force applied to the adjoint structure pile cap that will produce unit shear force at the pile number j under consideration,

Vj = the shear force produced at the top of pile number j under consideration by the application of the force Pg to the pile cap of the primary structure.

The following equation should be applied in order to determine the internal forces and deflections of adjoint structure described by the model (Figure 6.45):

$$(c) = (d) - (b) \tag{6.17}$$

where (c) = method of determination of internal forces and deflections of the adjoint structure with Pg_l applied at the pile cap,

(d) = structure that has the same physical properties as the primary structure but loaded by the force $(Pg + Pg_l)$ applied to the pile cap since the sensitivity analysis is conducted in the vicinity of load Pg,

(b) = primary structure loaded by the force Pg.

239
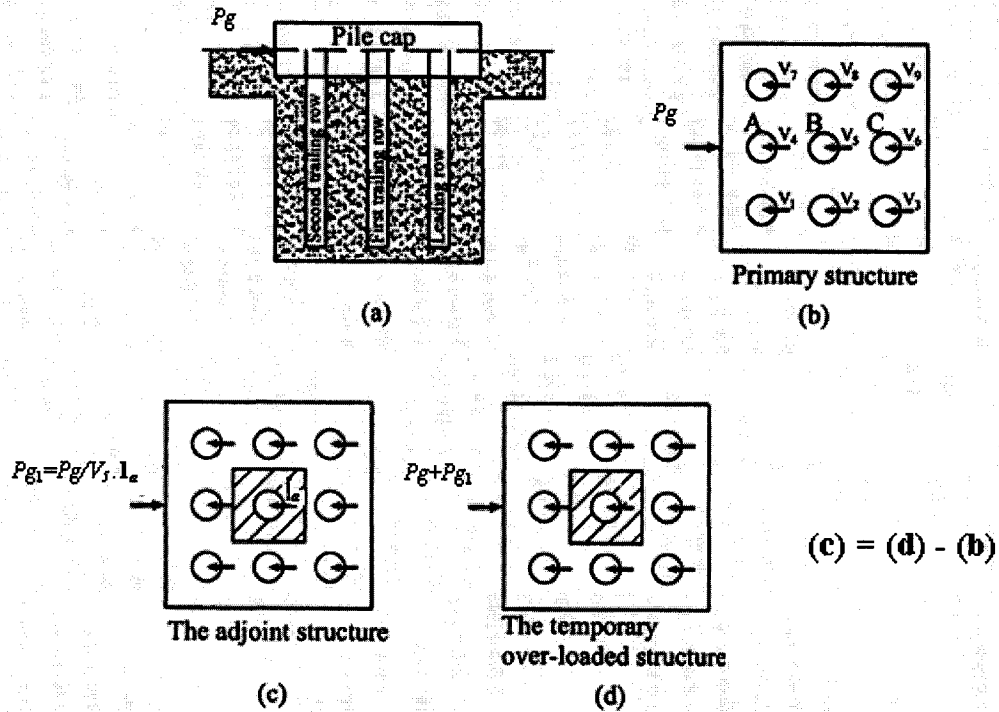
Figure 6.45 Method used to determine the force Pg_1 applied to the adjoint structure

6.3.3.2 Modeling of primary and adjoint piles for support type 3 (subjected to bending moment)

The bending moment denoted as Mg, is the bending moment applied to the pile head of each pile in the primary pile group. Similar to support types 1 and 2, the concept is based on the principle that the pile group will produce the same pile head deflection under the bending moment Mg, which is applied to the pile heads directly inside the pile group, as the single pile under bending moment M_t.

The lateral deflections of the single pile and pile groups versus the applied moments are plotted in Figure 6.46 (as an example) to demonstrate the method used to obtain the bending moment Mg applied at the pile head. The figure is for piles pinned to the pile group cap with variable spacing, s, embedded in a soil with 20% clay layer thickness.

240
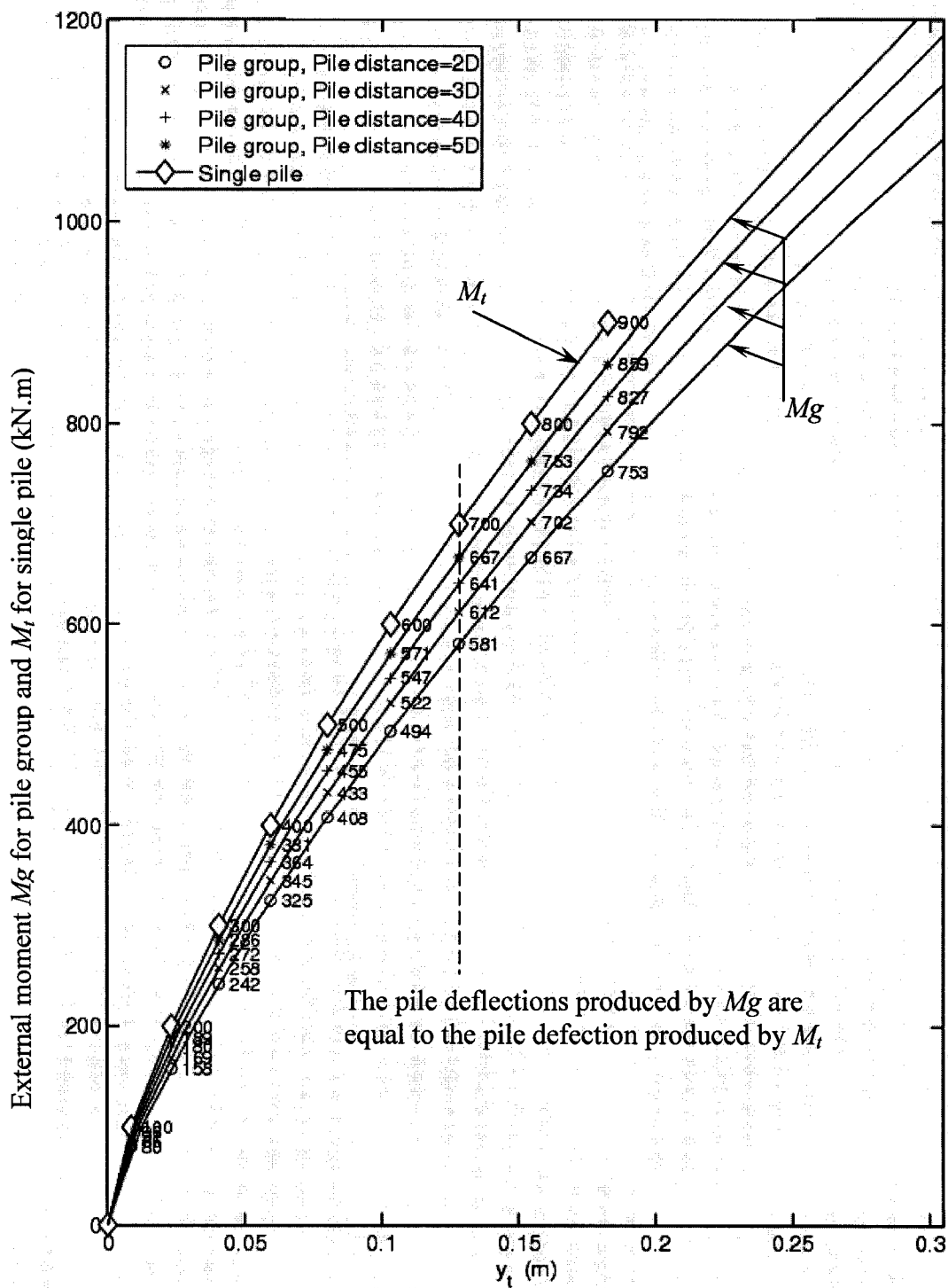
Figure 6.46 Determination of the bending moment *Mg* applied at the pile heads of piles pinned to the cap for different pile group spacing (*s* = 2*D*, 3*D*, 4*D* and 5*D*)

241

To model the adjoint pile, the values of lateral forces Pg_1 applied at the pile cap that will result in unit shear force reaction at the pile head of the pile member under investigation should be determined. In order to find out the force Pg_1, it is necessary to introduce a pile group load shown in Figure 6.47(c), in which a force $\overline{9}$ is applied in addition to the primary structure shown in Figure 6.47(b). The force $\overline{9}$ is the multiple of 1_a and the number of pile members (9) in the pile group arrangement.

Figure 6.47 presents in graphical way the methodology used for the determination of the adjoint load applied to the adjoint structure when the primary pile group is subjected to bending moment Mg. The final value of the force Pg_1 can be reached by subtracting the shear forces produced at the pile heads of structure shown in Figure 6.47(b) from the shear forces produced at the pile heads of structure shown in Figure 6.47(c).The resultant of the operation "(c)-(b)" is indicated in Figure 6.47(d), in which the shear force differences $\Delta V_1 - \Delta V_9$ exist at the heads of each pile in the pile group.

$$\overline{9} = \sum_{i=1}^{9} \Delta V \tag{6.18}$$

As an example to demonstrate the understanding of the methodology of the load application to the adjoint pile group system, the pile number 5 that appears inside of the shaded area in the Figure 6.47(e) is used. The force Pg_1 applied to the pile cap of the adjoint structure that will produce unit shear force at the pile head of pile 5 (the shaded pile) can be calculated as follows:

$$Pg_1 = \frac{\sum_{i=1}^{9} \Delta V_i}{\Delta V_s} \bullet 1_a = \frac{\overline{9}}{\Delta V_s} \tag{6.19}$$

The force Pg_1 for the pile group (3x3) consists of 9 piles that can be obtained by means of the following equation:

242

$$(Pg_1)_j = \frac{\sum\limits_{i=1}^{9} \Delta V_i}{\Delta V_j} \bullet 1_a = \frac{\overline{9}}{\Delta V_j} \qquad\qquad (6.20)$$

where $(Pg_1)_j$ = the lateral force applied to the adjoint pile group cap that will produce unit shear force at the pile head of pile j under analysis,

ΔV_i = the shear forces difference produced at the pile head due to application of force $\overline{9}$ (obtained by subtracting the shear forces produced at the pile heads of pile group system shown in Figure 6.47(b) from the shear forces produced at the pile heads of pile group system shown in Figure 6.47(c)),

ΔV_j = the shear force difference produced at the top of the pile subjected to analysis due to application of force $\overline{9}$ (obtained by subtracting the shear forces produced at the pile head j of pile group system shown in Figure 6.47(b) from the shear forces produced at the pile head j of pile group system shown in Figure 6.47(c)).

The following equation is then used for determination of the adjoint shear forces:

$$(e) = (f)-(b) \qquad\qquad (6.21)$$

where (e) = the adjoint structure with Pg_1 applied at the pile cap,

(f) = the pile group system which has the same physical properties as the primary structure and subjected to the lateral force Pg_1 applied to the pile cap in addition to the Mg acting at the pile heads in a pile group,

(b) = the primary structure subjected to Mg acting at the pile head of piles in a pile group.
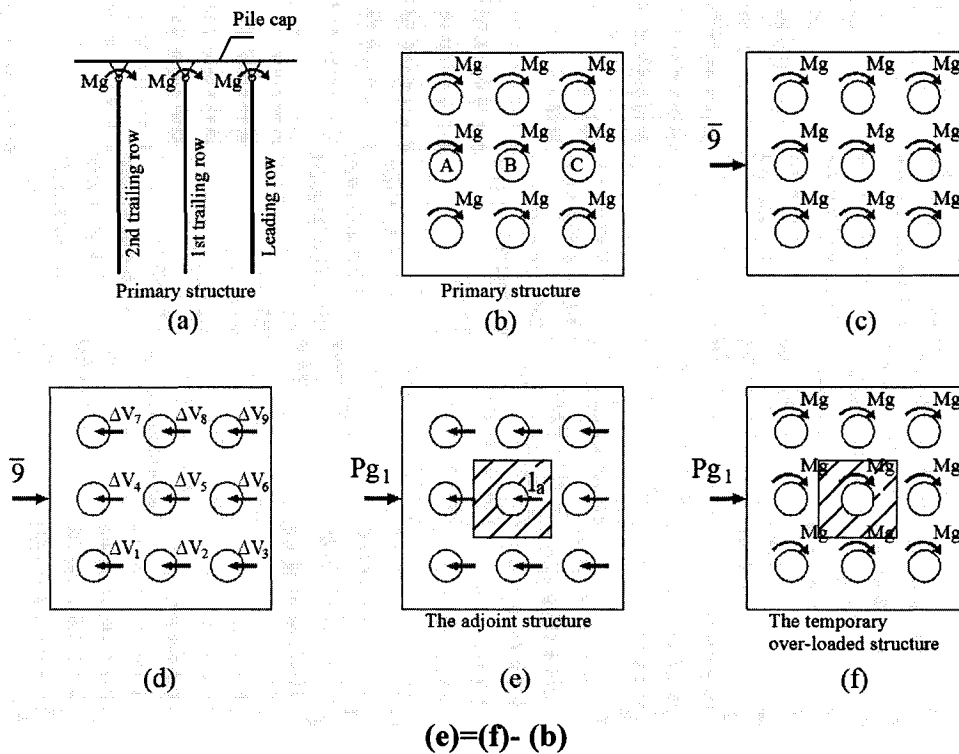
Figure 6.47 Method used to determine load Pg_1 applied to the adjoint pile group when the primary pile groups is loaded by bending moment Mg applied to the pile head of members in a pile group

6.3.4 Analysis of results

The results of the 396 cases mentioned above for the pile group study are given in the attached CD. The details of the contents of the CD and how to get the numerical values of the five forms of results and their graphical presentation are given in Appendix C. In the current section, a sample of the results is presented and compared to the results of a single pile and the effect of the pile location and pile spacing on the sensitivity results is studied.

6.3.4.1 Sample of results

The results of pile B in a pile group with piles pinned to the cap subjected to lateral force Pg (support type 1) with 20% clay layer thickness and pile spacing $3D$ are presented in

244

this Section. Figures 6.48 and 6.49 show the distribution of the sensitivity operators S for the eight studied parameters (clay, sand and pile parameters, respectively). The values of the sensitivity results A, PCR, TF and GF are given in Table 6.33. The bar charts for these results are available in the attached CD.

6.3.4.2 Comparison with single piles

The results given in Figure 6.48 and 6.49 for pile B in a group are compared to those in Figure 6.9 and 6.10 for the free head single pile subjected to lateral forces that give the same deflections as those of a pile group (Figure 6.43). The two piles have the same length (18 m) and embedded in the same thickness of clay (20% clay layer thickness = 3.6 m).

From the distribution of the sensitivity operators S for both piles, it is observed that both the single pile and pile B in the group have the same patterns. However, the values of the operators for the pile group are lower than those of the single pile. This is due to the use of p-multipliers f_m for the pile group that account for the shadowing effect. Therefore although the deflection is the same, the soil resistance p for the pile group is reduced for the pile group ($p_{group} = f_m \times p_{single}$ (Figure 2.3)). Since the operators for all parameters, except the pile's stiffness EI, involve the differentiation of the soil resistance with respect to the deflection, the operators for the group are reduced by the value of f_m ($f_m < 1$).

By comparing Table 6.33 to Tables 6.12, 6.13 , 6.14 and 6.15, the same observations apply above for the sensitivity factors A (since A is the integration of S) and the percent change ratio PCR (since $PCR = A/y_t$ and y_t is equal for both piles). However, the sensitivity factors (TF and GF) are similar (very close) for the two piles and the order of the parameters relative to all parameters and relative to their group is the same, in general. (order is not similar for the sand parameters at the lowest level of load).

It is concluded from the above discussion that due to the presence of the multiplier f_m that physically reflects the interaction between piles for the group, the sensitivity results S, A, PCR are lower for a pile in a group than that for a single isolated pile (except for EI).

245
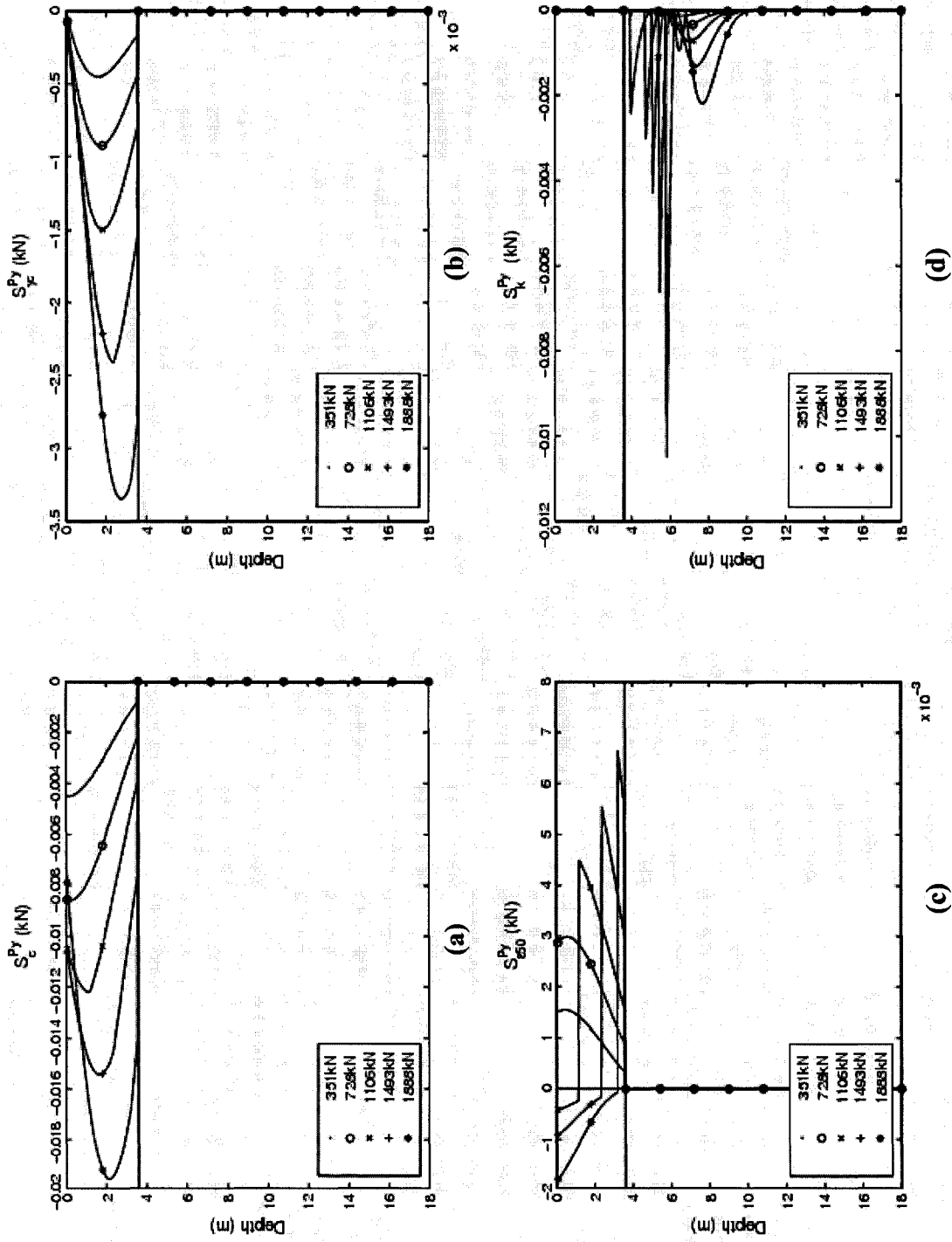
Figure 6.48 Sensitivity operators for pile B in a pile group embedded in soil with 20% clay layer thickness, spacing 3D and piles pinned to cap subjected to lateral loads (a) S_c^{Py}, (b) $S_{\gamma c}^{Py}$, (c) $S_{\varepsilon 50}^{Py}$ and (d) S_k^{Py}

246

Figure 6.49 Sensitivity operators for pile B in a pile group embedded in soil with 20% clay layer thickness, spacing 3D and piles pinned to cap subjected to lateral loads (a) S_{fs}^{Py}, (b) S_{ϕ}^{Py}, (c) S_{EI}^{Py} and (d) S_{b}^{Py}

247
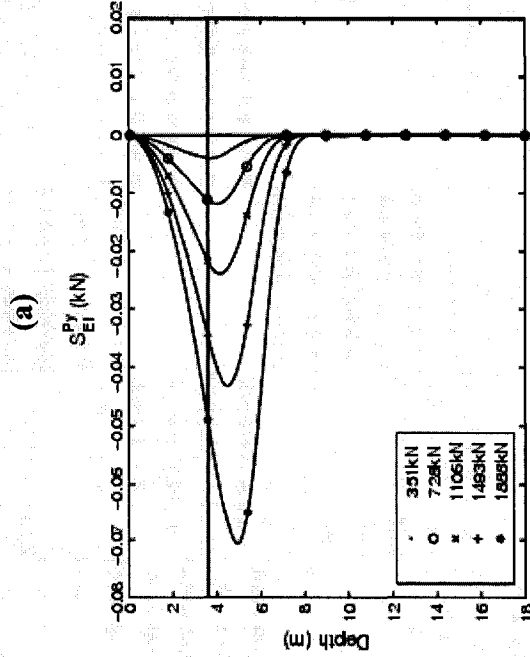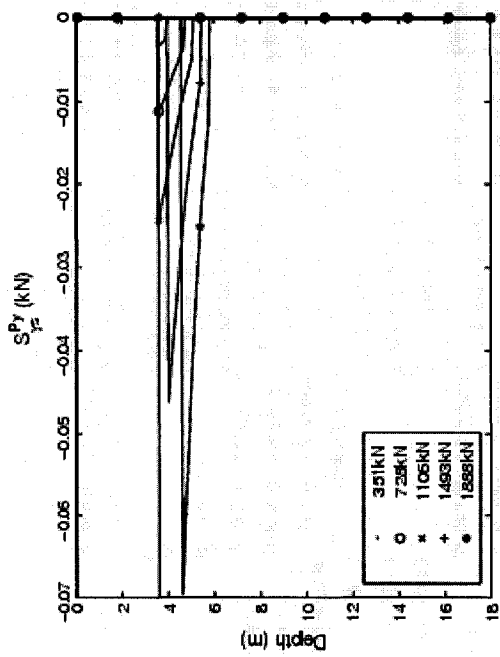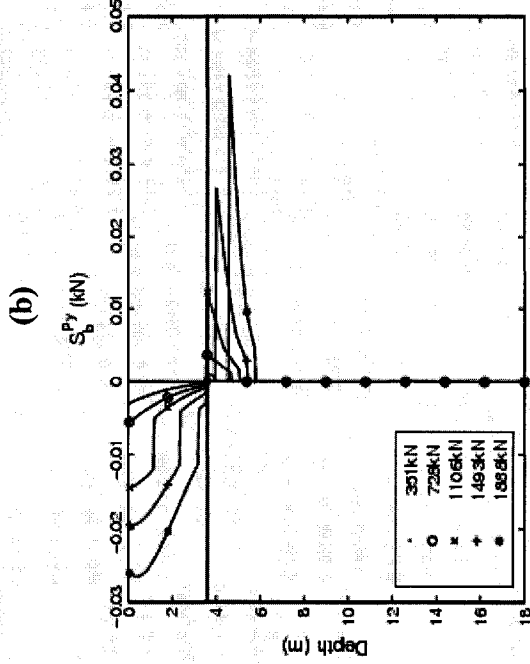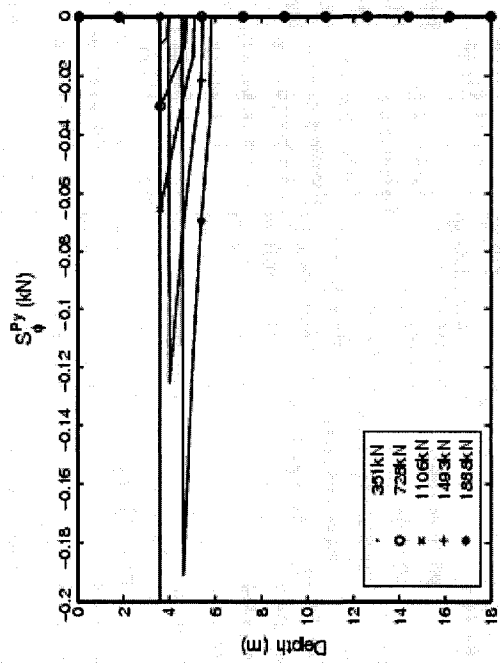
Table 6.33 Values of sensitivity results A, PCR, TF and GF for each variable at different load levels (support type = 1, % clay layer thickness = 20%, Pile B)

	Pg = 351 kN	Pg = 728 kN	Pg =1106 kN	Pg =1493 kN	Pg =1888 kN
A_c^{Py}	-0.011	-0.022	-0.033	-0.047	-0.058
$A_{\gamma c}^{Py}$	-0.001	-0.002	-0.004	-0.006	-0.008
$A_{\varepsilon 50}^{Py}$	0.004	0.008	0.007	0.004	-0.001
A_k^{Py}	-0.001	-0.001	-0.002	-0.004	-0.006
$A_{\gamma s}^{Py}$	-0.001	-0.008	-0.021	-0.036	-0.045
A_ϕ^{Py}	-0.003	-0.023	-0.057	-0.099	-0.124
A_{EI}^{Py}	-0.012	-0.037	-0.077	-0.142	-0.240
A_b^{Py}	-0.004	-0.006	-0.013	-0.025	-0.045
PCR_c^{Py}	-0.64	-0.45	-0.38	-0.33	-0.27
$PCR_{\gamma c}^{Py}$	-0.07	-0.05	-0.04	-0.04	-0.04
$PCR_{\varepsilon 50}^{Py}$	0.24	0.17	0.08	0.03	0.00
PCR_k^{Py}	-0.06	-0.03	-0.03	-0.03	-0.03
$PCR_{\gamma s}^{Py}$	-0.07	-0.17	-0.24	-0.25	-0.21
PCR_ϕ^{Py}	-0.18	-0.47	-0.64	-0.69	-0.57
PCR_{EI}^{Py}	-0.72	-0.77	-0.87	-0.99	-1.10
PCR_b^{Py}	-0.25	-0.13	-0.15	-0.17	-0.21
TF_c^{Py}	28.80	20.11	15.52	12.90	11.08
$TF_{\gamma c}^{Py}$	3.15	2.27	1.84	1.66	1.54
$TF_{\varepsilon 50}^{Py}$	10.65	7.46	3.35	1.09	0.10
TF_k^{Py}	2.91	1.35	1.05	1.01	1.11
$TF_{\gamma s}^{Py}$	2.94	7.69	9.74	9.97	8.55
TF_ϕ^{Py}	7.93	20.85	26.47	27.28	23.55
TF_{EI}^{Py}	32.56	34.61	35.91	39.27	45.55
TF_b^{Py}	11.06	5.66	6.13	6.84	8.50
GF_c^{Py}	67.61	67.39	74.96	82.47	87.09
$GF_{\gamma c}^{Py}$	7.39	7.61	8.86	10.59	12.11
$GF_{\varepsilon 50}^{Py}$	25.00	25.00	16.18	6.94	0.80
GF_k^{Py}	21.13	4.52	2.82	2.63	3.35
$GF_{\gamma s}^{Py}$	21.34	25.72	26.14	26.07	25.73

248

Table 6.33 Values of sensitivity results A, PCR, TF and GF for each variable at different load levels (support type =1, % clay layer thickness =20%, Pile B)(continued)

	Pg =351 kN	Pg =728 kN	Pg =1106 kN	Pg =1493 kN	Pg =1888 kN
GF_ϕ^{Py}	57.53	69.76	71.04	71.30	70.91
GF_{EI}^{Py}	74.65	85.94	85.43	85.17	84.27
GF_b^{Py}	25.35	14.06	14.57	14.83	15.73

However, it is noticed that also the deflection along the pile affects the sensitivity results. Although the single pile and the pile in a group are compared for piles that give equal deflection at the pile head, the deflection along the pile is not exactly similar for the single and pile groups. This difference in the deflection along the pile affects the sensitivity results. This effect appears in the sand operators where the results S, A and PCR for sand parameters show lower values for single pile than for pile B in the group at some levels of applied load.

6.3.4.3   Effect of pile location

The sensitivity operators for the three piles A, B and C for a pile group with piles pinned to the cap subjected to lateral load (support type 1) with spacing $3D$ and 20% clay layer thickness are plotted for the eight parameters in Figures 6.50 and 6.51 at load Pg = 1493 kN. The other four results are compared in Table 6.34. It is observed that the values of the sensitivity operators for piles A are smaller than those for B smaller than those for C. This can be attributed to the values of f_m which are ordered from smaller to higher for A, B then C, respectively. i.e., the leading row has the highest values of S. However, the order of the piles with respect to S values is different for the parameter k (Figure 6.50d).

By reexamining the expressions of the sensitivity operators S, it is found that, besides the values of f_m, the values of S are affected by the deflection of the primary pile and the adjoint pile. For the primary pile, although the lateral top deflections y_t of piles A, B, C are equal, it is noticed from the deflection patterns of the 3 piles that along the pile length the deflection decreases from A to C (i.e. deflection y for pile A $> y$ of B $> y$ of C). In addition, the adjoint piles for A, B and C, are obtained by applying a load Pg_1 at the pile

249

cap that will produce a unit shear at the pile head. Due to the difference in the f_m values for the three piles, the load Pg_1 applied for pile A is higher than pile B and pile B is higher than pile C. Therefore the adjoint deflection y_a for pile A is higher than B higher than C. Accordingly, as we move from trailing rows to leading row (pile A to pile C), the values of f_m increase, however, deflections of primary pile y and adjoint pile y_a decreases.

The effect of f_m is dominating for the clay parameters and the parameter b for all levels of load resulting in values of S increasing from pile A to pile C. For the sand parameters, it is not clear which effect dominates and accordingly the order of piles with respect to values of S changes depending on level of load and parameter under investigation (at load Pg=1493 kN (Table 6.34), f_m dominates for S_{js}^{Py} and S_{ϕ}^{Py} but not for S_k^{Py}, however, at lower loads results are different). For the parameter EI, the values of S are not a function of the f_m multiplier since they don't depend on the p-y relationship. The values of S_{EI} depend only on the bending moments of the primary and adjoint piles. As we move from pile A to C, the moment of primary pile increases while that for the moment of adjoint pile decreases resulting in close values of S_{EI} for the three piles.

Similar to the sensitivity operators results, the values of the sensitivity factors A (given in Table 6.34) for piles A are lower than B lower than C (except for k as explained above and EI). This implies that the change in lateral top deflection will be different for each pile. However, since the three piles are under the same cap, the change in the deflection should be equal for the three piles due to the constraint imposed by the pile cap. The results obtained from the sensitivity study are different for each pile since each pile is treated as an individual pile and for each pile there is a different value of Pg_1 applied to the cap that results in a unit load at the pile head under investigation (A, B or C). Therefore each pile can be treated individually, or it is suggested to obtain delta y_t for the group by taking the average of the sensitivity factors A of the three piles since there is little difference between results of the three piles.

250
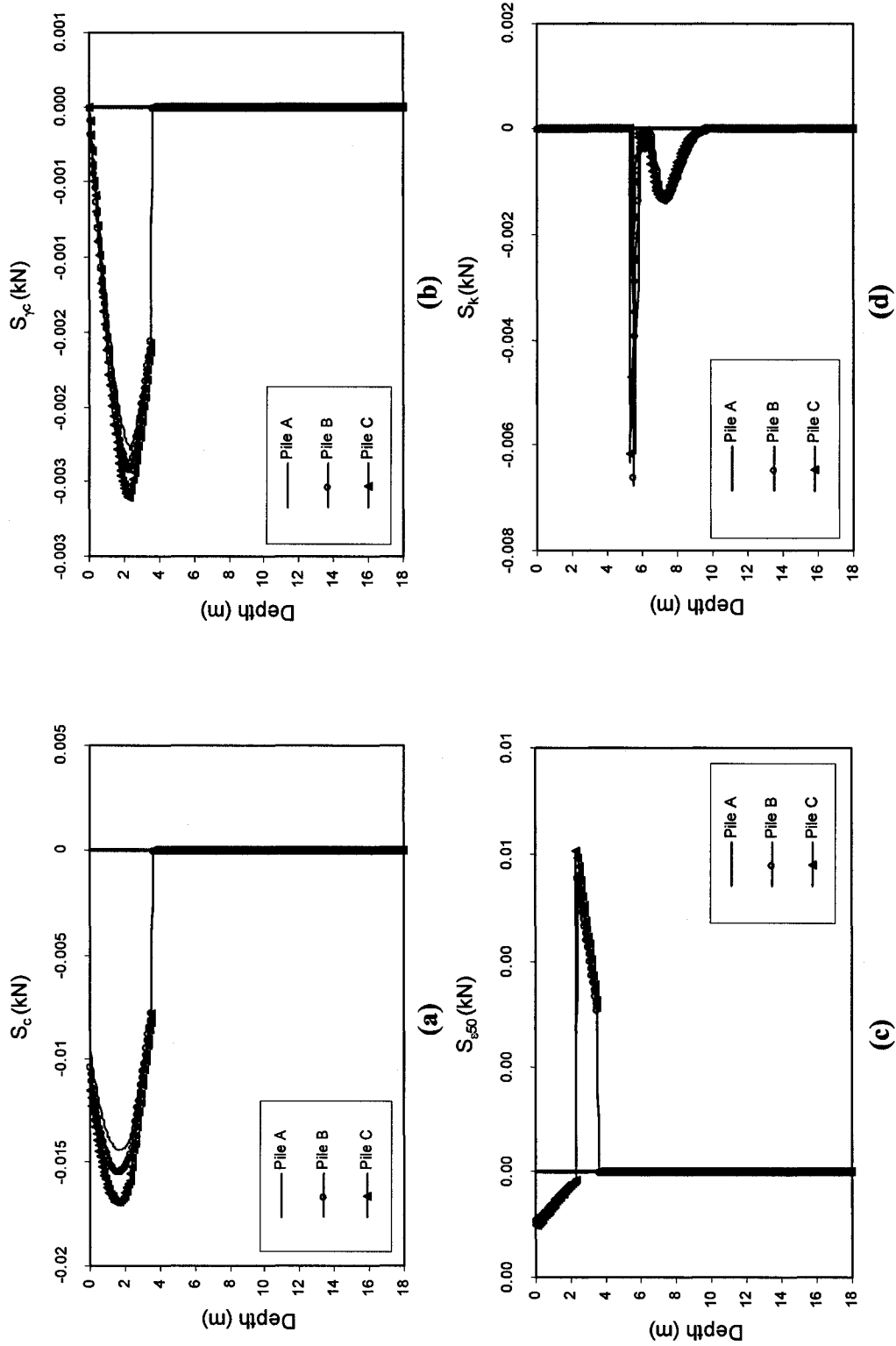
Figure 6.50 Comparison between the sensitivity operators of piles A, B and C in a pile group embedded in soil with 20% clay layer thickness, spacing 3*D* and piles pinned to cap subjected to lateral loads (a) S_c^{Py}, (b) $S_{\gamma c}^{Py}$, (c) $S_{\varepsilon 50}^{Py}$ and (d) S_k^{Py}

251
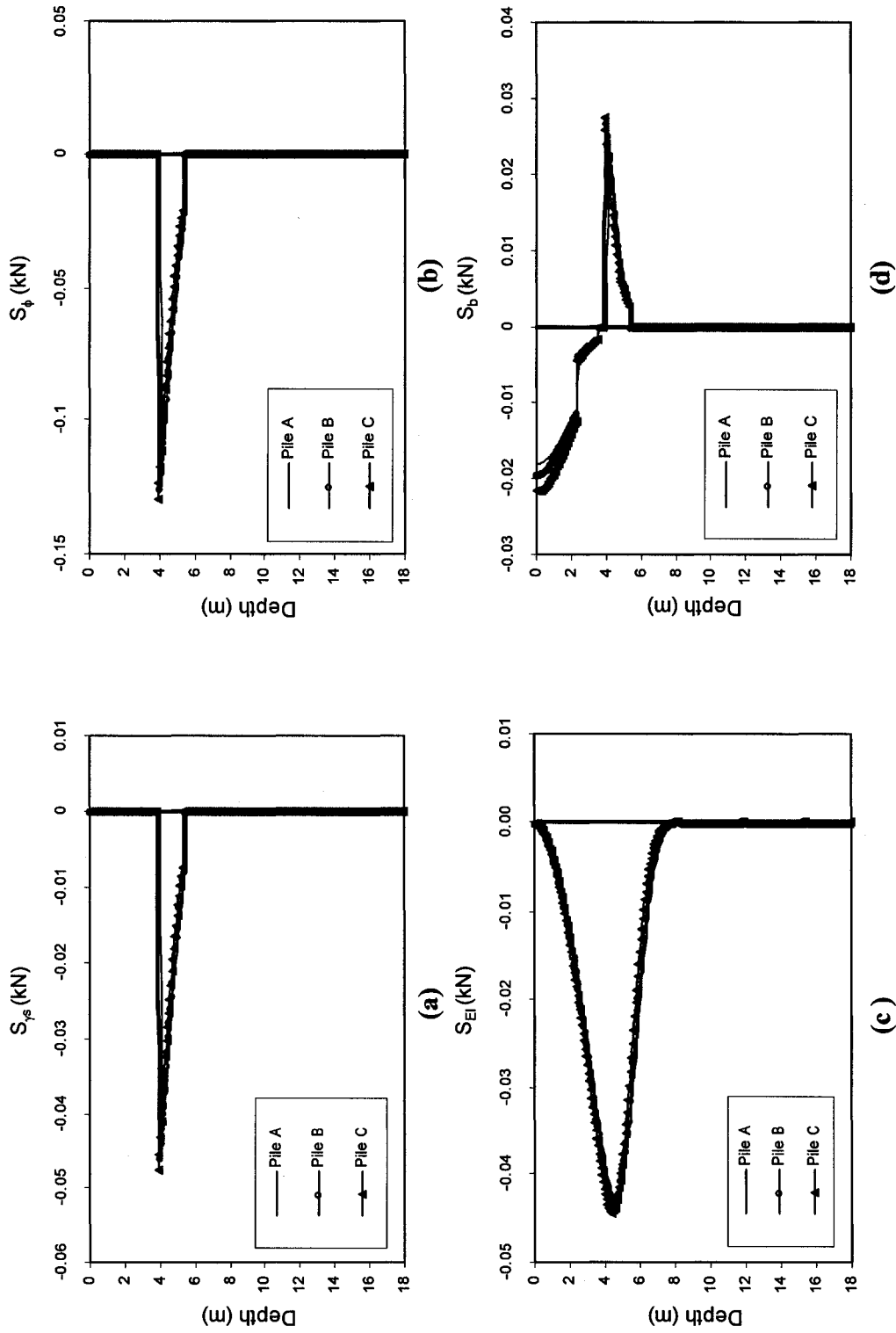
Figure 6.51 Comparison between the sensitivity operators of piles A, B and C in a pile group embedded in soil with 20% clay layer thickness, spacing 3D and piles pinned to cap subjected to lateral loads (a) S_{ys}^{Py}, (b) S_{ϕ}^{Py}, (c) S_{EI}^{Py} and (d) S_{b}^{Py}

252

Table 6.34 Values of sensitivity results A, PCR, TF and GF at Pg =1493 kN for piles A, B and C (different pile locations for support type =1, % clay layer thickness =20%)

|	Pile A (2nd trailing row)	Pile B (1st trailing row)	Pile C (leading row)
A_c^{Py}	-0.044	-0.047	-0.051
$A_{\gamma c}^{Py}$	-0.006	-0.006	-0.006
$A_{\varepsilon 50}^{Py}$	0.004	0.004	0.005
A_k^{Py}	-0.004	-0.004	-0.003
$A_{\gamma s}^{Py}$	-0.036	-0.036	-0.037
A_ϕ^{Py}	-0.098	-0.099	-0.100
A_{EI}^{Py}	-0.143	-0.142	-0.141
A_b^{Py}	-0.022	-0.025	-0.028
PCR_c^{Py}	-0.31	-0.33	-0.35
$PCR_{\gamma c}^{Py}$	-0.04	-0.04	-0.04
$PCR_{\varepsilon 50}^{Py}$	0.03	0.03	0.03
PCR_k^{Py}	-0.02	-0.03	-0.02
$PCR_{\gamma s}^{Py}$	-0.25	-0.25	-0.26
PCR_ϕ^{Py}	-0.69	-0.69	-0.70
PCR_{EI}^{Py}	-1.00	-0.99	-0.98
PCR_b^{Py}	-0.15	-0.17	-0.19
TF_c^{Py}	12.33	12.90	13.64
$TF_{\gamma c}^{Py}$	1.59	1.66	1.74
$TF_{\varepsilon 50}^{Py}$	1.07	1.09	1.22
TF_k^{Py}	1.00	1.01	0.92
$TF_{\gamma s}^{Py}$	10.07	9.97	9.90
TF_ϕ^{Py}	27.59	27.28	27.03
TF_{EI}^{Py}	40.17	39.27	38.03
TF_b^{Py}	6.18	6.84	7.52
GF_c^{Py}	82.22	82.47	82.18
$GF_{\gamma c}^{Py}$	10.62	10.59	10.46
$GF_{\varepsilon 50}^{Py}$	7.16	6.94	7.36
GF_k^{Py}	2.59	2.63	2.43

253

Table 6.34 Values of sensitivity results A, PCR, TF and GF at Pg =1493 kN for piles A, B and C (different pile locations for support type =1, % clay layer thickness =20%) (continued)

	Pile A (2nd trailing row)	Pile B (1st trailing row)	Pile C (leading row)
$GF_{\gamma s}^{Py}$	26.05	26.07	26.16
GF_{ϕ}^{Py}	71.36	71.30	71.41
GF_{EI}^{Py}	86.67	85.17	83.49
GF_{b}^{Py}	13.33	14.83	16.51

The observations regarding the values of *PCR* are similar to those for the values of sensitivity factors *A*. However, the sensitivity factors (*TF* and *GF*) are similar (very close) for the three piles and the order of the parameters relative to all parameters and relative to their group is the same, irrespective of the pile location.

6.3.4.4 Effect of pile spacing

The pile B (first trailing row) for pile groups with spacings 2*D*, 3*D*, 4*D* and 5*D* are compared in Figures 6.52 and 6.53. The comparison can be explained in view of the f_m values, and deflection results. The values of f_m increase as the pile spacing increases. However, the deflection of the adjoint pile decreases as the pile spacing decreases. The values of the loads applied at the top of the primary pile *Pg* (that give the same top deflection for all spacings) and the adjoint pile Pg_1 (calculated from Eq. 6.15) for the different spacings and the corresponding deflections are given in Table 6.35. The values of Pg_1 decrease as spacing increases (i.e. adjoint piles are subjected to lower load) leading to the decrease in y_a. The results *A, PCR, TF* and *GF* are compared in Table 6.36.

According to the above observation, the same comments given for the pile location apply to the pile spacing. In other words, as the pile spacing increases, the maximum values of *S* (and accordingly *A* and *PCR*) increase for the clay parameters and pile diameter *b* while they can increase or decrease for the sand parameters depending on which effect (effect of f_m or y_a) is more dominant. The parameter *EI* has very close values for the different pile spacings. The order of the parameters for *TF* and *GF* is similar for all pile spacings.

254
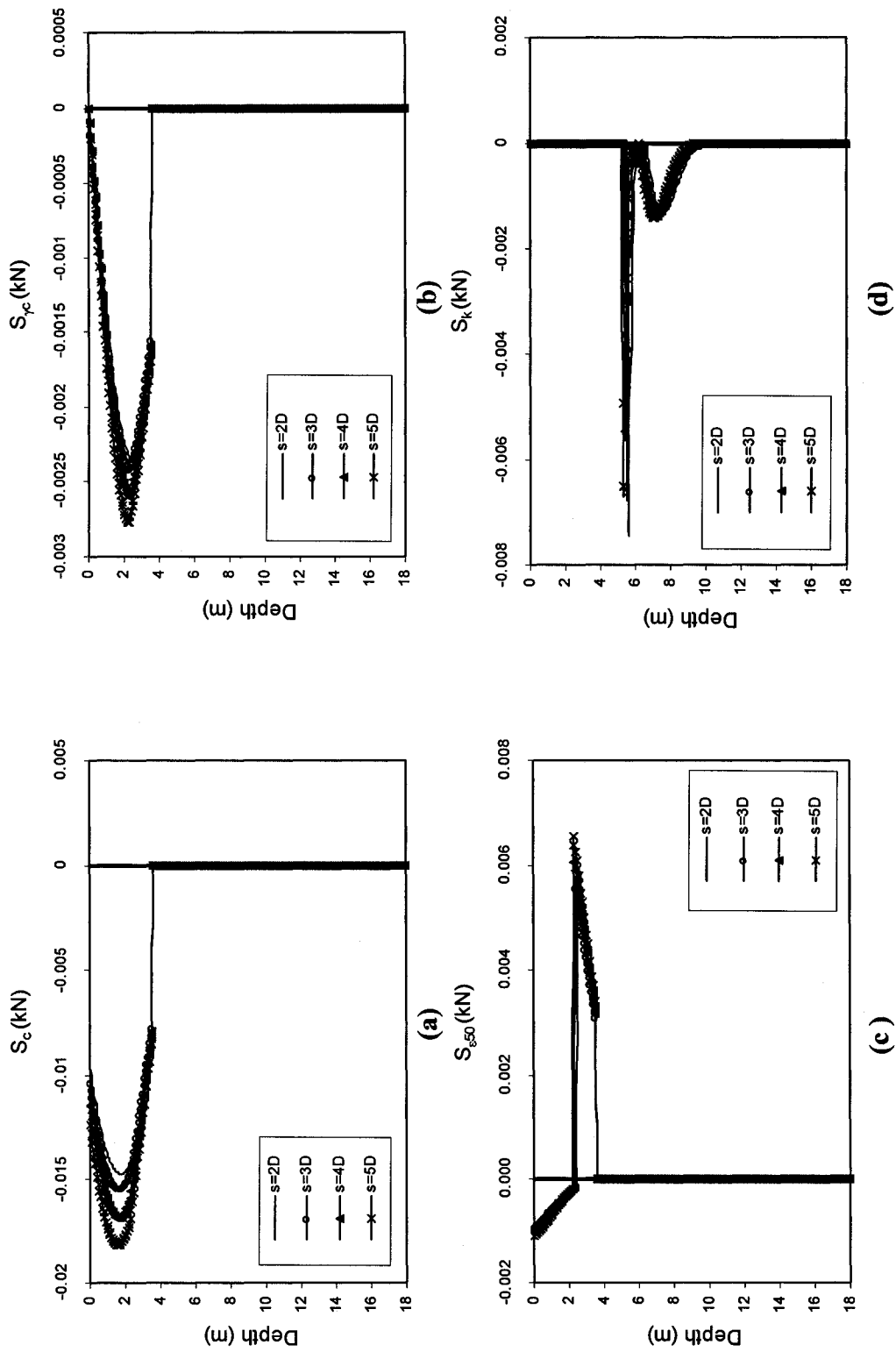
Figure 6.52 Comparison between the sensitivity operators of pile B in pile groups with different spacings (*2D*, *3D*, *4D* and *5D*), 20% clay layer thickness and piles pinned to cap subjected to lateral loads (a) S_c^{Py}, (b) $S_{\gamma c}^{Py}$, (c) $S_{\varepsilon 50}^{Py}$ and (d) S_k^{Py}

255
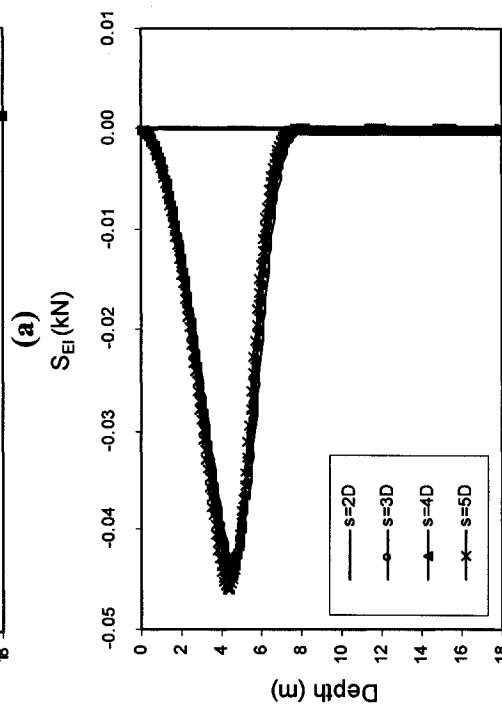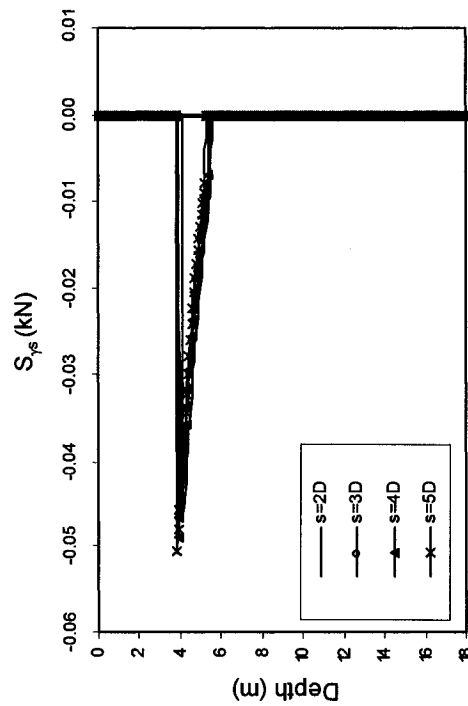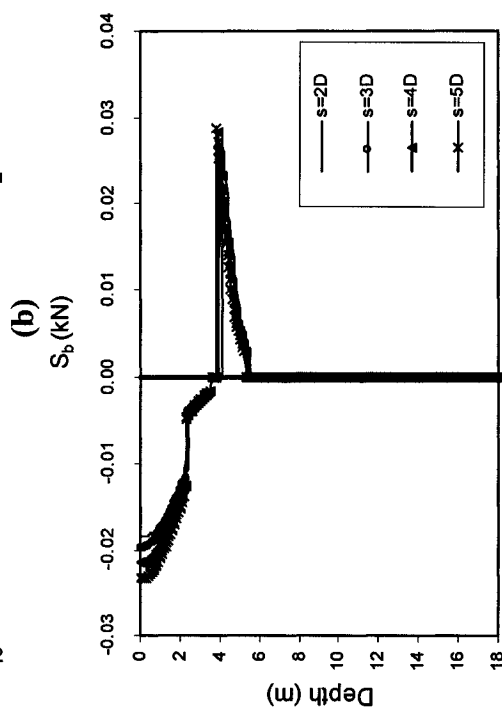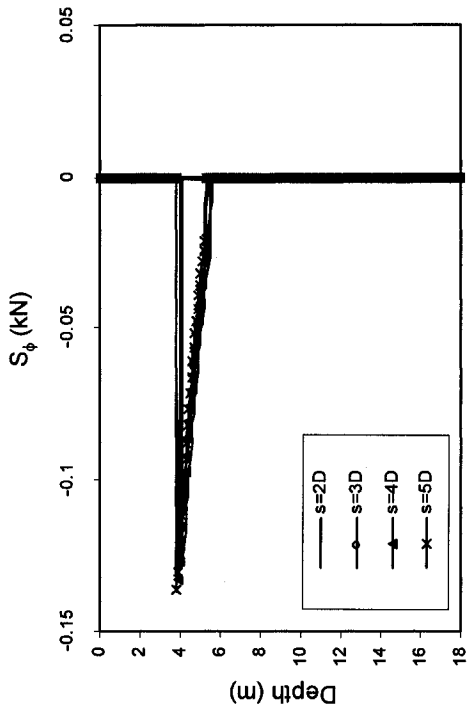
Figure 6.53 Comparison between the sensitivity operators of pile B in pile groups with different spacings (*2D*, *3D*, *4D* and *5D*), 20% clay layer thickness and piles pinned to cap subjected to lateral loads (a) $S_{\gamma s}^{Py}$, (b) S_{ϕ}^{Py}, (c) S_{EI}^{Py} and (d) S_{b}^{Py}

256

Table 6.35 Values of Pg, Pg₁, yₜ and yₐ(top) for different pile spacings (for support type =1, % clay layer thickness =20%, Pile B)

Spacing (s)	2D	3D	4D	5D
Pg (kN)	1381	1493	1591	1688
Pg_1 (kN)	9.1371	9.09929	9.06215	9.0291
y_t (m)	0.143898	0.14359	0.14303	0.14325
y_a (m)	0.001658	0.001474	0.00139	0.00132

Table 6.36 Values of sensitivity results A, PCR, TF and GF for different pile spacings (for support type =1, % clay layer thickness =20%, Pile B)

Spacing s	$s = 2D$	$s = 3D$	$s = 4D$	$s = 5D$
A_c^{Py}	-0.045	-0.047	-0.051	-0.054
$A_{\gamma c}^{Py}$	-0.006	-0.006	-0.006	-0.007
$A_{\varepsilon 50}^{Py}$	0.004	0.004	0.005	0.005
A_k^{Py}	-0.004	-0.004	-0.003	-0.003
$A_{\gamma s}^{Py}$	-0.037	-0.036	-0.039	-0.038
A_ϕ^{Py}	-0.102	-0.099	-0.106	-0.103
A_{EI}^{Py}	-0.146	-0.142	-0.144	-0.145
A_b^{Py}	-0.023	-0.025	-0.027	-0.030
PCR_c^{Py}	-0.31	-0.33	-0.35	-0.38
$PCR_{\gamma c}^{Py}$	-0.04	-0.04	-0.05	-0.05
$PCR_{\varepsilon 50}^{Py}$	0.03	0.03	0.03	0.03
PCR_k^{Py}	-0.03	-0.03	-0.02	-0.02
$PCR_{\gamma s}^{Py}$	-0.26	-0.25	-0.27	-0.26
PCR_ϕ^{Py}	-0.71	-0.69	-0.74	-0.72
PCR_{EI}^{Py}	-1.02	-0.99	-1.00	-1.01
PCR_b^{Py}	-0.16	-0.17	-0.19	-0.21
TF_c^{Py}	12.29	12.90	13.31	14.01
$TF_{\gamma c}^{Py}$	1.59	1.66	1.70	1.78
$TF_{\varepsilon 50}^{Py}$	1.03	1.09	1.21	1.30
TF_k^{Py}	1.09	1.01	0.83	0.87
$TF_{\gamma s}^{Py}$	10.13	9.97	10.21	9.83
TF_ϕ^{Py}	27.77	27.28	27.89	26.83
TF_{EI}^{Py}	39.93	39.27	37.85	37.51
TF_b^{Py}	6.16	6.84	7.01	7.87

257

Table 6.36 Values of sensitivity results A, PCR, TF and GF for different pile spacings (for support type =1, % clay layer thickness =20%, Pile B) (continued)

Spacing s	$s = 2D$	$s = 3D$	$s = 4D$	$s = 5D$
GF_c^{Py}	82.42	82.47	82.10	82.00
$GF_{\gamma c}^{Py}$	10.68	10.59	10.46	10.40
$GF_{\varepsilon 50}^{Py}$	6.90	6.94	7.44	7.61
GF_k^{Py}	2.80	2.63	2.14	2.33
$GF_{\gamma s}^{Py}$	25.98	26.07	26.23	26.20
GF_ϕ^{Py}	71.22	71.30	71.63	71.47
GF_{EI}^{Py}	86.63	85.17	84.37	82.65
GF_b^{Py}	13.37	14.83	15.63	17.35

6.3.5 Verification of results

The results of the pile group are verified in a similar manner to that used for the single piles. The error in the predicted lateral top deflection y_t due to change in each parameter is given in Table 6.37 (as an example) for pile B for the 18 m long pile embedded in soil with 20% clay layer thickness with spacing 3D. The error in predicting y_t for all the studied cases for pile groups (297 cases) is given in the attached CD (see Appendix C).

Table 6.37 Assessment of error (in %) in the predicted lateral top deflection y_t due to change in the eight studied parameters at different levels of applied load for pile B in a group pinned to the pile cap (18 m long pile with 20% clay layer thickness)

% change		1%	5%	10%	15%	20%	25%	30%	40%	50%
Error$_c$ (%)	Pg=351 kN	0.001	0.050	0.226	0.337	0.278	0.888	1.734	3.253	6.460
	Pg=728 kN	0.003	0.008	0.074	1.780	1.530	1.198	0.803	1.383	0.077
	Pg=1106 kN	0.002	0.007	0.052	2.495	2.323	2.109	1.866	3.451	2.474
	Pg=1493 kN	0.007	0.047	0.030	3.918	3.827	3.705	3.560	6.534	5.869
	Pg=1888 kN	0.007	0.035	0.060	4.945	4.901	4.821	4.762	9.259	8.971
Error$_{\gamma c}$ (%)	Pg=351 kN	0.093	0.389	0.912	1.272	1.770	2.176	2.569	3.308	4.856
	Pg=728 kN	0.068	0.340	0.670	0.988	1.295	1.590	1.873	2.403	4.952
	Pg=1106 kN	0.060	0.301	0.591	0.866	1.132	1.385	1.628	2.081	5.182
	Pg=1493 kN	0.065	0.322	0.653	0.948	1.209	1.478	1.734	2.211	6.576
	Pg=1888 kN	0.068	0.340	0.669	0.986	1.292	1.585	1.862	2.380	7.827
Error$_{\varepsilon 50}$ (%)	Pg=351 kN	0.001	0.024	0.025	0.228	0.398	0.534	0.850	1.349	2.025
	Pg=728 kN	0.001	0.014	0.071	0.164	0.291	0.449	0.633	1.074	1.597
	Pg=1106 kN	0.038	0.176	0.317	0.428	0.515	0.582	0.635	0.690	0.701
	Pg=1493 kN	0.077	0.363	0.675	0.942	1.168	1.361	1.522	1.767	1.927
	Pg=1888 kN	0.113	0.535	1.000	1.405	1.744	2.050	2.316	2.732	3.044

258

Table 6.37 Assessment of error (in %) in the predicted lateral top deflection y_t due to change in the eight studied parameters at different levels of applied load for pile B in a group pinned to the pile cap (18 m long pile with 20% clay layer thickness)(continued)

% change		1%	5%	10%	15%	20%	25%	30%	40%	50%
Error$_k$ (%)	Pg=351kN	0.004	0.001	0.114	0.183	0.282	0.404	0.546	0.884	1.277
	Pg=728 kN	0.004	0.007	0.003	0.031	0.067	0.119	0.175	0.319	0.487
	Pg=1106 kN	0.001	0.009	0.032	0.064	0.107	0.156	0.213	0.342	0.491
	Pg=1493 kN	0.002	0.007	0.034	0.050	0.090	0.161	0.198	0.313	0.473
	Pg=1888 kN	0.004	0.024	0.058	0.103	0.155	0.215	0.281	0.429	0.593
Error$_{ys}$ (%)	Pg=351 kN	0.215	0.997	0.765	1.462	1.990	1.603	2.172	2.910	2.811
	Pg=728 kN	0.296	1.375	0.315	1.281	2.033	0.465	0.950	1.509	0.358
	Pg=1106 kN	0.358	1.624	0.085	1.156	1.993	0.210	0.290	0.808	1.925
	Pg=1493 kN	0.598	2.762	0.929	2.861	4.426	1.643	2.705	4.137	0.969
	Pg=1888 kN	0.868	4.097	2.429	5.527	8.203	5.252	7.300	10.561	7.752
Error$_\phi$ (%)	Pg=351 kN	0.013	1.265	1.616	3.180	4.846	5.552	7.284	9.913	12.576
	Pg=728 kN	0.021	2.188	2.329	4.885	7.638	8.410	11.511	16.184	21.526
	Pg=1106 kN	0.040	2.794	2.965	6.211	9.681	10.554	14.405	20.037	26.485
	Pg=1493 kN	0.348	2.552	1.383	4.636	8.212	8.124	12.235	17.514	24.041
	Pg=1888 kN	0.794	1.407	1.962	0.283	2.934	0.764	4.118	6.844	11.243
Error$_{EI}$ (%)	Pg=351kN	0.068	0.455	1.197	2.216	3.505	5.109	6.865	11.226	16.577
	Pg=728 kN	0.067	0.472	1.261	2.361	3.742	5.461	7.429	12.250	18.162
	Pg=1106 kN	0.077	0.572	1.566	2.963	4.749	6.914	9.441	15.552	23.005
	Pg=1493 kN	0.073	0.581	1.687	3.295	5.405	7.999	11.065	18.567	27.834
	Pg=1888 kN	0.095	0.714	2.054	3.981	6.489	9.568	13.220	22.183	33.320
Error$_b$ (%)	Pg=351 kN	0.003	0.008	0.002	0.100	0.053	0.109	0.198	0.488	0.054
	Pg=728 kN	0.000	0.009	0.029	0.063	0.109	0.162	0.221	0.333	2.421
	Pg=1106 kN	0.006	0.009	0.062	0.148	0.266	0.420	0.612	1.127	0.600
	Pg=1493 kN	0.076	0.349	0.644	0.880	1.075	1.177	1.240	1.234	3.916
	Pg=1888 kN	0.074	0.374	0.700	0.990	1.255	1.478	1.665	1.924	6.055

From Tables 6.37 the following can be observed:

1. The maximum error obtained is for the design variable *EI* and the minimum error obtained is for the modulus *k*.

2. To achieve an error in predicting y_t less than 5%, the range of change in the parameter can be taken up to 15% for all variables (except for ϕ = 6%).

3. For all the parameters, the change of the parameter up to 50%, gave an error in predicting y_t less than 15% (except for *EI* and ϕ, maximum error reached = 33% and 26%, respectively). This reflects the small values of error verifying the sensitivity results obtained from the study

4. The range of applicability of the first variation of lateral top deflection and top rotation obtained from the study depends on the tolerable percent of error and the level of applied load.

259

CHAPTER 7

SENSITIVITY ANALYSIS PROGRAM

7.1 INTRODUCTION

Although previous theoretical and numerical studies were performed for laterally loaded piles embedded in homogeneous soils (Budkowska, 1998, Priyanto, 2002, Suwarno, 2003, Abedin, 2004, Liu, 2004, Rahman, 2004, and Mora, 2006), no attempts were made to provide a program for engineers who wish to perform a sensitivity analysis using their own input data. This limited the applicability of the previous conducted researches. Therefore, the third part in the current research concentrates on developing a user-friendly program for sensitivity analysis.

The sensitivity analysis program is developed in the current research for single laterally loaded piles based on the theoretical formulation developed in Chapter 5. The five forms of sensitivity results derived in Chapter 5 can be numerically and graphically obtained by employing the developed sensitivity analysis program. The developed program is referred to in the present study as "SA-program". The SA-program was created using MATLAB version 7. The SA-program uses COM624P to obtain the deflections and internal forces of laterally loaded piles required for the sensitivity analysis. The SA-program is provided in the attached CD.

In this chapter, the features of the program and the program requirements are first presented. The modules and logic used in the SA-program are then explained. Finally a guide for execution of SA-Program and a sample of input and output are provided to enable the user to employ the program conveniently and effectively.

7.2   PROGRAM FEATURES

7.2.1   Application scope

The program provides the sensitivity of the lateral pile head deflection and pile head rotation to changes in the design parameters for laterally loaded single piles embedded in the following **soil stratifications**:

1. Homogeneous soft clay layer below water table (cyclic loading)
2. Homogeneous sand layer below water table (cyclic loading)
3. Non-homogeneous soil consisting of soft clay overlying sand both below water table (cyclic loading).

The program is based on the theoretical formulation provided in Chapter 5 which considers that the p-y curves (discussed in Chapter 4) can properly model the soil behavior. The design parameters that can be investigated using SA-program are the clay, sand and pile parameters defining the system (eight parameters given in Eq. 5.5).

The program covers piles that are subjected to lateral horizontal loads or bending moment applied at the pile head. The pile head can be free or fixed. Accordingly the results for any of the following three **support types** can be obtained:

1. free head pile subjected to lateral horizontal load at the pile head
2. fixed head pile subjected to lateral horizontal load at the pile head
3. free head pile subjected to bending moment at the pile head

7.2.2   Input to the program

The SA-program allows the user to:

1. choose one of the soil stratifications mentioned above
2. choose one of the support types mentioned above
3. input values of pile and soil parameters
4. input pile length and layer dimensions

261

5. input range of load applied and load increments
6. input the maximum allowable moment and maximum allowable deflection of the pile
7. input number of pile increments along the pile length
8. computational control information for the COM624P program (Number of iterations and tolerance)

7.2.3 Output from the program

The sensitivity of the lateral pile head deflection y_t to changes in the design parameters of the system for free head and fixed head piles (support types 1, 2 and 3) and the sensitivity of the pile head rotation θ_t for free head piles (support types 1 and 3) can be obtained using the SA-program. The output of the program includes the following for each response studied (y_t and θ_t):

1. values of the sensitivity operators S (Section 5.2.6) for each parameter along the pile length at the given load increments.
2. graphical distribution of the sensitivity operators S along the pile length for each parameter at the given load increments.
3. values of sensitivity results A, PCR, TF, and GF (Section 5.2.6) for each parameter at the given load increments.
4. graphical presentation of the sensitivity results A, PCR, TF, GF in the form of bar charts at the given load increments.

In addition, the output includes the numerical and graphical presentation of deflection, moment, shear, soil resistance of the primary and adjoint piles at the given load increments obtained from COM624P.

It should be noted that values of the percent change ratio PCR are not available for the pile head rotation sensitivity. This is because the rotation of the pile head θ_t (slope) required for the evaluation of PCR ($PCR = A/\theta_t$) is not offered by COM624P.

262

7.3   PROGRAM REQUIRMENTS

The program can run on any personal computer with windows operating system. The program MATLAB (version 7) should be installed on the computer. The user is assumed to have basic knowledge on how to use MATLAB.

7.4   MODULES AND LOGIC

The SA-program consists of MATLAB developed programs that are used to

1. obtain the input data from the user through a user-friendly interface *(data input module)*

2. call COM624P to calculate the deformation and internal forces *(calculating module)*

3. read the output of COM624P and use the output to calculate and plot the sensitivity operators *(sensitivity operators results module)*

4. calculates and plots the other four forms of sensitivity results *(A, PCR, TF, GF)* *(sensitivity results module)*

The SA-program is divided into four modules. Each module should be run individually in a certain executing sequence since each module depends on the previous one. The sequence of the modules is shown in Figure 7.1. Each module is explained in the following subsections.

7.4.1   Data input module

The source file for this module is "inputdata.m". This module is used to input the data of the pile, soil, loading, and all other necessary data needed to solve the pile system through a user-friendly interface. The input data is saved in a data file with the name specified by the user at the beginning of the run. The flow chart for the data input module is shown Figure 7.2

263
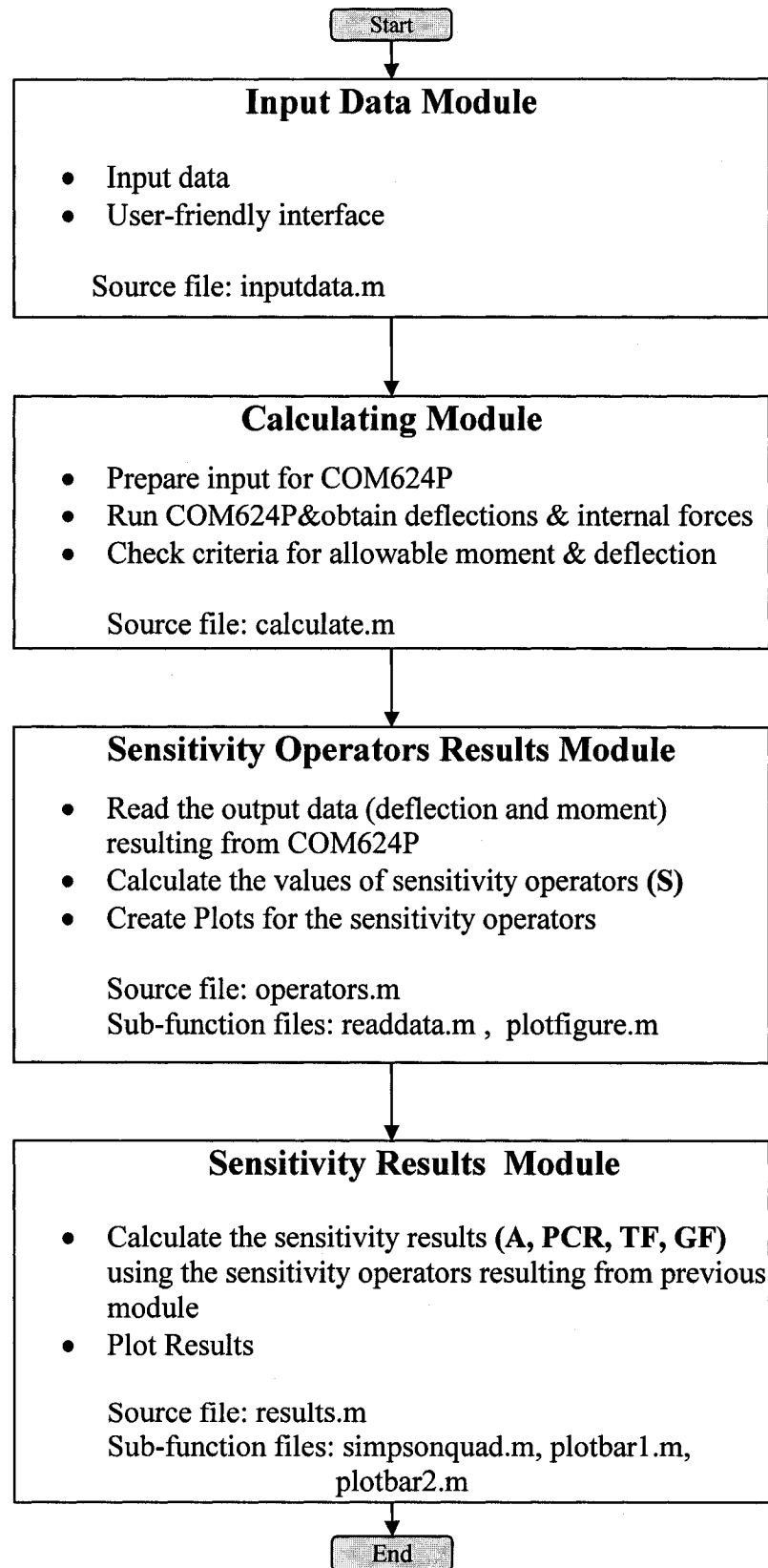
Figure 7.1 The executing sequence for the modules of SA-program

264
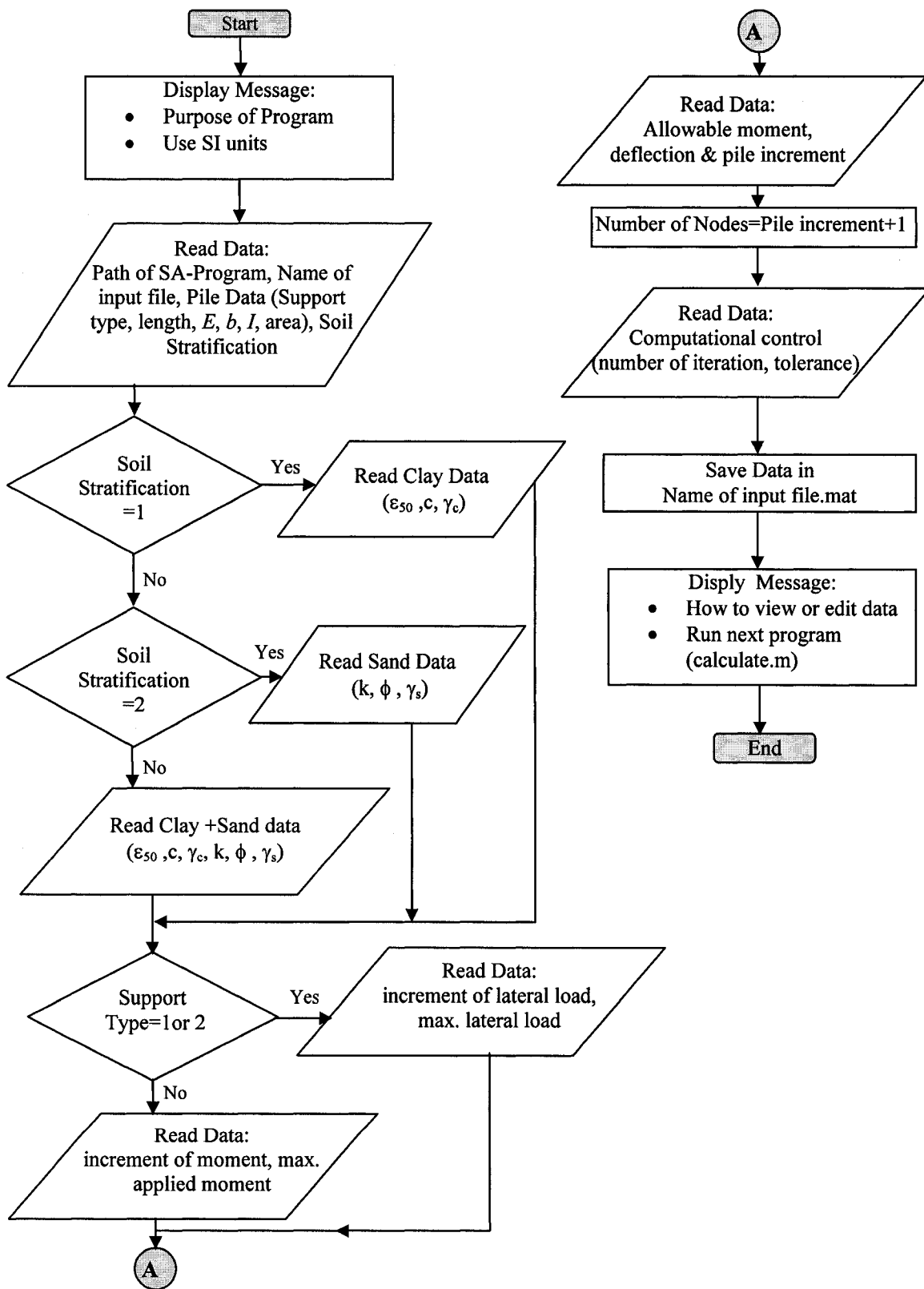
Figure 7.2 Flow chart for the input data module of SA-program

265

7.4.2 Calculating module

The source file for this module is "calculate.m". This module is used to

1- create the input files for primary and adjoint piles required for COM624P from the data file entered by the user. The name of the files consist of the force value followed by pr, ad1 and ad2 for primary pile, adjoint pile 1 (used to obtain δy_i) and adjoint pile 2 (used to obtain $\delta \theta_i$), respectively. For example, an input file for a primary pile subjected to force 100kN will carry the name "100pr.inp". A typical input file created by this module for COM624P is given in Figure 7.3. Refer to Manual of COM624P for details of the input file.

2- call COM624P to calculate the deflection and internal forces of both primary and adjoint piles. The MATLAB function dos( ) is used to call the executable file of COM624P. For example, to call Com624P to calculate the file 100pr.inp and save output file as 100pr.out and the graphic file as 100pr.grh, the source code will be written as:

dos('C:\SA-program\subfunctions\Com624p.exe 100pr.inp 100pr.out 100pr.grh')

3- create a folder with the same name of the data file. This folder will contain all the output results for this data file. In this module, the input, output and graphic files will be stored in this folder.

4- check the criteria for allowable moment and deflection

The flow chart for the calculating module is shown Figure 7.4

```
Free Head Lateral Force F=050 L=18 Clay Thickness=3.6
        2      1      0
 300          2      1       0
        4      4      0
 18          200000000      0.000      0.000
        0      1
 1       1      0      10
 400          1.000000e-005      100.00000000
        0.0000      4.060000e-001      3.000000e-004      1.420000e-002
        1      1      0      3.600000      10000.000000
        2      4      3.600000      38.000000      16285.800000
        0.0000      7.500000
 3.600000      7.500000
 3.600000      10.000000
 38.000000      10.000000
        0.0000      18.000000      0      0.020000
 3.600000      18.000000      0      0.020000
 3.600000      0      33.000000      0
 38.000000      0      33.000000      0
 1
 1      51.000000      0.000000      0.000000
```

Figure 7.3 Sample of input file created for COM624P

266
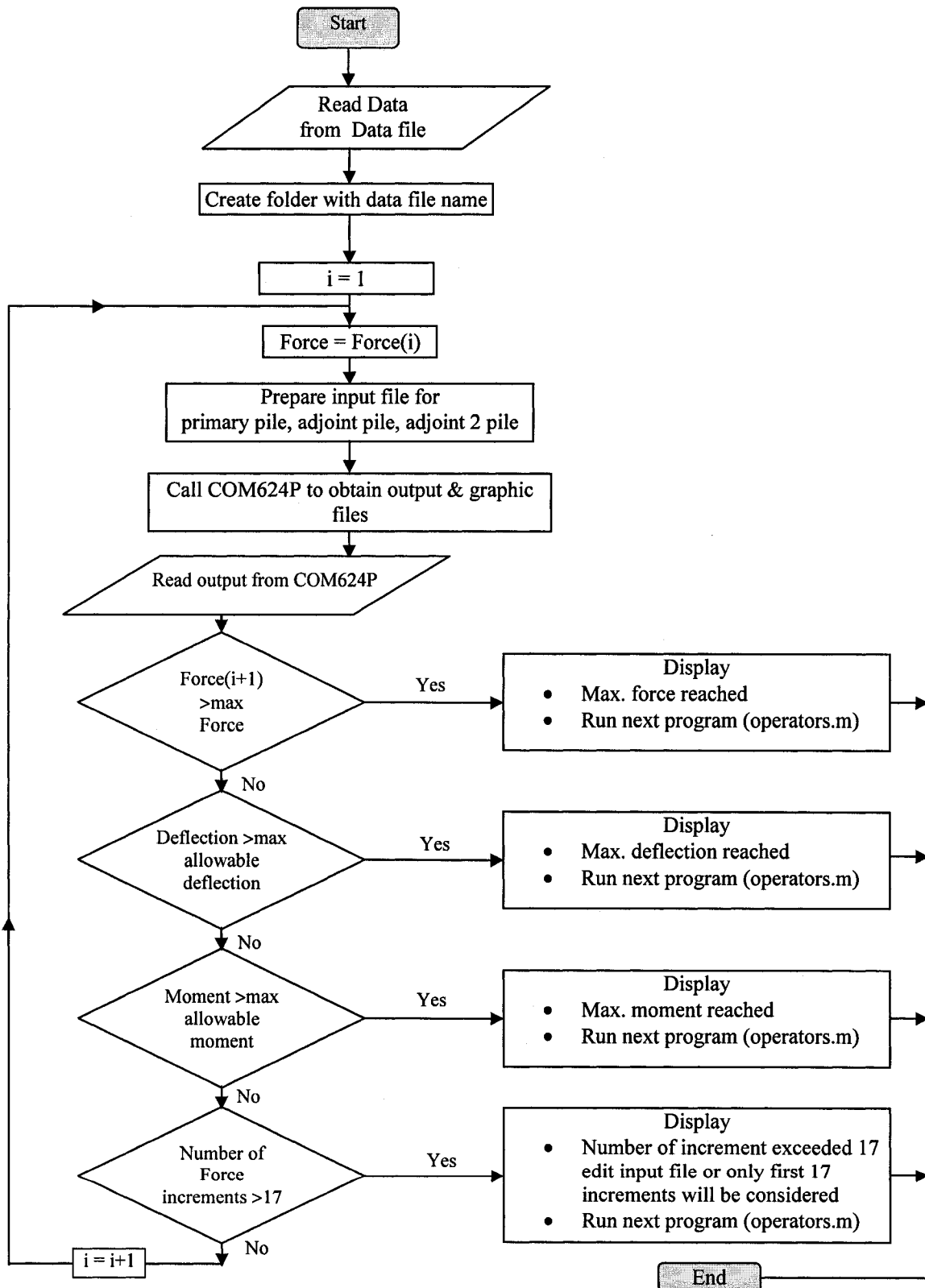
Figure 7.4 Flow chart for the calculating module of SA-program

267

7.4.3 Sensitivity operators results module

The source file for this module is "operators.m". This file uses two sub-functions, the developed source files for these two sub-functions are "readdata.m" and "plotfigure.m". The sensitivity operators module performs the following operations:

1- Reads the output data (deflection and moment) resulting from COM624P using the sub-function readdata( ). The sub-function reads the output data from the graphic file provided by COM624P instead of the output file provided by COM624P since it provides 4-effective-digits instead of 3 digits.

2- Calculates the values of sensitivity operators at the nodes along the pile length (number of nodes = number of pile increments +1) according to the different expressions for sensitivity operators (see Appendix A) that depend on the depth and deflection.

3- Plots the sensitivity operators for each parameter along the pile length as well as the moment, shear, deflection and soil reaction for primary and adjoint piles. This is performed by using the sub-function plotfig( ).

4- Saves the numerical values of the results in the output folder in a MATLAB format file named "operators.dat".

5- Saves the figures of the sensitivity operators in the output folder in a MATLAB figure format with extension .fig.

The flow chart for the data input module is shown in Figure 7.5.
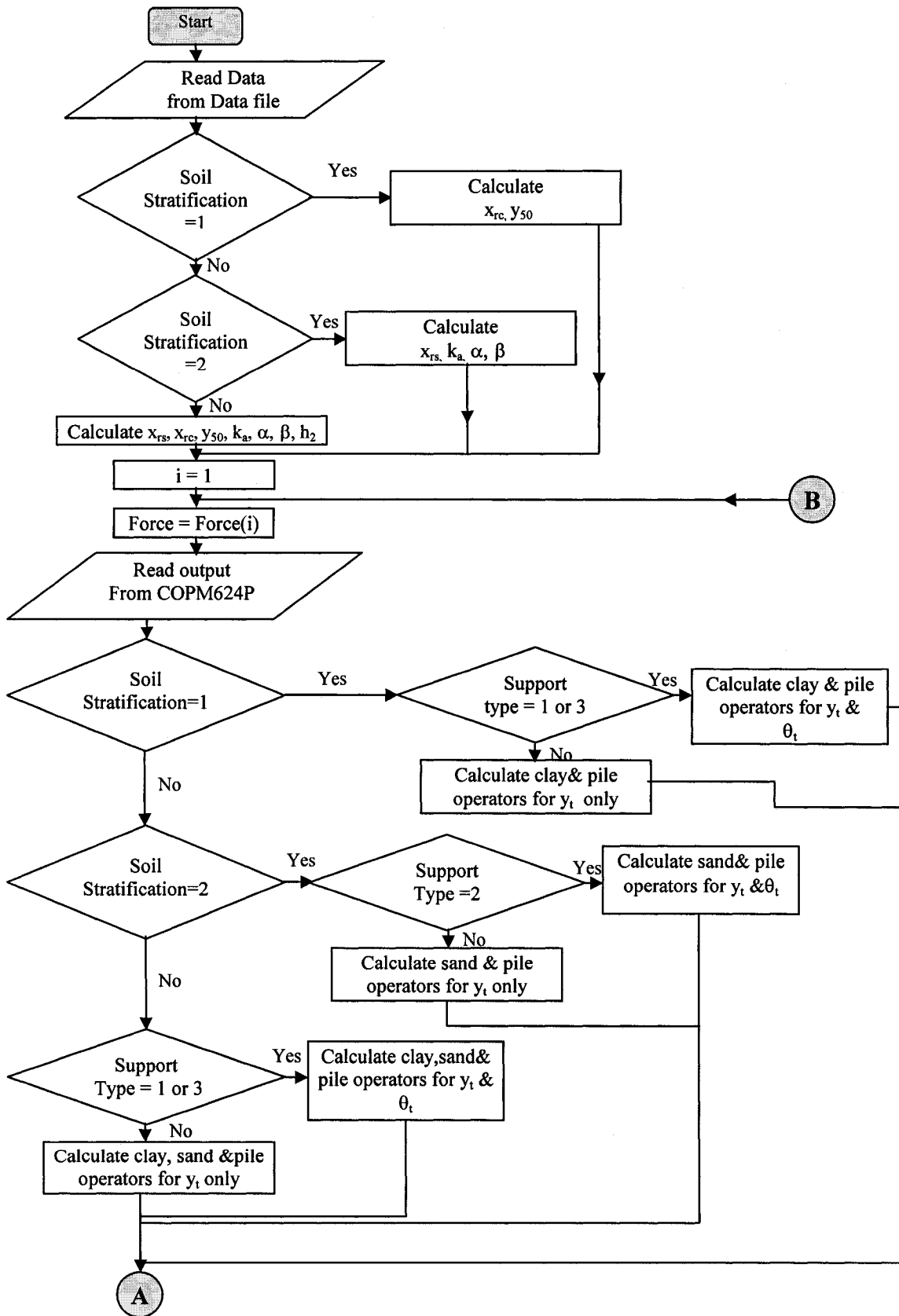
Figure 7.5 Flow chart for the sensitivity operators results module of SA-program

269
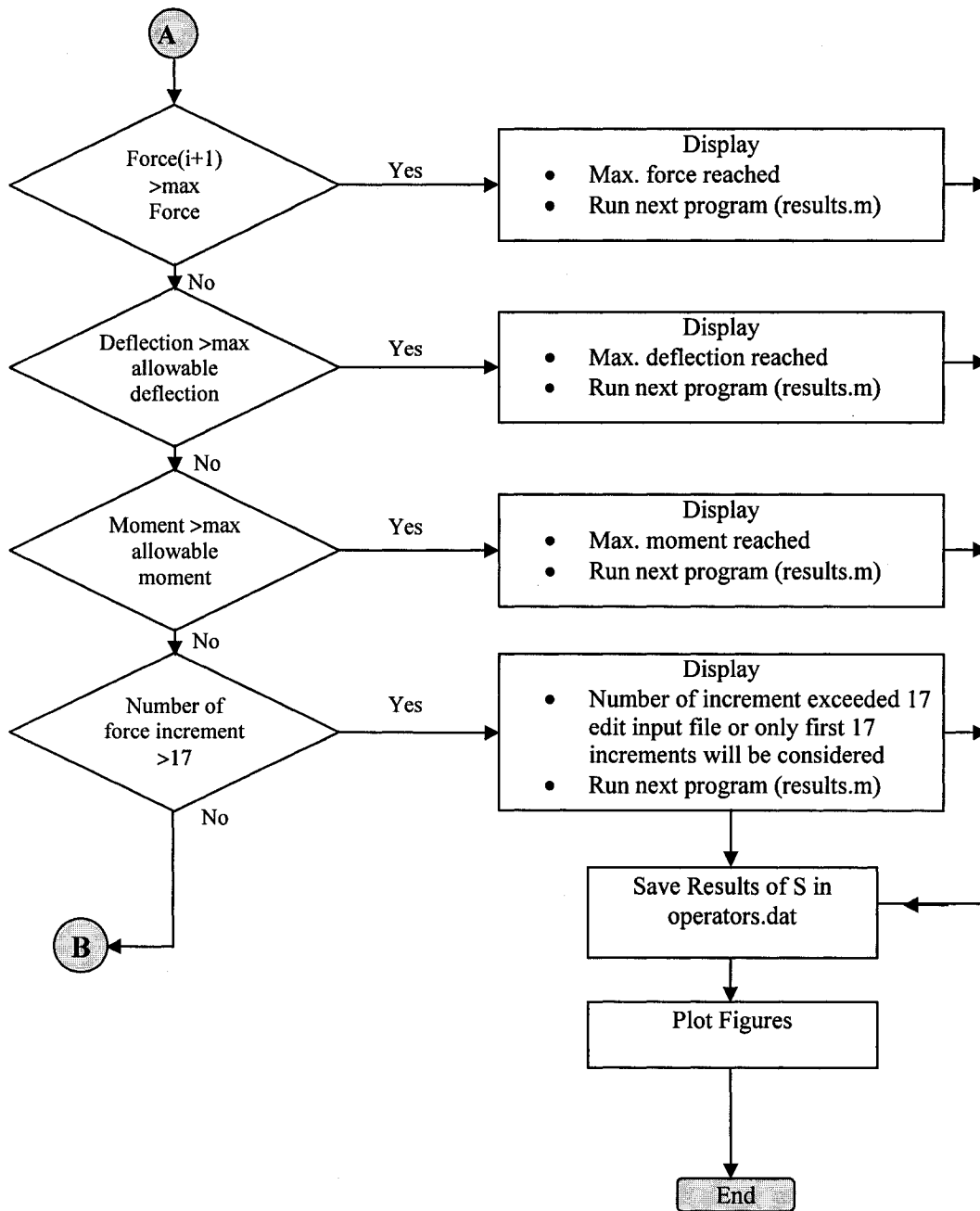
Figure 7.5 Flow chart for the sensitivity operators results module of SA-program (continued)

270

7.4.4 Sensitivity results module

The source file for this module is "results.m". This file uses three sub-functions, the developed source files for these sub-functions are "simpsonquad.m", "plotbar1.m" and "plotbar2.m". The sensitivity results module performs the following operations:

1- Loads the sensitivity operators numerical results calculated in the previous module using MATLAB function load( ).

2- Integrates the sensitivity operators along the pile length to obtain the sensitivity factors A using the developed sub-function simpsonquad( ).

3- Calculates *PCR*, *TF* and *GF* using the values of sensitivity factors A.

4- Saves these results in the MATLAB format file named "results.dat".

5- Plots these results in the form of bar charts using the developed sub-functions plotbar1( ) and plotbar2( ). The bar charts are saved in the MATLAB figure format with extension .fig.

The flow chart for this module is given in Figure 7.6.

7.5   VALIDATION OF RESULTS

The program was executed and the output from the program was numerically checked in a similar fashion to that used in the error analysis (Section 6.2.6). If the program is run with the same input used in the current study, the SA-program should provide results exactly similar to those given in Chapter 6 which were verified using the error analysis provided in Section 6.2.6.

271
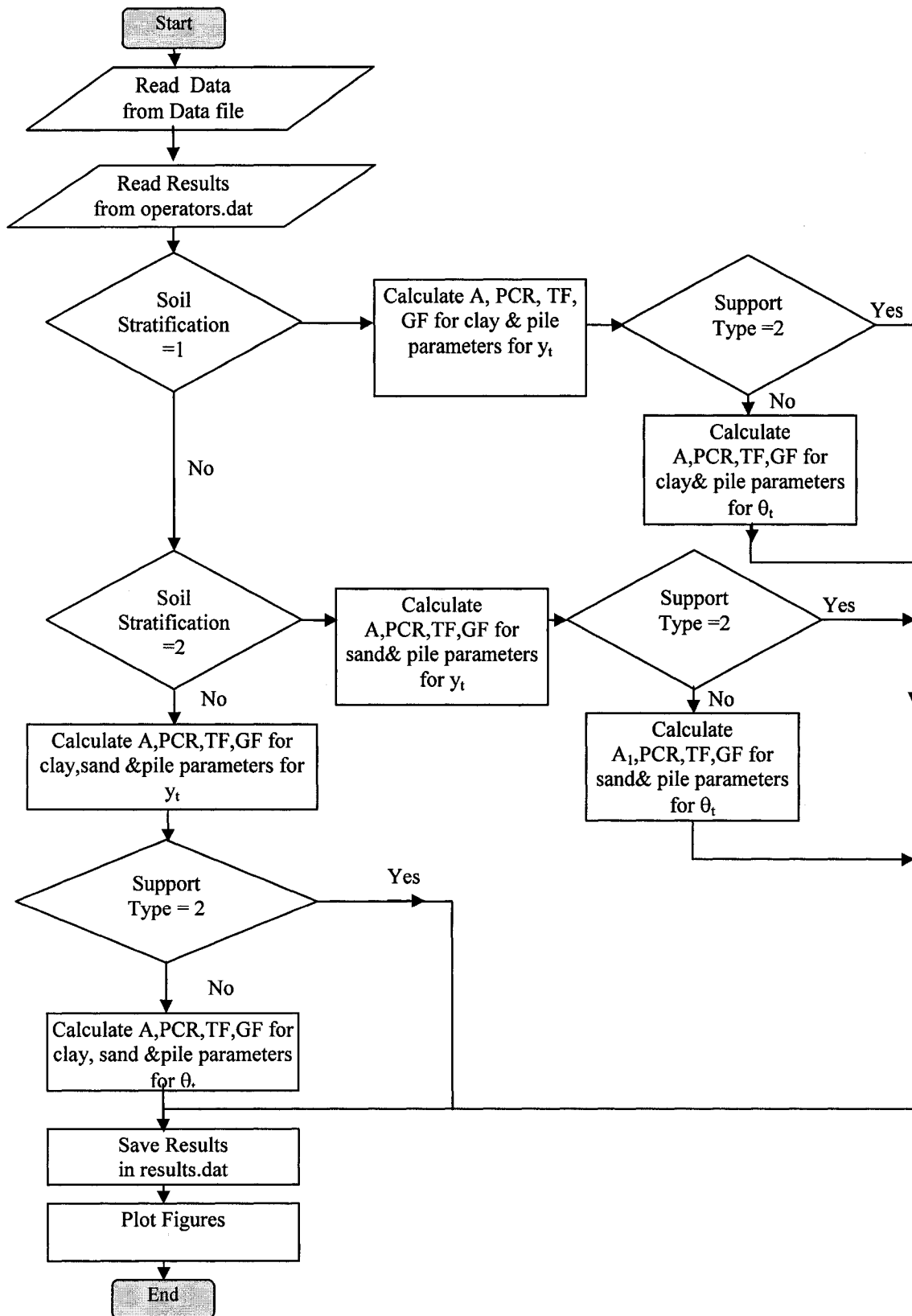
Figure 7.6 Flow chart for the sensitivity results module of SA-program

272

7.6   GUIDE FOR EXCUTION OF SA-PROGRAM

The purpose of this section is to provide detailed information to enable the user to employ the program conveniently and effectively. The SA-program folder provided in the attached CD contains four program files, one folder named 'subfunctions' and an example (consists of input data file "example.mat" and its output folder 'example'). The four program files are:

1. "inputdata.m"
2. "calculate.m"
3. "operators.m"
4. "results.m"

The four program files are to be run by the user through MATLAB in the sequence listed above. The 'subfunctions' folder contains the source files for the five sub-functions used by the four program files The five source files are: "plotfig.m", "readdata.m", "plotbar1.m", "plotbar2" and "simpsonquad.m". In addition, the file "Com624P.exe" is included in the 'subfunctions' folder (Note: Permission was taken from the US department of transportation to include the file "Com624P.exe" in the SA-program).The user doesn't need to open the folder 'subfunctions'.

The example provided for the user in the SA-program folder consists of a sample-data file "example.mat" and its output folder 'example'. The output folder 'example' contains all results for the laterally loaded free head 18 m long pile with 20% clay layer thickness studied in Chapter 6 (Section 6.2.5.1) obtained by running the SA-program. (Note: only 4 load increments are considered in the example instead of 5 increments in Chapter 6 because the allowable moment criteria is satisfied in the SA-program while it is neglected in Chapter 6)

7.6.1   Running the SA-program

The following points describe the step-by-step procedure to run the SA-program:

1. have the program MATLAB (version 7) installed on the computer

273

2. copy the SA-program folder provided in the attached CD with all its contents on the hard disk drive C such that the path of the program would be C:\SA-program

3. load MATLAB (version 7).

4. In MATLAB, choose the SA-program folder as the current directory. It is necessary to keep the current directory as C:\SA-program to be able to run any of the four main program files of SA-program.

5. Run the file "inputdata.m". (Note: to run any file, type the file name in the command window or right click on the file in the current directory and chose run or open the file using MATLAB editor (by double clicking on the file) and run the file through the editor).
   When the program is run:
   - Three statements are displayed: (1) purpose of the program; (2) SI units should be used and (3) no units should be written beside the values entered
   - The user has the option of changing the path of SA-program. If the program was saved in the default path mentioned above (C:\SA-program) it is sufficient to press "enter".
   - The user is asked to enter the name of the input data file where the input entered by the user will be saved. (note: all results obtained for this data will be stored in a folder having the same name)
   - The user is asked to enter the pile data as follows: a menu will appear containing the three choices for the pile's head boundary condition and type of loading. The chosen condition will be saved in the data file under the name 'SupportType' (1, 2 or 3). A number of command statements are displayed to ask the user to enter the pile length, stress-strain modulus, diameter, moment of inertia, and area.

274

- The user is asked to enter the soil data as follows: a menu will appear displaying the three choices for the soil stratification: the chosen stratification will be saved in the input file under the name 'SoilStratification'. Depending on the chosen soil stratification, the user is asked to enter the appropriate soil properties as follows:
  - If soil stratification = 1, the user enters the values of ε_{50}, c, and γ_c'.
  - If soil stratification = 2, the user enters the values of γ_s', k, and ϕ.
  - If soil stratification = 3, the user enters the values of clay thickness, c, γ_c', ε_{50}, k, γ_s' and ϕ
- The user is asked to enter the load increments of force or bending moment applied at the pile head as follows:
  - If SupportType = 1 or 2, the user is asked to enter the increments of lateral load and maximum lateral load to be reached. For example, an increment of 20 kN and a maximum load = 100 kN will produce sensitivity results of five loads on the same graph. These loads are 20, 40, 60, 80 and 100 kN. The load range should be between 10 and 999 kN.
  - If support style = 3, the program will ask for the increment of bending moment and maximum bending moment to be reached.
  - The number of load increments for any SupportType should not exceed 17, if they exceed 17 only the first 17 increments will be calculated and displayed on the obtained curves to avoid crowded unclear figures.
- The user is asked to enter:
  - the maximum allowable moment and maximum allowable deflection.
  - the number of pile length increments, default value is 300 (should not exceed 300).
  - the two computational control information for the COM624P program which are: (1)Numiterations: the maximum number of iterations

275

allowed (default value is 400). (2)Tolerance: the pile deflection tolerance indicating solution convergence (default value is 0.00001 m).

- The data entered is saved in a data file with extension .mat that could be viewed or edited anytime by the user as follows:

  a. The workspace is cleared by typing "clear" in the command window.

  b. The input file is loaded by typing: "load (*file name*)" in the command window.

  c. When the workspace is opened, the variable to be edited is double-clicked then edited.

  d. Save the workspace.

- The run of this file ends by displaying a statement indicating that the next file the user should run is "calculate.m"

6. Run the file "calculate.m".

- A statement is displayed asking the user to enter the name of the data file containing the input data entered in "inputdata.m".

- The program "calculate.m" will call COM624P to run automatically. Although the input file, output and graphic file names have been specified in the dos( ) function used to call COM624P the user will still be asked to enter them. It is sufficient to hit the enter key three times when asked about the input file name, output file name and graphic file name and the specified files will be used automatically.

- The run of this file ends by displaying statements indicating (1) criteria at which force increments stopped (i.e allowable deflection or moment or maximum force reached or number of force increments exceeded 17), (2) the next file the user should run is "operators.m"

- The input, output and graphic files will be saved in the output folder.

7. Run the file "operators.m".

- A statement is displayed asking the user to enter the name of the data file containing the input data.

276

- The program is executed and the run will end by displaying a statement indicating that the next file the user should run is "results.m" if the user wants to obtain the other four forms of sensitivity results

- The numerical results of the pile analysis (deflection, moment, shear and soil resistance) and the sensitivity operators S are saved in the output folder in a MATLAB format file named "operators.dat". The file "operators.dat" is viewed in an imported wizard by double clicking on the output folder in the current directory window then double clicking on "operators.dat" (after viewing the results choose cancel to close wizard.

- The results for sensitivity of lateral deflection y_t contain the number 1 in their name while the results for sensitivity of rotation θ_t contain the number 2. The following results will be displayed when opening "operators.dat"** and each result can be viewed by clicking on it:

```
x: vector containing the nodes along the depth x
yMatrix: Matrix containing the deflections y of primary pile
MMatrix Matrix containing the Moments M of primary pile
VMatrix: Matrix containing the shear of primary pile
pMatrix: Matrix containing the soil reaction p of primary pile
ya1Matrix: Matrix of deflections y of adjoint pile 1 (used for yt)
Ma1Matrix: Matrix of moments Ma of adjoint pile 1 (used for yt)
SEI1Matrix: Matrix of operators S for EI parameter (sensitivity of yt)
Sc1Matrix: Matrix of operators S for c parameter (sensitivity of yt)
Sgamac1Matrix: Matrix of operators S for γc parameter (sensitivity of yt)
Se501Matrix: Matrix of operators S for ε50 parameter (sensitivity of yt)
Sb1Matrix: Matrix of operators S for b parameter (sensitivity of yt)
Sk1Matrix: Matrix of operators S for k parameter (sensitivity of yt)
Sgamas1Matrix: Matrix of operators S for γs parameter (sensitivity of yt)
Sphi1Matrix: Matrix of operators S for φ parameter (sensitivity of yt)
ya2Matrix: Matrix of deflections y of adjoint pile 1 (used for θt)
Ma2Matrix: Matrix of moments Ma of adjoint pile 1 (used for θt)
SEI2Matrix: Matrix of operators S for EI parameter (sensitivity of θt)
Sc2Matrix: Matrix of operators S for c parameter (sensitivity of θt)
Sgamac2Matrix: Matrix of operators S for γc parameter (sensitivity of θt)
Se502Matrix: Matrix of operators S for ε50 parameter (sensitivity of θt)
Sb2Matrix: Matrix of operators S for b parameter (sensitivity of θt)
Sk2Matrix: Matrix of operators S for k parameter (sensitivity of θt)
Sgamas2Matrix: Matrix of operators S for γs parameter (sensitivity of θt)
Sphi2Matrix: Matrix of operators S for φ parameter (sensitivity of θt)
```

** Each column in a matrix represents the value along the pile length for each load increment. Accordingly, the number of columns for all matrices equal to the number of

277

force increments. For homogeneous soils, only clay or sand operators are displayed. Any of these outputs can be viewed by double clicking on the required matrix.

- The graphical presentations of the numerical results are saved directly in the output folder in a MATLAB figure format with extension .fig. The operators that end with 1 are for y_t while those that end with 2 are for θ_t. (for example: Sc1 will display a figure for sensitivity operators of parameter c at all levels of applied load for the sensitivity of lateral deflection y_t). They can be easily viewed by double clicking on the required result in the current directory.

8. Run the file results.m
   - A statement is displayed asking the user to enter the name of the data file containing the input data.
   - The program is executed and the obtained values of A, PCR, TF and GF are saved in the file "results.dat" under the output folder. Similar to the operators, the name of results ends with 1 for sensitivity of y_t while they end with 2 for sensitivity of θ_t. For example, Ac1 is a row vector with values of sensitivity factors A for the parameter c for sensitivity of y_t. Each column is the value of A at an increment of load.
   - The bar charts of each result will be given in a separate figure for each parameter in the form of a MATLAB figure file (having an extension ".fig"). These figures are saved in the output folder. The figure file can be opened by just clicking on the required figure.

7.6.2 Sample of input and output

The input is entered to the program through a user-friendly interface using the command window of MATLAB. A sample of the user interface for SA-program is shown in Figure 7.7. The figure shows the contents of the SA-program in the current directory window (four files used in running the program, 'subfunctions' folder, example.mat file and

278

'example' folder). The command window shows the input entered through command statements or menus.

Figures 7.8 to 7.10 show views of numerical and graphical results given in the output folder "example" attached in SA-program. A sample of the numerical output for the sensitivity operators obtained from "operators.dat" is given in Figure 7.8. In the figure, the import wizard shows the results saved in "operators.dat". The values of the Sc1matrix are displayed where each column shown in the wizard corresponds to a given load increment. For each column (load), the values of Sc1 along the pile length (at each node) are displayed.

A sample of the graphical form for sensitivity operator Sc1 is given in Figure 7.9. A view of the file "results.dat" containing sensitivity results A, PCR, TF and GF is shown in Figure. 7.10, where the values of Ac1 are displayed in the wizard. Figure 7.11 displays a sample of the bar chart for the sensitivity factor Ac1 .
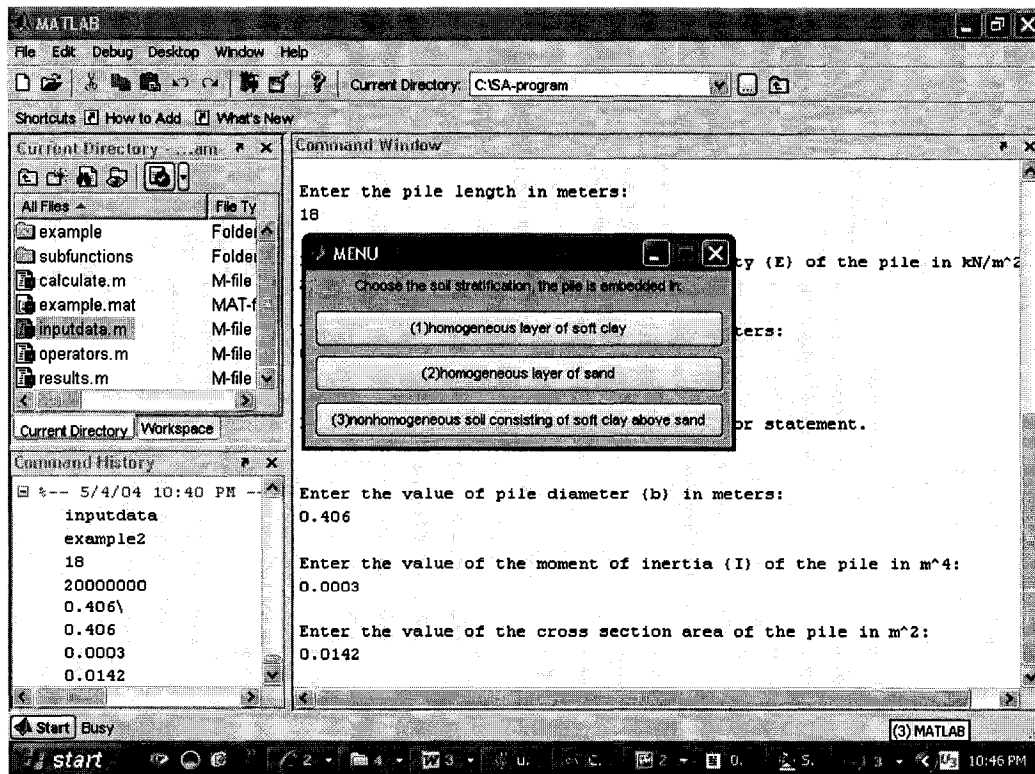
Figure 7.7 A sample of the user-interface of SA-program

279
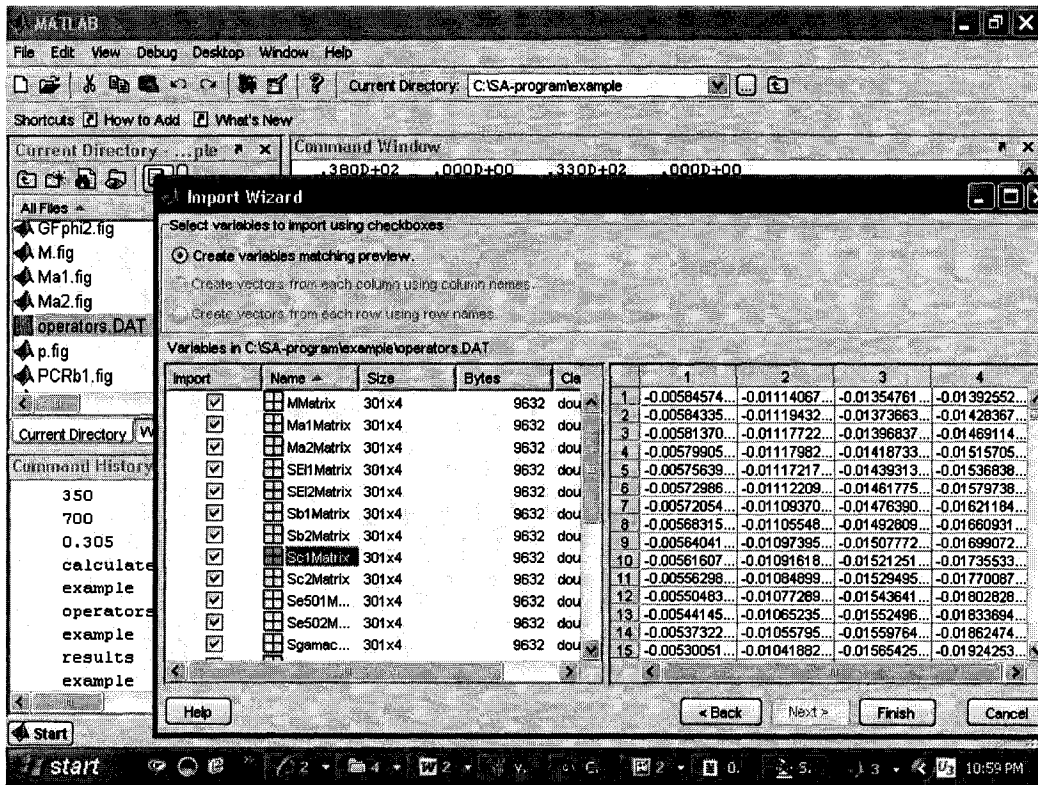
Figure 7.8 A view of the numerical output for sensitivity operators
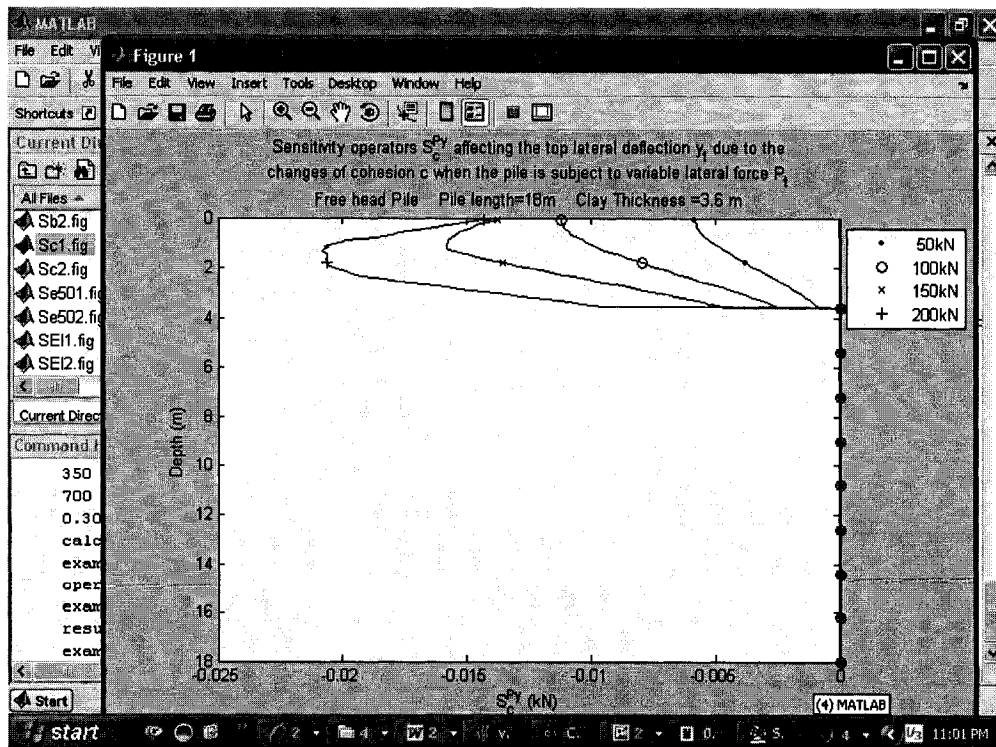
Figure 7.9 A view of the graphical output for sensitivity operators

280
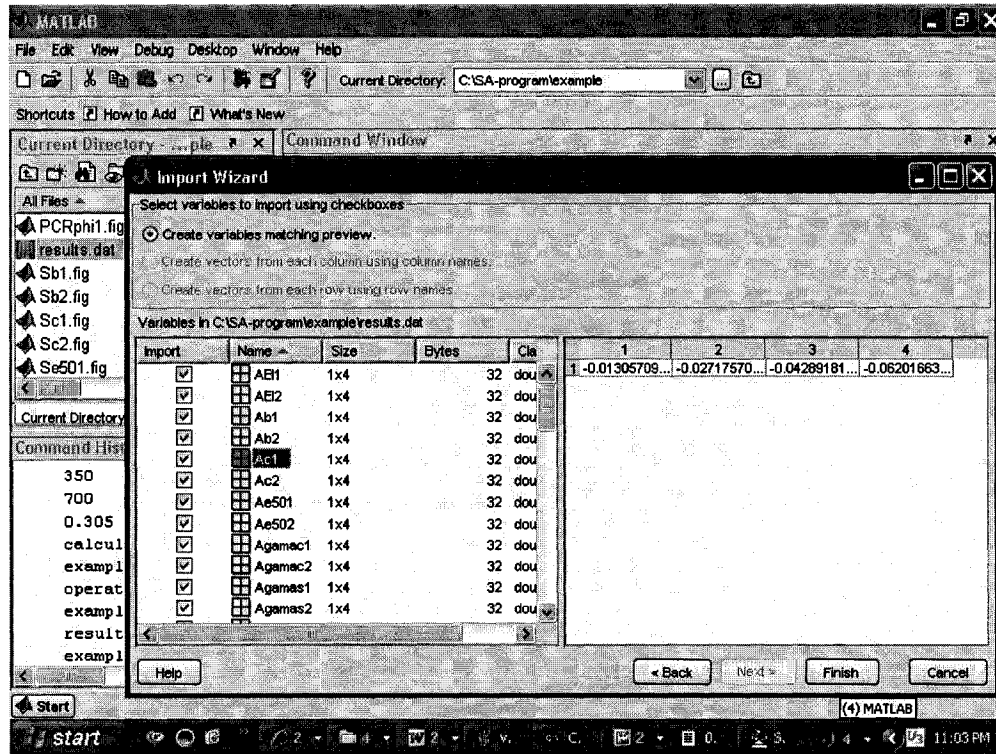
Figure 7.10 A view of the numerical output for sensitivity results in results.dat
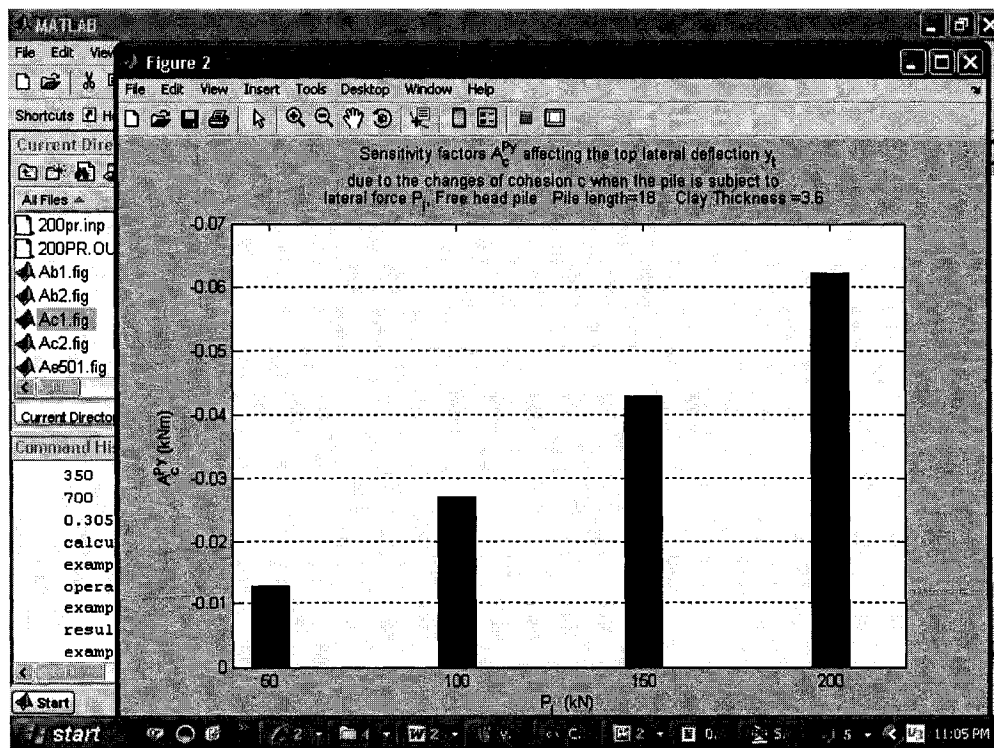
Figure 7.11 A view of the graphical output for the sensitivity factor Ac1

281

CHAPTER 8

CONCLUSIONS AND RECOMMENDATIONS

8.1   SUMMARY

8.1.1   Study topic

This dissertation focused on the application of the distributed parameter sensitivity analysis to laterally loaded piles embedded in non-homogeneous soil consisting of soft clay overlying sand subjected to cyclic loading. The sensitivities of the system responses to changes in the design parameters of the system were presented. The investigated system responses were the pile head deflection and the pile head rotation which are important serviceability measures. The design parameters considered in this research were the clay, sand and pile parameters defining the system. The study covered both single and pile groups.

8.1.2   Main parts of the study

The study consisted of the following three parts:

Part I: Theoretical formulation

The distributed parameter approach was used to develop the theoretical formulation of sensitivity analysis for both single and pile groups as given in Chapter 5. The formulation was developed using three different techniques of the adjoint method. The three techniques are the virtual work principle, the energy and load forms and the Lagrange multipliers method. The three techniques resulted in a similar final formulation. The pile was modeled as a one-dimensional beam on elastic foundation and the non-linear p-y

282

curves were used to model the soil behavior. The following five forms of sensitivity results were obtained from the formulation:

1. *Sensitivity operators S*, which are calculated and plotted along the pile length. These operators show where the change of the parameter has a maximum and minimum influence on the change of the system response under investigation.

2. *Sensitivity factors A*. When the sensitivity factor is multiplied by the percent change in the studied parameter (change along the entire pile length), it gives a numerical value of the change in the lateral top deflection or top rotation

3. *Percent change ratio PCR*. When *PCR* is multiplied by the percent change in the studied parameter (change along the entire pile length), it gives the percent change in the lateral top deflection or top rotation.

4. *Total relative sensitivity factor TF*, which gives the effect of the studied variable relative to all studied variables.

5. *Group relative sensitivity factor GF*, which gives the effect of the studied variable relative to the variables in its material group (clay, sand or pile).

Part II: Numerical investigations

Based on the developed theoretical formulation, the numerical investigations discussed in Chapter 6 were performed. The five forms of sensitivity results were calculated and graphically presented. The numerical sensitivity analysis was carried out for single piles by developing computer codes for sensitivity using MATLAB with the aid of the readily available computer code COM624P for single laterally loaded piles.

A total number of 297 cases were studied including free and fixed head piles subjected to lateral loads and bending moments with 11 cases of soil stratification ranging between 0% and 100% clay layer thickness. The following effects on the sensitivity results were investigated:

1. Effect of nonlinearity
2. Effect of non-homogeneity of the soil (thickness of overlying clay layer)

283

3. Effect of boundary condition (free and fixed head)
4. Effect of the load type (lateral load and bending moment)
5. Effect of studied pile response (lateral top deflection and top rotation)

Furthermore, the sensitivity numerical investigation for pile groups was conducted by developing computer codes using MATLAB with the aid of the FB-Pier program for pile groups. The investigation covered the variation of the lateral top deflection for long piles pinned and fixed to the pile cap subjected to lateral loads and bending moments. Different pile spacings and pile locations were considered, resulting in a total number of 396 cases investigated. The results for pile groups were compared to those for single piles. The following effects were studied:

1. Effect of pile location in the group
2. Effect of pile spacing on the sensitivity results

The sensitivity results for both single and pile groups were verified by checking the error resulting from the estimation of the lateral top deflection and rotation due to the variation in each parameter. This was achieved by the aid of COM624P and FB-Pier for single piles and pile groups, respectively.

Part III: Sensitivity program

A user friendly program for sensitivity analysis of laterally loaded single piles was developed using MATLAB with the aid of COM624P. The program is based on the developed theoretical formulation and offers the user the five forms of sensitivity results mentioned above in both a numerical and graphical form. The sensitivity of the lateral pile head deflection and rotation can be obtained for the following soil stratifications:

1. Homogeneous soft clay layer
2. Homogeneous sand layer
3. Non-homogeneous soil consisting of soft clay overlying sand.

284

8.2   CONCLUSIONS

The research conducted in this dissertation offers the answers to the following questions:

1. Where along the pile length is the maximum and minimum influence of each parameter on the system performance?
2. How is the effect of each parameter distributed along the pile length?
3. What is the quantitative value of the effect of change of each variable on each system performance measure?
4. What is the most effective parameter on the system performance?
5. What is the most effective clay parameter on the system performance?
6. What is the most effective sand parameter on the system performance?
7. What is the most effective pile parameter on the system performance?
8. If a certain parameter changes by a certain percent what will be the percent change in the lateral pile head deflection and the pile head rotation?

These answers are not only offered for the studied numerical cases but can also be obtained for any case of a single pile embedded in non-homogeneous soil consisting of soft clay overlying sand using the developed computer program.

In addition, the conducted numerical analysis presented in Chapter 6 reveals the following conclusions:

1. The sensitivity of lateral head deflection and rotation to changes in *EI* depends on the bending moments of piles while the sensitivity to changes in the other parameters depends on the pile deflection.

2. For a given design variable, the sensitivity is strongly dependent on the magnitude of the load applied at the pile head.

285

3. The values of the sensitivity operators $S_{\gamma s}$, S_ϕ, S_k, $S_{\gamma c}$, S_c, S_b and S_{EI} are negative implying that an increase in the parameter will cause a decrease in the studied performance measure. On the other hand, the value of $S_{\varepsilon 50}$ is positive as expected since it is a measure of deformability. However the following two exceptions were observed:

    a. The value of $S_{\varepsilon 50}$ was negative when the soft clay experienced the linear softening behavior (Stage 2), i.e. as ε_{50} increases, the pile lateral head deflection decreases.

    b. The values of S_b were negative in clay as expected but positive in sand. This implies that an increase in b in the sand layer increases the deflection.

4. The study of the *effect of the non-homogeneity* on the sensitivity results shows the following:

    a. For load-based comparison, the different non-homogeneous cases are compared at same load. In this case, the sensitivity of lateral head deflection to changes in the clay parameters (c, γ'_c and ε_{50}) and the pile parameter EI increases in general as the thickness of clay layer increases. On the other hand the sensitivity to changes in the sand parameters (k, γ'_s and ϕ) decreases as the clay thickness increases. For the pile diameter b, as the thickness of clay increases, the values of the sensitivity factor A_b changes its sign from positive to negative. This is because the effect of the negative values of the sensitivity factor S_b for clay dominates over the positive values in sand.

    b. For the deflection-based comparison, the different cases are compared at loads that give the same deflection at the pile head. In this case, the same conclusions for the load-based comparison apply. The only exception is that the sensitivity of the pile parameter EI decreases as the thickness of the clay increases.

286

5. The study of the *effect of the head constraint in case of free and fixed-head piles* on the sensitivity results shows that the head constraint affects mostly the results connected with the pile bending stiffness *EI*. In addition, for the load-based comparison, the fixed head pile lateral top deflection is, in general, less sensitive for variation of design variables, with the exception of design variables *EI* and ε_{50}.

6. The *effect of the load type (lateral load and bending moment)* on the sensitivity results of lateral head deflection is limited. The sensitivity of the piles subjected to moment is slightly lower than the sensitivity of piles subjected to lateral load, when both piles have the same deflection at the pile head.

7. The effect of the *system response under investigation* (y_t and θ_t) on sensitivity depends on the load type. When the investigated pile is subjected to M_t, the distribution of S_{EI} will be completely different in its pattern for the two responses lateral top deflection and top rotation. On the other hand, the distribution will be slightly different in its pattern for the two responses when the pile is subjected to P_t.

8. The study of the *effect of pile length* on the sensitivity results shows that the distribution of the sensitivity operators differs considerably in case of long and short piles, especially for the sand and pile parameters.

9. The comparison between *single pile and pile groups* that produce the same deflection at the pile head indicates a difference in the sensitivity. In general the sensitivity of single pile is less than the sensitivity of the pile in a group. This is always true for clay parameters. However, it is sometimes not the case for sand parameters and the pile diameter *b*.

10. The study of the *effect of the pile location* within a pile group on the sensitivity results indicates the following. The sensitivity due to changes in the clay

parameters for the piles in the second trailing row is less than that of the first trailing row and that of the first trailing row is less than that of the leading row. For the sand parameters and the pile diameter b, this order depends on the level of applied load. For the pile's bending stiffness, the sensitivities for the three piles are very close since the p-multipliers are not involved.

11. The study of the *effect of the pile spacing* on the sensitivity results shows the following. As the pile spacing increases, the sensitivity of lateral top deflection due to changes in the clay parameters increases. For sand parameters, the sensitivity can increase or decrease as the pile spacing increases. The pile spacing doesn't affect the sensitivity due to changes in EI.

12. The order of the eight parameters from most to least effective on the system response is not unique. It can differ by changing any of the following: the level of applied load, the percent of clay in the soil stratification, the pile's boundary condition, the type of applied load and the pile length. However, the order of parameters is the same for both responses y_t and θ_t for piles subjected to Pt.

13. The order of all parameters relative to their group is not influenced by the change in the boundary condition (deflection-based criteria only), the type of applied load, the type of response investigated, and the pile length (deflection-based criteria only).

14. The order of clay parameters is not influenced by the change in the percent of clay layer thickness in the soil stratification. However, this order differs with the change in the level of applied load. On the contrary, the order of the pile parameters is not affected by the level of applied load but affected by the percent of clay in the soil stratification. The order of the sand parameters is affected by the change in both the level of applied load and the soil stratification.

15. For all the studied cases, the cohesion c is the best clay parameter to change. The angle of friction is the best sand parameter if deflection is high enough to produce the second stage of the sand behavior. Furthermore, the pile's bending stiffness is the best pile parameter to change. The pile diameter b becomes slightly more effective than EI at high percentage of clay.

16. For pile groups, the pile location and spacing in the pile group do not affect the order of the eight parameters nor the order of the parameters with respect to its material group.

17. The error analysis used for verification of the obtained sensitivity results shows that the error in predicting y_t and θ_t for single piles and in predicting y_t for pile groups is less than 5% for a change in the parameter up to 15%. The error regarding EI was the maximum (39% error for 50% change in the value of EI).

8.3   RESEARCH APPLICATIONS

This research has significant applicability and importance in the following areas:

1. Design stage
   a. Assessment of the significance of each change of material properties and its effect on the maximum displacements of deep foundations.
   b. Understanding the system behavior and its relation to the system parameters.
   c. Development of rational basis for improvements of the soil-pile system performance.
2. Rehabilitation and aging process
   a. Quantification of the effects of degradation of the system's physical parameter during the aging process.
   b. Planning the maintenances, repairs, and replacement of the infrastructures.
3. Determining the best locations for placing monitoring devices along the pile.

289

4. Geotechnical field in general and the field of laterally loaded piles in particular, due to uncertainties in the soil parameters associated with the nature of the soil and the limited access to the pile system.

8.4 RECOMMENDATIONS FOR FUTURE RESEARCH

Future research in the same field of study could deal with the following points:

1. Conducting experimental laboratory and field studies regarding the sensitivity of laterally loaded piles to be compared to the numerical study.
2. Developing theoretical formulations and sensitivity analysis for non-homogeneous soils with different types of soil other than soft clay and sand.
3. Performing sensitivity analysis for soil stratifications, which consist of multiple layered soils.
4. Developing sensitivity analysis programs for pile groups.

8.5 SUMMARY OF CONTRIBUTIONS

The main contributions of the present study could be summarized in the following points:

1. The research presented the first theoretical formulation developed for sensitivity of laterally loaded piles embedded in non-homogeneous soil.
2. A comprehensive numerical analysis study was conducted to explore the effect of different conditions on the sensitivity results. The reported analysis will enhance the knowledge of pile designers in selecting optimal parameters and in better understanding of the system.
3. The research presented the first program developed for sensitivity of laterally loaded piles. The program offers five different forms of sensitivity results for piles embedded in homogeneous sand, homogeneous clay, non-homogeneous soil consisting of clay overlying sand.

290

REFERENCES

1. Abedin, Z.A. (2004), "Piles Embedded in p-y Sand Below Water Table Subjected to Static Loading-Sensitivity Investigations", *M. A. Sc. Thesis*, University of Windsor, Windsor, Ontario.

2. Adelman, H. M. and Haftka, R. T. (1986), "Sensitivity Analysis of Discrete Structural Systems", *AIAA Journal*, Vol. 24, No. 5, pp. 823-832.

3. Akhiezer, N. I. (1962), *The Calculus of Variations*, Blaisdell Publishing Company, New York.

4. Arnod, S., Battaglio, M. and Bellomo, N. (1996), "Nonlinear Models in Soils Consolidation Theory Parameter Sensitivity Analysis", *Mathematical and Computer Modelling*, Vol. 24, No. 3, pp. 11-20.

5. Arora, J. S. and Haug J. E. (1979), "Methods of Design Sensitivity Analysis in Structural Optimization", *AIAA Journal*, Vol. 17, No.9, pp. 970-974.

6. Arsoy, S. and Prakash, S. (2001), "Evaluating Group Action of Piles under Lateral Loads in Sand", *Proceedings of the Fifteenth International Conference on Soil Mechanics and Geotechnical Engineering*, Istanbul, 27-31 August, Vol. 2, pp. 835-837.

7. Aschenbrenner, R. (1967), "Three Dimensional Aanalysis of Pile Foundations", *Journal of the Structural Division, ASCE*, Vol. 93 (ST1,5097), pp. 201-219.

8. Ashour, M. and Norris, G. (2000), "Modeling Lateral Soil-Pile Response Based on Soil-Pile Interaction", *Journal of Geotechnical and Geoenvironmental Engineering, ASCE*, Vol.126, No. 5, pp. 420-428.

9. Ashour, M. and Norris, G. (2003), "Lateral Loaded Pile Response in Liquefiable Soil", *Journal of Geotechnical and Geoenvironmental Engineering*, Vol. 129, No. 5, May 2003, pp. 404-414.

10. Ashour, M., Norris, G. and Pilling P. (2002), "Strain Wedge Model Capability of Analyzing Behavior of Laterally Loaded Isolated Piles, Drilled Shafts, and Pile Groups" Journal of Bridge Engineering., Vol. 7, Issue 4, pp. 245-254.

11. Ashour, M., Norris, G. and Pilling, P. (1998b), "Lateral Loading of a Pile in Layered Soil Using the Strain Wedge Model," *Journal of Geotechnical and Geoenvironmental Engineering, ASCE*, Vol.124, No. 4, pp. 303-315.

12. Ashour, M., Pilling, P. and Norris, G. (2004), "Lateral Behavior of Pile Groups in Layered Soils", *Journal of Geotechnical and Geoenvironmental Engineering, ASCE*, Vol.130, No. 6, pp. 580-592.

13. Ashour, M., Pilling, P. and Norris, G. M. (1998a), "Updated Documentation of The Strain Wedge Model Program for Analyzing Laterally Loaded Piles and Pile Groups", *Proceedings of the 33rd Engineering Geology and Geotechnical Engineering Symposium*, Reno, Nevada, pp. 177-178.

14. Asplund, S. O. (1956), "Generalized Elastic Theory for Pile Groups," *International Association for Bridge and Structural Engineering*, Vol.16, pp. 1-22.

15. Awshika, K. and Reese, L. C. (1971), "Analysis of Foundations with Widely Spaced Batter Piles", *Proceedings of the International Symposium on the Engineering Properties of Sea-Floor Soils and their Geophysical Identification*, Seattle, Washington, 25 July 1971, University of Washington.

16. Banarjee, K. and Davies, T. G. (1980), "Analysis of Some Reported Case Histories of Laterally Loaded Pile Groups", *Proceedings of Conference on Numerical Methods in Offshore Piling*, Institute of Civil Engineers, England, pp. 101-108.

17. Bathe, K.J. (1996), *Finite Element Procedures*, Prentice-Hall, Englewood Cliffs, NJ.

18. Beatty, C. I. (1970), "Lateral Test on Pile Groups", *Foundation Facts*, Vol.6, No.1, pp.18–21.

19. Belegundu, A. D. (1985). "Lagrangian Approach to Design Sensitivity Analysis", *Journal of Engineering Mechanics Division*, ASCE, Vol. 111, pp. 680-695.

20. Belegundu, A. D. and Arora, J. S. (1985), "A Sensitivity Interpretation of Adjoint Variables in Optimal Design", *Computer Methods in applied Mechanics and Engineering*, Vol. 48, pp. 81-89.

21. Bhowmik, S. K. and Long, J. H. (1991), "An Analytical Investigation of The Behavior of Laterally Loaded Piles", *Proceedings of the Congress sponsored by Geotechnical Engineering Division of the American Society of Civil Engineering,* Geotechnical Special Publication, No. 27.

22. Bogard, D. and Matlock, H. (1983), "Procedures for Analysis of Laterally Loaded Pile Group in Soft Clay", *Proceedings of Conference on Geotechnical Practice in Offshore Engineering, ASCE,* New York, pp. 499-535.

23. Bransby, M. F. (1999), "Selection of p-y Curves for The Design of Single Laterally Loaded Piles", *International Journal for Numerical and Analytical Methods in Geomechanics,* Vol. 23, pp. 1909-1926.

24. Bristow, D. R. and Hawk, J. D. (1983), "Subsonic Panel Method for Designing Wing Surfaces from Pressure Distributions", *NASA* CR-3717.

25. Broms, B. B. (1964a), "Lateral Resistance of Piles in Cohesive Soils." *Journal of the Soil Mechanics and Foundations Division,* ASCE 90 (SM2), pp. 27-63.

26. Broms, B. B. (1964b), "Lateral Resistance of Piles in Cohesionless Soils." *Journal of the Soil Mechanics and Foundations Division,* ASCE 90 (SM3), pp. 123-156.

27. Broms, B. B. (1965), "Design of Laterally Loaded Piles." *Journal of the Soil Mechanics and Foundations Division,* ASCE 91 (SM3), pp. 77-99.

28. Brown, D. A. and Reese, L. C. (1985), "Behavior of A Large Scale Pile Group Subjected to Cyclic Lateral Loading", Report to the minerals Management Service, U.S. Dept. of Interior, Reston, VA; Dept. of Research, FHWA, Washington DC; and the U. S. Army Engineer Waterways Experiment Station, Vicksburg, Mississippi.

29. Brown, D. A. and Shie, C. F. (1991), "Modification of p-y Curves to Account for Group Effects of Laterally Loaded Piles", *Proceedings of the Geotechnical Engineering Congress 1991, ASCE,* Vol.1 (Geotechnical Special Publication 27), pp.479-490.

30. Brown, D. A., Morrison, C. and Reese, L. C. (1988), "Lateral Load Behavior of Pile Group in Sand", *Journal of Geotechnical Engineering,* ASCE, Vol. 114, no. 11, pp. 1261-1276.

31. Brown, D.A. and Shie, C.F. and Kumar, M (1989), "*p-y* Curves for Laterally Loaded Piles Derived from Three Dimensional Finite Element Model". *Proceedings of the III International Symposium, Numerical Models in Geomechanics (NUMOG III)*, Niagara Falls, Canada. New York: Elsevier Applied Science: pp. 683-690.

32. Budkowska, B. B., Sekulovic, D. and Saha, C.R. (1999b), "Sensitivity of Piles Due to Variable Thickness and Location of the Soil Layer. Part II. Numerical Investigation", *Archives of Civil Engineering*, Vol. 45, No. 3, pp. 427-441.

33. Budkowska, B. B. (1997a), "Sensitivity Analysis of Short Piles Subjected to Bending in Homogeneous Soil. Part I: Theoretical Formulation", *Computers and Geotechnics*, Vol. 21, No. 2, pp. 87-101.

34. Budkowska, B. B. (1997b), "Sensitivity Analysis of Short Piles Subjected to Bending in Homogeneous Soil. Part II: Numerical Formulation", *Computers and Geotechnics*, Vol. 21, No. 2, pp. 103-119.

35. Budkowska, B. B. (1998a), "Investigation of the Effect of Variable Length of Piles during Bending- Sensitivity Analysis", *Archives of Civil Engineering*, Vol. 44, No. 3, pp. 315-337.

36. Budkowska, B. B. (1998b), "Application of Sensitivity Theory to Analysis of Piles Subject to Bending and penetrating a Homogeneous Soil", *Archives of Civil Engineering*, Vol. 44, No. 3, pp. 299-314.

37. Budkowska, B. B. (1999), "Effect of Variable Location of Soil Layers on the Behavior of Laterally Loaded Piles", *Computers and Geotechnics*, Vol.25, pp.25-43.

38. Budkowska, B. B. and Cean, A. E. (1995), "Sensitivity Analysis of Short Piles Subject to Bending Moment", *Proceedings of the 14th Australian Conference on the*

Mechanics of Structures and Materials, University of Tasmania , Hobart, 11-13 December 1995, pp.357-362.

39. Budkowska, B. B. and Cean, A. E. (1996), "Comparative Sensitivity Analysis of Laterally Loaded Piles", *Proceedings of the 6th International Offshore and Polar Engineering Conference*, Los Angeles, USA, May 26-31,Vol. 1, pp.499-505.

40. Budkowska, B. B. and Priyanto, D. (2002a), "Comparative Analysis of Lateral Deformations of Short and Long Piles Embedded in Nonlinear Soft Clay-Sensitivity Analysis", *International Symposium on Lowland Technology*, Saga, Japan

41. Budkowska, B. B. and Priyanto, D. (2002b), "Investigation of Pile Group in Soft Clay Subjected to Horizontal Loading- Sensitivity Analysis", *Proceedings of the 8th International Symposium on Numerical Models in Geomechanics-NUMOG VII*, Rome, Italy, pp. 481-486.

42. Budkowska, B. B. and Suwarno, D. (2002a), "Distributed Parameter Sensitivity Analysis of Nonlinear Behaviour of Laterally Loaded Piles", *Proceedings of 8th International Symposium on Numerical Models in Geotechnics-NUMOG*. Vol. II, Rome, Italy.

43. Budkowska, B. B. and Suwarno, D. (2002b), "Assessment of Horizontal Loading of Pile Group Penetrating Stiff Clay Below the Water Table – Sensitivity Analysis", *International Symposium on Lowland Technology*, Saga, Japan.

44. Budkowska, B. B. and Szymczak, C. (1992a), "Application of Reanalysis Method of Laterally Loaded Piles", *Numerical Models in Geomachanics, Balkema*, pp. 817-825.

45. Budkowska, B. B. and Szymczak, C. (1992b), "Sensitivity Analysis of Laterally Loaded Piles by Means of Adjoint Method", *Computers and Geotechnics, An International Journal*, Vol. 13, pp. 37-49

46. Budkowska, B. B. and Szymczak, C. (1993a), "Sensitivity Analysis of Axially Loaded Piles", *Architectural Civil Engineering*, Vol. XXXIX, No. 1, pp. 93-105.

47. Budkowska, B. B. and Szymczak, C. (1993b), "Sensitivity Analysis of Piles Undergoing Torsion", *Computers and Structure*, Vol. 48, No. 5, pp. 827-834.

48. Budkowska, B. B. and Szymczak, C. (1994a), "Effect of Varying Length of Pile Undergoing Torsion. Undergoing Torsion", *Computers and Structure*, Vol. 48, No. 5, pp. 827-834.

49. Budkowska, B. B. and Szymczak, C. (1994b), "Some Problems of Sensitivity Analysis of Axially Loaded Piles", *Proceedings of the 4th International Offshore and Polar Engineering Conference*, Part 1, pp. 554-558.

50. Budkowska, B. B. and Szymczak, C. (1995a), "On the First Variation of Exremum Values of Displacements and Internal Forces of Laterally Loaded Piles", *Computers and Structure*, Vol. 57, No. 6, pp. 303-307.

51. Budkowska, B. B. and Szymczak, C. (1995b), "The Analysis of an Axially Loaded Piles with Account for Its Varying Length", *Computers and Structure*, Vol. 54, No. 6, pp. 1149-1154.

52. Budkowska, B. B. and Szymczak, C. (1996), "Partially Embedded Piles Subjected to Critical Buckling Load- Sensitivity Analysis", *Computers and Structure*, Vol. 61, No. 1, pp. 193-196.

53. Budkowska, B. B. and Szymczak, C. (1997), "Initial Post-Buckling Behaviour of Piles Partially Embedded in Soil", *Computers and Structure*, Vol. 62, No. 5, pp. 831-835.

54. Budkowska, B. B. Sekulovic, D. and Saha, C.R. (1999a), "Sensitivity of Piles Due to Variable Thickness and Location of the Soil Layer. Part I. Theoretical formulation", *Archives of Civil Engineering*, 45(3), pp. 553-570.

55. Burg, C. O. E. (2002), "Groundwater Parameter Estimation via the Unsteady Adjoint Variable Formulation of Discrete Sensitivity Analysis", *Communications in Numerical Methods in Engineering*, Vol. 18, pp. 391–398.

56. Canadian Institute of Steel Construction (2000), *Hollow Structural Sections to ASTM A500 grade C*, Willowdale, Ontario.

57. Cao, Y., Li, S. and Petzold, L. (2002), "Adjoint Sensitivity Analysis for Differential-Algebraic Equations: Algorithms and Software", *Journal of Computational and Applied Mathematics*, Vol.149, pp. 171–191.

58. Cardoso, J. B. and Arora, J. S. (1988), "Variational Method for Design Sensitivity Analysis in Nonlinear Structural Mechanics", *AIAA Journal*, Vol. 26, pp.595-603.

59. Choi, K. K. (1985), "Shape Design Sensitivity Analysis of Displacement and Stress Constraints", *Journal of Structural Mechanics* Vol. 13, No. 1, pp.27-41.

60. Choi, K. K. and Haug, E. J. (1983), "Shape Design Sensitivity Analysis of Elastic Structures", *Journal of Structural Mechanics,* Vol. 11, pp. 231-269.

61. Choi, K. K. and Santos, J. L. T. (1987), "Design Sensitivity Analysis of Non-Linear Structural Systems Part I: Theory", *International Journal for numerical methods in Engineering*, Vol. 24, pp. 2039-2055.

62. Coduto, D.P. (1994), *Foundation Design, Principles and Practice.* Prentice Hall Inc., Englewood Cliffs.

63. Cook, R. D., Malkus, D. S., Plesha, M. E. and Witt, R. J. (2002), *Concepts and Applications of Finite Element Analysis*, Fourth Edition, John Wiley and Sons, NY.

64. Cox, W. R., Dixon, D. A. and Murphy, B. S. (1984), "Lateral-loaded Tests on 25.4-mm Diameter Piles in Very Soft Clay in Side-by-side and in-line Groups", Laterally Loaded Deep Foundations: Analysis and Performance, ASTM, STP 835, pp.122-139.

65. Cox, W. R., Reese, L. C. and Grubbs, B. R. (1974), "Field Testing of Laterally Loaded Piles in Sand", *Proceedings of the Sixth Annual Offshore Technology Conference*, Houston, Texas, paper 2079.

66. Craig, R. F. (1978), *Soil Mechanics*, Van Nostrand Reinhold Company, Ltd., Berkshire, England.

67. Das, B. M. (1999), *Principles of Foundation Engineering,* Fourth Edition, PWS-Kent Publishing Company, Boston.

68. Davisson, M. T. (1970), "Lateral Load Capacity of Piles", Hwy Res. No. 333. Transportation Research Board, National Research Council, Washington, D.C., pp.104-112.

69. Dems, K. and Mroz, Z. (1983), "Variational Approach by Means of Adjoint Systems to Structural Optimization and Sensitivity Analysis-I: Variation of Material Parameters within Fixed Domain", *International Journal of Solids and Structures*, Vol. 19, No. 8, pp. 677-692.

70. Dems, K. and Mroz, Z. (1985), "Variational Approach to First-and Second-Order Sensitvity Analysis of Elastic Structures", *International Journal for Numerical Methods in Engineering*, Vol. 21, pp. 637-661.

71. Drewko, J. and T. D. Hien, T. D. (2005), "First- and Second-Order Sensitivities of Beams with Respect to Cross-Sectional Cracks", *Archive of Applied Mechanics*, Vol. 74, pp. 309-324.

72. Duncan, J. M., Evans, L. T. Jr. and Ooi, P. S. K. (1994), "Lateral Load Analysis of Single Piles and Drilled Shafts", *Journal of Geotechnical Engineering*, ASCE, Vol. 120, No. 6, Pp. 1018-1033..

73. Dunnavant, T. W. and O'Neill, M. w. (1986), "Evaluation of Design-oriented Methods for Analysis of Vertical Pile Groups Subjected to Lateral Loads", *Proceedings of the 3rd International Conference on Numerical Methods in Offshore Pilling,* Nantes, France, Technip., Paris, France, pp. 303-316.

74. Dunnavant, T.W. and O'Neill, M.W. (1989), "Experimental *p-y* Model for Submerged Stiff Clay." *Journal of Geotechnical Engineering*, Vol. 115, No. 1, pp. 95-114.

75. Dwyer, H. A., and Peterson, T. (1980), "A Study of Turbulent Flow with Sensitivity Analysis", *AIAA* Paper 80-1397.

76. Dwyer, H. A., and Peterson, T. and Brewer, J. (1976), "Sensitivity Analysis Applied to Boundary Layer Flow", *Proceedings of the 5th International Conference on Numerical Methods in Fluid Dynamics*, Springer-Verlag, NY.

77. El Naggar, M. H. and Novak, M. (1996), "Nonlinear Analyses for Dynamic Lateral Pile Response", *Soil Dynamics and Earthquake Engineering* 15, pp. 233-244.

78. Eringen, A. C. (1962). *Nonlinear Theory of Continuous Media.* Mcgraw-Hill, New York.

79. Evans, L.T. and Duncan, J.M. (1982), "Simplified Analysis of Laterally Loaded Piles." *Report No. UCB/GT 82-04*, Berkeley: Department of Civil Engineering, University of California.

80. FB-Pier, Version 3.01, Florida Bridge Software Institute, copyright 2000, University of Florida, http://bsi-web.ce.ufl.edu

81. Fellenius, B. H. (1999), *Basics of Foundation Design*, 2nd Edition, Bitech Publishers, Richmond, British Coumbia.

82. Focht, J. A. and Koch, K. J. (1973), "Rational Analysis of the Lateral Performance of Offshore Pile Groups", *Proceedings of the 5th Offshore Technology Conference*, Dallas, Texas, pp. 701-708.

83. Francis, A. J. (1964), "Analysis of Pile Groups with Flexural Resistance", *Journal of Soil Mechanics and Foundations Division, ASCE*, No. 3887, pp.1-32.

84. Frank, P. M. (1978), *Introduction to Sensitivity Theory*, Academic Press, Orlando, FL.

85. Gabr, M. A., Lunne, T. and Powel, J. J. (1994), "p-y Analysis of Laterally Loaded Piles in Clay Using DMT", *Journal of Geotechnical Engineering*, Vol. 120, No. 5, pp. 816-837.

86. Gadala, M. S., Dokainish, M. A., and Oravas, AE. G. (1984) "Formulation Methods of Geometric and Material Nonlinear Problems", *International Journal for numerical methods in Engineering*, Vol. 20, pp. 887-914.

87. Gandhi, S. R. and Selvam, S. (1997), "Group Effect on Driven Piles under Lateral Load", *Journal of Geotechnical and Geoenvironmental Engineering, ASCE*, Vol.123, No. 8, pp. 702-709.

88. Gelfand, I. M. and Fomin, S. V. (1964) *Calculus of Variations*, Prentice Hall, Englewood Cliffs, New Jersey.

89. Georgiadis, M. (1983), "Development of p-y Curves For Layered Soils," *Proceedings of the Geotechnical Practice in Offshore Engineering, ASCE*, pp. 536-545.

90. Ghosh, R., Chakraborty, S. and Bhattacharyya, B. (2001), "Stochastic Sensitivity Analysis of Structures Using First-order Perturbation", *Meccanica*, Vol. 36, pp. 291–296, 2001.

91. Ghostgum Software Pty Ltd., GSview program, Version 4.6, Copyright 1993-2002, http://www.ghostgum.com.au

92. Guo, Wei Dong and Lee, F.H. (2001), "Load Transfer Approach for Laterally Loaded Piles", *International Journal for Numerical and Analytical Methods in Geomechanics,* Vol. 25, pp. 1101-1129.

93. Hafez, D. H. and Budkowska, B. B. (2004), "Sensitivity Investigations of Fixed Head Pile Penetrating Non-homogenous Soil of Layered Type Below Water Table Subjected to Horizontal Forces of Cyclic Type", *Proceedings of the International symposium on Lowland Technology ISLT*, Bangkok, Thailand, September 1-3, pp. 159-164.

94. Hafez, D. H. and Budkowska, B. B. (2005a), "On Distributed Parameter Sensitivity Performance of Laterally Loaded Long Pile Embedded in Nonhomogeneous p-y Soil Subjected to Cyclic Loading", *Proceedings of the fifth International Geotechnical Engineering Conference*, Cairo, January 11-13, pp. 565-585.

95. Hafez, D. H. and Budkowska, B. B. (2005b), "Nonlinear Sensitivity Performance of Long Piles Embedded in Non-homogenous p-y Soil Subjected to Horizontal Cyclic Forces – Effect of Boundary Conditions", *Proceedings of the 16th ICSMGE 2005*, Osaka, Japan, September 12-16, pp.2119-2124.

96. Hafez, D. H. and Budkowska, B. B. (2006a), "Deformation of Laterally Loaded Fixed Head Short Pile Subjected To Variable Lateral Force Embedded in Non-Homogeneous p-y Soils of Layered Type – Sensitivity Analysis of Distributed Parameters", *Proceedings of the Civil Engineering Conference: Toward Sustainable Civil Engineering Practice*, Surabaya, August 25-26.

97. Hafez, D. H. and Budkowska, B. B. (2006b), "Effect of Thickness of Overlaying Clay Layer of Lowland Region on Sensitivity of Lateral Deflection of Long Piles

Embedded in Non-homogeneous Soil. Part I: Theoretical Formulation", *Lowland Technology International Journal*, June 2006, Vol. 8, No.1, pp.27-36

98. Hafez, D. H. and Budkowska, B. B. (2006c), "Effect of Thickness of Overlaying Clay Layer of Lowland Region on Sensitivity of Lateral Deflection of Long Piles Embedded In Non-Homogeneous Soil. Part IIA: Numerical Study of Sand Parameters", *Lowland Technology International Journal*, December 2006, Vol. 8, No.2, pp.9-20.

99. Hafez, D. H. and Budkowska, B. B. (2006d), "Effect of Thickness of Overlaying Clay Layer of Lowland Region on Sensitivity of Lateral Deflection of Long Piles Embedded In Non-Homogeneous Soil. Part IIB: Numerical Study of Clay and Pile Parameters", *Lowland Technology International Journal*, December 2006, Vol. 8, No.2, pp.21-31.

100. Hafez, D. H. and Budkowska, B. B. (2007a), "Performance of Fixed Head Pile Group Embedded in Non-Homogeneous Soil Subjected To Lateral Cyclic Loading – Distributed Parameter Sensitivity Analysis," *Proceedings of the seventeenth (2007) International Offshore and Polar Engineering Conference*, Lisbon, July1-7, pp. 1388-1395.

101. Hafez, D. H. and Budkowska, B. B. (2007b), "Comparative Sensitivity Analysis of Laterally Loaded Piles Embedded in Non-Homogeneous Soil", *Proceedings of the 60th Canadian Geotechnical Conference and 8th Joint CGS/IAH-CNC Groundwater Conference*, Ottawa, October 21-25, 2007 (accepted).

102. Haftka, R. T. (1982), "Second-Order Sensitivity Derivatives in Structural Analysis", *AIAA Journal*, Vol. 20, pp. 1765-1766.

103. Haftka, R. T. and Mroz, Z. (1986), "First- and Second- Order Sensitivity Analysis of linear and nonlinear Structures", *AIAA Journal*, Vol. 24, pp.1187-1192.

104. Hariharan, M. and Kumarasamy, K. (1982), "Analysis of Pile Groups Subjected to Lateral Loads", *Proceedings of the 3rd International Conference on Behavior of Offshore Structures*, 2, Hemisphere Publishing Corp., Washington, D. C., pp. 383-390.

105. Haug, E. J. (1981), "Second-Order Design Sensitivity Analysis of Structural Systems", *AIAA Journal*, Vol. 19, pp.1087-1088.

106. Haug, E. J. and Arora, J. S. (1978), "Design Sensitivity Analysis of Elastic Mechanical Systems", *Computer Methods in Applied Mechanics and Engineering*, Vol. 15, pp. 35-62.

107. Haug, E. J. and Ehle, P. E. (1982), "Second-Order Design Sensitivity Analysis of Mechanical System Dynamics", *International Journal for Numerical Methods in Engineering*, Vol. 18, pp. 1699-1717.

108. Haug, E. J. and Rousselet, B. (1980), "Design Sensitivity Aanalysis in Structural Mechanics, I. Static Response Variation", *Journal of Structural Mechanics*, Vol. 8, pp. 17-41.

109. Haug, J. E. and Arora, J. S. (1979), *Applied Optimal Design*, Wiley, New York.

110. Haug, J. E., Choi, K. K. and Komkov, V. (1986), *Design Sensitivity Analysis of Structural Systems*, Academic Press, New York.

111. Haung, A., Hseuh, C., O'Neill, M. W., Chern, S. and Chen, C. (2001), "Effects of Construction on Laterally Loaded Pile Groups", *Journal of Geotechnical and Geoenvironmental Engineering, ASCE*, Vol.127, No. 5, pp. 385-397.

112. Hetenyi, M. (1946), *Beams on Elastic Foundation.* Ann Arbor: The University of Michigan Press.

113. Horsnell, M. R., Aldridge, T. R. and Erbrich, C. (19900, "Lateral Group Behavior of Piles in Offshore Soil Conditions", *Proceedings of the 22nd Offshore Technology Conference*, pp. 417-424.

114. Hrennikoff, A. (1950), "Analysis of Pile Foundation with Batter Piles", *Transactions, ASCE,* 115(2401).

115. Hsiung, Yun-mei and Chen, Ya-ling (1997), "Simplified Method for Analyzing Laterally Loaded Single Piles in Clays", *Journal of Geotechnical and Geoenvironmental Engineering*, Vol. 123, No 11, pp. 1018-1029.

116. Hwang, J. T., Dougherty, E. P., Rabitz, S. and Rabitz, H. (1978), "The Green's Function, Method of Sensitivity Analysis in Chemical Kinetics", *Journal of Chemical Physics,* Vol. 69, pp. 5180-5191.

117. Ilyas, T., Leung, C. F., Chow, Y. K. and Budi, S. S. (2004), " Centrifuge Model Study of Laterally Loaded Pile Groups in Clay", *Journal of Geotechnical and Geoenvironmental Engineering, ASCE,* Vol.130, No. 3, pp. 274-283.

118. Irwin, C. L. and O'Brien, T. J. (1982), "Sensitivity Analysis of Thermodynamic Calculations", *U.S. Dept. of Energy Rept.* DOE/METC/82-53.

119. Jawed, A. H. and Morris, A. J. (1984), "Approximate Higher-Order Sensitivities in Structural Design", *Engineering Optimization,* Vol. 7, No. 2, pp. 121-142.

120. Kaminski, M. (2001), "Material Sensitivity Analysis in Homogenization of Linear Elastic Composites" *Archives of Applied Mechanics,* Vol. 71, pp. 679-694.

121. Karol, R. H. (1960), *Soils and Soil Engineering,* Prentice Hall, Englewood Cliffs.

122. Kim, B. T., Kim, N., Lee, W. J. and Kim, Y. S. (2004), "Experimental Load-Transfer Curves of Laterally Loaded Piles in Nak-Dong River Sand", *Journal of Geotechnical and Geoenvironmental Engineering,* Vol. 130, No 4, pp. 416 – 425.

123. Kim, J. B. and Singh, L. P. (1974), "Effect of Pile Cap-Soil Interaction on Lateral Capacity of Pile Groups", *MS Thesis,* Department of Civil Engineering, Bucknell University, Lewisburg, Pa.

124. Kleiber, M., Antunez., H., Hien, T. D and Kowalczyk, P. (1997), *Parameter Sensitivity in Nonlinear Mechanics, Theory and Finite Element Computations,* John Wiley and Sons.

125. Konagai, K., Yin, Y. and Murono, Y. (2003), "Single Beam Analogy for Describing Soil-pile Group Interaction", *Soil Dynamics and Earthquake Engineering,* Vol. 23, pp. 213-221.

126. Kooijman, A.P. (1989), "Comparison of as Elastoplastic Quasi Three-Dimensional Model for Laterally Loaded Piles with Field Test." *Proceedings of the III*

International Symposium, Numerical Models in Geomechanics (NUMOG III), Niagara Falls, Canada, Elsevier Applied Science, New York, pp. 675-682.

127. Kubo, K. (1965), "Experimental Study of The Behavior of Laterally Loaded Piles", *Proceedings of the VI International Conference on Soil Mechanics and Foundation Engineering*, Montreal, Canada, Vol. 2, pp. 275-279.

128. Lee, B. W. and Lim, O. K. (1997), "Design Sensitivity Analysis Extended To Perturbation Treatment In Problems of Uncertain Structural System", *Computers and Structures*, Vol. 62, No. 4, Feb, 1997, pp. 757-762

129. Leonard, J. I. (1974), "The Application of Sensitivity Analysis to Models of Large Scale Physiological Systems", *NASA* CR-160228.

130. Liu, L. (2004), "Sensitivity Analysis of Laterally Loaded Piles Embedded in Stiff Clay Above Water Table", *Thesis*, University of Windsor Libraries, Windsor, Ontario.

131. Liu, L. and Budkowska, B. B. (2004), "Sensitivity Investigations of Short Piles in Stiff Clay Subjected to Cyclic Loading", Eighth Pan-American Congress of Applied Mechanics , Havana International Conference Center, Cuba, January 5-9.

132. Long, J. H. and Vanneste, G. (1994), "Effects of Cyclic Lateral Loads on Piles in Sand", *Journal of Geotechnical Engineering*, Vol. 120, No. 1, pp. 225-244.

133. Malvern, L. E. (1969), *Introduction to the Mechanics of a Continuous Medium*, Englewood Cliffs, N.J., Prentice-Hall.

134. MATLAB program, Version 7.0.1.24704, Release 14, copyright 1984-2004, the Mathworks Inc.

135. Matlock, H. (1970), "Correlations for Design of Laterally Loaded Piles in Soft Clay", *Proceedings of the Second Annual Offshore Technology Conference*, Houston, Texas, Vol. 1, Paper No. OTC 1204, pp. 577-594.

136. Matlock, H., Ingram, W. B., Kelley, A. E., and Bogard, D. (1980), "Field Tests of the Lateral Load Behavior of Pile Groups in Soft Clay", *Proceedings of the 12th*

Offshore Technology Conference, Offshore Technology Conference, Dallas, Texas, pp.163-174.

137. McClelland, B. and Focht Jr., J. A. (1958), "Soil Modulus for Laterally Loaded Piles." *Transactions of ASCE*, Vol. 123, pp. 1049-1063.

138. McVay, M. C., Zhang, L. M., Molnit, T. and Lai, P. (1998), "Centrifuge Testing of Large Laterally Loaded Pile Groups in Sands", *Journal of Geotechnical and Geoenvironmental Engineering, ASCE*, Vol.124, No. 10, pp. 1016-1026.

139. McVay, M., Casper, R. and Shang, T. (1995), "Lateral Response of Three Row Groups in Loose to Dense Sand at 3D and 5D Pile spacing", *Journal of Geotechnical and Geoenvironmental Engineering, ASCE*, Vol.121, No. 5, pp. 436-441.

140. Meyerhof, G. G. and Ranjan, G. (1973), "The Bearing Capacity of Rigid Piles under Inclined Loads in Sand II: Batter Piles", *Canadian Geotechnical Journal*, Ottawa, Vol.10, pp. 71–85.

141. Mokwa R. L. and Duncan, J. M. (2001a), "Experimental Evaluation of Lateral-load Resistance of "Pile Caps", *Journal of Geotechnical and Geoenvironmental Engineering, ASCE*, Vol.127, No. 2, pp. 185-192.

142. Mokwa, R. L. and Duncan, J. M. (2001b), "Laterally Loaded Pile Group Effect and p-y multipliers", *Foundation and Ground improvement (Proceedings of a specialty Conference: June 9-13, 2001)*, Blacksburg, Virginia, pp. 728-742.

143. Mora, M. R. (2006), "Investigations of Nonlinear P-Y Piles and Pile Groups In Soft Clay Subjected To Static Loading-Distributed Parameter Sensitivity Analysis", *M. A. Sc. Thesis*, University of Windsor, Windsor, Ontario.

144. Morrison, C. and Reese, L. C. (1986), "A Lateral Load Test of Full-scale Pile Group in Sand", GR86-1, FHWY, Washington D. C.

145. Mostafa, Y. E. and El Naggar, M. H. (2002), "Dynamic Analysis of Laterally Loaded Pile Groups in Sand and Clay", *Canadian Geotechnical Journal*, Vol. 39, No. 6, pp. 1358–1383.

305

146. Ng, C. W. W., Zhang, L., Nip, D. C. N. (2001), "Response of Laterally Loaded Large-Diameter Bored Pile Groups", *Journal of Geotechnical and Geoenvironmental Engineering, ASCE*, Vol.127, No. 8, pp. 658-669.

147. Nogami, T. and Paulson, S. K. (1985), "Transfer Matrix Approach for Nonlinear Pile Group Response Analysis", *International Journal of Numerical and Analytical Methods in Geomechanics*, Vol. 9, pp. 289-316.

148. Novozhilov, V. V. (1953), *Foundations of the Nonlinear Theory of Elasticity.* Graylock Press, New York.

149. O'Neill, M. W. (1983), "Group Action in Offshore Piles", *Proceedings of the Conference of Geotechnical Practice in Offshore Engineering*, University of Texas at Austin, Texas, pp. 25-46.

150. O'Neill, M. W. and Gazioglu, S. M. (1984), "Evaluation of p-y Relationship in Sand. Proceedings, Analysis and Design of Pile Foundation", *ASCE Technical Council on Codes and Standards, ASCE National Convention,* San Francisco, California, J. Meyers Edition, pp. 192-213.

151. O'Neill, M. W. and Haung, A. (2003), "Comparative Behavior of Laterally Loaded Groups of Bored and Driven Piles in Cohesionless Soil", *International Journal of Offshore and Polar Engineering*, Vol. 13, No. 3, pp.161-167.

152. O'Neill, M. W. and Tsai, C. N. (1984), "Investigation of Soil Nonlinearity and Pile-Soil-Pile-Interaction in Pile Group Analysis", *Research Report No. UHUC 84-9,* U.S. Army Engineer Waterways Experiment Station, Vicksburg, Miss.

153. O'Neill, M. W., Ghazzaly, O. I., and Ha, H. B. (1977), "Analysis of three-dimensional pile groups with non-linear soil response and pile-soil-pile-interaction", *Proceedings of the 9th Offshore Technology Conference*, Offshore Technology Conference, Dallas, Texas, pp. 245-256.

154. Ooi, P. S. K., and Duncan, J. M. (1994), "Lateral Load Analysis of Groups of Piles and Drilled Shafts", *Journal of Geotechnical Engineering*, Vol. 120, No. 6, Pp. 1034-1050.

155. Patra, N. R. and Pise, P. J. (2001), "Ultimate Lateral Resistance of Pile Groups in Sand", *Journal of Geotechnical and Geoenvironmental Engineering, ASCE,* Vol.127, No. 6, pp. 481-487.

156. Perloff, W. H. and Baron, W. (1976), *Soil Mechanics, Principles and Applications.* The Ronald Press Company, New York.

157. Phelan, D. G. and Haber, R. B. (1989), "Sensitivity Analysis of Linear Elastic Systems using Domain Parameterization and a Mixed Mutual Energy Principle", *Computer Methods in Applied Mechanics and Engineering,* Vol. 77, pp. 31-59.

158. Phelan, D. G., Vidal, C. and Robert, B. H. (1991), "Adjoint Variable Method for Sensitivity Analysis of Non-linear Elastic Systems", *International Journal for numerical methods in Engineering,* Vol. 31, pp. 1649-1667.

159. Poldneff, M. J., Rai, I. S. and Arora, J. S. (1993), "Implementation of Design Sensitivity Analysis for Nonlinear Elastic Structures", *The American Institute of Aeronautics and Astronautics, AIAA,* Vol. 31, No. 11, pp. 2137-2142.

160. Poulos, H. G. (1971), "Behavior of Laterally Loaded Piles: II-Pile Groups," *Journal of Soil Mechanics and Foundations Division, ASCE,* Vol. 97, No. 5, 733-751.

161. Poulos, H. G. and Davis, E. H. (1980), *Pile Foundation Analysis and Design,* John Wiley & Sons, New York.

162. Poulos, H. G. and Hull, T.S. (1989), "The Role of Analytical Mechanics in Foundation Engineering." *Foundation Engineering, Current Principals and Practices, ASCE,* Vol. 2, pp. 1578-1606.

163. Poulos, H. G. and Madhav, M. R. (1971), "Analysis of Movement of Battered Piles", *Research Report No. R173,* University of Sydney, Australia, pp. 1–18.

164. Prakash, S. (1962), "Behavior of pile groups subjected to lateral loads", *PhD. Thesis,* University of Illinois, Urbana, III.

165. Prakash, S. and Prakash, Sally. (1989), "Reanalysis of Piles under Static and Dynamic Lateral Loads", *In Burland, J. B. and Mitchell, J. M. (eds), Proceedings of the International Conference on Pilling and Deep Foundations,* London.

166. Prakash, Shamsher and Kumar, Sanjeev (1996), "Nonlinear Lateral Pile Deflection Prediction in Sands", *Journal of Geotechnical Engineering*, Vol. 122, No. 2, pp. 130 – 138.

167. Priyanto, D. (2002), "Piles Embedded in Soft Clay Located Below the Water Table Subjected to Lateral Cyclic Loadings – Sensitivity Analysis", *M. A. Sc. Thesis*, University of Windsor, Windsor, Ontario.

168. Radanovic, L. (1966), *Sensitivity Methods in Control Theory*, Pergamon Press, Oxford, England.

169. Rahman, N. (2004), "Analysis of Piles Embedded in *p-y* Sand Below Water Table Subjected to Cyclic Lateral Loading – Sensitivity Analysis", *M. A. Sc. Thesis*, University of Windsor, Windsor, Ontario.

170. Rajashree, S. S. and Sitharam, T. G. (2001), "Nonlinear Finite –Element Modeling of Batter Piles under Lateral Load", *Journal of Geotechnical and Geoenvironmental Engineering, ASCE*, Vol.127, No. 7, pp. 604-612.

171. Rajashree, S. S. and Sundaravadivelu, R., (1996), "Degradation Model for One-Way Cyclic Load on Piles In Soft Clay", *Computers and Geotechnics*, Vol. 19, No 4, pp. 289-300.

172. Rajashree, S. S., and Sitharam, T. G. (1999), "Nonlinear Cyclic Load Analysis for Lateral Response of Batter Piles in Soft Clay with A Rigorous Degradation Model", *Proceedings of the International Conference on Offshore and Nearshore Geotechnical Engineering, (Geoshore)*, pp.309–314.

173. Reese, L. C. and Matlock, H. (1960), "Numerical Analysis of Laterally Loaded Piles", *Proceedings of the 2ⁿᵈ structural Division Conference on Electronic Computation*, Pittsburg, Pennsylvania, ASCE, pp. 657-668.

174. Reese, L. C. and Matlock, H. (1966), "Behavior of a Two-Dimensional Pile Group under Inclined and Eccentric Loading", *Proceedings of the Offshore Exploration Conference*, Long Beach, California.

175. Reese, L. C. and O'Neill, M. W. (1967), "The Analysis of Three-dimensional Pile Foundations Subjected to Inclined and Eccentric Loads", *Proceedings of the Conference on Civil Engineering,* ASCE, pp. 245-276.

176. Reese, L. C. and Van Impe, W. F. (2001), *Single Piles and Group of Piles under Lateral Loading.* A.A. Balkema, Rotterdam.

177. Reese, L. C., Cox, W. R. and Koop, F. D. (1975), "Field Testing and Analysis of Laterally Loaded Piles in Stiff Clay", *Proceedings of the Seventh Annual Offshore Technology Conference,* Houston, Texas, Vol. 2 (OTC 2312), pp. 672-690.

178. Reese, L. C., O'Neill, M. W. and Smith, R. E. (1970), "Generalized Analysis of Pile Foundations", *Journal of Soil Mechanics and Foundations Division, ASCE,* Vol. 96, No. 1, pp. 235-250.

179. Reese, L.C. and Matlock, H. (1956) "Nondimensional Solutions for Laterally Loaded Piles With Soils Modulus Assumed Proportional to Depth", *Proceedings of the VIII Texas Conference on Soil Mechanics and Foundations Engineering,* University of Texas, Austin.

180. Reese, L.C. and Welch, R.C. (1975), "Lateral Loading of Deep Foundation in Stiff Clay", *Journal of the Geotechnical Engineering Division,* ASCE, Vol. 101, No. GT7, pp.633-649.

181. Reese, L.C., Cox, W.R. and Koop, F.D. (1974), "Analysis of Laterally Loaded Piles in Sand." *Proceedings of Sixth Annual Offshore Technology Conference,* Houston, Texas, Vol. 2, Paper No. 2080, pp. 473-483.

182. Rollins, K. M., Gerber, T. M., Lane, J. D. and Ashford, S. A.(2005b), "Lateral Resistance of a Full-Scale Pile Group in Liquefied Sand", *Journal of Geotechnical and Geoenvironmental Engineering, ASCE,* Vol.131, No. 1, pp. 115-125.

183. Rollins, K. M., Lane, J. D. and Gerber, T. M. (2005a), "Measured and Computed Lateral Response of a Pile Group in Sand", *Journal of Geotechnical and Geoenvironmental Engineering, ASCE,* Vol.131, No. 1, pp. 103-114.

184. Rollins, K. P., Peterson, K. T. and Weaver, T. J. (1998), "Lateral Load Behavior of Full-Scale pile group in Clay", *Journal of Geotechnical and Geoenvironmental Engineering, ASCE*, Vol.124, No. 6, pp. 468-478.

185. Rollins, M. K., Weaver, T. J. and Peterson, K. T. (1997), "Statnamic Lateral Load Testing of A Full-Scale Fixed-Head Pile Group", *Report for the Utah Department of Transportation, Region 2*.

186. Rousselet, B. (1983), "Note on the Design Differentiability of the Static Response of Elastic Structures", *Journal of Structural Mechanics*, Vol. 10, No. 3, pp. 353-358.

187. Ruesta, P. F. and Townsend, F. C. (1997), "Evaluation of Laterally Loaded Pile Group", *Journal of Geotechnical and Geoenvironmental Engineering, ASCE*, Vol.123, No. 12, pp. 1153-1174.

188. Ryu, Y. S., Harrian, M., Wu, C. C. and Arora, J. S. (1985), "Structural Design Sensitivity Analysis of nonlinear response", *Computers and Structures*, Vol. 13, pp. 245-266.

189. Sanders, B. F. and Katopodes, N. D. (2000), "Adjoint Sensitivity Analysis for Shallow-Water Wave Control", *Journal of Engineering Mechanics*, Vol. 126, No. 9, pp. 909-919.

190. Saul, W. E. (1968), "Static and dynamic Analysis of Pile Foundations", *Journal of Structural Division, ASCE*, Vol. 94, ST5, pp. 1077-1100.

191. Shen, W. Y. and The, C.I. (2004), "Analysis of Laterally Loaded Piles in Soil with Stiffness Increasing with Depth", *Journal of Geotechnical and Geoenvironmental Engineering*, Vol. 130, No 8, pp. 878 – 882.

192. Shibata, T., Yashima, A., Kimura, M. and Fukada, H. (1988), "Analysis of Laterally Loaded Pies by Quasi-three Dimensional Finite Element Method", *Proceedings of the 6th International Conference on Numerical Methods in Geomechanics*, A. A. Balkema, Rotterdam, The Netherlands, Vol. 2, 1051-1058.

193. Suwarno, D. (2003), "Nonlinear Deformations of Laterally Loaded Piles embedded in Stiff Clay Located below Water Table-Sensitivity Analysis", *M. A. Sc. Thesis*, University of Windsor, Windsor, Ontario.

194. Terzaghi, K. (1955), "Evaluation of Coefficients of Subgrade Reaction." *Geotechnique*, Vol. V, pp. 297-326.

195. Terzaghi, K. (1956), *Theoretical Soil Mechanics*. John Wiley and Sons, New York, pp. 363-366.

196. Terzaghi, K. and Peck, R. B. (1967), *Soil Mechanics in Engineering Practice*, Second Edition, John Wiley & Sons, Inc., New York.

197. Thompson, G. R. (1977), "Application of Finite Element Method to The Development of P-Y Curves for Saturated Clays". Thesis, University of Texas, Austin.

198. Tomovic, R. (1963), *Sensitivity Analysis of Dynamic Systems*, McGraw-Hill Book Co., New York.

199. Tsai, J. J. and Arora, J. S. (1989), "Optimal Design of Nonlinear Structures with Path Dependent Response", *AIAA/ASME/ ASCE/ AHS/ASC 30th Structures, Structural Mechanics and Materials Conf.*, Mobile , Alabama, pp. 553-563.

200. Valliappan, S., Tandjiria, V. and Khalili, N. (1997), "Design Sensitivity and Constraint Approximation Methods for Optimization in Non-linear Analysis", *Communications in Numerical Methods in Engineering*, Vol. 13, 999-1008.

201. Valliappan, S., Tandjiria, V. and Khalili, N. (1999), "Design of Raft-pile Foundation Using Combined Optimization and Finite Element Approach", *International Journal of Numerical and Analytical Methods in Geomechaincs*, Vol. 23, 1043-1065.

202. Van Belle, H. (1982), "Higher Order Sensitivities in Structural Systems," *AIAA Journal*, Vol. 20, pp. 286-288.

203. Veeresh, C. (1996), "Behaviour of Batter Piles in Marine Clays", *PhD Thesis*, Indian Institute of Technology, Madras, India.

204. Wang, S.T., and Reese, L.C. (1993), *COM624P-Laterally Loaded Pile Analysis Program for the Microcomputer*, Version 2.0. Report FHWA-SA-91-048, Washington, USDT.

205. Weinstock, R. (1974), *Calculus of Variations*, Dover Publications, Inc., New York.

206. Welch, R. C. and Reese, L. C. (1972), "Laterally Loaded Behavior of Drilled Shafts", *Research Report 3-5-65-89*. Center for Highway Research, University of Texas, Austin.

207. Wu, C. C. and Arora, J. S. (1987), "Design Sensitivity Analysis of nonlinear response using incremental procedure", *AIAA Journal*, Vol. 25, pp. 1118-1125.

208. Yang, R. J. and Choi, K. K.(1985), "Accuracy of Finite Element Based Shape Design Sensitivity Analysis", *Journal of Structural Mechanics*, Vol. 13, No. 2, pp. 223-239.

209. Yegian, M and Wrigth, S.G. (1973). "Lateral Soil Resistence-Displecement Relationship for Pile Foundation in Soft Clays", *Proceedings of The Offshore Technology Conference,* Houston, Texas, Paper No. OTC 1893, pp. 663-676.

210. Yoo, Y. M., Haug, E. J. and Choi, K. K. (1984), "Shape Optimal Design of an Engine Connecting Rod", *Journal of Mechanisms, Transmission, and Automation in Design*, Vol. 106, No. 3, pp. 415-419.

211. Zafir, Z. and Vanderpool, W. E. (1998), "Lateral Response of Large Diameter Drilled Shafts: I-15/US 95 Load Test Program", *Proceedings of the 33rd Engineering Geological and Geotechnical Engineering Symposium*, University of Nevada, Reno, Nevada, pp. 161-176.

212. Zhang, L., McVay, M. C. and Lai, P. (1999), "Numerical Analysis of Laterally Loaded 3×3 to 7 ×3 Pile Groups in Sands", *Journal of Geotechnical and Geoenvironmental Engineering, ASCE*, Vol.125, No. 11, pp. 936-946.

APPENDIX A

EXPRESSIONS USED FOR SENSITVITY OPERATORS

The different expressions used for the sensitivity operators S defined in Equation 5.84 based on Equation 5.83 are given in this Appendix for the eight studied parameters. The expressions of S (for all parameters except EI) is based on the differentiation of the p-y relationships and depend on the depth x and deflection y. The sensitivity operator related to EI has a single expression along the pile length. The pile parameter b has different expressions when pile is surrounded by clay than that when the pile is surrounded by sand. The pile diameter b is included in the p-y relationships of both the clay and sand. The different expressions for the sensitivity operators are given below:

Sensitivity operator for EI

For any depth,

$$S_{EI} = -y'' y_a'' EI$$

Sensitivity operators for clay parameters and b in clay layer

The different p-y relationships for the soft clay behavior are given in Table 4.1 based on the p-y curves given in Figure 4.5. By performing the required operations given in Equation 5.83, the following expressions are obtained depending on the depth x and the deflection y:

For $x \leq x_{rc}$ and $y \leq 3y_{50}$

$$S_c = -c y_a \frac{1}{2} (3b + Jx) \left(\frac{y}{y_{50}} \right)^{\frac{1}{3}}$$

313

$$S_{\gamma c} = -\gamma'_c y_a \frac{1}{2}(bx)(\frac{y}{y_{50}})^{\frac{1}{3}}$$

$$S_{\varepsilon 50} = \varepsilon_{50} y_a \frac{1}{6}[(3b + Jx)c + \gamma'_c bx](\frac{y}{y_{50}})^{\frac{1}{3}}(\frac{1}{\varepsilon_{50}})$$

$$S_b = -by_a(c + \frac{1}{3}\gamma'_c x - \frac{Jxc}{6b})\left(\frac{y}{y_{50}}\right)^{\frac{1}{3}}$$

For $x \leq x_{rc}$ **and** $3y_{50} \leq y \leq 15y_{50}$

$$S_c = -cy_a(3b + Jx)\left\{(0.9 - 0.18\frac{x}{x_{rc}}) - 0.06\left(\frac{y}{y_{50}}\right)(1 - \frac{x}{x_{rc}})\right\}$$

$$S_{\gamma c} = -\gamma'_c y_a(bx)\left\{(0.9 - 0.18\frac{x}{x_{rc}}) - 0.06\left(\frac{y}{y_{50}}\right)(1 - \frac{x}{x_{rc}})\right\}$$

$$S_{\varepsilon 50} = \varepsilon_{50} y_a(0.06)\frac{1}{\varepsilon_{50}}(1 - \frac{x}{x_{rc}})\left(\frac{y}{y_{50}}\right)[3cb + \gamma'_c bx + Jcx]$$

$$S_b = -by_a\left\{\begin{array}{l}(3c + \gamma'_c x)\left[(0.9 - 0.18\frac{x}{x_{rc}}) - 0.06\left(\frac{y}{y_{50}}\right)(1 - \frac{x}{x_{rc}})\right] + \\ 0.06[3c + \gamma'_c x + \frac{Jxc}{b}]\left(\frac{y}{y_{50}}\right)(1 - \frac{x}{x_{rc}})\end{array}\right\}$$

For $x \geq x_{rc}$ **and** $y \leq 3y_{50}$

$$S_c = -cy_a 4.5b\left(\frac{y}{y_{50}}\right)^{\frac{1}{3}}$$

314

$$S_{\gamma c} = 0$$

$$S_{\varepsilon 50} = \varepsilon_{50} y_a 1.5cb \left(\frac{y}{y^{50}} \right)^{\frac{1}{3}} \frac{1}{\varepsilon_{50}}$$

$$S_b = -by_a 3c \left(\frac{y}{y^{50}} \right)^{\frac{1}{3}}$$

For $x \geq x_{rc}$ **and** $3y_{50} \leq y \leq 3y_{50}$

$$S_c = 0$$

$$S_{\gamma c} = 0$$

$$S_{\varepsilon 50} = 0$$

$$S_b = 0$$

Note : All expressions equal to zero since flow occurs in this stage (Figure 4.5)

315

Sensitivity operators for sand parameters and *b* in sand layer

The different *p-y* relationships for the sand behavior are given in Table 4.2 based on the *p-y* curves given in Figure 4.7. By performing the required operations given in Equation 5.83, the following expressions are obtained depending on the depth x (local coordinates of sand are used in determining the proper x) and the deflection y:

For $x<x_{rs}$ and $y \leq y_k$

$$S_k = -ky_a yx$$

$$S_b = 0$$

$$S_{\gamma s} = 0$$

$$S_\phi = 0$$

For $x<x_{rs}$ and $y_k \leq y \leq y_m$

$$S_k = 0$$

$$S_b = -by_a B_c \gamma_s x \left\{ \begin{array}{l} \left[\dfrac{\tan\beta}{\sqrt{K_a}} - K_a\right]\left(\dfrac{60}{b}y\right)^{0.8\left(\frac{\tilde{A}_c}{B_c}-1\right)} + 0.8\left(\dfrac{\tilde{A}_c}{B_c}-1\right)\left(-\dfrac{60}{b^2}y\right)\left(\dfrac{60}{b}y\right)^{\left(0.8\frac{\tilde{A}_c}{B}-1.8\right)} \\ \times\left[\dfrac{K_o x \tan\phi \sin\beta}{\sqrt{k_a}\cos\alpha} + \dfrac{\tan\beta}{\sqrt{K_a}}(b + x\tan\beta\tan\alpha) + \right. \\ \left. K_o x \tan\beta(\tan\phi\sin\beta - \tan\alpha) - K_a b \right] \end{array} \right\}$$

$$S_{\gamma s} = -\gamma_s y_a B_c x \left[\dfrac{K_o x \tan\phi \sin\beta}{\sqrt{K_a}\cos\alpha} + \dfrac{\tan\beta}{\sqrt{K_a}}(b + x\tan\beta\tan\alpha) + \atop K_o x \tan\beta(\tan\phi\sin\beta - \tan\alpha) - K_a b \right]\left(\dfrac{60}{b}y\right)^{0.8\left(\frac{\tilde{A}_c}{B_c}-1\right)}$$

316

$$S_\phi = -\phi \ y_a B_c \gamma_s' x \left(\frac{60}{b} y\right)^{0.8(\frac{\tilde{A}_c}{B_c}-1)}$$

$$\left\{ \begin{array}{l} \left[\dfrac{\left(0.5\tan\phi\cos\beta + \dfrac{\sin\beta}{\cos^2\phi}\right)\left(\tan(45-\dfrac{\phi}{2})\cos\alpha\right) + 0.5\tan\phi\sin\beta\left(\tan(45-\dfrac{\phi}{2})\sin\alpha + \dfrac{\cos\alpha}{\cos^2(45-\dfrac{\phi}{2})}\right)}{\tan^2(45-\dfrac{\phi}{2})\cos^2(\dfrac{\phi}{2})} \right] \\[2em]
+ \dfrac{\tan(45+\dfrac{\phi}{2})}{\tan(45-\dfrac{\phi}{2})}\left(0.5x\tan(45+\dfrac{\phi}{2})\dfrac{1}{\cos^2(\dfrac{\phi}{2})} + 0.5x\dfrac{1}{\cos^2(45+\dfrac{\phi}{2})}\tan\alpha\right) \\[2em]
+ \left(\dfrac{0.5\dfrac{1}{\cos^2\beta}\tan(45-\dfrac{\phi}{2}) + 0.5\tan\beta\dfrac{1}{\cos^2(45-\dfrac{\phi}{2})}}{\tan^2(45-\dfrac{\phi}{2})}\right)\left(b + x\tan(45+\dfrac{\phi}{2})\tan\dfrac{\phi}{2}\right) \\[2em]
+ K_o\left[\tan\beta\left(0.5\tan\phi\cos\beta + \dfrac{\sin\beta}{\cos^2\phi}\right) - \dfrac{0.5}{\cos^2\alpha}\right] + \dfrac{0.5}{\cos^2\beta}(\tan\phi\sin\beta - \tan\alpha)\right] + \dfrac{b\tan(45-\dfrac{\phi}{2})}{\cos^2(45-\dfrac{\phi}{2})}
\end{array} \right\}$$

For $x < x_{rs}$ and $y_m \le y \le y_u$

$$S_k = 0$$

$$S_b = -by_a\gamma_s' x \left\{ \begin{array}{l} \left[\dfrac{\tan\beta}{\sqrt{K_a}} - K_a\right]\left[B_c + \left(y - \dfrac{b}{60}\right)\left(\dfrac{48(\tilde{A}_c - B_c)}{b}\right)\right] - \\[1.5em]
\left[\left(\dfrac{48(\tilde{A}_c - B_c)}{b}\right)\left(\dfrac{1}{60}\right) + \left(y - \dfrac{b}{60}\right)\left(\dfrac{48(\tilde{A}_c - B_c)}{b^2}\right)\right] \times \\[1.5em]
\left[\dfrac{K_o x \tan\phi\sin\beta}{\sqrt{K_a}\cos\alpha} + \dfrac{\tan\beta}{\sqrt{K_a}}(b + x\tan\beta\tan\alpha) + \right. \\[1em]
\left. K_o x \tan\beta(\tan\phi\sin\beta - \tan\alpha) - K_a b \right]
\end{array} \right\}$$

317

$$S_{ys} = -\gamma_s' y_a x \left\{ \begin{bmatrix} \left[\dfrac{K_o x \tan\phi \sin\beta}{\sqrt{K_a}\cos\alpha} + \dfrac{\tan\beta}{\sqrt{K_a}}(b + x\tan\beta\tan\alpha) + \right] \times \\ K_o x \tan\beta(\tan\phi\sin\beta - \tan\alpha) - K_a b \end{bmatrix} \\ \left[B_c + \left(y - \dfrac{b}{60}\right)\left(\dfrac{48}{b}(\tilde{A}_c - B_c)\right) \right] \end{bmatrix} \right\}$$

$$S_\phi = -\phi\, y_a \gamma_s' x \left[B_c + \left(y - \dfrac{b}{60}\right)\left(\dfrac{48}{b}(\tilde{A}_c - B_c)\right) \right] \times$$

$$\left\{ \begin{array}{l} \left[\dfrac{\left(0.5\tan\phi\cos\beta + \dfrac{\sin\beta}{\cos^2\phi}\right)\left(\tan(45 - \dfrac{\phi}{2})\cos\alpha\right) + 0.5\tan\phi\sin\beta\left(\tan(45 - \dfrac{\phi}{2})\sin\alpha + \dfrac{\cos\alpha}{\cos^2(45 - \dfrac{\phi}{2})}\right)}{\tan^2(45 - \dfrac{\phi}{2})\cos^2(\dfrac{\phi}{2})} \right] \\[4ex] + \dfrac{\tan(45 + \dfrac{\phi}{2})}{\tan(45 - \dfrac{\phi}{2})}\left(0.5x\tan(45 + \dfrac{\phi}{2})\dfrac{1}{\cos^2(\dfrac{\phi}{2})} + 0.5x\dfrac{1}{\cos^2(45 + \dfrac{\phi}{2})}\tan\alpha\right) \\[4ex] + \left(\dfrac{0.5\dfrac{1}{\cos^2\beta}\tan(45 - \dfrac{\phi}{2}) + 0.5\tan\beta\dfrac{1}{\cos^2(45 - \dfrac{\phi}{2})}}{\tan^2(45 - \dfrac{\phi}{2})}\right)\left(b + x\tan(45 + \dfrac{\phi}{2})\tan\dfrac{\phi}{2}\right) \\[4ex] + K_o\left[\tan\beta\left(0.5\tan\phi\cos\beta + \dfrac{\sin\beta}{\cos^2\phi}\right) - \dfrac{0.5}{\cos^2\alpha}\right] + \dfrac{0.5}{\cos^2\beta}(\tan\phi\sin\beta - \tan\alpha)\right] + \dfrac{b\tan(45 - \dfrac{\phi}{2})}{\cos^2(45 - \dfrac{\phi}{2})} \end{array} \right\}$$

318

For $x \geq x_{rs}$ **and** $y_k \leq y \leq y_m$

$$S_k = 0$$

$$S_\gamma = B_c bx \left[K_a(\tan^8 \beta - 1) + K_o \tan\phi \tan^4 B \left(\frac{60}{b} y \right)^{0.8\left(\frac{\tilde{A}_c}{B_c} - 1 \right)} \right]$$

$$S_b = -by_a B_c \left\{ \begin{matrix} \left[K_a \gamma'_s x(\tan^8(45 + \frac{\phi}{2}) - 1) + K_o \gamma'_s x \tan\phi \tan^4(45 + \frac{\phi}{2}) \right] \left(\frac{60}{b} y \right)^{0.8\left(\frac{\tilde{A}_c}{B_c} - 1 \right)} + \\ 0.8\left(\frac{\tilde{A}_c}{B_c} - 1 \right)\left(\frac{60}{b} y \right)^{\left[0.8(\frac{\tilde{A}_c}{B_c} - 1) - 1 \right]} \cdot \left(-\frac{60}{b^2} y \right) \begin{bmatrix} K_a by'_s x \left(\tan^8(45 + \frac{\phi}{2}) - 1 \right) \\ + K_o by'_s x \tan\phi . \tan^4(45^o + \frac{\phi}{2}) \end{bmatrix} \end{matrix} \right\}$$

$$S_\phi = -\phi \, y_a B_c \gamma'_s x \left(\frac{60}{b} y \right)^{0.8\left(\frac{\tilde{A}_c}{B_c} - 1 \right)} \left[\begin{matrix} \dfrac{4\tan^2(45 - \frac{\phi}{2})\tan^7 \beta}{\cos^2 \beta} - \dfrac{\tan(45 - \frac{\phi}{2})}{\cos^2(45 - \frac{\phi}{2})}(\tan^8 \beta - 1) + \\ K_o \left(2\dfrac{\tan\phi \tan^3 \beta}{\cos^2 \beta} + \dfrac{\tan^4 \beta}{\cos^2 \phi} \right) \end{matrix} \right]$$

For $x \geq x_{rs}$ **and** $y_m \leq y \leq y_u$

$$S_k = 0$$

$$S_{\gamma s} = -\gamma'_s y_a bx \left[K_a(\tan^8 \beta - 1) + K_o \tan\phi \tan^4 \beta \right] \left[B_c + (y - \frac{b}{60})(\frac{48}{b}(\tilde{A}_c - B_c)) \right]$$

$$S_b = -by_a \left\{ \begin{matrix} \left[K_a \gamma'_s x(\tan^8 \beta - 1) + K_o \gamma'_s x \tan\phi \tan^4 \beta \right] \left[B_c + (y - \frac{b}{60})(\frac{48}{b}(\tilde{A}_c - B_c)) \right] + \\ \left[K_a by'_s x(\tan^8 \beta - 1) + K_o by'_s \tan\phi \tan^4 \beta \right] \\ \left[(-\frac{1}{60})(\frac{48}{b}(\tilde{A}_c - B_c)) + (y - \frac{b}{60})(-\frac{48}{b^2}(\tilde{A}_c - B_c)) \right] \end{matrix} \right\}$$

319

$$S_\phi = -\phi \, y_a b \gamma_s' x \left[B_c + (y - \frac{b}{60})(\frac{48}{b}(\tilde{A}_c - B_c)) \right] \left[\begin{array}{l} \dfrac{4\tan^2(45 - \frac{\phi}{2})\tan^7 \beta}{\cos^2 \beta} - \dfrac{\tan(45 - \frac{\phi}{2})}{\cos^2(45 - \frac{\phi}{2})}(\tan^8 \beta - 1) + \\[4ex] K_o\left(2\dfrac{\tan\phi \tan^3 \beta}{\cos^2 \beta} + \dfrac{\tan^4 \beta}{\cos^2 \phi}\right) \end{array} \right]$$

320

APPENDIX B

PROGRAMS USED FOR NUMERICAL SENSITVITY ANALYSIS

The programs used for the numerical sensitivity analysis studied in Chapter 6 are discussed in this appendix. They are given in the attached CD along with the results obtained from their execution.

Developed programs for single pile sensitivity analysis

MATLAB programs were developed for the sensitivity analysis of single piles conducted in Chapter 6 (Section 6.2) with the aid of COM624P and FB-Pier. The role of each developed program is given below. The programs should be executed in the given order.

1. Sgendirectory.m

This program prepares the directory system used to differentiate between the different studied cases: support types, pile lengths and % clay layer thickness for the laterally loaded single piles embedded in non-homogeneous soil studied in Chapter 6. The names of the directories assigned to the different cases are shown in Figure B.1.

2. Sgeninput.m

This program creates the input files required by COM624P for the different studied cases. The input file names assigned to different cases are shown in Figure B.2.

3. Scalculate.m

This program calls COM624P to calculate the deflections, moments, shear, and soil resistance required for the sensitivity analysis. Only the allowable deflection criteria is used to check the condition of the maximum force reached as mentioned in Section 6.2.1. In addition a data file is developed if the force at which the allowable moment was exceeded and points out this force.

321

4. Soperatorsa.m

This program reads the output from COM624P using the developed sub-function file "readdata.m" calculates the sensitivity operators along the pile length using the different expressions given in Appendix A depending on the depth and deflection. The results are saved in a data file named "Soperators.dat".

5. Soperatorsb.m

This program loads the data from "Soperators.dat" and plots the sensitivity results in a picture format (with extension .eps). Each four Figures are plotted in one page using the developed sub-function file "plotfig4pp.m". The sensitivity operators for c, γ'_c, ε_{50}, k, γ'_s, ϕ, EI and b are saved in the picture files S1.eps and S1(cont), respectively for sensitivity of y_t. The sensitivity operators of lateral top rotation θ_t are saved in S2 and S2(cont).

6. Sresultsa.m

This program loads the data file "Soperators.dat" to obtain the values of S and calculates the values of the sensitivity results A, PCR, TF, and GF. The results are saved in a data file named "Sresults.dat".

7. Scheckrange.m

This program checks the results according to the error analysis presented in Section 6.2.6. It uses two developed sub-functions "groupreaddata" and "readcheckrange". This check is performed with the aid of the FB-Pier software for pile groups since it provides the slope θ in its output required for the checking criteria of the top rotation. The errors in the predicted y_t and θ_t are given in percent for the range of 1% to 50% change in the parameter (as explained in Section 6.2.6). The error is saved in the data file "Scheck.dat".

8. Sresultsb.m

This program plots the results A, PCR, TF and GF in the form of bar charts. Each four Figures are plotted in one page using the developed sub-functions plotbar4pp1.m and plotbar4pp2.m The results are saved in a picture format with the same name convention used for the operators, i.e. A1, A1(cont.), A2, A2(cont), PCR1, PCR1(cont), ..etc.

322

S I N G L E \ X \ X \ X X

0, 1, 2, 3, 4, 5, 6, 7, 8, 9 or 10. The directories contain the results for clay layer thickness equal to 0, 10, 20 ,30, 40, 50, 60, 70, 80, 90 or 100%, respectively.

An interger between 0-9, the directories contain the sensitivity analysis results of the single piles with lengths $l = 2T, 3T, 4T, 5T, 6T, 7T, 8T, 9T, 10T$, respectively.

1, 2 or 3. The directories contain the sensitivity analysis results of the single piles having support types. "1' stands for free head pile subjected to concentrated lateral force; "2"stands for fixed head pile subjected to concentrated lateral force; "3"stands for free head pile subjected to bending moment.

Directory used to hold the sensitivity analysis results of the single

Figure B.1 The subdirectory structure used to store the results for single pile

XXXXXXXX . i n p

0, 1 or 2. The indicator used to differentiate between primary, adjoint1 and adjoint2 piles, respectively.

Value of applied lateral load or bending moment

0, 1, 2, 3, 4, 5, 6, 7, 8, 9 or 10 Stands for clay layer thickness equal 0,10, 20,30, 40, 50, 60, 70, 80, 90 or 100%, respectivly

An integer between 1-9. Stands for pile length l =2T, 3T, 4T, 5T, 6T, 7T, 8T, 9T or 10T, respectively.

1, 2 or 3. Support type indicator."1" stands for free head pile subjected to concentrated lateral force; "2" stands for fixed head pile subjected to concentrated lateral force; "3' stands for free head pile subjected to bending moment.

Figure B.1 Name convention of the created input file for COM624P for single pile

323

Developed programs for sensitivity analysis of pile groups

MATLAB programs were developed for the sensitivity analysis of pile groups conducted in Chapter 6 (Section 6.3) with the aid of FB-Pier. The role of each developed program is given below. The programs should be executed in the given order.

1. GGenDirectory.m

This program is used to generate the directory system in which the preparation and result data are saved. There are two directories generated, ':\G' and ":\Group'. The directory ':\G' is used to store preparing data while ':\Group' is used to store the sensitivity analysis result data. The names of the directories assigned to the different cases of sensitivity analysis results are shown in Figure B.3.

2. GGenInputProducePdelta.m

This program creates the input file that produce the force versus pile head deflection graphs used in the calculation of forces Pg and Mg as shown in Figure 6.44 and Figure 6.46. The input files are saved in the folder ':\G'.

3. GCalculate.m

This program calls FB-Pier to calculates the input files produced by Groupgeninputproducedelta.m using the MATLAB function dos( ). The output from FB-pier is saved in the directory ':\G'

4. GPlotPdelta.m

This program calculates the force Pg and Mg determined and plot the Pg or Mg versus y_t graphs presented in Figures 6.44 and 6.46, respectively. The plots are saved in the directory 'G'

5. GGenPrimaryInput.m

This program generates the input files for FB-Pier to calculate the primary structures shown in Figure 6.45 and Figure 6.47. The force Pg and Mg determined by

324

Groupplotpdelta.m are used as the force series applied at the primary structure. The input files are saved in the dierectory 'Group'. The input file names assigned to different cases are shown in Figure B.4.

6. GPrimaryCalculate.m

This program calls FB-Pier to calculate the deflections and internal forces of the input files generated in Ggenprimaryinput.m

7. GTransferResults_PrimaryOnly.m

This program reads the output results of FB-Piers for the primary structures and saves them into MATLAB format data files.

8. GCalculatePg1_S1_2.m

This program calculates force Pg_1, determined by the method shown in Figure 6.45 for the pile groups under lateral concentrated load (SupportType =1 and 2). The force Pg_1 is obtained through the application of Eq. (6.15) and the results of force Pg_1 are saved into a MATLAB data file named ForcePg1.dat.

9. GGenUnitAppliedF_S3.m

This program generates the input files for FB-Piers to calculate the structure shown in

Figure 6.47 (c) in which a force $\bar{9}$ is applied in addition to the primary structure shown in Figure 6.47(b).

10. GCalculateUnitAppliedF_S3.m

This program calls FB-Pier software to calculate the input files generated in the program GgenunitappliedF_S3.m.

11. GCalculatePg1_S3.m

This program reads the results obtained from the program GroupCalculateUnitAppliedF_S3.m and calculates Pg_1, determined in Figure 6.47, for the pile groups with bending moments Mg applied at the pile heads(SupportStyle= 3).The

325

forces Pg_1 are obtained though the application of Equation(6.17). The results of force Pg_1 are saved into a MATLAB data file named ForcePg1.dat.

12. GGenAdjointInput.m

This program generates the input file for FB-Pier to calculate the temporary overloaded structures shown in Figure 6.45 (d) and 6.47 (f).The results in the MATLAB data file ForcePg1.dat, which are obtained by the application of GroupCalculatePg1_S1_2.m and GroupCalculatePg1_S3.m, are loaded and introduced into the input files for the calculationof the adjoint structures.

13. GAdjointCalculate.m

This Program calls FB-Pier to calculate the input files generated through the application of program Groundgenadjointinput.m.

14. GTransferResult.m

This Program reads the output results of of FB-Pier for the adjoint structures and saves them into MATLAB format data files.

15. Goperatorsa.m

In this program, the sensitivity operators for the pile groups are evaluated and saved in MATLAB data files named "Goperators.dat".

16. Goperatorsb.m

This program loads the data "Goperators.dat" and plots the sensitivity operators. The results are saved in the attached CD as a picture format file (.eps).

17. Gresultsa.m

This program loads the data file "Goperators.dat" to obtain the values of S and calculates the values of the sensitivity results *A*, *PCR*, *TF*, and *GF*. The results are saved in a data file named "Gresults.dat".

18. Gresultsb.m

This program plots the results A, PCR, TF and GF for the pile groups in the form of bar charts. Each four Figures are plotted in one page using the developed sub-functions plotbar4pp1.m and plotbar4pp2.m The results are saved in a picture format with the same name convention used for the operators, i.e. A1, A1(cont.), A2, A2(cont), PCR1, PCR1(cont), ..etc.

19. Gcheckrange.m

This program checks the results according to the error analysis presented in Section 6.2.6. The error is saved in the data file "Gcheck.dat".

GROUP \ X \ X \ X X \ X

1, 2, or 3.The directories contain results for pile located in centre of the 2nd trailing row,1st, trailing row or leading row, respectively.

0, 1, 2, 3, 4, 5, 6, 7, 8, 9 or 10. The directories contain results for pile groups with clay layer thickness equal to 0, 10, 20, 30, 40, 50, 60,70, 80, 90 or 100% , respectively.

2, 3, 4 or 5. The directories contains results of pile groups with spacing equal 2D, 3D, 4D or 5D respectively.

1, 2 or 3 The directories contains the sensitivity analysis results of different support types."1" stands for a pile pined to a cap subjected to concentrated lateral force; "2" stands for a pile fixed to a cap subjected to concentrated lateral force: "3' stands for a pile pinned to a can

Directory used to hold the sensitivity analysis results of pile groups.

Figure B.3 The subdirectory structure used to store the results for pile groups

327

XXXXXXXXX.inp

0, 1 or 2. The indicator used to differentiate the files used to calculate the forces and deformations of adjoint structure

Value of applied lateral load or moment

0, 1, 2, 3, 4, 5, 6, 7, 8, 9 or 10 Stands for clay layer thickness equal   0, 10,   20 ,30, 40, 50, 60, 70, 80, 90, 100%, respectively.

2, 3, 4 or 5, Stands for pile spacing equal 2D, 3D, 4D or 5D, respectively.

1, 2 or 3. Support type indicator."1" stands for a pile pined to a cap subjected to concentrated lateral force; "2" stands for a pile fixed to a cap subjected to concentrated lateral force; "3' stands for a pile pinned to a cap subjected to bending moment applied at each pile head.

Figure B.4 Name convention of the created input file for COM624P for pile groups

328

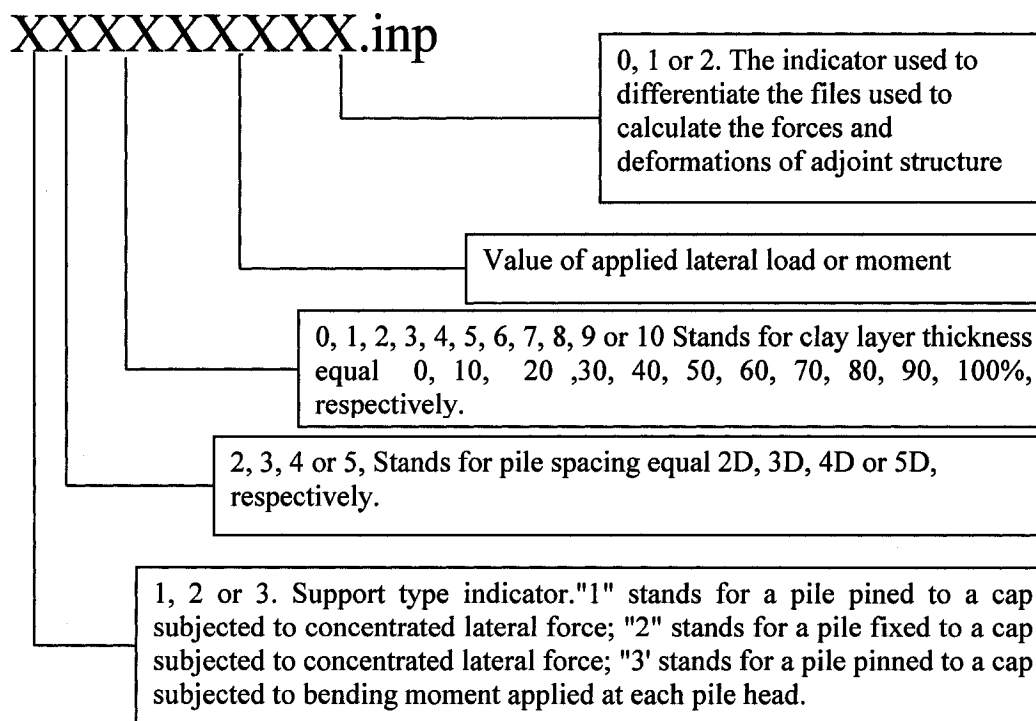# APPENDIX C

CONTENTS OF ATTACHED CD

The CD (Compact Disk) attached to this study contains the following two folders:

1. "SA-program" folder

This folder contains the developed user-friendly sensitivity analysis program "SA-program" discussed in Chapter 7. The folder contains the four main program files (inputdata.m, calculate.m, operators.m, results.m), the folder "sub-functions", in addition to the input data file "example.dat" and the output folder "example" as a sample for input and output. The execution of the SA-program is discussed in detail in Chapter 7.

2. "Numerical sensitivity analysis" folder

This folder contains the programs and result for the numerical sensitivity analysis conducted in Chapter 6, in addition to the program GSView used to view the sensitivity analysis results. The following four folders are included in this folder:

a. "Programs" folder

The developed MATLAB programs used to conduct the sensitivity analysis for single and pile groups discussed in Appendix B are saved in this folder. The files included in the directory are the MATLAB source files which should be opened with the MATLAB software and executed in the MATLAB command windows. Please refer to the manual or the help menu of the MATLAB program for the details about how to open, edit, execute and save the MATLAB source files. The source files should be executed in a certain sequence because the execution of one file might depend on the results of

329

another. The execution sequences of the source files for the sensitivity analysis of single piles and pile groups were presented in Appendix B.

b. "Single" folder

This folder contains the sensitivity analysis results of the laterally loaded single piles conducted in Chapter 6. The sensitivity analysis results for different support types, pile lengths, and soil stratifications (% clay) are saved in different sub-directories. The structure of the sub-directory system used to hold the sensitivity analysis results of the laterally loaded piles embedded in the non-homogeneous soil are presented in Figure B.2 in Appendix 2.

The numerical results are given in a MATLAB data file format that has an extension ".dat" and can be opened with MATLAB software by clicking on the required result. The graphical results are given in a picture format that has an extension ".eps" that can be opened with GSView program provided in the directory "GSView".

The Matalab data file containing the numerical results of sensitivity operators S is "Soperators.dat". The results of S are given in the form of matrices for each parameter, where each column in a matrix corresponds to a given load increment. In addition, the file "Soperators.dat" contains the lateral deflections, bending moments, soil resistance and shear matrices for the primary piles and the lateral deflection and bending moment matrices for both the adjoint piles.

The numerical results for A, PCR, TF and GF are saved in "Sresults.dat". They are in the form of a row vector for each design variable (for example Ac1 is the row vector for the design variable c for the lateral deflection sensitivity) where each column represents the value at a given load increment. For easy comparison between all variables the row vectors for all the design

330

variables are collected in one matrix Aall1 (or Aall2, PCRall1, PCRall2, TFall1, etc.) where each row represents a design variable. Accordingly the matrix consists of 8 rows where the order of the design variables in the rows is as follows: c, γ'_c, ε_{50}, k, γ'_s, ϕ, EI and b.

The error (in%) is given in the data file "Scheck.dat". The error for each parameter is given in a form of a matrix. The first row in the matrix displays the percent change in the parameter (1% to 50% change in the parameter). Each following row represents the error at a given load increment due to the % change mentioned in the first row.

The graphical results S, A, PCR, TF and GF are denoted for the different variables as mentioned in Appendix B. The number 1 included in the names of all graphical and numerical results (for example Sc1Matrix, Ac1, PCRc1, TFc1, GFc1, and Errorc1, Sc1.fig, Sc1(cont), Ac1.fig, Ac1(cont).fig, ...etc. for the parameter c) refers to results of the sensitivity of lateral top deflection y_t while the number 2 refers to the sensitivity of the top rotation θ_t.

c. **"Group" folder**

The sensitivity analysis results of laterally loaded pile groups conducted in Chapter 6 are saved in this folder. The structure of the sub-directory system used to hold the sensitivity analysis results of the laterally loaded pile groups are presented in Figure B.4 in Appendix B. The graphical and numerical sensitivity analysis results can be opened and viewed in the similar way to that of the single pile.

d. **"GSView" folder**

The GSView program is provided in this folder. It is needed to view graphical results obtained from the analysis in Chapter 6. The installation can be done

331

simply by running both of the executable files gs814w32.exe and gsv46w32.exe included in the directory "\GSView". The free GSView program installer can be obtained from the website www.ghostgum.com.au.

VITA AUCTORIS

Name: Dahlia Hisham Hafez

Place of birth: Windsor, Canada

Date of birth: November 13, 1977

Education: B. Sc. Civil Engineering, Cairo University, Egypt.
                   (1995-2000)

                   M. Sc. Civil Engineering, Cairo University, Egypt.
                   (2000-2003)

                   Civil and Environmental Engineering, University of
                   Windsor, Windsor, Ontario, Canada (2003-2007)